The ecological role of the activation of oxylipin biosynthesis in plants as a response to insect herbivory

Dissertation

zur Erlangung des akademischen Grades doctor rerum naturalium
(Dr. rer. nat.)

vorgelegt dem Rat der Chemisch-Geowissenschaftlichen Fakultät der
Friedrich-Schiller-Universität Jena

von Mario Kallenbach, Dipl. Chemie

geboren am 29.11.1980 in Gotha

Gutachter:

1. Prof. Dr. Georg Pohnert; IAAC Chemisch-geowissenschaftlich Fakultät, Friedrich-Schiller-Universität Jena

2. Prof. Dr. Ian Thomas Baldwin, Abt. Molekulare Ökologie, Max-Planck-Institut für chemische Ökologie Jena

3. Prof. Dr. Jean-Luc Wolfender, Pharmazeutisches Institut, Universität Genf

Tag der öffentlichen Verteidigung: 26.09.2012

(bitte nur in den Pflichtexemplaren ausfüllen)

Table of contents

Table of contents

General introduction

Interactions between plants and invertebrate herbivores have a long history; the first evidence of plant damage by arthropods dates back 400 million years ago (Labandeira, 2007). This timeframe has allowed plants and insects to develop sophisticated mechanisms to recognize one another and respond accordingly. On the one hand, phytophagous insects use plants as food, mating and oviposition sites; on the other hand, plants are not defenseless against their attack and have evolved a broad arsenal of defenses that are either constitutively present or produced upon attack. These defenses are tightly regulated by plant hormones such as jasmonates, salicylic acid, abscisic acid and ethylene (Fujita et al., 2006) which are rapidly produced in response to biotic stress.

Nicotiana attenuata as a plant model

Nicotiana attenuata (Solanaceae) is a wild annual tobacco plant native to the Southwestern US which germinates after fires from long-lived seed banks in nitrogen-rich soils after the seeds are exposed to cues contained in wood smoke (Baldwin and Morse, 1994; Preston and Baldwin, 1999). This synchronized germination behavior creates strong intra-specific competition, and *N. attenuata* plants must allocate their resources to sustain rapid growth and maximize seed set. *N. attenuata* monocultures also experience high herbivore pressure and *N. attenuata* plants respond strongly and specifically to the attack of insects from different feeding guilds, presumably in order to maximize the efficiency of their defense while maintaining competitive growth (Baldwin, 1998; Voelckel and Baldwin, 2004; Diezel et al., 2009). The short generation time, the complexity of induced defenses, self-compatibility and the availability of genetic transformation tools makes *N. attenuata* plants an ideal model plant for the study of biochemical processes in plants upon herbivore attack and the role of these processes in nature.

Perception of insect attack by plants

When plants are attacked by insect herbivores, they can recognize insect feeding by the perception of components present in the insect's oral secretions (OS) (Alborn et al., 1997;

Halitschke et al., 2003; Schmelz et al., 2009), multiple sequential wounding events (Mithöfer et al., 2005), or a combination of both. Among the insect elicitors of plant defense responses, the first to be isolated was the fatty acid-amino acid-conjugate (FAC) volicitin (17-OH-18:3-Gln), which was found in the OS of *Spodoptora exigua* larvae feeding on maize (*Zea mays*) plants and was shown to induce a volatile blend different from that induced by wounding alone (Alborn et al., 1997). Glucose oxidase was first identified in the saliva from *Helicoverpa zea* (Eichenseer et al., 1999) and it has been demonstrated to suppress the plant's defense response (Musser et al., 2002) and activate the salicylic acid (SA) pathway (Diezel et al., 2009). Inceptins were found in the OS of *S. frudgiperda* larvae feeding on cowpea (*Vigna unguiculata*) and have the capacity to induce the differential production of jasmonic acid (JA), SA and volatiles in these plants (Schmelz et al., 2006). More recently, sulfur-containing compounds, named caeliferins, were identified as elicitors in grasshopper (*Schistocerca americana*) OS (Alborn et al., 2007). In a recent study, different elicitors were applied on various plant species and the results indicated that elicitation by different insect-derived components is a plant species-specific process (Schmelz et al., 2009).

In the OS of the tobacco hornworm *Manduca sexta* (a specialized herbivore feeding on various Solanaceae species) the main elicitors that induce insect specific defense responses are FACs. FACs in *M. sexta* OS are composed predominantly of linoleic acid (18:2) or α-linolenic acid (18:3) conjugated to glutamic acid (Glu) or glutamine (Gln) (Halitschke et al., 2001). When applied to wounded *N. attenuata* leaves, FACs induce the differential production of signaling molecules such as JA and ethylene (Halitschke et al., 2001; von Dahl et al., 2007), large scale transcriptomic and proteomic changes (Halitschke et al., 2003; Giri et al., 2006), and the release of herbivory induced plant volatiles (Gaquerel et al., 2009). Moreover, when removed from *M. sexta* OS, the remaining FAC-free OS fraction loses its capacity to elicit insect specific responses in *N. attenuata* (Halitschke et al., 2003; Giri et al., 2006; Gaquerel et al., 2009).

In contrast to elicitors derived from plant pathogens, insect elicitor perception and mode of action is poorly understood. It is known that in maize, volicitin binds to a membrane-associated protein suggesting a ligand-receptor interaction (Truitt et al., 2004). Additional proposed mechanisms for FAC elicitation include their capacity to increase ion

permeability in membrane bilayers (Maischak et al., 2007). It has been previously demonstrated that volicitin can be transferred from the caterpillar OS into the wound surfaces of maize leaves (Truitt et al., 2004) and although the transferred amounts may be low (Peiffer and Felton, 2009), they seem sufficient to elicit specific responses against insect herbivores (Schittko et al., 2000). In **manuscript I,** I contributed to the investigation of the metabolism of one of the major FACs in *M. sexta* OS, 18:3-Glu, on wounded *N. attenuata* leaves. We studied the consequences of its metabolism on two processes associated to herbivory, the regulation of JA biosynthesis and terpenoid volatile emission.

Oxylipins – signaling molecules in response to stress

Oxylipins comprise a large family of oxidized fatty acids and their derivatives and are abundant molecules in a diverse range of organisms including mammals, mosses, algae, bacteria and fungi (Andreou et al.; Funk, 2001; Brodhun and Feussner, 2011). In plants, the production of oxylipins from polyunsaturated fatty acids (PUFAs) is immediately induced in response to diverse stresses including wounding, and insect and pathogen attacks (Turner et al., 2002; Farmer et al., 2003; Mueller, 2004; Taki et al., 2005; Matsui, 2006; Howe and Jander, 2008; Browse, 2009). The enzymatic biosynthesis of oxylipins in plants is initiated by lipoxygenases (9- and 13-LOXs) (Sanz et al., 1998; Hamberg et al., 1999; Feussner and Wasternack, 2002). These enzymes catalyze the di-oxygenating of PUFAs such as linoleic acid ($18:2^{\Delta9,12}$, 18:2) and α-linolenic acid ($18:3^{\Delta9,12,15}$, 18:3) to generate 9- and 13-hydroperoxy dienoic (9- and 13-HPODE) and trienoic (9- and 13-HPOTE) acids, respectively. These hydroperoxides can be metabolized by allene oxide synthase (AOS) to initiate the biosynthesis of JA or by hydroperoxide lyase (HPL) to initiate the biosynthesis of C_6 aldehydes and C_{12} ω-oxo-acids (Mosblech et al., 2009).

Oxylipins play essential roles as signaling molecules during plant responses to environmental stresses. For example, JA is essential for the induction of defense responses against pathogens and insect herbivores (Farmer et al., 2003; Kessler et al., 2004; Browse, 2005), C_6 aldehydes act as signals during pathogenesis and plant–insect communication (Croft et al., 1993; Matsui, 2006; Baldwin, 2010) and C_{12} diacids and ω-oxo-acids were originally described as wound-associated hormones (Bonner and English, 1937; Zimmerman and Coudron, 1979).

Jasmonic acid, an important mediator of plant responses to herbivory

JA together with some of its precursors and derivatives are signal molecules that function as essential mediators of the plant's wound, antiherbivore, and antipathogen responses, as well as in growth and development (Farmer, 1994; Creelman and Mullet, 1997; Turner et al., 2002). In *N. attenuata* these responses are governed by a strong transient burst of JA within one hour after herbivore attack that is amplified by elicitors in the insect's OS such as FACs (Halitschke et al., 2001; Howe and Jander, 2008; Schmelz et al., 2009; Stork et al., 2009). In unelicited mature leaves, JA is maintained at very low levels, however, upon specific stimulations, its biosynthesis is induced within a few minutes (Glauser et al., 2008). This rapid biosynthetic response results from the activation of constitutively expressed JA biosynthetic enzymes which can be activated by substrate availability and/or posttranslational modifications. According to the canonical mechanism for JA biosynthesis (Vick and Zimmerman,1983), free 18:3 (**1,** Fig 1.1) forms 13(S)-hydroperoxy-18:3 (13S-(OOH)-18:3, **2**, Fig 1.1) by the action of 13-lipoxygenase (13-LOX) in plastids. 13S-(OOH)-18:3 can be converted by allene oxide synthase (AOS) into a highly unstable allene oxide intermediate that is processed by allene oxide cyclase (AOC) to yield (9S,13S)-12-oxo-phytodienoic acid (OPDA, **4**, Fig 1.1). Similarly, (7S,11S)-10-oxo-phytodienoic acid (dinor-OPDA) can be formed from 16:3 through the same pathway (Weber et al. 2007). OPDA and dinor-OPDA are transported from the plastid into the peroxisome, where they are reduced by the action of OPDA reductase 3 (OPR3) and after two and three cycles of β-oxidation, respectively, (3R,7S)-JA (**6**) is formed (Fig 1.1). JA can be modified, for example, by jasmonyl-O-methyl transferase (JMT) to form methyl-jasmonic acid (MeJA) (Seo et al., 2001) or by JASMONATE RESISTANT (JAR) that conjugates isoleucine to form JA-Ile (**7**, Fig 1.1) (Wang et al., 2007; Suza and Staswick, 2008). JA-Ile activates the SCF^{COII}-JAZ complex (Fonseca et al., 2009) which transcriptionally activates genes involved in the biosynthesis of defense molecules, among other responses (Fig1.1; Chini et al., 2007; Thines et al., 2007).
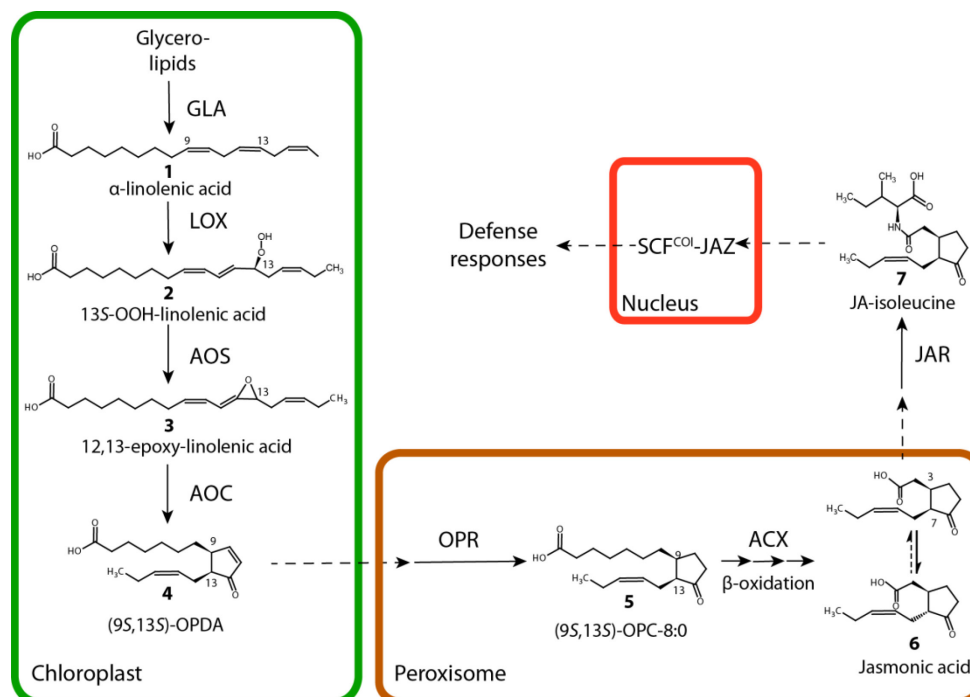
Figure 1.1: Schematic representation of the jasmonic acid biosynthesis pathway in plants. Free α-linolenic acid (**1**) forms 13(*S*)-hydroperoxy-18:3 (**2**) by the action of 13-lipoxygenase (13-LOX) in plastids. **2** is converted by allene oxide synthase (AOS) into a highly unstable allene oxide intermediate (**3**) that is processed by allene oxide cyclase (AOC) to yield (9*S*,13*S*)-12-oxo-phytodienoic acid (OPDA, **4**). **4** is transported from the plastid into the peroxisome where it is reduced by the action of an OPDA reductase (OPR), and after three cycles of β-oxidation involving an acetyl-CoA-transferase (ACX), (3*R*,7*S*)-JA (**6**) is formed. **6** can be modified by JASMONATE RESISTANT (JAR) that conjugates isoleucine to form JA-Ile (**7**). **7** activates the SCF^COI1^-JAZ complex which transcriptionally activates genes involved in the biosynthesis of defense molecules.

Analysis of intermediates of the JA biosynthesis pathway

To understand how JA biosynthesis is activated in response to wounding and herbivory, the quantitative analysis of low abundant intermediates of the JA biosynthesis pathway is of major importance. The use of mass spectrometry (MS) coupled to liquid chromatography (LC) is ideal for the analysis of the complex mixture of signaling molecules which are commonly found in plant tissues. One of the advantages of LC–MS is that separation and structural elucidation of compounds can be achieved in a continuous manner without the need for purification or derivatization steps. Another advantage of LC–MS is the use of tandem MS (MS–MS), in which a precursor ion is mass-selected by mass analyzer 1, focused into a collision region preceding a second mass analyzer (collision

chamber), and their mass fragments analyzed in a third mass analyzer (Lima and Abdalla, 2002). The capacity to perform multi reaction monitoring (MRM) has the advantage of rapid and sensitive detection of several compounds even if they show similar retention times during chromatography. Ionization by electrospray (ESI) is one of the most widely used tools for LC–MS analysis (Johnson, 2005). However, the efficiency of ion formation differs widely among compounds depending on their chemical structure (Nishikaze and Takayama, 2007). For example, while small molecules containing free carboxyl groups and high numbers of heteroatoms such as JA are ionized efficiently by ESI (Forcat et al., 2008; Pan et al., 2008; Diezel et al., 2009), aliphatic molecules such as free fatty acids are relatively poorly ionized by this technique (Valianpour et al., 2003).

In **manuscript II**, I present a method for the simultaneous determination of aliphatic (e.g., free fatty acids and oxygenated derivatives) and more polar compounds (e.g. OPDA, JA and JA-Ile) by using picolinyl ester derivatives of crude leaf samples an analysis by with LC-(ESI)-MS. The method provides a one-step procedure to simultaneously analyze aliphatic and polar compounds in small quantities of tissue extracts.

Regulation of JA biosynthesis in N. attenuata

Due to the large number of enzymes and different cellular compartments involved in JA biosynthesis, it is expected that the pathway is regulated at multiple steps. Resolution of the structures of the tomato (*Solanum lycopersicum*) OPR3 and Arabidopsis AOC2 and ACX1 has provided insights into potential regulatory mechanisms for these enzymes (e.g. oligomerization and phosphorylation; Pedersen and Henriksen, 2005; Breithaupt et al., 2006; Hofmann et al., 2006). The identification of two plastidial glycerolipases in Arabidopsis, DAD1 and DGL (Ishiguro et al., 2001; Hyun et al., 2008), has provided genetic evidence for the importance of the release of trienoic fatty acids from plastidial lipids in the activation of JA biosynthesis. Some oxylipins have been found esterified to galactolipids in Arabidopsis leaves and in this species, preformed JA precursors may supply the JA biosynthesis pathway after their release from lipids (Stelmach et al., 2001; Hisamatsu et al., 2003; Buseman et al., 2006; Schäfer et al., 2011). Lipid-bound oxylipins appear to be restricted to Arabidopsis species (Böttcher and Weiler, 2007).

Several regulatory factors with a potential function upstream of JA biosynthesis have been identified (Ludwig et al., 2005; Takabatake et al., 2006; Schweighofer et al., 2007; Takahashi et al., 2007); however, how these regulators affect JA biosynthesis is at present unknown. For example, wounding and herbivory in tobacco and tomato activate the mitogen-activated protein kinases salicylate-induced protein kinase (SIPK) and wound-induced protein kinase (WIPK) (Seo et al., 1999; Kandoth et al., 2007; Wu et al., 2007). When SIPK and WIPK expression is silenced in tobacco, the plants accumulate 60% to 70% less JA than wild type after wounding or OS elicitation (Seo et al., 2007; Wu et al., 2007). Another regulatory component that affects JA production in *N. attenuata* is Nonexpressor of PR-1 (NPR1), an essential component of the SA signal transduction pathway first identified in Arabidopsis (Cao et al., 1994). *N. attenuata* NPR1-silenced plants accumulate 60% to 70% lower JA levels after elicitation than wild type (Rayapuram and Baldwin, 2007). NPR1 interacts with the JA and ethylene signaling cascades, and a cytosolic role for this factor in the regulation of JA-dependent responses/biosynthesis has been proposed (Spoel et al., 2003). In contrast to the mechanisms acting upstream of JA biosynthesis, the mechanisms mediating downstream JA responses are better characterized (Kazan and Manners, 2008; Browse, 2009). Among the best-characterized regulators of these responses is CORONATIVE INSENSITIVE1 (COI1), a gene that participates in jasmonate perception and regulates gene expression through its interaction with the JASMONATE ZIM-DOMAIN repressors (Chini et al., 2007; Thines et al., 2007).

In **manuscript III**, I quantified the initial rates of accumulation of plastid-derived JA precursors after wounding and FAC elicitation in *N. attenuata* leaves to understand the early processes regulating the activation of JA biosynthesis after these stimuli in wild type and four JA-deficient genotypes previously described: ir-*sipk*, ir-*wipk*, ir-*npr1*, and ir-*coi1* (Rayapuram and Baldwin, 2007; Paschold et al., 2008; Meldau et al., 2009). We show that SIPK, WIPK, NPR1, and FACs contribute to the activation of *de novo* JA biosynthesis by affecting diverse early enzymatic steps in this pathway. The identification of a plastidial glycerolipase A1 type I protein (GLA1) essential for JA biosynthesis pointed to this enzyme as one potential target of some of these activating mechanisms.

Figure 1.2: The wild tobacco *Nicotiana attenuata* (**A**) germinates after fires in its natural habitat, Southwestern US, and has to cope with an unpredictable community of herbivore like *Manduca* spp larvae (**B**) and *Empoasca* spp leafhoppers (**C**).

The ecological role of JA biosynthesis activation in response to insect herbivory

In its natural habitat, *N. attenuata* has to cope with an unpredictable insect community including piercing-sucking herbivores such as mirids (*Tupiocoris notatus*) and chewing herbivores such as grasshoppers (*Trimerotropis* spp), armyworm larvae (*Spodoptera* spp) and larvae of the specialist herbivores, the tomato hornworm (*Manduca quinquemaculata*) and the tobacco hornworm (*M. sexta*) (Fig 1.2). To defend against this great diversity of herbivores, *N. attenuata* evolved a cocktail of JA regulated inducible defense molecules like nicotine (Baldwin, 2001; Steppuhn et al., 2004), trypsine protease inhibitors (TPIs) (Ussuf et al., 2001; Steppuhn and Baldwin, 2007), 17-hydroxygeranyllinalool diterpene glycosides (HGL-DTGs) (Heiling et al., 2010) and phenylpropanoid-polyamine conjugates (PPCs) (Kaur et al., 2010). Field studies have demonstrated the essential role of the activation of JA biosynthesis and the induction of JA regulated defenses in *N. attenuata* to respond to insect herbivore attack (Kessler et al. 2004; Paschold et al. 2007; Stitz et al., 2011). For example, when *N. attenuata* plants are rendered deficient in JA biosynthesis by silencing NaLOX3 (as-*lox3*), these plants are notably stronger damaged by herbivores (Kessler et al., 2004). Moreover, the generalist leafhoppers of the genus *Empoasca* (Fig

1.2), a hemipterans that feed on phloem and cell contents of a broad range of host plants (Carter, 1952; Gyrisco, 1958), heavily damage as-*lox3* whereas these insect are only rarely found on WT *N. attenuata* plants (Kessler et al., 2004).

In **manuscript IV**, I used a set of eleven *N. attenuata* transgenic lines deficient in specific steps of JA biosynthesis and perception, and in the accumulation of major insecticidal molecules, to disentangle the mechanisms underlying the selection of host plants by *Empoasca* leafhoppers. I demonstrate that the choice of plants for feeding by *Empoasca* leafhoppers is independent of the accumulation of major insecticidal molecules, and were not associated with detectable changes in plant volatiles, but depends on the plant´s capacity to mediate JA signaling. I exploited this trait and used different levels of damage by *Empoasca* leafhoppers in natural *N. attenuata* populations as markers of genetic variation in JA accumulation and signaling in these plants.

Oxylipins of the hydroperoxide lyase pathway

Similar to the rapid activation of the JA biosynthesis pathway induced after stress, another oxylipin pathway generates the green leaf volatiles (GLVs) hexanal and (3*Z*)-hexenal as a result of the cleavage of 13*S*-HPODE and –HPOTE by Hydroperoxide lyase (HPL) (Fig. 1.3). In *N. attenuata* leaves, the supply of 13*S*-HPODE and 13*S*-HPOTE for the biosynthesis of hexanal and (3*Z*)-hexenal requires the activity of the lipoxygenase-2 gene (Na*LOX2*); plants with reduced expression of Na*LOX2* have a greatly reduced production of GLVs (Allmann et al., 2010). *N. attenuata* plants with reduced expression of Na*HPL* have similarly reduced production of GLVs (Halitschke et al., 2004). GLVs play essential roles as signaling molecules in indirect plant defenses (Croft et al., 1993; Matsui, 2006; Allmann and Baldwin, 2010; Baldwin, 2010).

In addition to GLV production, the cleavage of 13*S*-HPODE and –HPOTE, respectively, by HPL also leads to the formation of 12-oxo-(9*Z*)-dodecenoic acid ((9*Z*)-traumatin, **1a**, Fig 1.3) (Vick and Zimmerman, 1976). In recent years, research has been focused primarily on the biochemical and functional characterization of GLVs during herbivore and pathogen attacks, and less attention has been paid to the metabolism and signal capacities of the C_{12} derivatives of the HPL pathway. As a result, the metabolic fluxes and fates of these molecules under stress conditions are largely unknown in plants. (9*Z*)-

traumatin undergoes rapid modifications by diverse enzymatic and non-enzymatic reactions, generating multiple potential chemical signals. These modifications change the physicochemical properties of the molecules, and in some cases the importance of the resulting modified molecules in biological processes has been demonstrated (Zimmerman and Coudron, 1979; Ivanova et al., 2001).
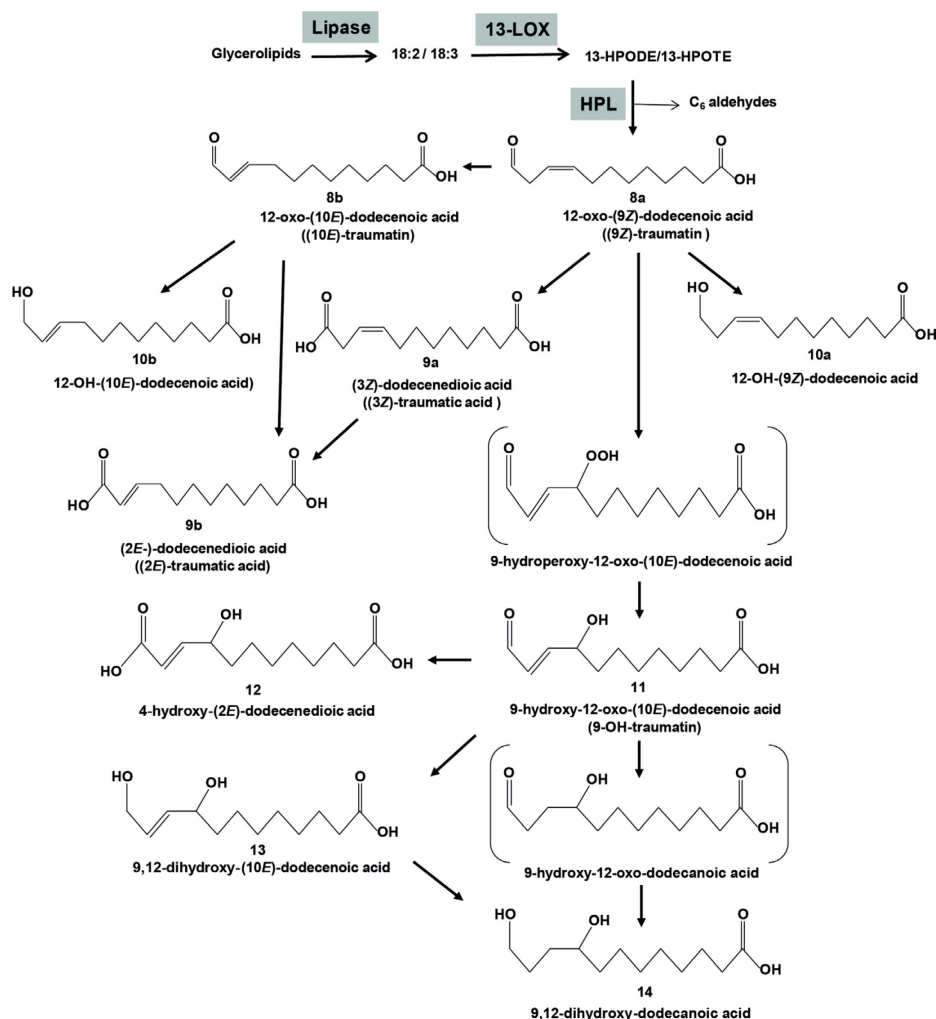
Figure 1.3: Schematic representation of the hydroperoxide lyase (HPL) pathway in plants and the generation of derivatives of 12-oxo-(9Z)-dodecenoic acid ((9Z)-traumatin). In leaves, 18:2 and 18:3 fatty acids are released from membranes and dioxygenated by 13-lipoxygenases (13-LOXs) to generate 13S-hydroperoxides (13-HPODE and 13-HPOTE, respectively). These molecules are cleaved by HPL to produce C_6 aldehydes and (9Z)-traumatin (**8a**). This molecule can undergo several enzymatic and nonenzymatic modifications to be converted into the products (10*E*)-traumatin (**8b**), (3Z) and (2*E*)-traumatic acid (**9a**, 9b), 12-OH-(9Z)- and 12-OH-(10*E*)-dodecenoic acid (**10a**, **10b**) and 9-OH-traumatin (**11**). **11** can be converted into 4-OH-traumatic acid (**12**), 9,12-OH-(10*E*)-dodecenoic acid (**13**) and 9,12-OH-dodecanoic acid (**14**).

In the case of (9*Z*)-traumatin (**8a,** Fig 1.3), the *Z*-C_9-C_{10} double bond rearranges to *E*-C_{10}-C_{11} to form 12-oxo-(10*E*)-dodecenoic acid ((10*E*)-traumatin, **8b**, Fig 1.3), and the aldehyde group can be auto-oxidized non-enzymatically to form (3*Z*)- or (2*E*)-dodecenedioic acid ((3*Z*)- or (2*E*)-traumatic acid **9a**, **9b**, Fig 1.3) (Zimmerman and Coudron, 1979) or be reduced to form (9*Z*)- or (10*E*)-12-hydroxydodecenoic acid ((9*Z*)- or (10*E*)-12-OH-dodecenoic acid, **10a**, **10b**, Fig 1.3) (Grechkin, 2002). (9*Z*)-traumatin can be oxidized to 9-hydroxy-12-oxo-(10*E*)-dodecenoic acid (9-OH-traumatin, **11**, Fig 1.3) either enzymatically by a LOX-mediated mechanism (Gardner, 1998) or non-enzymatically (Noordermeer et al., 2000). A recent study showed that 9-OH-traumatin can be subsequently converted into 4-hydroxy-(2*E*)-dodecenedioic acid (4-OH-traumatic acid, **12**, Fig 1.3), 9,12-dihydroxy-(10*E*)-dodecenoic acid (9,12-OH-(10*E*)-dodecenoic acid, **13**, Fig 1.3) and 9,12-dihydroxy-dodecanoic acid (9,12-OH-dodecanoic acid, **14**, Fig 1.3) in pea (*Pisum sativum*) seedlings (Mukhtarova et al., 2011).

In **manuscript V**, I present a detailed analysis of the fluxes and metabolism of C_{12} derivatives of the HPL pathway in *N. attenuata* plants induced by wounding and simulated herbivory. Part of this analysis is based on a new LC-MS/MS method developed for the quantification of these metabolites. The study reveals new aspects of the biogenesis of C_{12} derivatives of the HPL pathway and opens new perspectives for possible roles of these metabolites in the regulation of stress responses.

References

Alborn, H.T., Turlings, T.C., Jones, T.H., Stenhagen, G., Loughrin, J.H., and Tumlinson, J.H. (1997). An elicitor of plant volatiles from beet armyworm oral secretion. Science **276,** 945-949.

Alborn, H.T., Hansen, T.V., Jones, T.H., Bennett, D.C., Tumlinson, J.H., Schmelz, E.A., and Teal, P.E. (2007). Disulfooxy fatty acids from the American bird grasshopper Schistocerca americana, elicitors of plant volatiles. Proc Natl Acad Sci U S A **104,** 12976-12981.

Allmann, S., and Baldwin, I.T. (2010). Insects betray themselves in nature to predators by rapid isomerization of green leaf volatiles. Science **329,** 1075-1078.

Allmann, S., Halitschke, R., Schuurink, R., and Baldwin, I. (2010). Oxylipin channelling in Nicotiana attenuata: lipoxygenase 2 supplies substrates for green leaf volatile production. Plant Cell Environ **33,** 2028-2040.

Andreou, A., Brodhun, F., and Feussner, I. Biosynthesis of oxylipins in non-mammals. Progress in Lipid Research **48,** 148-170.

Arimura, G., Kost, C., and Boland, W. (2005). Herbivore-induced, indirect plant defences. Biochimica Et Biophysica Acta-Molecular and Cell Biology of Lipids **1734,** 91-111.

Baldwin, I.T. (1998). Jasmonate-induced responses are costly but benefit plants under attack in native populations. Proceedings of the National Academy of Sciences of the United States of America **95,** 8113-8118.

Baldwin, I.T. (2001). An ecologically motivated analysis of plant-herbivore interactions in native tobacco. Plant Physiology **127,** 1449-1458.

Baldwin, I.T. (2010). Plant volatiles. Curr Biol **20,** R392-397.

Baldwin, I.T., and Morse, L. (1994). Up in Smoke 2. Germination of Nicotiana attenuata in response to smoke-derived cues and nutrients in burned and unburned soils. Journal of Chemical Ecology **20,** 2373-2391.

Bonner, J., and English, J. (1937). Purification of traumatin, a plant wound hormone. Science **86,** 352-353.

Böttcher, C., and Weiler, E.W. (2007). cyclo-Oxylipin-galactolipids in plants: occurrence and dynamics. Planta **226,** 629-637.

Breithaupt, C., Kurzbauer, R., Lilie, H., Schaller, A., Strassner, J., Huber, R., MacHeroux, P., and Clausen, T. (2006). Crystal structure of 12-oxophytodienoate reductase 3 from tomato: Self-inhibition by dimerization. Proceedings of the National Academy of Sciences **103,** 14337-14342.

Brodhun, F., and Feussner, I. (2011). Oxylipins in fungi. FEBS Journal **278,** 1047-1063.

Browse, J. (2005). Jasmonate: an oxylipin signal with many roles in plants. J Chem Ecol **72,** 431-456.

Browse, J. (2009). Jasmonate Passes Muster: A Receptor and Targets for the Defense Hormone. Annu. Rev. Plant Biol **60,** 183-205.

Buseman, C.M., Tamura, P., Sparks, A.A., Baughman, E.J., Maatta, S., Zhao, J., Roth, M.R., Esch, S.W., Shah, J., and Williams, T.D. (2006). Wounding Stimulates the Accumulation of Glycerolipids Containing Oxophytodienoic Acid and Dinor-Oxophytodienoic Acid in Arabidopsis Leaves. Plant Physiology **142,** 28.

Cao, H., Bowling, S.A., Gordon, A.S., and Dong, X. (1994). Characterization of an Arabidopsis Mutant That Is Nonresponsive to Inducers of Systemic Acquired Resistance. The Plant Cell **6,** 1583-1592.

Carter, W. (1952). Injuries to plants caused by insect toxins.2. Botanical Review **18,** 680-721.

Chen, M.-S. (2008). Inducible direct plant defense against insect herbivores: A review. Insect Science **15,** 101-114.

Chini, A., Fonseca, S., Fernández, G., Adie, B., Chico, J., Lorenzo, O., García-Casado, G., López-Vidriero, I., Lozano, F., Ponce, M., Micol, J., and Solano, R. (2007). The JAZ family of repressors is the missing link in jasmonate signalling. Nature **448,** 666-671.

Creelman, R.A., and Mullet, J.E. (1997). Biosynthesis and action of jasmonates in plants. Annual Reviews in Plant Physiology and Plant Molecular Biology **48,** 355-381.

Croft, K., Juttner, F., and Slusarenko, A.J. (1993). Volatile Products of the Lipoxygenase Pathway Evolved from Phaseolus vulgaris (L.) Leaves Inoculated with Pseudomonas syringae pv phaseolicola. Plant Physiol **101,** 13-24.

Diezel, C., von Dahl, C.C., Gaquerel, E., and Baldwin, I.T. (2009). Different lepidopteran elicitors account for cross-talk in herbivory-induced phytohormone signaling. Plant Physiol **150,** 1576-1586.

Eichenseer, H., Mathews, M.C., Bi, J.L., Murphy, J.B., and Felton, G.W. (1999). Salivary glucose oxidase: multifunctional roles for helicoverpa zea? Arch Insect Biochem Physiol **42,** 99-109.

English, J., and Bonner, J. (1937). The wound hormones of plants I. Traumatin, the active principle of the bean test. Journal of Biological Chemistry **121,** 791-799.

Esterbauer, H., Ertl, A., and Scholz, N. (1976). The reaction of cysteine with α,β-unsaturated aldehydes. J Chem Ecol **32,** 285-289.

Farmer, E.E. (1994). Fatty-Acid Signaling in Plants and Their Associated Microorganisms. Plant Molecular Biology **26,** 1423-1437.

Farmer, E.E., Almeras, E., and Krishnamurthy, V. (2003). Jasmonates and related oxylipins in plant responses to pathogenesis and herbivory. Curr. Opin. Plant Biol. **6,** 372-378.

Feussner, I., and Wasternack, C. (2002). The lipoxygenase pathway. Annual Review of Plant Biology **53,** 275-297.

Fonseca, S., Chini, A., Hamberg, M., Adie, B., Porzel, A., Kramell, R., Miersch, O., Wasternack, C., and Solano, R. (2009). (+)-7-iso-Jasmonoyl-L-isoleucine is the endogenous bioactive jasmonate. Nature Chemical Biology **5,** 344-350.

Forcat, S., Bennett, M.H., Mansfield, J.W., and Grant, M.R. (2008). A rapid and robust method for simultaneously measuring changes in the phytohormones ABA, JA and SA in plants following biotic and abiotic stress. Plant Methods **4**.

Fujita, M., Fujita, Y., Noutoshi, Y., Takahashi, F., Narusaka, Y., Yamaguchi-Shinozaki, K., and Shinozaki, K. (2006). Crosstalk between abiotic and biotic stress responses: a current view from the points of convergence in the stress signaling networks. Curr. Opin. Plant Biol. **9,** 436-442.

Funk, C. (2001). Prostaglandins and Leukotrienes: Advances in Eicosanoid Biology. J Chem Ecol **294,** 1871-1875.

Gaquerel, E., Weinhold, A., and Baldwin, I.T. (2009). Molecular interactions between the specialist herbivore Manduca sexta (Lepidoptera, Sphigidae) and its natural host Nicotiana attenuata. VIII. An unbiased GCxGC-ToFMS analysis of the plant's elicited volatile emissions. Plant Physiol **149,** 1408-1423.

Gardner, H.W. (1998). 9-Hydroxy-traumatin, a new metabolite of the lipoxygenase pathway. Lipids **33,** 745-749.

Giri, A.P., Wunsche, H., Mitra, S., Zavala, J.A., Muck, A., Svatos, A., and Baldwin, I.T. (2006). Molecular interactions between the specialist herbivore Manduca sexta (Lepidoptera, Sphingidae) and its natural host Nicotiana attenuata. VII. Changes in the plant's proteome. Plant Physiology **142,** 1621-1641.

Glauser, G., Grata, E., Dubugnon, L., Rudaz, S., Farmer, E.E., and Wolfender, J.L. (2008). Spatial and temporal dynamics of jasmonate synthesis and accumulation in Arabidopsis in response to wounding. J Biol Chem **283,** 16400-16407.

Grechkin, A.N. (2002). Hydroperoxide lyase and divinyl ether synthase. Prostaglandins & Other Lipid Mediators **68-69,** 457-470.

Gyrisco, G.G. (1958). Forage insects and their control. Annual Review of Entomology **3,** 421-448.

Halitschke, R., Ziegler, J., Keinanen, M., and Baldwin, I.T. (2004). Silencing of hydroperoxide lyase and allene oxide synthase reveals substrate and defense signaling crosstalk in Nicotiana attenuata. Plant Journal **40,** 35-46.

Halitschke, R., Schittko, U., Pohnert, G., Boland, W., and Baldwin, I.T. (2001). Molecular interactions between the specialist herbivore Manduca sexta (Lepidoptera, Sphingidae) and its natural host Nicotiana attenuata. III. Fatty acid-amino acid conjugates in herbivore oral secretions are necessary and sufficient for herbivore-specific plant responses. Plant Physiology **125,** 711-717.

Halitschke, R., Gase, K., Hui, D.Q., Schmidt, D.D., and Baldwin, I.T. (2003). Molecular interactions between the specialist herbivore Manduca sexta (Lepidoptera, Sphingidae) and its natural host Nicotiana attenuata. VI. Microarray analysis reveals that most herbivore-specific transcriptional changes are mediated by fatty acid-amino acid conjugates. Plant Physiology **131,** 1894-1902.

Hamberg, M., Sanz, A., and Castresana, C. (1999). α-Oxidation of Fatty Acids in Higher Plants. Journal of Biological Chemistry **274,** 24503-24513.

Heil, M. (2009). Damaged-self recognition in plant herbivore defence. Trends Plant Sci **14,** 356-363.

Heiling, S., Schuman, M.C., Schoettner, M., Mukerjee, P., Berger, B., Schneider, B., Jassbi, A.R., and Baldwin, I.T. (2010). Jasmonate and ppHsystemin Regulate Key Malonylation Steps in the Biosynthesis of 17-Hydroxygeranyllinalool Diterpene Glycosides, an Abundant and Effective Direct Defense against Herbivores in Nicotiana attenuata. Plant Cell **22,** 273-292.

Hisamatsu, Y., Goto, N., Hasegawa, K., and Shigemori, H. (2003). Arabidopsides A and B, two new oxylipins from Arabidopsis thaliana. Tetrahedron Letters **44,** 5553-5556.

Hofmann, E., Zerbe, P., and Schaller, F. (2006). The Crystal Structure of Arabidopsis thaliana Allene Oxide Cyclase: Insights into the Oxylipin Cyclization Reaction. THE PLANT CELL **18,** 3201-3217.

Howe, G.A., and Jander, G. (2008). Plant Immunity to Insect Herbivores. Annual review of plant biology **59,** 41-66.

Hyun, Y., Choi, S., Hwang, H.-J., Yu, J., Nam, S.-J., Ko, J., Park, J.-Y., Seo, Y.S., Kim, E.Y., Ryu, S.B., Kim, W.T., Lee, Y.-H., Kang, H., and Lee, I. (2008). Cooperation and functional diversification of two closely related galactolipase genes for jasmonate biosynthesis. Developmental cell **14,** 183-192.

Ishiguro, S., Kawai-Oda, A., Ueda, J., Nishida, I., and Okada, K. (2001). The DEFECTIVE IN ANTHER DEHISCIENCE gene encodes a novel phospholipase A1 catalyzing the initial step of jasmonic acid biosynthesis, which synchronizes pollen maturation, anther dehiscence, and flower opening in Arabidopsis. The Plant cell **13,** 2191-2209.

Ivanova, A.B., Yarin, A.Y., Antsygina, L.L., Gordon, L.K., and Grechkin, A.N. (2001). (9Z)-12-Hydroxy-9-dodecenoic Acid Is an Inducer of Oxygen Consumption and Extracellular pH Changes by Cut Wheat Roots. Doklady Biochemistry and Biophysics **379,** 302-303.

Johnson, D.W. (2005). Contemporary clinical usage of LC/MS: Analysis of biologically important carboxylic acids. Clinical biochemistry **38,** 351-361.

Kandoth, P.K., Ranf, S., Pancholi, S.S., Jayanty, S., Walla, M.D., Miller, W., Howe, G.A., Lincoln, D.E., and Stratmann, J.W. (2007). Tomato MAPKs LeMPK1, LeMPK2, and LeMPK3 function in the systemi n-mediated defense response against herbivorous insects. Proceedings of the National Academy of Sciences of the United States of America **104,** 12205-12210.

Kaur, H., Heinzel, N., Schoettner, M., Baldwin, I.T., and Galis, I. (2010). R2R3-NaMYB8 Regulates the Accumulation of Phenylpropanoid-Polyamine Conjugates, Which Are Essential for Local and Systemic Defense against Insect Herbivores in Nicotiana attenuata. Plant Physiology **152,** 1731-1747.

Kazan, K., and Manners, J. (2008). Jasmonate Signaling: Toward an Integrated View. Plant Physiology **146,** 1459-1468.

Kessler, A., and Baldwin, I. (2002). Plant responses to insect herbivory: the emerging molecular analysis. Annual review of plant biology **53,** 299-328.

Kessler, A., Halitschke, R., and Baldwin, I.T. (2004). Silencing the jasmonate cascade: induced plant defenses and insect populations. Science **305,** 665-668.

Labandeira, C. (2007). The origin of herbivory on land: Initial patterns of plant tissue consumption by arthropods. Insect Science **14,** 259-275.

Lawrence, P.K., and Koundal, K.R. (2002). Plant protease inhibitors in control of phytophagous insects. Electronic Journal of Biotechnology **5**.

Lima, E.S., and Abdalla, D.S.P. (2002). High-performance liquid chromatography of fatty acids in biological samples. Analytica Chimica Acta **465,** 81-91.

Ludwig, A.A., Saitoh, H., Felix, G., Freymark, G., Miersch, O., Wasternack, C., Boller, T., Jones, J.D.G., and Romeis, T. (2005). Ethylene-mediated cross-talk between calcium-dependent protein kinase and MAPK signaling controls stress responses in plants. Proceedings of the National Academy of Sciences of the United States of America **102,** 10736-10741.

Maischak, H., Grigoriev, P.A., Vogel, H., Boland, W., and Mithofer, A. (2007). Oral secretions from herbivorous lepidopteran larvae exhibit ion channel-forming activities. Febs Letters **581,** 898-904.

Matsui, K. (2006). Green leaf volatiles: hydroperoxide lyase pathway of oxylipin metabolism. Curr Opin Plant Biol **9,** 274-280.

Meldau, S., Wu, J., and Baldwin, I.T. (2009). Silencing two herbivory-activated MAP kinases, SIPK and WIPK, does not increase Nicotiana attenuata's susceptibility to herbivores in the glasshouse and in nature. New Phytol **181,** 161-173.

Mithöfer, A., Wanner, G., and Boland, W. (2005). Effects of feeding Spodoptera littoralis on lima bean leaves. II. Continuous mechanical wounding resembling insect feeding is sufficient to elicit herbivory-related volatile emission. Plant Physiology **137,** 1160-1168.

Mosblech, A., Feussner, I., and Heilmann, I. (2009). Oxylipins: structurally diverse metabolites from fatty acid oxidation. Plant Physiol Biochem **47,** 511-517.

Mueller, M.J. (2004). Archetype signals in plants: the phytoprostanes. Curr Opin Plant Biol **7,** 441-448.

Mueller, M.J., and Berger, S. (2009). Reactive electrophilic oxylipins: pattern recognition and signalling. Phytochemistry **70,** 1511-1521.

Mukhtarova, L.S., Mukhitova, F.K., Gogolev, Y.V., and Grechkin, A.N. (2011). Hydroperoxide lyase cascade in pea seedlings: Non-volatile oxylipins and their age and stress dependent alterations. Phytochemistry **72,** 356-364.

Musser, R.O., Hum-Musser, S.M., Eichenseer, H., Peiffer, M., Ervin, G., Murphy, J.B., and Felton, G.W. (2002). Herbivory: caterpillar saliva beats plant defences. Nature **416,** 599-600.

Myher, J.J., and Kuksis, A. (1995). General strategies in chromatographic analysis of lipids. Journal of Chromatography B: Biomedical Sciences and Applications **671,** 3-33.

Nishikaze, T., and Takayama, M. (2007). Study of factors governing negative molecular ion yields of amino acid and peptide in FAB, MALDI and ESI mass spectrometry. International Journal of Mass Spectrometry **268,** 47-59.

Noordermeer, M.A., Feussner, I., Kolbe, A., Veldink, G.A., and Vliegenthart, J.F.G. (2000). Oxygenation of (3Z)-alkenals to 4-hydroxy-(2E)-alkenals in plant extracts: A nonenzymatic process. Biochemical and Biophysical Research Communications **277,** 112-116.

Pan, X., Welti, R., and Wang, X. (2008). Simultaneous quantification of major phytohormones and related compounds in crude plant extracts by liquid chromatography-electrospray tandem mass spectrometry. Phytochemistry **69,** 1773-1781.

Paschold, A., Halitschke, R., Baldwin, I.T. (2007) Co(i)-ordinating defenses: NaCOI1 mediates herbivore-induced resistance in Nicotiana attenuata and reveals the role of herbivore movement in avoiding defenses. Plant J **51,** 79-91.

Paschold, A., Bonaventure, G., Kant, M., and Baldwin, I.T. (2008). Jasmonate perception regulates jasmonate biosynthesis and JA-Ile metabolism: the case of COI1 in *Nicotiana attenuata*. Plant and Cell Physiology **49,** 1165 -1175.

Pedersen, L., and Henriksen, A. (2005). Acyl-CoA Oxidase 1 from Arabidopsis thaliana. Structure of a Key Enzyme in Plant Lipid Metabolism. Journal of Molecular Biology **345,** 487-500.

Peiffer, M., and Felton, G.W. (2009). Do caterpillars secrete "oral secretions"? J Chem Ecol **35,** 326-335.

Preston, C.A., and Baldwin, I.T. (1999). Positive and negative signals regulate germination in the post-fire annual, Nicotiana attenuata. Ecology **80,** 481-494.

Rayapuram, C., and Baldwin, I.T. (2007). Increased SA in NPR1-silenced plants antagonizes JA and JA-dependent direct and indirect defenses in herbivore-attacked Nicotiana attenuata in nature. Plant Journal **52,** 700-715.

Rezanka, T. (2002). Identification of very long chain fatty acids by atmospheric pressure chemical ionization liquid chromatography-mass spectroscopy from green alga Chlorella kessleri. Journal of Separation Science **25**.

Sanz, A., Moreno, J.I., and Castresana, C. (1998). PIOX, a new pathogen-induced oxygenase with homology to animal cyclooxygenase. Plant Cell **10,** 1523-1537.

Schäfer, M., Fischer, C., Meldau, S., Seebald, E., Oelmüller, R., and Baldwin, I.T. (2011). Lipase Activity in Insect Oral Secretions Mediates Defense Responses in Arabidopsis. Plant Physiology **156,** 1520-1534.

Schittko, U., Preston, C.A., and Baldwin, I.T. (2000). Eating the evidence? Manduca sexta larvae can not disrupt specific jasmonate induction in Nicotiana attenuata by rapid consumption. Planta **210,** 343-346.

Schmelz, E.A., Engelberth, J., Alborn, H.T., Tumlinson, J.H., and Teal, P.E.A. (2009). Phytohormone-based activity mapping of insect herbivore-produced elicitors. Proceedings of the National Academy of Sciences **106,** 653-657.

Schmelz, E.A., Carroll, M.J., LeClere, S., Phipps, S.M., Meredith, J., Chourey, P.S., Alborn, H.T., and Teal, P.E. (2006). Fragments of ATP synthase mediate plant perception of insect attack. Proc Natl Acad Sci U S A **103,** 8894-8899.

Schweighofer, A., Kazanaviciute, V., Scheikl, E., Teige, M., Doczi, R., Hirt, H., Schwanninger, M., Kant, M., Schuurink, R., and Mauch, F. (2007). The PP2C-Type Phosphatase AP2C1, Which Negatively Regulates MPK4 and MPK6, Modulates Innate Immunity, Jasmonic Acid, and Ethylene Levels in Arabidopsis. Plant Cell **19,** 2213-2224.

Seo, H.S., Song, J.T., Cheong, J.J., Lee, Y.H., Lee, Y.W., Hwang, I., Lee, J.S., and Choi, Y.D. (2001). Jasmonic acid carboxyl methyltransferase: A key enzyme for jasmonate-regulated plant responses. Proceedings of the National Academy of Sciences of the United States of America **98,** 4788-4793.

Seo, S., Sano, H., and Ohashi, Y. (1999). Jasmonate-based wound signal transduction requires activation of WIPK, a tobacco mitogen-activated protein kinase. Plant Cell **11,** 289-298.

Seo, S., Katou, S., Seto, H., Gomi, K., and Ohashi, Y. (2007). The mitogen-activated protein kinases WIPK and SIPK regulate the levels of jasmonic and salicylic acids in wounded tobacco plants. Plant Journal **49,** 899-909.

Spoel, S.H., Koornneef, A., Claessens, S., Korzelius, J.P., Van Pelt, J.A., Mueller, M.J., Buchala, A.J., Metraux, J.P., Brown, R., and Kazan, K. (2003). NPR1 Modulates Cross-Talk between Salicylate-and Jasmonate-Dependent Defense Pathways through a Novel Function in the Cytosol. The Plant Cell **15,** 760.

Stelmach, B., Müller, A., Hennig, P., Gebhardt, S., Schubert-Zsilavecz, M., and Weiler, E. (2001). A novel class of oxylipins, sn1-O-(12-oxophytodienoyl)-sn2-O-(hexadecatrienoyl)-monogalactosyl Diglyceride, from Arabidopsis thaliana. J Biol Chem **276,** 12832-12838.

Steppuhn, A., and Baldwin, I.T. (2007). Resistance management in a native plant: nicotine prevents herbivores from compensating for plant protease inhibitors. Ecology Letters **10,** 499-511.

Steppuhn, A., Gase, K., Krock, B., Halitschke, R., and Baldwin, I.T. (2004). Nicotine's defensive function in nature. Plos Biology **2,** 1074-1080.

Stitz, M., Baldwin, I. T., Gaquerel, E. (2011). Diverting the flux of the JA pathway in Nicotiana attenuata compromises the plant's defense metabolism and fitness in nature and glasshouse. PLoS One, **6,** e25925.

Stork, W., Diezel, C., Halitschke, R., Galis, I., and Baldwin, I.T. (2009). An ecological analysis of the herbivory-elicited JA burst and its metabolism: plant memory processes and predictions of the moving target model. J Chem Ecol **4,** e4697.

Suza, W.P., and Staswick, P.E. (2008). The role of JAR1 in Jasmonoyl-L: -isoleucine production during Arabidopsis wound response. Planta **227,** 1221-1232.

Takabatake, R., Seo, S., Ito, N., Gotoh, Y., Mitsuhara, I., and Ohashi, Y. (2006). Involvement of wound-induced receptor-like protein kinase in wound signal transduction in tobacco plants. Plant Journal **47,** 249-257.

Takahashi, F., Yoshida, R., Ichimura, K., Mizoguchi, T., Seo, S., Yonezawa, M., Maruyama, K., Yamaguchi-Shinozaki, K., and Shinozaki, K. (2007). The mitogen-activated protein kinase cascade MKK3-MPK6 is an important part of the jasmonate signal transduction pathway in Arabidopsis. Plant Cell **19,** 805-818.

Taki, N., Sasaki-Sekimoto, Y., Obayashi, T., Kikuta, A., Kobayashi, K., Ainai, T., Yagi, K., Sakurai, N., Suzuki, H., Masuda, T., Takamiya, K., Shibata, D., Kobayashi, Y., and Ohta, H. (2005). 12-oxo-phytodienoic acid triggers expression of a distinct set of genes and plays a role in wound-induced gene expression in Arabidopsis. Plant Physiol **139,** 1268-1283.

Thines, B., Katsir, L., Melotto, M., Niu, Y., Mandaokar, A., Liu, G.H., Nomura, K., He, S.Y., Howe, G.A., and Browse, J. (2007). JAZ repressor proteins are targets of the SCFCO11 complex during jasmonate signalling. Nature **448,** 661-U662.

Truitt, C., Wei, H.-X., and Pare, P. (2004). A Plasma Membrane Protein from Zea mays Binds with the Herbivore Elicitor Volicitin. Plant Cell **16,** 523-532.

Turner, J.G., Ellis, C., and Devoto, A. (2002). The jasmonate signal pathway. Plant Cell **14,** S153-S164.

Uchida, K. (2003). 4-Hydroxy-2-nonenal: a product and mediator of oxidative stress. J Chem Ecol **42,** 318-343.

Ussuf, K.K., Laxmi, N.H., and Mitra, R. (2001). Proteinase inhibitors: Plant-derived genes of insecticidal protein for developing insect-resistant transgenic plants. Current Science **80,** 847-853.

Valianpour, F., Selhorst, J.J.M., van Lint, L.E.M., van Gennip, A.H., Wanders, R.J.A., and Kemp, S. (2003). Analysis of very long-chain fatty acids using electrospray ionization mass spectrometry. Molecular Genetics and Metabolism **79,** 189-196.

Vick, B.A., and Zimmerman, D.C. (1976). Lipoxygenase and hydroperoxide lyase in germinating watermelon seedlings. Plant Physiol **57,** 780-788.

Vick, B.A., and Zimmerman, D.C. (1983). The biosynthesis of jasmonic acid: a physiological role for plant lipoxygenase. Biochem Biophys Res Commun **111,** 470-477.

Voelckel, C., and Baldwin, I.T. (2004). Herbivore-induced plant vaccination. Part II. Array-studies reveal the transience of herbivore-specific transcriptional imprints and a distinct imprint from stress combinations. Plant Journal **38,** 650-663.

von Dahl, C., Winz, R., Halitschke, R., Kühnemann, F., Gase, K., and Baldwin, I. (2007). Tuning the herbivore-induced ethylene burst: the role of transcript accumulation and ethylene perception in Nicotiana attenuata. Plant Journal **51,** 293-307.

Wang, L., Halitschke, R., Kang, J.H., Berg, A., Harnisch, F., and Baldwin, I.T. (2007). Independently silencing two JAR family members impairs levels of trypsin proteinase inhibitors but not nicotine. Planta **226,** 159-167.

Weber H, Vick BA, Farmer EE (1997) Dinor-oxo-phytodienoic acid: a new hexadecanoid signal in the jasmonate family. Proc Natl Acad Sci USA **94:** 10473-10478

Wittstock, U., and Gershenzon, J. (2002). Constitutive plant toxins and their role in defense against herbivores and pathogens. Curr. Opin. Plant Biol. **5,** 300 - 307.

Wu, J.Q., Hettenhausen, C., Meldau, S., and Baldwin, I.T. (2007). Herbivory rapidly activates MAPK signaling in attacked and unattacked leaf regions but not between leaves of Nicotiana attenuata. Plant Cell **19,** 1096-1122.

Zimmerman, D.C., and Coudron, C.A. (1979). Identification of Traumatin, a Wound Hormone, as 12-Oxo-trans-10-dodecenoic Acid. Plant Physiol **63,** 536-541.

Manuscript overview

Manuscript I

Rapid modification of the insect elicitor *N*-linolenoyl-glutamate via a lipoxygenase mediated mechanism on *Nicotiana attenuata* leaves

Arjen van Doorn, Mario Kallenbach, Alejandro A. Borquez, Ian T. Baldwin and Gustavo

Bonaventure

In manuscript I, we describe the metabolism of the insect elicitor *N*-linolenoyl-glutamate (18:3-Glu) on the wounded leaf surface, and show that 18:3-Glu is metabolized into at least three different 18:3-Glu derivatives. One of these derivatives was shown to be active as an elicitor of jasmonic acid and monoterpenes.

A. van Doorn and G. Bonaventure planned and performed the experiments, analyzed data and wrote the manuscript. A. A. Borquez performed experiments and M. Kallenbach interpreted the MS/MS spectra and was involved in structural elucidation. I. T. Baldwin planed the experiments and corrected the manuscript.

Manuscript II

A rapid and sensitive method for the simultaneous analysis of aliphatic and polar molecules containing free carboxyl groups in plant extracts by LC-MS/MS

Mario Kallenbach, Ian T. Baldwin and Gustavo Bonaventure

In manuscript II, we describe a method for the simultaneous detection and quantification of free aliphatic molecules and small polar molecules containing free carboxyl groups by direct derivatization of leaf extracts with Picolinyl reagent followed by LC-MS/MS analysis. The method presented was used to detect 16 compounds in leaf extracts of *N. attenuata* plants.

M. Kallenbach carried out the experiments, analyzed the data and drafted the manuscript. I. T. Baldwin participated in the design and coordination of the study and helped to draft the manuscript. G. Bonaventure conceived of the study, participated in its design and coordination and drafted the manuscript.

Manuscript III

Nicotiana attenuata SIPK, WIPK, NPR1, and fatty acid-amino acid conjugates participate in the induction of jasmonic acid biosynthesis by affecting early enzymatic steps in the pathway

Mario Kallenbach, Fiammetta Alagna, Ian T. Baldwin, and Gustavo Bonaventure

Manuscript III describes the early processes regulating the activation of JA biosynthesis by wounding and fatty acid- amino acid conjugate (FAC) elicitation in *N. attenuata* leaves. We show that NaSIPK, NaWIPK, NaNPR1, and FACs contribute to the activation of *de novo* JA biosynthesis by affecting diverse early enzymatic steps in this pathway and identified a plastidial glycerolipase A1 type I family protein (GLA1) essential for JA biosynthesis.

M. Kallenbach and F. Alagna designed and performed the experiments, analyzed the data and drafted the manuscript. I.T. Baldwin was involved in experimental design and helped to draft the manuscript. G. Bonaventure conceived of the study, designed and performed experiments and drafted the manuscript.

Manuscript IV

***Empoasca* leafhoppers attack the wild tobacco *Nicotiana attenuata* in a jasmonate-dependent manner and identify jasmonate mutants in nature**

Mario Kallenbach, Gustavo Bonaventure, Paola Gilardoni, Antje Wissgott, and Ian T.

Baldwin

Submitted to *PNAS*

In Manuscript IV, we studied host choice mechanisms of *Empoasca* leafhoppers using *Nicotiana attenuata* plants. These plants are attacked by the leafhoppers when plants are rendered deficient (by transformation) in JA accumulation and perception but not in the plant's main JA-elicited defenses in both field and glasshouse experiments. We also report that this JA-dependent mechanism of host selection also occurs in native *N. attenuata* populations.

M. Kallenbach carried out the experiments, analyzed the data and drafted the manuscript. G. Bonaventure participated in the design and coordination of the study and helped to draft the manuscript. P. Gilardoni carried out experiments and helped to draft the manuscript. A. Wissgott performed PCR analyses and helped to draft the manuscript. I.T. Baldwin carried out field experiments, conceived of the study and its design and coordinated and drafted the manuscript.

Manuscript V

C$_{12}$ derivatives of the hydroperoxide lyase pathway are produced by product recycling through lipoxygenase-2 in *Nicotiana attenuata* leaves

Mario Kallenbach, Paola A. Gilardoni, Silke Allmann, Ian T. Baldwin and Gustavo

Bonaventure

In Manuscript V, we studied the fluxes and metabolism of C$_{12}$ derivatives of the HPL pathway in *Nicotiana attenuata* plants after wounding and fatty acid- amino acid conjugate (FAC) elicitation. The quantification of these metabolites was achieved by the development of a new LC-MS∕MS method. We reveal new aspects of the biogenesis of C$_{12}$ derivatives of the HPL pathway and rise new hypotheses for possible roles of these metabolites in the regulation of stress responses.

M. Kallenbach carried out the experiments, analyzed the data and drafted the manuscript. P. Gilardoni carried out experiments. S. Allmann provided the data for the characterization of ir-*hpl* plants. I.T. Baldwin participated in the design and coordination of the study and helped to draft the manuscript. G. Bonaventure conceived of the study, participated in its design and coordination and drafted the manuscript.

BMC
Plant Biology

Open Access

Rapid modification of the insect elicitor N-linolenoyl-glutamate via a lipoxygenase-mediated mechanism on *Nicotiana attenuata* leaves

Arjen VanDoorn, Mario Kallenbach, Alejandro A Borquez, Ian T Baldwin, Gustavo Bonaventure[*]

Abstract

Background: Some plants distinguish mechanical wounding from herbivore attack by recognizing specific constituents of larval oral secretions (OS) which are introduced into plant wounds during feeding. Fatty acid-amino acid conjugates (FACs) are major constituents of *Manduca sexta* OS and strong elicitors of herbivore-induced defense responses in *Nicotiana attenuata* plants.

Results: The metabolism of one of the major FACs in *M. sexta* OS, *N*-linolenoyl-glutamic acid (18:3-Glu), was analyzed on *N. attenuata* wounded leaf surfaces. Between 50 to 70% of the 18:3-Glu in the OS or of synthetic 18:3-Glu were metabolized within 30 seconds of application to leaf wounds. This heat-labile process did not result in free α-linolenic acid (18:3) and glutamate but in the biogenesis of metabolites both more and less polar than 18:3-Glu. Identification of the major modified forms of this FAC showed that they corresponded to 13-hydroxy-18:3-Glu, 13-hydroperoxy-18:3-Glu and 13-oxo-13:2-Glu. The formation of these metabolites occurred on the wounded leaf surface and it was dependent on lipoxygenase (LOX) activity; plants silenced in the expression of *NaLOX2* and *NaLOX3* genes showed more than 50% reduced rates of 18:3-Glu conversion and accumulated smaller amounts of the oxygenated derivatives compared to wild-type plants. Similar to 18:3-Glu, 13-oxo-13:2-Glu activated the enhanced accumulation of jasmonic acid (JA) in *N. attenuata* leaves whereas 13-hydroxy-18:3-Glu did not. Moreover, compared to 18:3-Glu elicitation, 13-oxo-13:2-Glu induced the differential emission of two monoterpene volatiles (β-pinene and an unidentified monoterpene) in ir*lox2* plants.

Conclusions: The metabolism of one of the major elicitors of herbivore-specific responses in *N. attenuata* plants, 18:3-Glu, results in the formation of oxidized forms of this FAC by a LOX-dependent mechanism. One of these derivatives, 13-oxo-13:2-Glu, is an active elicitor of JA biosynthesis and differential monoterpene emission.

Background

Interactions between plants and invertebrate herbivores have a long history; the first evidence of plant damage by arthropods dates back 400 m years ago [1]. This timeframe has allowed plants and insects to develop sophisticated mechanisms to recognize one another and respond accordingly. Plants activate a plethora of defense responses upon insect feeding, and one way of decreasing the herbivore load is to emit volatiles that attract predators or parasitoids of the herbivore [2,3]. These herbivore-induced plant volatiles (HIPVs) consist of different compounds, for example C_6 green leaf volatiles (GLVs) and isoprenoids such as C_{10} monoterpenes. The plant's ability to produce different volatile signals when attacked by herbivores is essential for the function of these molecules as indirect defenses. Depending on the plant species, the recognition of insect feeding may be primarily mediated by mechanisms such as the perception of components in insect oral secretions (OS) [4-6], multiple sequential wounding events that mimic larvae feeding [7], or a combination of both.

* Correspondence: gbonaventure@ice.mpg.de
Department of Molecular Ecology, Max Planck Institute for Chemical Ecology, Hans Knöll Strasse 8, D-07745 Jena, Germany
Full list of author information is available at the end of the article

Recently, the discovery of digested fragments of a plant ATP synthase, named inceptins, as elicitors of insect responses added a plant 'self-recognition' mechanism to the repertoire of mechanism for insect's feeding perception [8,9]. Among the insect elicitors of plant defense responses, the first to be isolated was the fatty-acid amino-acid conjugate (FAC) volicitin (17-OH-18:3-Gln), which was found in the OS of *Spodoptora exigua* (*S. exigua*) larvae feeding on maize (*Zea mays*) plants and shown to induce a volatile blend different from that induced by wounding alone [6]. Glucose oxidase was first identified from the corn earworm, *Helicoverpa zea;* [10] and it has been demonstrated to suppress the plant's defense response [11] and activate the salicylic acid (SA) pathway [12]. Inceptins were found in the OS of *Spodoptora frudgiperda* larvae feeding on cowpea (*Vigna unguiculata*) and have the capacity to induce the differential production of jasmonic acid (JA), SA and volatiles in cowpea plants [9]. More recently, sulfur-containing compounds, named caeliferins, were isolated from grasshopper OS (*Schistocerca americana*) and were able to induce volatile production in maize plants [13]. Finally, in a recent study, different elicitors were applied on a variety of plant species, and phytohormones and volatile production were monitored. The results indicated that elicitation by different insect-derived components is a plant-species specific process [5].

M. sexta's main elicitors to induce insect specific defense responses in *Nicotiana attenuata* plants are FACs, which are composed predominantly of linoleic acid (18:2) or linolenic acid (18:3) conjugated to Glu or Gln [14]. When applied to wounded *N. attenuata* leaves, synthetic FACs induce the differential production of jasmonic acid (JA) and ethylene [14,15], large scale transcriptomic and proteomic changes [4,16], and the release of HIPVs [17]. Moreover, when removed from *M. sexta* OS, the remaining FAC-free OS fraction loses its capacity to elicit insect specific responses in *N. attenuata* [4,16,17] which can be recovered after reconstitution of the FAC-free OS fraction with synthetic FACs [4]. The long-standing question of why a caterpillar would produce these potent elicitors was addressed in a recent study demonstrating the essential role of Gln containing FACs in nitrogen assimilation by *Spodoptora litura* larvae [18].

In contrast to elicitors derived from plant pathogens, insect elicitor perception and mode of action is poorly understood. It is known that in maize, volicitin binds to a membrane-associated protein suggesting a ligand-receptor interaction [19]. Additional proposed mechanisms for FAC elicitation include their capacity to increase ion permeability in membrane bilayers [20]. It has been previously demonstrated that volicitin can be transferred from the caterpillar OS into the wound surfaces of maize leaves [21] and although the transferred

amounts may be low [22], they seem sufficient to elicit specific responses against insect herbivores [23].
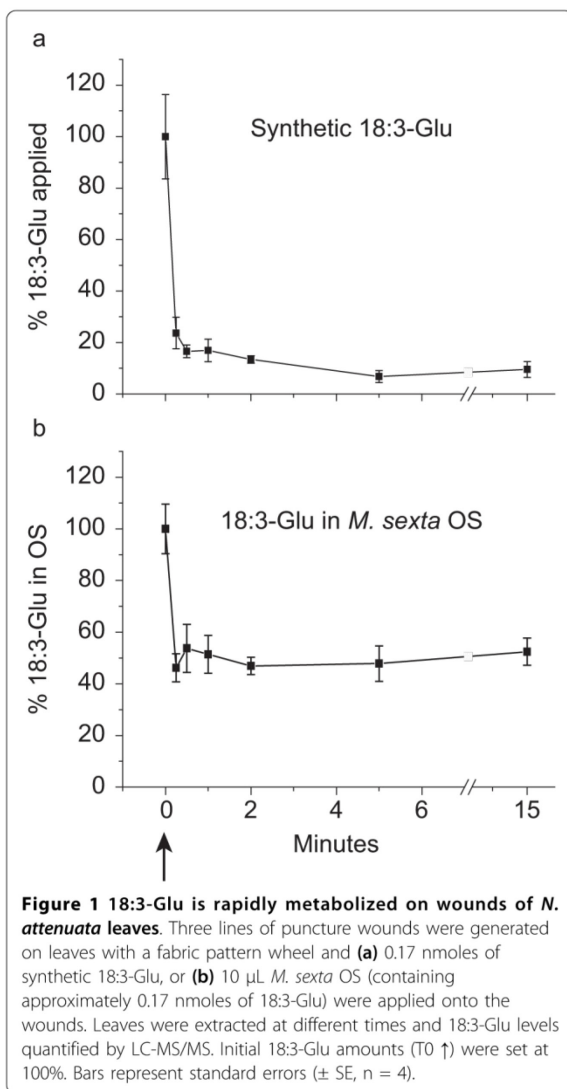
To understand the metabolic fate of FACs in plants and to gain novel insights into their mode of action, we investigated the metabolism of one of the major FACs in *M. sexta* OS, 18:3-Glu, on *N. attenuata* leaves. We studied the consequences of its metabolism on two processes associated to herbivory, the regulation of JA biosynthesis and terpenoid volatile emission.

Results
N-linolenoyl-glutamate is rapidly metabolized on wounded *N. attenuata* leaf surfaces

To investigate the turnover rate of 18:3-Glu on wounded *N. attenuata* leaves, 0.17 nmoles of synthetic 18:3-Glu, the amount naturally occurring in 10 μL *M. sexta* OS [14], were applied onto puncture wounds. Leaf material was harvested at different time points and 18:3-Glu levels were quantified by LC-MS/MS. The results showed that 18:3-Glu levels decreased rapidly, with 70% of the initial 18:3-Glu being metabolized within 30 seconds (Fig. 1a). To assess whether the endogenous 18:3-Glu in the insect's OS was also rapidly metabolized, 10 μL of *M. sexta* OS were applied on wounded leaf tissue and the 18:3-Glu levels were analyzed. The results again revealed a rapid decline of the 18:3-Glu levels in the OS with 50% of the initial 18:3-Glu metabolized within 30 seconds (Fig. 1b).

The metabolic fate of 18:3-Glu on the wounded leaf surface was investigated by applying both, synthetic radiolabeled [1-^{14}C]18:3-Glu and *M. sexta* OS spiked with [1-^{14}C]18:3-Glu, onto wounded leaf tissue for 2 min. After extraction and chromatographic separation of the ^{14}C-labeled metabolites by thin layer chromatography (TLC), the results showed that 18:3-Glu was not hydrolyzed into free 18:3 and Glu, but converted into different 18:3-Glu modified forms (Fig. 2a, Additional file 1). As evaluated by their Rfs, the major modified compounds were more polar than the unmodified 18:3-Glu, however, minor (less polar modified forms) were also detected (Additional file 1). Consistent with the rapid metabolism of unlabeled 18:3-Glu, radiolabeled 18:3-Glu derivatives appeared within the first minutes upon contact with wounded leaf tissue (Additional file 1). The ^{14}C-labeled metabolites were also separated and quantified by reverse phase (RP) radio-HPLC, which detected three major peaks with retention times consistent with an increased polarity compared to 18:3-Glu (Fig. 2a and 2b). The total radioactivity recovered after extraction was ca. 90% of the initial radioactivity applied onto the leaf surface, and the peak areas corresponding to metabolites 1, 2, 3 and to the unmodified 18:3-Glu (Fig. 2a) accounted for ca. 8, 15, 35 and 30% of the recovered radioactivity, respectively. These results were

Figure 1 18:3-Glu is rapidly metabolized on wounds of *N. attenuata* leaves. Three lines of puncture wounds were generated on leaves with a fabric pattern wheel and **(a)** 0.17 nmoles of synthetic 18:3-Glu, or **(b)** 10 µL *M. sexta* OS (containing approximately 0.17 nmoles of 18:3-Glu) were applied onto the wounds. Leaves were extracted at different times and 18:3-Glu levels quantified by LC-MS/MS. Initial 18:3-Glu amounts (T0 ↑) were set at 100%. Bars represent standard errors (± SE, n = 4).

Figure 2 Radio-HPLC chromatograms of wounded *N. attenuata* leaves treated with [14]C-18:3-Glu. (a) Leaves of rosette stage *N. attenuata* plants were wounded with a pattern wheel and 0.1 µCi of [1-^{14}C]18:3-Glu were immediately applied onto leaf wounds. The damaged tissue was harvested immediately (T0) or 2 min after the treatment. After extraction, the radiolabeled metabolites were separated by RP-radio-HPLC. The numbers (1 to 3) indicate the different fractions collected for further analysis. CPM: counts per minute. **(b)** *M. sexta* OS was spiked with 0.1 µCi [14]C 18:3-Glu, applied onto wounded leaf tissue, extracted after different time points and separated by TLC (W+OS). Plates were exposed for 24 h to ^{14}C-sensitive screens. Time 0: [14]C 18:3-Glu was applied onto wounded leaves and immediately extracted. W+: [14]C-18:3-Glu was applied onto wounded leaves and extracted after 2 min. 18:3-Glu[m1] and 18:3-Glu[m2] indicate different modified forms of 18:3-Glu.

consistent with the rate of 18:3-Glu metabolism shown in Fig. 1 and indicated that the metabolites corresponding to peaks 1, 2 and 3 in Fig. 2a were the major metabolites produced.

Isolation and chemical characterization of 18:3-Glu derivatives

For the purification of the three major polar 18:3-Glu derivatives, a leaf extract derived from wounded 18:3-Glu-treated *N. attenuata* leaves was fractionated by HPLC as described in Materials and Methods. Based on the retention times of the radiolabeled forms of 18:3-Glu, three HPLC fractions were collected and analyzed by LC-ESI-ToF to identify candidate ions corresponding to modified forms of 18:3-Glu. After mass/charge based
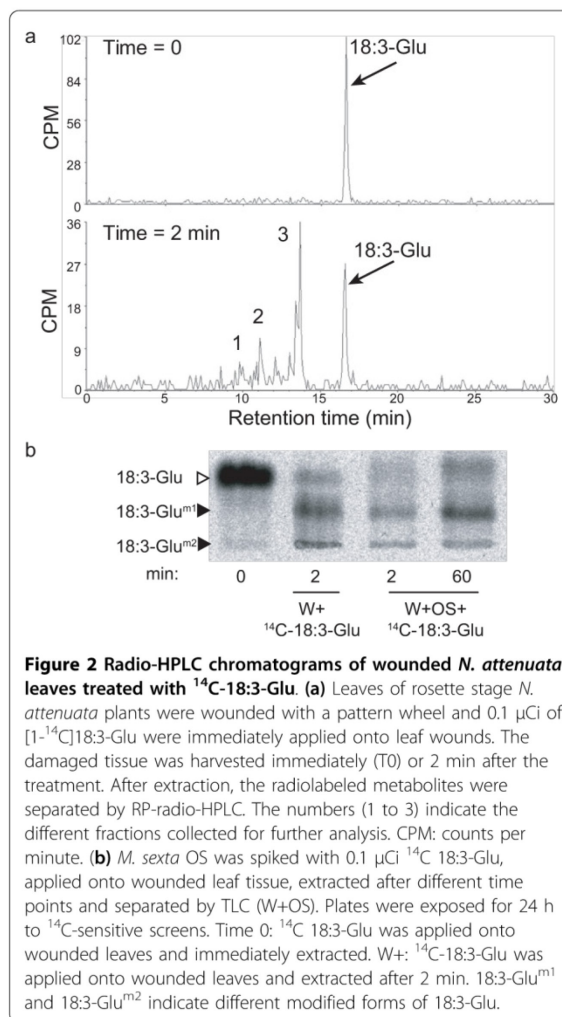
selection (600 >m/z > 200) and retention times, three compounds corresponding to the major ions m/z 352.1779, 422.2549 and 438.2550 in fractions 1, 2 and 3 (Fig. 2a), respectively, were selected and further purified by preparative TLC (see Material and Methods). These compounds were used for all subsequent analyses. To confirm that these compounds were derivatives of 18:3-Glu, they were directly injected into a triple-quad ESI-MS/MS system. After fragmentation of their molecular ions by collision induced dissociation (CID), all compounds released an intense ion with m/z 128, a specific ion generated from the rearrangement of the Glu moiety [24]. Additionally, fragmentation of the ions with m/z 422.3 and 438.3 using increasing fragmentation energies clearly showed an energy-dependent neutral loss of water from both ions. However, the ion with

m/z 438.3 lost water already with a fragmentation energy of 10V while the ion with m/z 422.3 with 15.5V, suggesting the presence of a more labile oxygenated functional group in the ion with m/z 438.3.
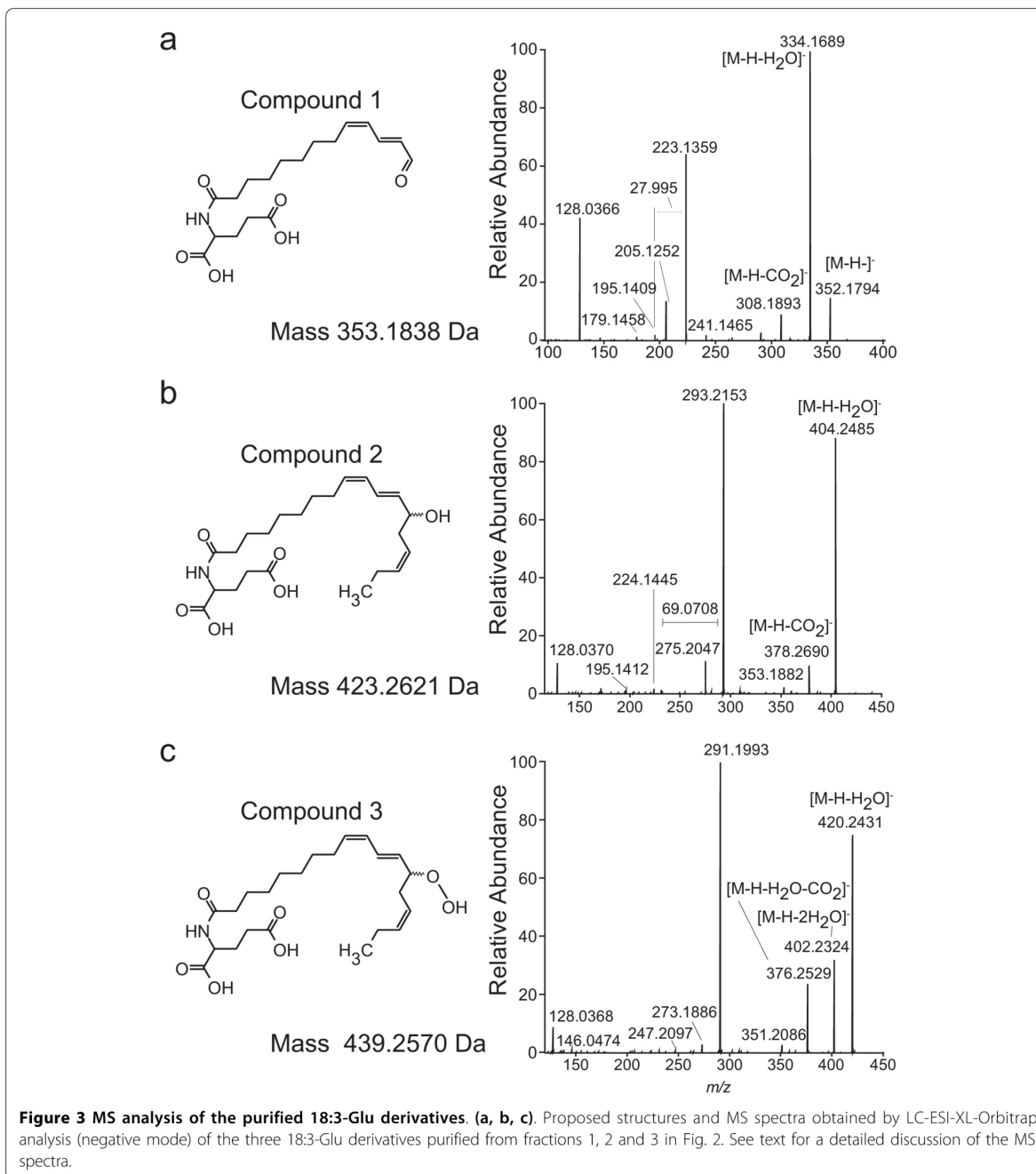
For structure elucidation, MS/MS was performed using an LC-ESI-XL-orbitrap. Consistent with the triplequad ESI-MS/MS analysis described above, all components released an intense ion with m/z 128.0368 [24]. For the compound purified from fraction 1 (Fig. 3a), an intense ion with m/z 223.1359 was released after fragmentation. This ion was generated from the acyl chain of the modified 18:3-Glu including the re-arrangement described in [24]. From this acyl fragment, a sub-fragment of m/z 195.1409 was released, giving a difference of 27.995 Da, which was consistent with the release of CO from the ω-position (Fig. 3a). The spectrum was consistent with compound 1 being 13-oxo-trideca-9,11-dienoyl-Glu. (13-oxo-13:2-Glu). For the compound purified from fraction 2 (Fig. 3b), an intense ion with m/z 404.2485 was detected and corresponded to the neutral loss of water from the molecular ion (m/z 422.2549), consistent with the triplequad ESI-MS/MS analysis described above. A second intense ion with m/z 293.2153 originated from the acyl chain of the modified 18:3-Glu including the re-arrangement described in [24] and the addition of a hydroxyl group (Fig. 3b). This fragment showed a subsequent neutral loss of 69.0708 Da giving m/z 224.1445, indicating the loss of C_5H_9 (calculated mass 69.0705 Da) from the end of the acyl chain (Fig. 3b) and the position of the hydroxyl group at C_{13} of the 18:3 moiety. Further evidence for the position of the hydroxyl group was the loss of 98.0739 from the m/z 293.2147 to give m/z 195.1408, corresponding to a loss of $C_6H_{10}O$ (calculated mass 98.0732 Da). The spectrum was consistent with compound 2 being 13-OH-octodeca-9,11,15-trienoyl-Glu (13-OH-18:3-Glu). For the compound purified from fraction 3 (Fig. 3c), an intense ion with m/z 420.2431 was detected and corresponded to the neutral loss of water from the molecular ion (m/z 438.2550), again consistent with the triplequad ESI-MS/MS analysis described above. A fragment with m/z 291.1996, generated from the acyl chain of the modified 18:3-Glu and including the re-arrangement described in [24] was consistent with the previous loss of water from a hydroperoxy group. Moreover, a fragment ion with m/z 352.1799 was also generated, which was identical to the molecular ion of 13-oxo-13:2-Glu and suggested the generation of this compound from a 13-hydroperoxydated precursor in the ion source. The proposed structure for fraction 3 was 13-OOH-octodeca-9,11,15-trienoyl-Glu (13-OOH-18:3-Glu).

Kinetic of formation of 18:3-Glu oxidized forms in wounded *N. attenuata* leaves

The formation of 18:3-Glu-modified forms on wounded *N. attenuata* leaves was analyzed after different times. Synthetic 18:3-Glu (0.17 nmoles) were applied on puncture wounds and after extraction samples were analyzed by LC-MS/MS and the results are presented in Fig. 4. Because ionization efficiencies vary substantially between compounds, the amounts of the different compounds are presented as normalized peak areas. Consistent with the rapid kinetic of 18:3-Glu metabolism (Fig. 1 and 2), the oxidized forms of 18:3-Glu were generated rapidly (Fig. 4). All three compounds, 13-OH-18:3-Glu, 13-OOH-18:3-Glu and 13-oxo-13:2-Glu started to accumulate within 15 seconds. 13-OH-18:3-Glu was the most abundant derivative and peaked at 15 seconds, while 13-OOH-18:3-Glu and 13-oxo-13:2-Glu showed a slower kinetic of accumulation and their relative levels were lower (Fig. 4). The relative levels of these oxygenated derivatives detected by LC-MS/MS (2 > 1 > 3; Fig. 4) differed from those detected by radio-HPLC (3 > 2 > 1; Fig. 2b) and, as mentioned above, these differences most likely reflected variations in ionization efficiencies between derivatives. The detection of 13-OH-18:3-Glu at time zero indicated that conversion of 18:3-Glu already occurred after a few seconds of its contact with wounded tissue (the time required to harvest the leaf after application of 18:3-Glu, ~3-5 seconds).

Formation of 13-oxo-18:3-Glu occurs on the leaf surface

It has been reported that formation of 13-oxo-tridecadienoic acid (13-oxo-13:2) from 13-OOH-linolenic acid (13-OOH-18:3) could occur by both enzymatic [25] and non-enzymatic mechanisms (thermal decomposition; [25,26]). To rule out the possibility that 13-oxo-13:2-Glu was generated by thermal decomposition during sample preparation or analysis (for example during solvent evaporation or electrospray ionization), wounded leaves supplemented with synthetic 18:3-Glu were extracted with and without the addition of 1% butylhydroxytoluene (BHT) as a radical scavenger and of 10 mg/ml of trimethylphosphite (TMP) as a reducing agent of the hydroperoxy groups [27] in the solvent. Samples were taken after 1 and 5 min of the treatment and extractions and solvent evaporation were conducted always on ice to prevent sample heating. After analysis by LC-MS/MS, the results showed that formation of 13-oxo-13:2-Glu was independent of the presence of BHT and TMP in the extraction solvents (Additional file 2) and demonstrated that its biogenesis took place on the leaf surface.

Figure 3 MS analysis of the purified 18:3-Glu derivatives. **(a, b, c)**. Proposed structures and MS spectra obtained by LC-ESI-XL-Orbitrap analysis (negative mode) of the three 18:3-Glu derivatives purified from fractions 1, 2 and 3 in Fig. 2. See text for a detailed discussion of the MS spectra.

Oxidation of 18:3-Glu on wounded *N. attenuata* leaves depends on lipoxygenase activity

To test if the metabolism of 18:3-Glu was enzymatic, steamed wounded leaves were supplemented with 18:3-Glu and its turnover rate and modifications determined by LC-MS/MS. In this experiment, control leaves (18:3-Glu control) were freeze killed before application of 18:3-Glu onto their frozen surface and 18:3-Glu levels represent the initial amounts applied. Consistent with the abovementioned results, more than 90% of the applied 18:3-Glu was metabolized after 5 min of the treatment in wounded leaves (Fig. 5a). In contrast, after steam treatment of leaves to inactivate heat-labile processes, the levels of 18:3-Glu remained higher compared

Figure 4 Accumulation of 18:3-Glu derivatives on wounded WT *N. attenuata* leaves. WT plants were wounded with a pattern wheel and 0.17 nmoles of 18:3-Glu were applied to the wounds and samples harvested after different times. After extraction, samples were analyzed by LC-MS/MS (n = 3, bars denote ± SE). Numbers between brackets correspond to compounds 1, 2 and 3 in Fig. 2 and 3.
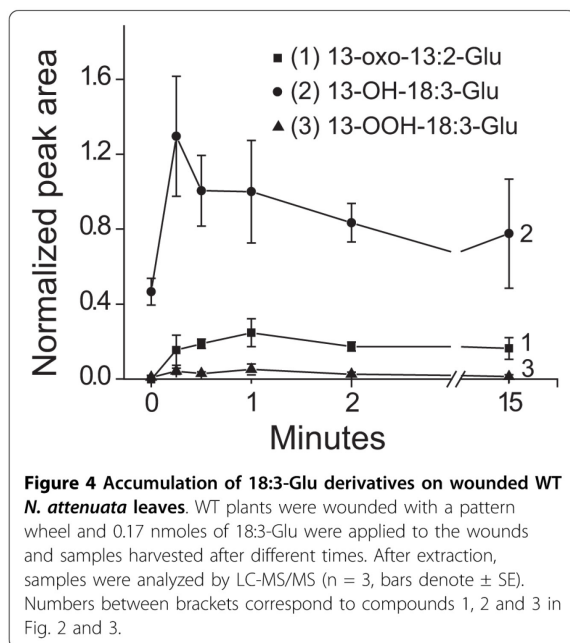
to wounded leaves and statistically similar to control levels (Fig. 5a). Consistently, the formation of 18:3-Glu derivatives was not detected in steamed leaves (data not shown). In the absence of wounding, the levels of 18:3-Glu were also not reduced compared to the control treatment (Fig. 5a). Together, these results indicated that the metabolism of 18:3-Glu was primarily enzymatic and that it required mechanical damage of the leaf.

Based on the identification of a 13-hydroperoxide derivative, we hypothesized that lipoxygenase activity was responsible for hydroperoxidation of 18:3-Glu. *N. attenuata* leaves express two major plastidial lipoxygenases, lipoxygenase 2 (NaLOX2) and lipoxygenase 3 (NaLOX3), involved in the supply of hydroperoxy-fatty acids for green leaf volatiles and JA biosynthesis, respectively [28,29]. Hence, we tested 18:3-Glu metabolism in *N. attenuata* plants silenced in the expression of either *NaLOX2* (ir*lox2*) or *NaLOX3* (ir*lox3*). The expression of *NaLOX2* and *NaLOX3* transcripts is reduced by 99% and 83% in ir*lox2* and ir*lox3* plants, respectively [29]. Importantly, the transcript levels of NaLOX3 are also reduced (by 94%) in ir*lox2* plants, most likely due to co-silencing [29]. In contrast, the transcript levels of NaLOX3 in ir*lox2* plants were similar to WT [29]. The accumulation of 18:3-Glu derivatives after 18:3-Glu treatment was first analyzed in these plants (Fig. 5b). All genotypes were substantially reduced in their ability to produce 18:3-Glu derivatives with ir*lox2* plants showing the strongest reduction in

Figure 5 Analysis of 18:3-Glu metabolism in steamed leaves and in LOX deficient plants. **(a)** 18:3-Glu (0.17 nmoles) was applied to either wounded leaves, wounded-steamed leaves, or unwounded leaves. The 18:3-Glu blank sample denotes an unwounded leaf onto which 18:3-Glu was added after freeze killing the leaf. Leaves were extracted after 5 min of the treatments and 18:3-Glu levels were analyzed by LC-MS/MS. Statistical analysis was performed using a non-parametric Moses extreme test with Bonferroni correction, * indicates $P < 0.017$, N.S. denotes non-significant differences (n = 3, bars denote ± SE). **(b)** Leaves of ir*lox2* and ir*lox3* plants were wounded, 0.17 nmoles of 18:3-Glu were applied on the wounds, and the samples were harvested after 2 min. After extraction, 18:3-Glu derivatives were analyzed by LC-MS/MS (n = 3, bars denote ± SE). Different letters indicate significant differences (univariate *ANOVA* 13-oxo-13:2-Glu: $F_{3,3} = 85.4$ $P < 0.001$, 13-OH-18:3-Glu: $F_{3,3} = 25.1$ $P < 0.001$ 13-OH-18:3-Glu: $F_{3,3} = 136.1$ $P < 0.001$ followed by a Scheffé *post-hoc* test, $P < 0.05$). **(c)** Turnover of 18:3-Glu on WT and ir*lox2* plants. Leaves were wounded, 18:3-Glu (0.17 nmoles) were applied onto the wounds, and the samples were harvested after different times. 18:3-Glu levels were analyzed by LC-MS/MS. Initial 18:3-Glu amounts (T0) were set at 100% (n = 4, bars denote ± SE).

their accumulation. The rate of 18:3-Glu turnover was further analyzed in ir*lox2* plants and, consistent with the reduced accumulation of oxygenated forms of 18:3-Glu on wounded leaves of this genotype, the turn-over rate was significantly reduced compared to wild-type plants (Fig. 5c). After 5 min, 40% of the applied amounts of 18:3-Glu remained on the wounded leaf surface compared to 7% on WT (Fig. 5c).

13-oxo-13:2-Glu is an active elicitor

FAC elicitation of leaves in *N. attenuata* plants induces an enhanced production (2 to 3-fold) of JA compared to mechanical damage and this response was used as a parameter to test elicitation activity [5,14]. For this experiment synthetic 18:3-Glu and purified 13-oxo-13:2-Glu and 13-OH-18:3-Glu were applied onto wounds of *N. attenuata* leaves and JA levels were quantified after 60 min of the treatments. This time point corresponds to the peak of JA accumulation in *N. attenuata* leaves after FAC elicitation [30]. For this and subsequent elicitation experiments, the amounts of elicitors applied corresponded to either 0.17 nmoles of synthetic 18:3-Glu or the corresponding amounts of 13-oxo-13:2-Glu and 13-OH-18:3-Glu produced by wounded leaves after 2 min (as assessed by LC-MS/MS; see Materials and Methods). The instability of the purified 13-OOH-18:3-Glu precluded its analysis as an elicitor. 13-oxo-13:2-Glu induced JA production to similar levels as 18:3-Glu and ~2-fold over wounding whereas 13-OH-18:3-Glu did not enhance JA production compared to wounding (Fig. 6a). Quantification of JA levels at 60, 90 and 120 min after 18:3-Glu and 13-oxo-13:2-Glu elicitation showed that both elicitors enhanced JA accumulation to similar levels at these 3 time points in both WT and ir*lox2* (data not shown).

The emission of terpenoid volatiles in *N. attenuata* plants is influenced by application of FACs to the wounds [17]. To investigate if the metabolism of 18:3-Glu could qualitatively or quantitatively affect terpenoid volatile emission, WT and ir*lox2* plants were analyzed after wounding and application of either 18:3-Glu or 13-oxo-13:2-Glu. Terpenoid volatiles in *N. attenuata* are released in a diurnal cycle [17] and for this experiment volatiles were trapped after 24 h of the treatments for a period of 8 h. The results showed that two monoter-penes, β-pinene and a monoterpene of unidentified structure (see Additional file 3 for MS spectra) were differentially emitted in ir*lox2* plants when 13-oxo-13:2-Glu and 18:3-Glu elicitation treatments were compared (Fig. 6b). In contrast, emission of these two monoter-penes in WT plants was similar between treatments (Fig. 6c). *trans*-α-bergamotene and an additional sesqui-terpene did not show significant differences between the treatments (data not shown).
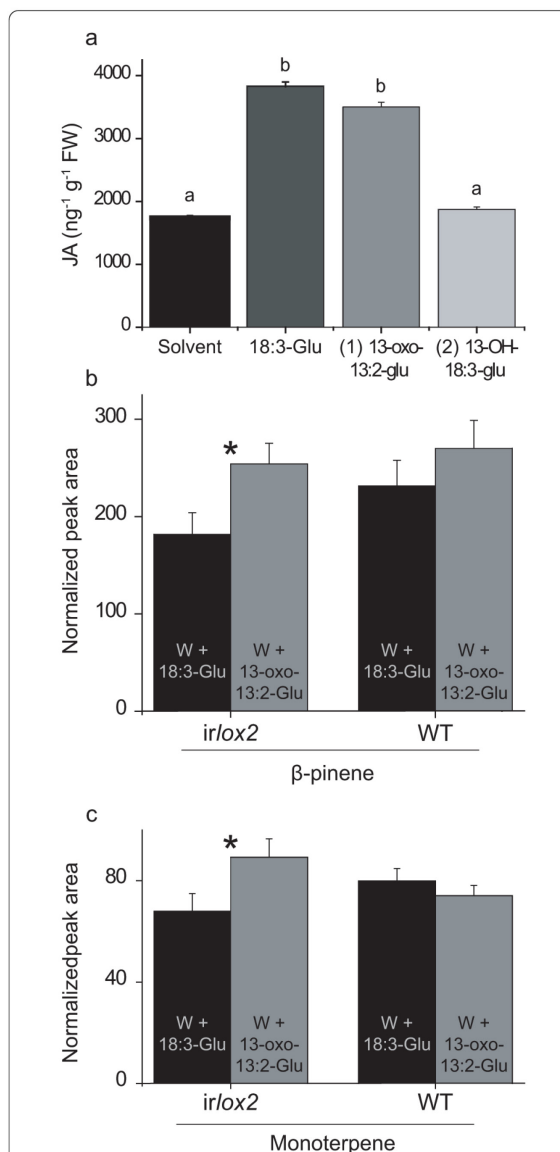

Figure 6 Analysis of JA and terpenoid volatiles in WT and ir*lox2* plants after elicitation. **(a)** WT plants were wounded and of the wounds immediately treated with either solvent alone, 18:3-Glu (0.17 nmoles), 13-oxo-18:3-Glu or 13-OH-18:3-Glu (see text for a description of the amounts used). Samples were taken after 60 min and JA quantified by LC-MS/MS (n = 3, bars denote ± SE). Different letters denote significant differences (univariate ANOVA $F_{3,3}$ = 17.9, $P < 0.001$ followed by a Scheffé *post-hoc* test, $P < 0.05$). **(b,c)** ir*lox2* and WT plants were wounded and treated with either 18:3-Glu (0.17 nmoles) or 13-oxo-13:2-Glu (see text for a description of the amounts used), the emitted volatiles were trapped for 8 h after 24 h of the treatment and analyzed by GCxGC-ToF. Injection of a β-pinene standard confirmed the structure of the first compound, while the second monoterpene remained unidentified. The MS spectra of the two compounds are shown in Additional file 3. Asterisks indicate significant difference ($P < 0.05$, Student's *t*-test).

Discussion

In this study, we demonstrated that one of the major elicitors present in the OS of *M. sexta* larvae, *N*-linolenoyl-glutamate (18:3-Glu), was rapidly oxidized by a LOX-dependent reaction upon contact with wounded leaf tissue; *N. attenuata* plants silenced in the expression of *NaLOX2* and *NaLOX3* (*irlox2* and *3*, respectively) were affected in their capacity to metabolize 18:3-Glu into its oxidized forms. This process occurred when either synthetic 18:3-Glu or OS were applied onto wounded leaves. Metabolism of 18:3-Glu was however slower when OS was applied, suggesting that the *M. sexta* OS may contain either inhibitors of the LOX-dependent reaction or that the FACs are less accessible to LOXs (e.g., by interacting with other OS components). The formation of the LOX product 13-OOH-18:3-Glu occurred within seconds and based on the metabolism of radioactive ^{14}C-18:3-Glu, we estimated that after 2 min of contact with wounded leaf tissue, 55 to 60% of the applied 18:3-Glu was metabolized by LOX activity. These results suggested that LOXs can rapidly utilize 18:3-Glu as a substrate and catalyze its 13-hydroperoxidation. ir*lox2* and ir*lox3* plants showed similar rates of 18:3-Glu metabolism (Fig. 5b), and due to the fact that ir*lox3* plants have also significantly reduced levels of NaLOX2 transcripts whereas ir*lox2* plants have WT levels of NaLOX3 transcripts [29], we conclude that most likely NaLOX2 is the major LOX isoform involved in 18:3-Glu metabolism. Without mechanical damage, 18:3-Glu was not metabolized in contact with leaf surfaces, suggesting that mechanical disruption of leaf cells releases LOX enzymes into the extracellular space where they come into rapid contact with 18:3-Glu. Consistently, heat treatment of the wounded leaves strongly reduced the metabolism of 18:3-Glu and prevented the accumulation of its LOX-dependent derivatives. Non-enzymatic mechanisms resulting in derivatives different from those produced by LOX activity (Supplemental file 1) were most likely responsible for the partial metabolism of 18:3-Glu after heat inactivation of the leaves (Fig. 5a).

In a previous study, beet armyworm caterpillars fed with radiolabeled plant material were allowed to feed on unlabeled maize plants, and the results showed that this FAC is transferred from the caterpillar's OS into the feeding site of the leaf [21]. In the same study, however, there is no indication of a plant-mediated conversion of volicitin, as no additional radioactive fractions could be recovered from leaf tissue after caterpillar feeding. These results may indicate that the presence of the hydroxyl group at the C_{17} position of the fatty-acid moiety of volicitin inhibits the lipoxygenase-mediated conversion of this insect elicitor.

Hydroperoxy fatty acids are substrates for a diverse set of enzymatic and non-enzymatic reactions in plant tissues [31]. Among the reactions involving 13-OOH-18:3 are the reduction of the hydroperoxy group into a hydroxyl group to form 13-OH-18:3 and the cleavage of the C_{13}-C_{14} bond to generate 13-oxo-C_{13} derivatives [25,26]. Consistent with these reactions we observed the formation of 13-oxo-13:2-Glu and 13-OH-18:3-Glu on the leaf surface of wounded *N. attenuata* plants. Similar to 13-OOH-18:3-Glu, the formation of these molecules was detected within seconds upon contact with wounded leaf tissue and based on the metabolism of radioactive ^{14}C-18:3-Glu, we estimated that together they accounted for approximately 20 to 25% of the initial amounts of 18:3-Glu applied (after 2 min of contact with wounded leaf tissue). Whether these two 13-OOH-18:3-Glu derivatives are produced via enzymatic or non-enzymatic mechanisms on the leaf surface is at present unknown. Formation of 13-oxo-13:2-Glu from 13-OOH-18:3-Glu requires the cleavage of the α-C_{13}-C_{14} bond and in soybean seeds an enzymatic activity that cleaved 13-OOH-18:3 into 13-oxo-trideca-9,11-tridecanoic acid and two isomeric pentenols has been described [25]. In animal cells, this reaction (reductive β-scission) has been proposed to be mediated by cytochrome P-450 enzymes [32]. Formation of 13-oxo-13:2 from 13-OOH-18:3 can also occur non-enzymatically by thermal decomposition [25,26], however, analysis of 18:3-Glu metabolism in the presence of a radical scavenger (BHT) and a reducing agent (TMP) [27] showed that this conversion took place on the leaf surface (Additional file 2). Whether this conversion occurs enzymatically or not in wounded leaves remains unknown. In the case of 13-OH-18:3-Glu, the reduction of the hydroperoxy group into a hydroxyl group is the most plausible mechanism and as mentioned above, the mechanism involved remains to be elucidated.

Elicitation of *N. attenuata* leaves with purified 13-oxo-13:2-Glu was sufficient to enhance JA production to levels similar to those induced by 18:3-Glu (Fig. 6a), indicating that this oxidized form of 18:3-Glu is active as an elicitor and that its relative activity is similar to that of unmodified 18:3-Glu in terms of JA induction. In contrast to 13-oxo-13:2-Glu, 13-OH-18:3-Glu was inactive in mediating an enhanced JA production, suggesting that some modifications could be important for the rapid inactivation of FACs and therefore for the control of the FAC-mediated elicitation stimulus. The activity of 13-oxo-13:2-Glu was also evidenced by the differential induction of two emitted monoterpenes (β-pinene and a monoterpene of unidentified structure) in ir*lox2* plants (Fig. 6b,c). In WT plants this difference disappeared, most likely because of a high 18:3-Glu conversion to 13-oxo-13:2-Glu. All together, our results suggest a degree

of specificity in the responses elicited by modified forms of 18:3-Glu.

Conclusions

The results presented showed that upon contact with wounded *N. attenuata* leaves, the FAC elicitor 18:3-Glu is rapidly metabolized by LOX activity to form additional active and inactive elicitors. In particular, 13-oxo-13:2-Glu was active as an elicitor of an enhanced JA biosynthesis and of the differential emission of two monoterpenes. Although speculative at this point, the results presented open the possibility that the metabolism of 18:3-Glu may play a role in the tuning of some plant responses to insects. Future investigations will be focus on the unraveling of these potential responses.

Methods
Plant growth and treatments

Seeds of the 22th generation of an inbred line of *Nicotiana attenuata* plants were used as the wild-type (WT) genotype in all experiments. Plants were grown at 26-28°C under 16 h of light. In all experiments, slightly elongated *N. attenuata* plants were used. For 18:3-Glu elicitation experiments, puncture wounds were generated using a fabric pattern wheel, wounds were immediately supplied with 10 µL of a solution containing 0.17 nmoles of synthetic *N*-linolenoyl-glutamic acid (18:3-Glu; dissolved in 0.02% (v/v) Tween-20/water). For elicitation with purified oxidized forms of 18:3-Glu, amounts corresponding to ion intensities (as analyzed by LC-MS/MS; see below) similar to those detected after 2 min of 18:3-Glu metabolism on wounded leaves were used. Similar to 18:3-Glu, these modified forms were dissolved in 0.02% (v/v) Tween-20/water. The total treated area was quickly excised and used immediately for extraction and subsequent analysis. The oral secretion (OS) treatment was performed similarly but the wounds were supplemented with freshly harvested OS from *M. sexta* larvae (3rd to 5th instar) reared on *N. attenuata* plants. The amounts of 18:3-Glu in the OS were quantified by LC-MS/MS (see conditions below). For the steam treatment, three *N. attenuata* leaves were exposed to steam for 2 min and treated as above.

Synthesis of ^{14}C-labeled 18:3-Glu and turnover analysis

Ten µCi of [1-^{14}C]-9,12,15-linolenic acid (51.7 mCi/mmol, Perkin-Elmer, Rodgau, Germany) were dissolved in 2 mL of dry tetrahydrofurane containing 27.5 µL (0.198 mmol) of triethylamine. While stirring, 19 µL (0.197 mmol) of ethylchloroformate were added at 0°C (ice-water). After 3 min, 20 mg Glu dissolved in 1.4 mL 0.3 N NaOH were added. After 5 min, the ice bath was removed and the mixture stirred for 30 min at room temperature. The reaction was adjusted to pH 3-4 with 5 N HCl and extracted 3 times with 3 mL of dichloromethane. The combined organic phases were dried with Na$_2$SO$_4$ and evaporated to dryness under N$_2$. For purification, a column of 3 g of silica 60 gel was preconditioned with 100/1 (v/v) chloroform/acetic acid. The sample reconstituted in 1 mL 100/1 (v/v) chloroform/acetic acid was loaded onto the column. Washes were: 5 mL of 100/1 (v/v) chloroform/acetic acid two times, 5 mL of 14/6/1 (v/v/v) chloroform/ethylacetate/acetic acid two times collecting the flow-through in between. Purity of the fractions was checked by TLC using 14/6/1 (v/v/v) chloroform/ethylacetate/acetic acid as the solvent system.

^{14}C-18:3-Glu (0.1 µCi; 1.9 nmoles) were applied onto leaf wounds (area of 4 cm^2) and tissue collected at 0, 1 and 2 min. Leaf material was extracted two times with 2 ml of ethylacetate and radioactivity was quantified by liquid scintillation (WinSpectral model; Hewlett-Packard, Boeblingen, Germany). Metabolites were separated by TLC on silica gel 60 plates (Merck, Darmstadt, Germany) using 14/6/1 (v/v/v) chloroform/ethylacetate/acetic acid as the solvent system. After drying, TLC plates were exposed to ^{14}C-sensitive screens and the screens scanned with an FLA-3000 densitometric scanner (Fujifilm, Düsseldorf, Germany). Commercial α-linolenic acid (18:3; Sigma, Taufkirchen, Germany) was co-run as a standard. For radio-HPLC analysis, radioactive extracts were run on an HPLC system (Agilent HPLC 1100 Series, Palo Alto, CA), using a gradient of solvent A (0.05% (v/v) formic acid/water) and solvent B (0.05% (v/v) formic acid/acetonitrile) starting with a linear gradient of 20% to 70% (v/v) solvent B for 20 min, 70% (v/v) solvent B for 5 min, and 20% (v/v) solvent B for 5 min. The extract was separated with an RP Sphinx column (C$_{18}$ and propylphenyl stationary phase, 15%C, 250 × 4.6 mm, 5 µm particle diameter, Macherey-Nagel, Düren, Germany) with a flow of 1 mL min^{-1}. For radio-detection, a flow scintillation analyzer 500 TR (Packard), using Ultima-Flo AP (Perkin Elmer, Jügesheim, Germany) scintillation liquid was used.

Purification and identification of 18:3-Glu derivatives

Ten mg of synthetic 18:3-Glu were dissolved in 0.5 mL water containing 0.02% (v/v) Tween-20 and applied to 20 wounded fully expanded leaves (500 µg leaf^{-1} or 1.2 µmoles leaf^{-1}). After 5 min, the treated leaves were cut and dipped for 30 seconds in 2:1 (v/v) chloroform/methanol. The solvent was evaporated under a gentle stream of nitrogen preventing heating, reconstituted in 70% (v/v) methanol/water and fractionated using the retention times from the radio-HPLC, with the same system connected to a fraction collector. After fractionation, samples were concentrated and injected in an ESI-ToF (MicroToF, Bruker Daltonics, Bremen, Germany)

system connected to an HPLC system (Agilent HPLC 1100 Series) equipped with a Phenomenex Gemini NX 3 μm column (150 × 2 mm) using the same solvents (A and B) as above. The gradient was first isocratic at 5% (v/v) solvent B for 2 min, and then a linear gradient to 80% (v/v) solvent B for 28 min, 80% (v/v) solvent B for 6 min, and 5% (v/v) solvent B for 9 min at a flow rate of 0.2 mL min^{-1} was used. Compounds were analyzed in the negative ion mode. Instrument settings were as follows: capillary voltage 4500 V, capillary exit 130 V, drying gas temperature 200°C, drying gas flow of 8 L min^{-1} and a ToF acceleration voltage of 2100 V. Ions were detected from *m/z* 100 to 1400. Using a syringe pump, samples were directly injected into an ESI-MS/MS (Varian 1200 Triple-Quadrupole-LC-MS system; Varian, Palo Alto, CA) system to confirm their identification as an 18:3-Glu derivative. 18:3-Glu derivatives were further purified by separation on preparative TLC silica gel 60 plates (Merck) and TLC fractions were eluted sequentially with 5 mL of dichloromethane, chloroform and ethylacetate. Fractions were concentrated under nitrogen and reconstituted in 70/30 (v/v) methanol/water for subsequent LC-ESI-ToF and LC-ESI-MS/MS analysis. For final structural elucidation, samples were injected on an LC-ESI-XL-Orbitrap (Thermo, Steingrund, Germany) using the linear ion trap for fragmentation. Conditions were: source voltage: 4050V, capillary voltage: -40V and a sheath gas flow rate of 25 L min^{-1}.

Extraction and analysis of JA and FACs

For analysis of JA, ~0.2 g of frozen leaf material was added to 2 mL SafeLock® (Eppendorf) tubes containing two steel beads, and homogenized in a Genogrinder® Model2000 (Munich, Germany) at 500 strokes min^{-1}. 1 mL ethylacetate spiked with 100 ng of [9,10-^{2}H]-dihydro-JA was added as an internal standard (IS), the samples were vortexed for 5 min and centrifuged under refrigeration (4°C) for 15 min at 13,200 × *g*. The upper organic phase was transferred to a fresh tube and the leaf material was re-extracted with 0.5 ml ethylacetate. The organic phases were pooled and evaporated to dryness. The dry residue was reconstituted in 0.4 mL of 70/30 (v/v) methanol/water for analysis by LC-ESI-MS/MS using previously described conditions [30].

FACs were extracted from leaves with 1 ml of ice-cold chloroform and chloroform/methanol 4/1 (v/v) with or without the addition of 1% (w/v) butylated hydroxytoluene (BHT; Sigma) and 10 mg/ml trimethyl phosphite (TMP; Sigma)[27] using the same grinding conditions as for JA extraction. The samples were spiked with 100 ng of [9,10-^{2}H]-dihydro-JA as an internal standard (IS) for normalization. The solvent was evaporated under a gentle stream of nitrogen keeping the samples on ice. Precautions were taken not to completely dry the samples and the residue was reconstituted in 0.4 mL of 70/30 (v/v) methanol/water for analysis with an LC-ESI-MS/MS system (Varian 1200 Triple-Quadrupole-LC-MS system). 10 μL of the sample was injected onto a ProntoSIL® column (C18, 5 μm, 50 × 2 mm, Bischoff, Leonberg, Germany) connected to a precolumn (C18, 4 × 2 mm, Phenomenex). As mobile phases 0.05%/1% (v/v/v) formic acid/acetonitrile/water (solvent A) and 0.05% (v/v) formic acid/acetonitrile (solvent B) were used, starting with 15% (v/v) solvent B for 1.5 min (pre-run), a linear gradient to 98% (v/v) solvent B for 3 min, 98% (v/v) solvent B for 8 min and 15% (v/v) solvent B for 2.5 min. Flow rates were: 0.4 mL min^{-1} for 1 min and 0.2 mL min^{-1} from 1 to 12 min, and 0.4 mL min^{-1} till the end of the run (15 min). Compounds were detected in the ESI negative mode and multiple reaction monitoring (MRM; see Additional file 4 for details on ion transitions and conditions used for analysis).

Volatile collection and GCxGC-ToF analysis

ir*lox2* and WT plants were induced with either wounding plus 18:3-Glu or wounding plus 13-oxo-13:2-Glu and the volatiles emitted by the induced leaves were trapped as described previously [17]. Briefly, a single leaf was enclosed in a plastic volatile collection chamber and volatiles were trapped on 20 mg of Super-Q absorbent (ARS, Philadelphia, PA) secured with glass wool in small glass cylinders. Ambient air filtered through activated charcoal was pulled at 200 to 300 ml min^{-1} into each collection chamber with a vacuum pump. Volatile trapping was performed after 24 h of the treatment for a period of 8 h. Traps were spiked with 400 ng tetraline as IS and eluted with 250 μL of dichloromethane. Eluted volatiles were injected into a GCxGC-ToF system (Leco, Germany) and the samples run using the same instrument parameters as previously described [17]. For analysis, a reference sample made by mixing all the different samples was injected and a reference library was created by software assisted peak finding. Non-relevant peaks (e.g. plasticizers) were manually removed, and all individual samples were processed against this reference. After manual correction of the peak integrated areas, data was normalized by the IS (tetraline) and the total ion current (TIC). Significant peaks were identified using an unpaired student's *t*-test.

Data analysis

All experiments were performed with at least three individual plants (biological replicates). Statistics were calculated using SPSS v. 17.0, data was *log*-transformed when the data was not homoscedastic.

Additional material

> **Additional file 1: Metabolism of ^{14}C labeled 18:3-Glu in wounded *N. attenuata* leaves.**
>
> **Additional file 2: Analysis of 13-oxo-13:2-Glu biogenesis on the leaf surface.**
>
> **Additional file 3: Mass spectra of two monoterpenes detected by GC-MS.**
>
> **Additional file 4: List of ion transitions used for analysis of compounds by LC-MS/MS.**

Authors' contributions
AVD and GB carried out the experiments, analyzed the data and drafted the manuscript. AAB carried out experiments and analyzed the data. MK analyzed the data. ITB participated in the design and coordination of the study and helped to draft the manuscript. GB conceived of the study, participated in its design and coordination and helped to draft the manuscript. All authors read and approved the final manuscript.

References
1. Labandeira C: **The origin of herbivory on land: Initial patterns of plant tissue consumption by arthropods.** *Insect Sci* 2007, **14**:259-275.
2. Kessler A, Baldwin IT: **Defensive function of herbivore-induced plant volatile emissions in nature.** *Science* 2001, **291**:2141-2144.
3. Turlings TCJ, Tumlinson JH, Lewis WJ: **Exploitation of herbivore-induced plant odors by host-seeking parasitic wasps.** *Science* 1990, **250**:1251-1253.
4. Halitschke R, Gase K, Hui D, Schmidt DD, Baldwin IT: **Molecular Interactions between the specialist herbivore *Manduca sexta* (Lepidoptera, Sphingidae) and its natural host *Nicotiana attenuata*. VI. Microarray analysis reveals that most herbivore-specific transcriptional changes are mediated by fatty acid-amino acid conjugates.** *Plant Physiol* 2003, **131**:1894-1902.
5. Schmelz EA, Engelberth J, Alborn HT, Tumlinson JH, Teal PEA: **Phytohormone-based activity mapping of insect herbivore-produced elicitors.** *Proc Natl Acad Sci USA* 2009, **106**:653-657.
6. Alborn HT, Turlings TCJ, Jones TH, Stenhagen G, Loughrin JH, Tumlinson JH: **An elicitor of plant volatiles from beet armyworm oral secretion.** *Science* 1997, **276**:945-949.
7. Mithöfer A, Wanner G, Boland W: **Effects of feeding spodoptera littoralis on lima bean Leaves. II. Continuous mechanical wounding resembling insect feeding is sufficient to elicit herbivory-related volatile emission.** *Plant Physiol* 2005, **137**:1160-1168.
8. Heil M: **Damaged-self recognition in plant herbivore defence.** *Trends Plant Sci* 2009, **14**:356-363.
9. Schmelz EA, Carroll MJ, LeClere S, Phipps SM, Meredith J, Chourey PS, Alborn HT, Teal PEA: **Fragments of ATP synthase mediate plant perception of insect attack.** *Proc Natl Acad Sci USA* 2006, **103**:8894-8899.
10. Eichenseer H, Mathews MC, Bi JL, Murphy JB, Felton GW: **Salivary glucose oxidase: Multifunctional roles for *Helicoverpa zea*?** *Arch Insect Biochem Physiol* 1999, **42**:99-109.
11. Musser RO, Hum-Musser SM, Eichenseer H, Peiffer M, Ervin G, Murphy JB, Felton GW: **Herbivory: Caterpillar saliva beats plant defences.** *Nature* 2002, **416**:599-600.
12. Diezel C, von Dahl CC, Gaquerel E, Baldwin IT: **Different lepidopteran elicitors account for cross-talk in herbivory-induced phytohormone signaling.** *Plant Physiol* 2009, **150**:1576-1586.
13. Alborn HT, Hansen TV, Jones TH, Bennett DC, Tumlinson JH, Schmelz EA, Teal PEA: **Disulfooxy fatty acids from the American bird grasshopper Schistocerca americana, elicitors of plant volatiles.** *Proc Natl Acad Sci USA* 2007, **104**:12976-12981.
14. Halitschke R, Schittko U, Pohnert G, Boland W, Baldwin IT: **Molecular interactions between the specialist herbivore *Manduca sexta* (Lepidoptera, Sphingidae) and its natural host *Nicotiana attenuata*. III. Fatty acid-amino acid conjugates in herbivore oral secretions are necessary and sufficient for herbivore-specific plant responses.** *Plant Physiol* 2001, **125**:711-717.
15. von Dahl CC, Winz RA, Halitschke R, Kühnemann F, Gase K, Baldwin IT: **Tuning the herbivore-induced ethylene burst: the role of transcript accumulation and ethylene perception in *Nicotiana attenuata*.** *Plant J* 2007, **51**:293-307.
16. Giri AP, Wünsche H, Mitra S, Zavala JA, Muck A, Svatoš A, Baldwin IT: **Molecular interactions between the specialist herbivore *Manduca sexta* (Lepidoptera, Sphingidae) and its natural host *Nicotiana attenuata*. VII. Changes in the plant's proteome.** *Plant Physiol* 2006, **142**:1621-1641.
17. Gaquerel E, Weinhold A, Baldwin IT: **Molecular Interactions between the Specialist Herbivore *Manduca sexta* (Lepidoptera, Sphigidae) and Its Natural Host *Nicotiana attenuata*. VIII. An Unbiased GCxGC-ToFMS Analysis of the Plant's Elicited Volatile Emissions.** *Plant Physiol* 2009, **149**:1408-1423.
18. Yoshinaga N, Aboshi T, Abe H, Nishida R, Alborn HT, Tumlinson JH, Mori N: **Active role of fatty acid amino acid conjugates in nitrogen metabolism in Spodoptera litura larvae.** *Proc Natl Acad Sci USA* 2008, **105**:18058-18063.
19. Truitt CL, Wei H-X, Paré PW: **A plasma membrane protein from *Zea mays* binds with the herbivore elicitor volicitin.** *Plant Cell* 2004, **16**:523-532.
20. Maischak H, Grigoriev PA, Vogel H, Boland W, Mithöfer A: **Oral secretions from herbivorous lepidopteran larvae exhibit ion channel-forming activities.** *FEBS Lett* 2007, **581**:898-904.
21. Truitt C, Paré P: **In situ translocation of volicitin by beet armyworm larvae to maize and systemic immobility of the herbivore elicitor in planta.** *Planta* 2004, **218**:999-1007.
22. Peiffer M, Felton G: **Do caterpillars secrete "oral secretions"?** *J Chem Ecol* 2009, **35**:326-335.
23. Schittko U, Preston CA, Baldwin IT: **Eating the evidence?** *Manduca sexta* larvae can not disrupt specific jasmonate induction in Nicotiana attenuata by rapid consumption. *Planta* 2000, **210**:343-346.
24. Shroff R, Svatoš A: **Proton sponge: A novel and versatile MALDI matrix for the analysis of metabolites using mass spectrometry.** *Anal Chem* 2009, **81**:7954-7959.
25. Salch YP, Grove MJ, Takamura H, Gardner HW: **Characterization of a C-5,13-cleaving enzyme of 13(S)-hydroperoxide of linolenic acid by soybean seed.** *Plant Physiol* 1995, **108**:1211-1218.
26. Frankel EN, Neff WE, Selke E: **Analysis of auto-oxidized fats by gas chromatography-mass spectrometry. 7. volatile thermal-decomposition products of pure hydroperoxides from auto-oxidized and photosensitized oxidized methyl oleate, linoleate and linolenate.** *Lipids* 1981, **16**:279-285.
27. Mueller MJ, Mene-Saffrane L, Grun C, Karg K, Farmer EE: **Oxylipin analysis methods.** *Plant J* 2006, **45**:472-489.
28. Kessler A, Halitschke R, Baldwin IT: **Silencing the jasmonate cascade: induced plant defenses and insect populations.** *Science* 2004, **305**:665-668.
29. Allmann S, Halitschke R, Schuurink RC, Baldwin IT: **Oxylipin channelling in Nicotiana attenuata: lipoxygenase 2 supplies substrates for green leaf volatile production.** *Plant, Cell Environ* 2010, PMID: 20584148..
30. Kallenbach M, Alagna F, Baldwin IT, Bonaventure G: **Nicotiana attenuata SIPK, WIPK, NPR1, and fatty acid-amino acid conjugates participate in the induction of jasmonic acid biosynthesis by affecting early enzymatic steps in the pathway.** *Plant Physiol* 2010, **152**:1760-1760.
31. Blée E: **Impact of phyto-oxylipins in plant defense.** *Trends Plant Sci* 2002, **7**:315-322.
32. Vaz AD, Roberts ES, Coon MJ: **Reductive beta-scission of the hydroperoxides of fatty acids and xenobiotics: role of alcohol-inducible cytochrome P-450.** *Proc Natl Acad Sci USA* 1990, **87**:5499-5503.
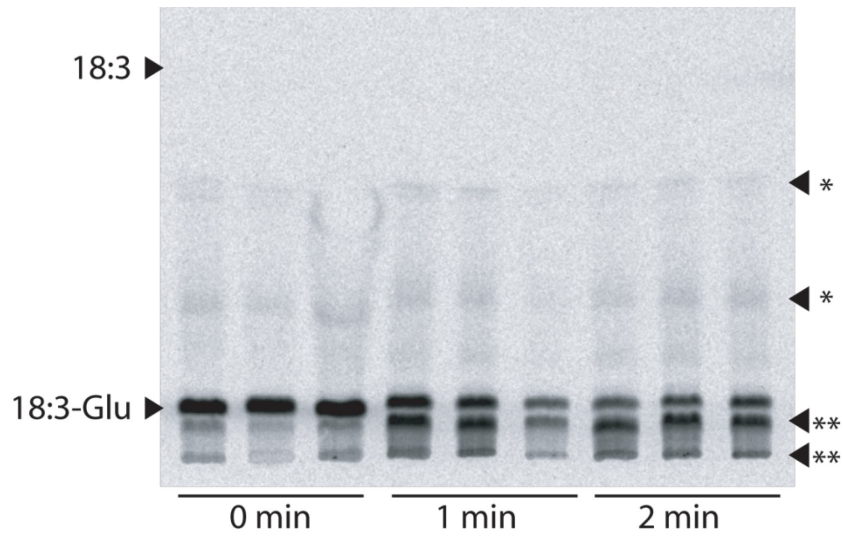
Additional file 1. Metabolism of ^{14}C labeled 18:3-Glu on wounded *N. attenuata* **leaves** Leaves of rosette stage *N. attenuata* plants were wounded with a pattern wheel and 0.1µCi of [1- ^{14}C]18:3-Glu were immediately applied onto leaf wounds. The damaged tissue was harvested harvested immediately (T0) and 1 and 2 min after the treatment and extracted. Radiolabeled metabolites were separated by TLC and plates were exposed for 24h to ^{14}C-sensitive screens. Major (**) and monor (*) [1-^{14}C]18:3-Glu derivatives were marked on the right, α-linolenic acid (18:3) and 18:3-Glu were co-run and their position of migration indicated on the left.
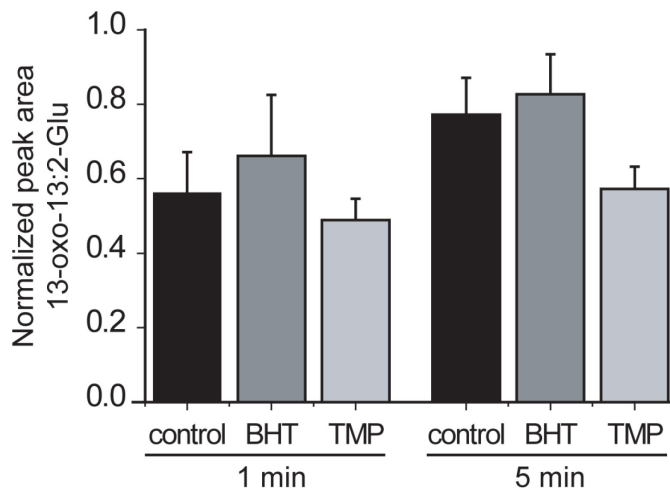
Additional file 2. Analysis of 13-oxo-13:2 biogenesis on the leaf surface. WT plants were wounded with a pattern wheel and 0.17 nmoles of 18:3-Glu were applied onto the wounds. After 1 and 5 min, leaf tissue was extracted without (control) or with the addition of butylated hydroxytoluene (BHT) or trimethyl phosphite (TMP) to the solvent. After extraction, samples were analyzed by LC-MS/MS (n=3, bars denote ± SE). Univariate *ANOVA* (1 Min $F_{3,3}$=0.799, *P*=0.492; 5 Min $F_{3,3}$=2.166 *P*=0.196).
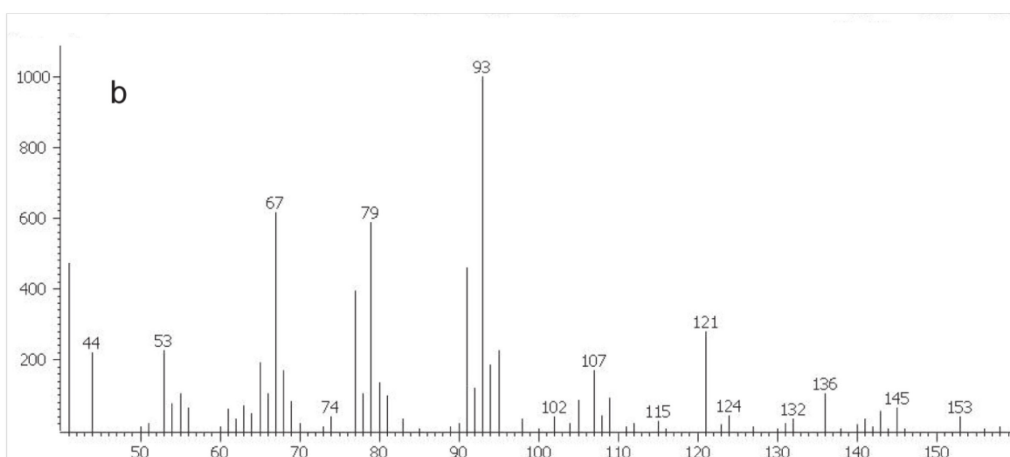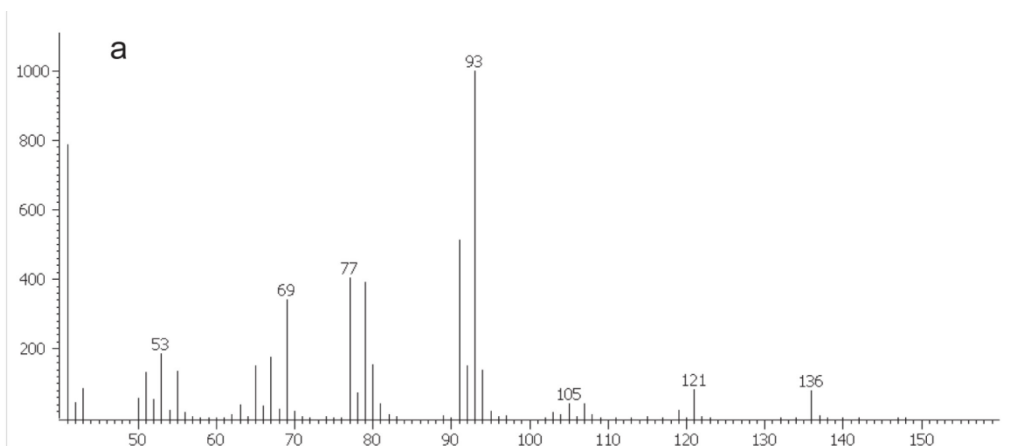
Additional file 3. Mass spectra of monoterpenes detected by GC-MS a. Mass spectrum of β-pinene. b. Unknown monoterpene. Average mass spectra were recorded after background substraction and compared against standards. β-pinene matched in both the mass spectrum and both retention times.

Name of analyte	Molecular ion [M-1]	Fragment ion	Capillary CID	Collision energy
JA	209	59	-35V	12V
$^2H_2$-dihydro-JA	213	59	-35V	12V
18:3-Glu	406	128	-35V	21.5V
13-OOH-18:3-Glu	438	352	-20V	19V
13-OH-18:3-Glu	422	293	-35V	18V
13-oxo-13:2-Glu	352	128	-35V	18V

Additional file 4. List of ion transitions used for analysis of compounds by LC-MS/MS.

Plant Methods

Methodology

A rapid and sensitive method for the simultaneous analysis of aliphatic and polar molecules containing free carboxyl groups in plant extracts by LC-MS/MS

Mario Kallenbach, Ian T Baldwin and Gustavo Bonaventure*

Address: Max Planck Institute for Chemical Ecology, Department of Molecular Ecology, Hans Knöll Str. 8, 07745 Jena, Germany

Email: Mario Kallenbach - mkallenbach@ice.mpg.de; Ian T Baldwin - baldwin@ice.mpg.de; Gustavo Bonaventure* - gbonaventure@ice.mpg.de
* Corresponding author

Abstract

Background: Aliphatic molecules containing free carboxyl groups are important intermediates in many metabolic and signalling reactions, however, they accumulate to low levels in tissues and are not efficiently ionized by electrospray ionization (ESI) compared to more polar substances. Quantification of aliphatic molecules becomes therefore difficult when small amounts of tissue are available for analysis. Traditional methods for analysis of these molecules require purification or enrichment steps, which are onerous when multiple samples need to be analyzed. In contrast to aliphatic molecules, more polar substances containing free carboxyl groups such as some phytohormones are efficiently ionized by ESI and suitable for analysis by LC-MS/MS. Thus, the development of a method with which aliphatic and polar molecules -which their unmodified forms differ dramatically in their efficiencies of ionization by ESI- can be simultaneously detected with similar sensitivities would substantially simplify the analysis of complex biological matrices.

Results: A simple, rapid, specific and sensitive method for the simultaneous detection and quantification of free aliphatic molecules (e.g., free fatty acids (FFA)) and small polar molecules (e.g., jasmonic acid (JA), salicylic acid (SA)) containing free carboxyl groups by direct derivatization of leaf extracts with Picolinyl reagent followed by LC-MS/MS analysis is presented. The presence of the N atom in the esterified pyridine moiety allowed the efficient ionization of 25 compounds tested irrespective of their chemical structure. The method was validated by comparing the results obtained after analysis of *Nicotiana attenuata* leaf material with previously described analytical methods.

Conclusion: The method presented was used to detect 16 compounds in leaf extracts of *N. attenuata* plants. Importantly, the method can be adapted based on the specific analytes of interest with the only consideration that the molecules must contain at least one free carboxyl group.

Background

The analysis of low abundant signalling molecules such as phytohormones (e.g., jasmonic acid (JA), salicylic acid (SA) and abscisic acid (ABA)) and intermediates of meta-bolic pathways (e.g., free fatty acids (FFA), oxygenated forms of fatty acids) in plants is an important tool to understand how plants grow, develop and respond to stress conditions. For high-throughput biochemical phe-

notyping of, for example, wild-type or genetically modified plants grown under diverse conditions, it is essential to develop methods for the rapid, simultaneous and reliable quantitative analysis of a broad range of molecules.

The use of tandem mass spectrometry (MS/MS) coupled to liquid chromatography (LC) is ideal for the analysis of complex mixtures of compounds which are commonly found in biological matrices such as plant tissues. One of the advantages of LC-MS/MS is that separation and structural elucidation of compounds can be achieved in a continuous manner without the need for purification or derivatization steps. Another advantage of LC-MS/MS is the use of tandem MS, in which a precursor ion is mass-selected by mass analyzer 1, focused into a collision region preceding a second mass analyzer (collision chamber), and their mass fragments analyzed in a third mass analyzer [1]. The capacity to perform multi reaction monitoring (MRM) has the advantage of rapid and sensitive detection of several compounds even if they show similar retention times during LC.

Ionization by electrospray (ESI) is one of the most widely used tools for LC-MS/MS analysis, and the ions can be selectively monitored in negative and positive mode [2]. In the ESI negative mode, analysis of small molecules containing free carboxyl groups, yields mainly the ion $[M-H]^-$, corresponding to their carboxylate anion. However, the efficiency of formation of carboxylate anions differs widely among compounds depending on their chemical structure [3]. For example, while small molecules containing free carboxyl groups and high numbers of heteroatoms such as the phytohormones JA, SA and ABA or aromatic substances are ionized efficiently by ESI [4-6], aliphatic molecules such as FFAs are relatively poorly ionized by this technique, in particular, as the aliphatic chain becomes longer and the degree of saturation higher [7]. This lower efficiency of carboxylate anion formation restricts the analysis of aliphatic molecules, specially, when small amounts of tissue are available for analysis (e.g., embryos, pollen, tissue sections obtained by laser micro-dissection).

Analytical methods to quantify aliphatic molecules are laborious, involving enrichment steps using chromatographic techniques such as thin layer chromatography (TLC), solid phase extraction (SPE) or LC previous to derivatization and gas chromatography (GC) for separation and analysis [8]. One strategy to improve the sensitivity of analysis of aliphatic molecules containing carboxyl groups by LC-MS/MS is the use of chemical derivatization that generates a strong ion in the ESI source [8]. Among these, the generation of pyridinium compounds has many advantages [9]. The presence of the N atom in the pyridine moiety allows for the efficient ionization of the com-

pounds [9] and due to the mild conditions used to generate the Picolinyl ester intermediates, analysis of sensitive molecules containing conjugated double bonds is possible [10]. Moreover, since ester bonds are resistant to the conditions used to generate Picolinyl ester derivatives, esterified fatty acids do not interfere with the analysis [10].

In this study, a method for the simultaneous determination of aliphatic molecules (e.g., FFAs and their oxygenated derivatives) and more polar (phytohormones, phenolics) compounds by using Picolinyl ester derivatives of leaf extracts coupled with LC-MS/MS is presented. The method was applied for the analysis of leaves of *N. attenuata* plants before and after wounding and elicitation by the insect elicitors fatty acid-amino acid conjugates (FACs)[11]; which are treatments known to stimulate the production of a large number of phytohormones and secondary metabolites [12].

Results and Discussion
Method development
Commercial chemical standards (Table 1) were first derivatized to their respective Picolinyl esters using the mild method proposed in [10]. Some examples of the molecules used are shown in Figure 1. This method allows the quantitative derivatization of free carboxyl group-containing molecules within 10 min using conditions that preserve sensitive molecules containing conjugated double bonds. The first step in the reaction involves the activation of the carboxyl group with 1,1'-carbonyldiimidazole to form an active carbimidazol amid (**1**, Figure 2). The second step involves the reaction of **1** with 3-(hydroxymethyl)-pyridine to form the corresponding β-Picolinyl ester (**2**, Figure 2).

As mentioned in the background section, the formation of Picolinyl esters by this method is restricted to free carboxyl groups [10]. To confirm the absence of hydrolysis of ester bonds from esterified fatty acids, 10 μg of commercial glycerolipids (monogalactosyldiglycerol: MGDG, phosphatidylcholine: PC and phosphatidylglycerol: PG) were first purified by TLC and then subjected to the reaction. No free fatty acids could be detected (data not shown and see below for the methodology used for detection), confirming that the reaction does not induce the hydrolysis of esterified fatty acids.

Analysis of the Picolinyl ester derivatives of the commercial standards was first accomplished by their direct injection into the MS-interface to determine their $[M+H]^+$ parent ion and their MS/MS fragmentation pattern by collision induced dissociation (CID) using increasing voltage energies. The third mass analyzer was set in the scan mode for ions with *m/z* between 50 and 500. Two major frag-
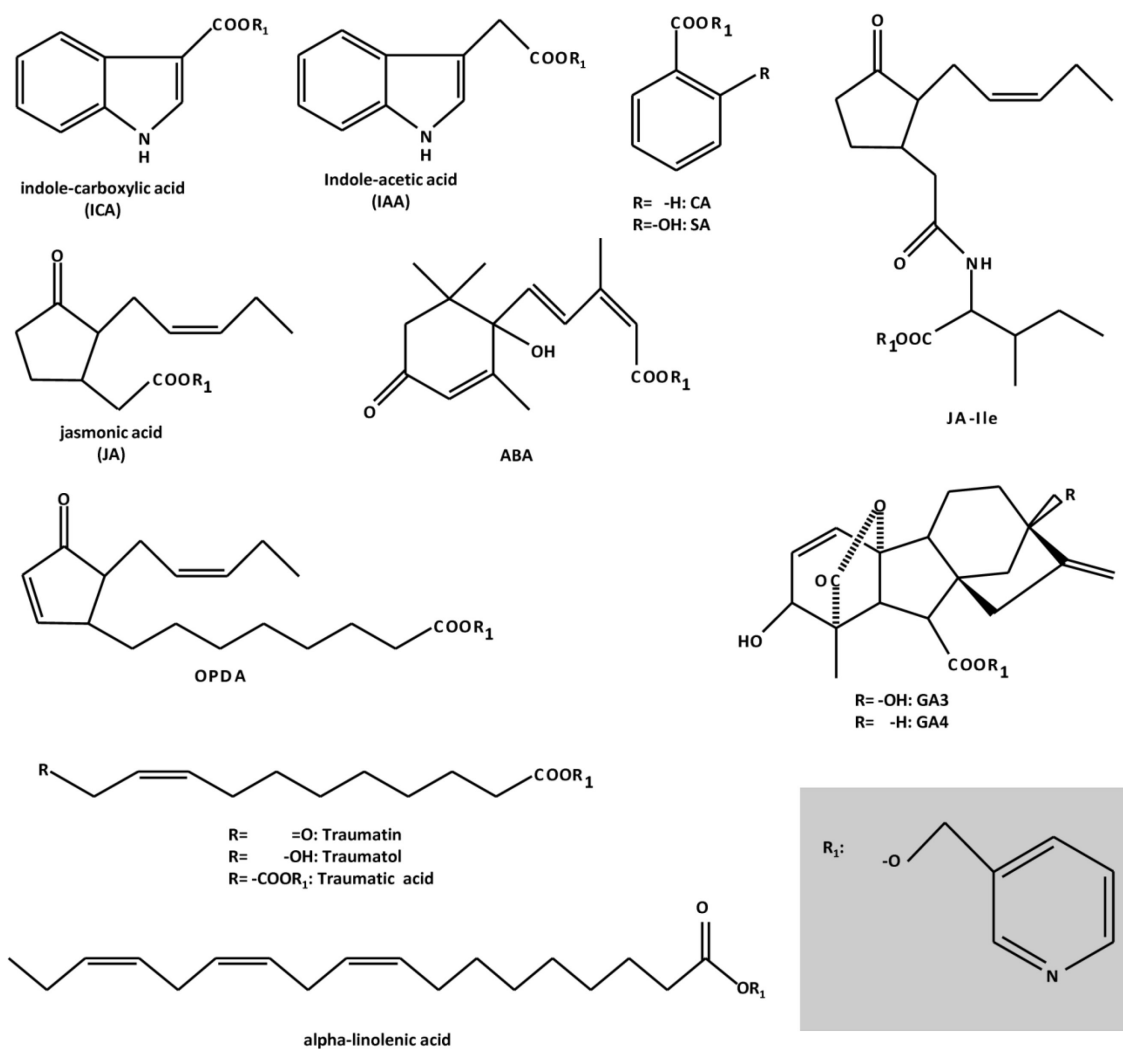
Figure 1
Examples of compounds analyzed as their Picolinyl ester derivatives by LC-MS/MS.

ments were generated, $m/z = 92$ and $m/z = 108$, resulting from the loss of the methyl-pyridine fragment and the hydroxymethyl-pyridine fragment, respectively (Figure 2). The ion $m/z = 92$ gave the strongest intensity at a collision energy of -25.5 V and therefore the $[M+H]^+ > 92$ m/z transition was used for specific detection of Picolinyl ester derivatives.

The chromatographic separation of Picolinyl ester derivatives was performed on a reverse-phase column using acidic water and methanol as solvents in a gradient mode.

In this case, the LC method was optimized for the analysis in plant extracts of small polar molecules and aliphatic molecules containing no more than 18 carbons. After a pre-run of 1.5 min, all substances of interest eluted from the column in 18.5 min. An additional post run of 6.5 min was added for column conditioning for a final run time of 25 min. An example of chromatograms (total ion current, TIC) for derivatized commercial standards and a derivatized leaf extract from *N. attenuata* is shown in Figures 3A and 3B, respectively.

http://www.plantmethods.com/content/5/1/17

Table 1: List of standards used for matrix free and matrix adapted calibration.

| Number	Substance	[M+H]⁺	Retention time [min]	Calibration[2]		Calibration[3]	
				Linearity (r)§	LOD [pg/μL]	Linearity (r)§	LOD [pg/μL]
1	$^{13}C_6$-jasmonic acid-isoleucine ($^{13}C_6$-JA-Ile)	421	6.86	1.00	20.60	0.99	116
2	Jasmonic acid-isoleucine (JA-Ile)	415	6.86	1.00	20.80	0.99	117
3	$^2H_4$-salicylic acid ($^2H_4$-SA)	234	8.77	0.98	24.40	0.98	167
4	Salicylic acid (SA)	230	8.77	0.97	24.80	0.98	165
5	$^2H_6$-abscisic acid ($^2H_6$-ABA)	362	9.01	0.98	19.40	0.98	163
6	Abscisic acid (ABA)	356	9.02	0.99	18.70	0.98	165
7	Indole-3-carboxylic acid (ICA)	253	9.08	0.93	41.30	0.91	355
8	Royal jelly acid (Tr IS)	278	9.26	0.99	12.00	0.98	181
9	Cinnamic acid (CA)	240	9.34	0.99	23.90	0.97	203
10	Jasmonic acid (JA)	302	9.43	0.98	19.60	0.98	155
11	Traumatol	306	9.85	0.99	12.90	0.98	174
12	Indole-3-acetic acid (IAA)	267	9.94	0.98	19.30	0.99	297
13	Traumatin	304	9.96	1.00	5.30	0.98	168
14	9,10-$^2H_2$-dihydro-jasmonic acid (D_2-JA)	306	10.13	1.00	11.30	0.98	180
15	Traumatic acid	320	10.15	0.99	11.20	0.96	250
16	Hexadecatrieonic acid (16:3)	342	10.29	0.99	17.00	0.99	132
17	(9 S, 13 S)-12-oxo-phytodienoic acid (OPDA)	384	10.89	1.00	10.30	0.98	147
18	Hexadecadienoic acid (16:2)	344	10.93	0.99	14.90	0.98	147
19	Gibberellin A_3 (GA_3)	438	11.27	0.93	42.30	0.96	246
20	$^2H_2$-OPC 8:0	388	11.59	0.94	*1	0.96	*1
21	Linolenic acid (18:3)	370	12.83	1.00	7.80	1.00	70
22	Hexadecenoic acid (16:1)	346	13.20	0.99	19.00	0.99	95
23	Heptadecenoic acid (17:1)	360	13.78	1.00	4.10	0.97	195
24	Linoleic acid (18:2)	372	14.22	0.97	8.60	0.96	123
25	Hexadecanoic acid (16:0)	348	14.53	1.00	5.20	0.99	114
26	Octadecenoic acid (18:1)	374	14.86	0.99	14.70	0.99	94
27	Heptadecanoic acid (17:0)	362	16.09	1.00	7.50	0.99	119
28	Stearic acid (18:0)	376	17.59	1.00	7.90	0.99	117

*1 Amount of standard unknown.
[2] Matrix free calibration
[3] Matrix adapted calibration
§Standard calibration curves were generated by injecting 10 μL of 100, 250, 375, 500, 750, 1000 pg/μL of the different standards (n = 3).

Mixtures of derivatized commercial standards ranging from 100 to 1000 pg/μL were first used to determine their linear range of detection and their limit of detection (LOD). These concentrations were in the same range as the endogenous compounds quantified in derivatized leaf extracts (see below). Within this range, most analytes presented a linear response (concentration vs. area) with r values higher than 0.97 with the exception of ICA, GA_3 and $^2H_2$-OPC 8:0 which presented r values between 0.93 and 0.94 (Table 1). The LODs, calculated based on the calibration plot method, were between 5 and 42 pg/μL (Table 1). To determine the injection precision, each derivatized commercial standard was injected 10 times at different concentrations and the coefficient of variation (CV) was calculated. For all compounds, the CV values were less than 0.1 for all concentrations tested (Additional file 1, Table S1).

To determine matrix suppression effects in a leaf extract, mixtures of derivatized standards were spiked at different concentrations in underivatized leaf extracts of *N. attenuata* plants and the linear range of detection and LOD were calculated (Table 1). In this case, the linearity of the response (r value, concentration vs. area) was similar to that presented by the derivatized standards in pure solvent, however, the LOD values were increased for all standards to amounts between 70 and 350 pg/μL.

Extraction and analysis of **N. attenuata** *leaves*
The extraction of polar and lipophilic compounds from *N. attenuata* leaves was performed as indicated by [13] with the modifications adopted by [14]. Additional modifications were included to increase the number of samples that can be processed simultaneously and to reduce

-44-
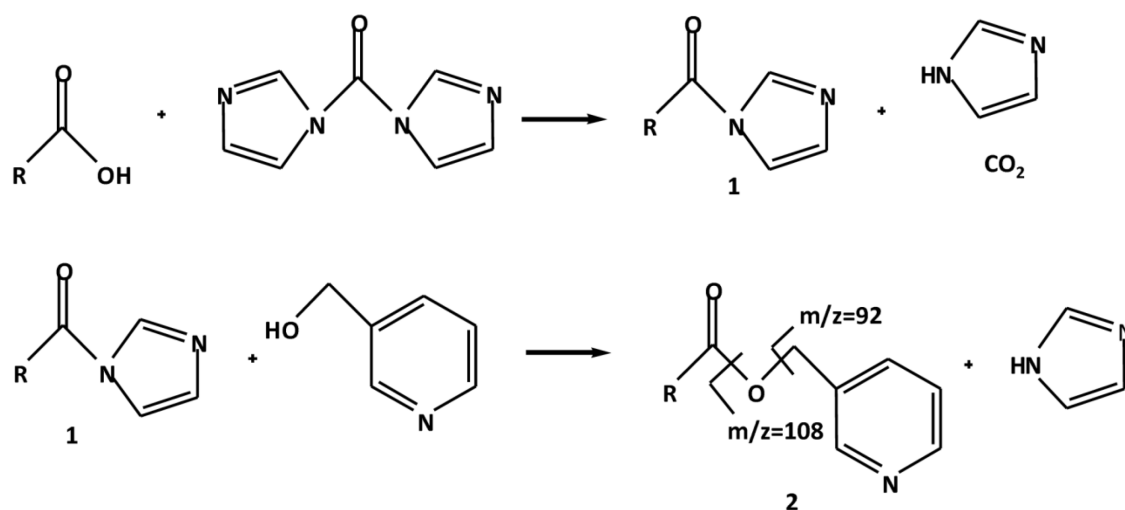
Figure 2
Reaction mechanisms for the formation of Picolinyl ester derivatives of carboxylic acids. The carboxyl group is first activated by reaction with 1,1'-carbidiimidazole to form the active amid 1. 1 is then transesterified with 3-(hydroxymethyl)-pyridine to form the Picolinyl ester derivative 2. After collision induced dissociation (CID), the major ion fragments obtained are $m/z = 92$ and $m/z = 108$.

the amount of sample material necessary for analysis (see Methods section).

The extraction method was first validated by performing 10 biological replicates of *N. attenuata* non-elicited and FAC-elicited leaves after 60 min of the treatment. For each replicate, 300 mg of leaf tissue were extracted, derivatized and analyzed by LC-MS/MS (Additional file 1, Table S2). The standard deviations were below 10% of the average values for all detectable compounds. To determine the extraction recovery rate, the residual leaf material obtained after the first extraction was re-extracted, derivatized and analyzed. The recovery rates were higher than 98% for all molecules tested (Additional file 1, Table S2). Sample stability was tested by re-analyzing the derivatized leaf extracts after two days of the first analysis (samples were kept at 10°C). The amounts of all compounds did not differ significantly between the first and second analyses (paired *t*-test, data not shown). The CV was analyzed for the detectable compounds in derivatized leaf extracts (analyzed the same day of extraction) from FAC-elicited leaves (60 min after the treatment). The CV values of two-day old extracts (kept at 10°C) were also analyzed. The CV values were below 0.1 for all detectable compounds (Additional file 1, Table S1). Finally, the efficiency of derivatization was evaluated by the analysis of the respective free compounds in derivatized leaf extracts (60 min after

FAC elicitation). No free molecules were detected, corroborating that the derivatization is quantitative [10].

To validate the results obtained with the method presented in this study, 300 mg of non-elicited leaves of *N. attenuata* plants and leaves wounded and elicited with FAC (30 and 60 min) were analyzed with the present method and additionally with well established analytical methods for aliphatic compounds and phytohormes. Aliphatic compounds (free fatty acids in this case) were analyzed by performing separation by TLC and GC-MS analysis of their methyl-ester derivatives (see Methods section) and phytohormones were analyzed by LC-MS/MS using underivatized leaf extracts [6].

A total of 25 compounds were analyzed, including FFAs, derivatives and intermediates of the lipoxygenase pathway (e.g., OPDA, dnOPDA, OPCs) and some phytohormones related to stress responses or growth (e.g., JA, SA, ABA, JA-Ile, GAs, IAA). The analysis showed that 16 compounds could be detected in derivatized *N. attenuata* leaf extracts after elicitation. ICA, CA, traumatol, dnOPDA, IAA, 16:2, GA_3, OPC-8:0 and GA_4 could not be detected by any of the methods used (Table 2). The phytohormones IAA, GA_3, and GA_4 accumulate to low levels in leaf tissue and their detection usually requires purification steps. Thus, these molecules were most likely below their LOD

Figure 3
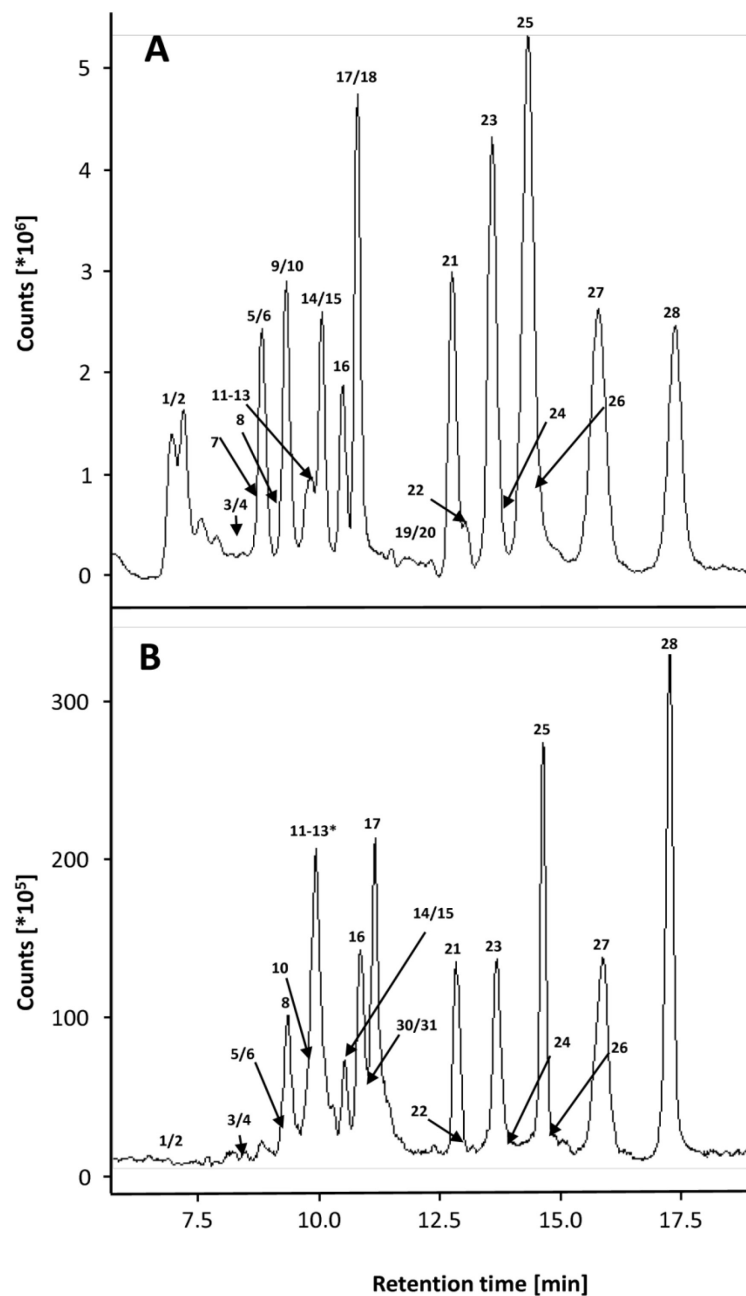**Example of chromatograms of Picolinyl ester derivatives from a standard mixture and a *N. attenuata* leaf extract**. A, Chromatogram (TIC) of a mix of derivatized commercial standards. B, Chromatogram (TIC) of a derivatized *N. attenuata* leaf extract after 60 min of FAC elicitation. *Analytes 11 to 13 are overlaid by a peak corresponding to an unknown compound in the leaf extract. Peaks are numbered according to Table 1.

http://www.plantmethods.com/content/5/1/17

Table 2: Quantification of Picolinyl ester derivatives of *N. attenuata* leaf extracts and comparison with two additional analytical methods.

| | | | Treatments | | | | | | | | | |
| | | | 0 min | | wound 30 min | | FAC 30 min | | wound 60 min | | FAC 60 min | |
Substance	RT	[M+H]+	Picol. esters ng gFW⁻¹ (± SE)	Method 2 or 3* ng gFW⁻¹ (± SE)	Picol. esters ng gFW⁻¹ (± SE)	Method 2 or 3* ng gFW⁻¹ (± SE)	Picol. esters ng gFW⁻¹ (± SE)	Method 2 or 3* ng gFW⁻¹ (± SE)	Picol. esters ng gFW⁻¹ (± SE)	Method 2 or 3* ng gFW⁻¹ (± SE)	Picol. esters ng gFW⁻¹ (± SE)	Method 2 or 3* ng gFW⁻¹ (± SE)
JA-Ile	6.86	415	-	1.1 (± 0.14)	-	-	-	-	-	-	-	-
SA	8.77	230	193 (± 31)	173 (± 23)	203 (± 24)	212 (± 19)	182 (± 11)	196 (± 11)	216 (± 22)	189 (± 17)	116 (± 18)	129 (± 22)
ABA	9.01	356	257 (± 7)	225 (± 8.0)	192 (± 35)	246 (± 9.0)	274 (± 16)	232 (± 14)	264 (± 6.0)	242 (± 10)	277 (± 12)	270 (± 14)
ICA	9.08	253	-	-	-	-	-	-	-	-	-	-
CA	9.34	240	-	-	-	-	-	-	-	-	-	-
JA	9.43	302	137 (± 20)	152 (± 23)	937 (± 150)	845 (± 95)	1845 (± 125)	1586 (± 110)	1564 (± 180)	1326 (± 42)	3820 (± 350)	3149 (± 223)
Traumatol	9.85	306	-	-	-	-	-	-	-	-	-	-
dnOPDA	9.85	356	-	-	-	-	-	-	-	-	-	-
IAA	9.94	267	-	-	-	-	-	-	-	-	-	-
Traumatin	9.96	304	11.3 (± 5.6)	14.4 (± 7.8)	17.1 (± 4.8)	15.2 (± 2.3)	14.6 (± 3.4)	12.4 (± 2.7)	13.8 (± 1.9)	15 (± 5.2)	12.2 (± 3.6)	21.4 (± 4.2)
Tr. acid**	10.15	320	-	5 (± 0.96)	19.6 (± 3.2)	24.3 (± 6.7)	23.8 (± 6.1)	20.4 (± 4.8)	17.1 (± 2.5)	19.6 (± 2.3)	20.9 (± 1.9)	-
OPC4:0	10.46	330	-	-	-	-	12.6 (± 8.1)	-	10.3 (± 4.9)	-	18.5 (± 4.7)	-
OPC6:0	10.67	358	-	-	-	-	5.3 (± 2.9)	-	8.6 (± 3.5)	-	11.2 (± 5.6)	-
OPDA	10.89	384	107 (± 60)	91 (± 53)	323 (± 47)	386 (± 45)	291 (± 11)	322 (± 15)	180 (± 45)	184 (± 15)	301 (± 31)	313 (± 30)
GA₃	11.27	438	-	-	-	-	-	-	-	-	-	-
OPC8:0	11.41	386	-	-	-	-	-	-	-	-	-	-
GA₄	11.99	424	-	-	-	-	-	-	-	-	-	-
18:3	12.83	370	446 (± 38)	398 (± 24)	480 (± 53)	497 (± 37)	523 (± 30)	497 (± 42)	605 (± 20)	596 (± 31)	476 (± 33)	424 (± 31)
16:1	13.2	346	52 (± 9)	26 (± 23)	41 (± 3.0)	22 (± 20)	48 (± 12)	51 (± 32)	91 (± 26)	147 (± 96)	103 (± 13)	121 (± 83)
16:2	10.93	344	-	-	-	-	-	-	-	-	-	-
16:3	10.29	342	45.6 (± 12)	-	41.1 (± 2.0)	28.2 (± 23.0)	64.1 (± 19)	40.5 (± 21)	130.2 (± 10)	80.9 (± 39)	37.2 (± 3.0)	-
18:2	14.22	372	245 (± 16)	190 (± 17)	251 (± 8.0)	189 (± 13)	316 (± 45)	398 (± 23)	377 (± 43)	415 (± 26)	333 (± 209)	367 (± 25)
16:0	14.53	348	21100 (± 3000)	22300 (± 4150)	16600 (± 930)	14100 (± 2300)	18600 (± 2800)	15400 (± 4700)	23200 (± 3200)	21600 (± 3000)	14600 (± 900)	15600 (± 3300)
18:1	14.86	374	625 (± 47)	502 (± 66)	603 (± 22)	572 (± 72)	805 (± 59)	716 (± 28)	791 (± 84)	778 (± 47)	894 (± 36)	813 (± 51)
18:0	17.59	376	46800 (± 12900)	44600 (± 7300)	47900 (± 1200)	33400 (± 9300)	49000 (± 5100)	36700 (± 4600)	45700 (± 6200)	41300 (± 3300)	39400 (± 5300)	33000 (± 2700)

Quantification of compounds was performed in triplicate (n = 3)
-: below limit of detection under the conditions tested
* Method 2: Analysis of underivatized molecules by LC-MS/MS, this method was used to quantify compounds in the upper list section
* Method 3: Analysis of methyl esters of FFA (FAMES) by GC-MS
** Tr. acid: Traumatic acid

-47-

(Table 1). Likewise, levels of free 16:2, CA, OPC-8:0, dnOPDA and traumatol could be either below their LOD or in some cases (CA and dnOPDA) absent in *N. attenuata* leaves. JA-Ile and traumatic acid could not be detected by the present method in non-elicited tissue however they were detected in low amounts by analysis of underivatized extracts (Table 2). Nevertheless, as the amount of these molecules increased after FAC elicitation, they became detectable in their Picolinyl ester forms (Table 2). In contrast, OPC-4:0 and OPC-6:0 could be detected only by the present method after FAC elicitation but not by the analysis of underivatized extracts. For the remaining compounds, a good correlation was observed between the methods used (Table 2).

Finally, increasing amounts of leaf material (5 to 200 mg; fresh weight) were also extracted from *N. attenuata* plants after 60 min of FAC elicitation to determine the range of tissue amounts in which a linear correlation with the amounts of detectable compounds was observed. The results showed a linear correlation between the amount of 11 compounds and the amount of leaf material extracted (Figure 4), indicating that as little as 5 mg of leaf tissue was sufficient for the reliable quantification of these molecules. In the case of JA-Ile, at least 50 mg of leaf tissue were required for detection while for OPC-6:0, OPC-4:0, traumatin and traumatic acid more than 100 mg of tissue were required (Additional file 1, Table S3).

Conclusion

A method was developed that enables the rapid, specific and simultaneous analysis of aliphatic compounds such as free fatty acids and small polar compounds such as phytohormones in *N. attenuata* leaves. Although in this study only a selected number of molecules were tested, the method can be adapted to the needs of the investigator. This method may prove useful in cases in which tissue amounts are limiting (e.g., embryos, ovules, pollen or specific tissue sections obtained by laser micro-dissection) and multiple analytical techniques cannot be used. Additionally, the rapid extraction procedure without additional purification steps may also facilitate the analysis of multiple samples quickly, making it compatible with high-throughput biochemical screenings.

Methods
Plant material and treatments
Seeds of the 30th generation of an inbred line of *Nicotiana attenuata* plants were used as the wild-type genotype (WT) in all experiments. Plants were grown as described in [15]. For all experiments, leaves at nodes +1 of rosette stage (40-day old) plants were used. Wounding was performed by rolling three times a fabric pattern wheel on each side of the midvein. For FAC treatment, the wounds were immediately supplied with 20 µL of synthetic *N*-lino-leoyl-glutamic acid (18:3-Glu; 0.03 nmol/µL in 0.02% (v/v) Tween-20/water). Leaf tissue was collected at 30 and 60 min after the treatments and frozen immediately in liquid nitrogen for subsequent analysis. Non-elicited leaf tissue was collected without any previous treatment.

Chemicals
Chloroform, dichloromethane, methanol and hexane were from VWR (International GmbH, Darmstadt, Germany). JA, SA, ABA, IAA, ICA, traumatic acid, 1, 1'-carbonyldiimidazole, 3-(hydroxymethyl)-pyridine and fatty acids were from Sigma (Taufkirchen, Germany). OPDA was from Cayman Chemicals (Ann Arbor, MI). Cinnamic acid was from Merck KGaA (Darmstadt, Germany). Gibberellins was from Carl Roth GmbH (Karlsruhe, Germany). Traumatin was from Larodan Chemicals (Malmö, Sweden). Traumatol was synthesized by the reduction of traumatin with $NaBH_4$ using standard conditions and $^2H_2$-OPC 8:0 was synthesized by deuteration of OPDA using standard conditions.

Leaf extraction
Extractions were performed according to [13] with the modifications adopted by [14]. Depending on the experiment, different amounts of frozen leaf material were homogenized in 2 mL microcentrifuge tubes (Eppendorf, Hamburg, Germany) containing 2 steel beads (ASK, Korntal-Muenchingen, Germany) by grinding in a Genogrinder (SPEX Certi Prep, Metuchen, NJ) for 30 sec at 1300 strokes min^{-1}. After homogenization, samples were extracted with 1 ml of 10/10/1/1 (v/v/v/v) chloroform/methanol/acetic acid/water spiked with internal standards (0.5 µg heptadecanoic acid, 0.4 µg [$^2H_2$]-JA, [$^2H_4$]-SA, [$^{13}C_6$]-Ja-Ile, [$^2H_6$]-ABA, royal jelly acid). After vortexing for 10 min, the phases were separated by centrifugation at 4°C for 10 min. The organic phase was transferred into a fresh tube and the leaf material re-extracted with 1 ml 5/5/1 (v/v/v) chloroform/methanol/water. After centrifugation, the organic phases were combined, evaporated to dryness under a gentle stream of nitrogen and reconstituted in 0.2 mL of dry dichloromethane for subsequent derivatization. Quantification was made based on the internal standards added and calibration curves.

Picolinyl ester derivatization
Formation of Picolinyl ester derivatives of free carboxylic acids was performed as described in [10]. Briefly, 0.2 mL of leaf extract in dichloromethane were mixed with 0.1 mL of freshly prepared 1% (w/v) 1, 1'-carbonyldiimidazole/dichloromethane. After 1 min, 0.2 mL of freshly prepared 0.1/1/1 (v/v/v) 3-(hydroxymethyl)-pyridine/dichloromethane/triethylamine containing catalytic amounts of 4-(1-pyrrolidinyl)-pyridine were added and the mixture heated for 10 min at 37°C. The reaction was stopped by the addition of 25 µL of acetic acid. Samples
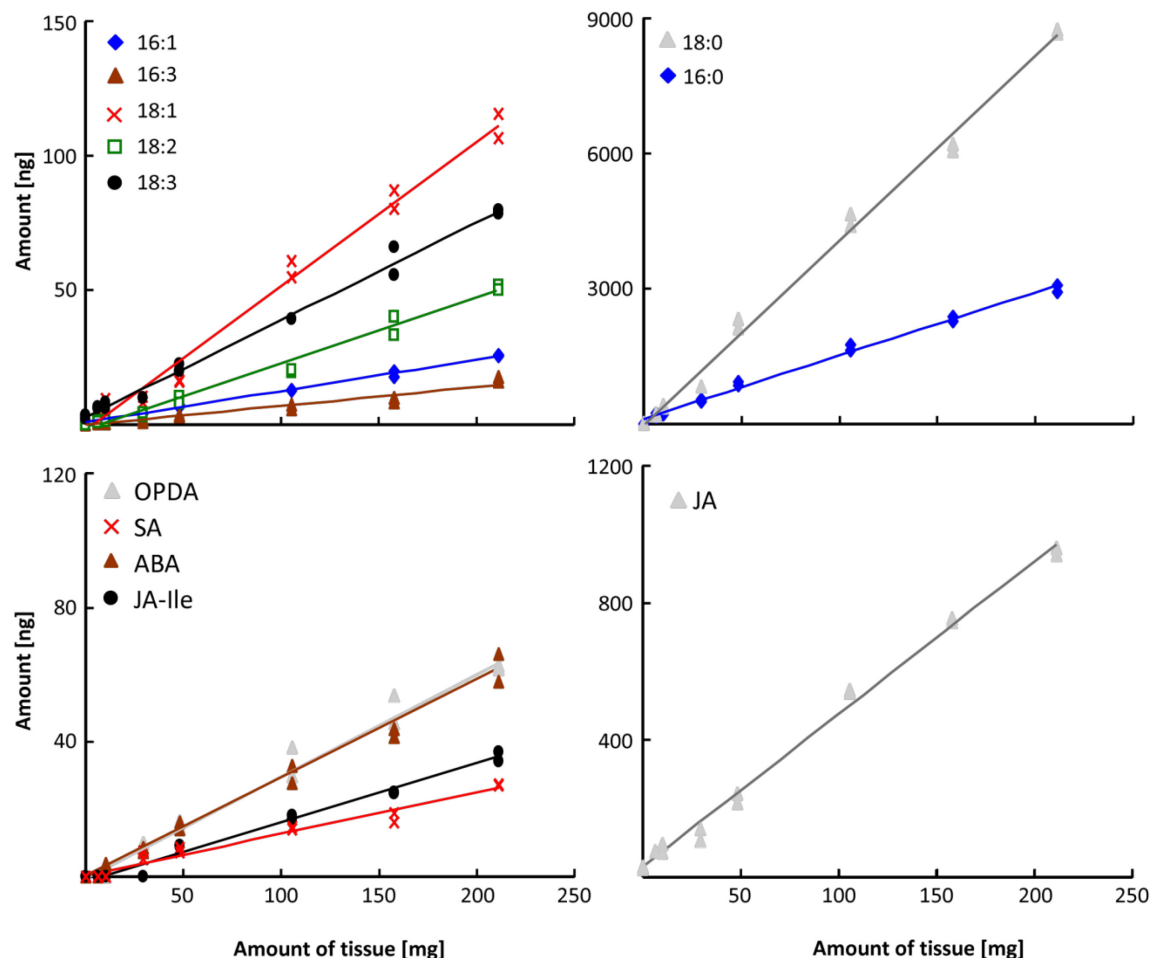
Figure 4
Example of the linear correlation between the amounts of leaf tissue extracted from FAC elicited *N. attenuata* leaves and the amounts of compounds detected. Different amounts of leaf tissue (5 to 250 mg; fresh weight) from *N. attenuata* plants were collected after 60 min of FAC elicitation. Leaf material was extracted, derivatized and analyzed by LC-MS/MS. Two biological replicates were performed for each amount of tissue.

were dried under a stream of nitrogen and 0.5 mL of water were added. Picolinyl ester derivatives were extracted twice with 0.5 mL hexane, the solvent evaporated under a stream of nitrogen and the samples reconstituted in 70/30 (v/v) methanol/water for LC-MS/MS analysis.

LC-MS/MS analysis

Picolinyl ester derivatives were analyzed in an LC-MS/MS system (Varian 1200 Triple-Quadrupole-LC-MS system; Varian, Palo Alto, CA, USA http://www.varianinc.com). Ten µL of the sample were injected onto a ProntoSIL® column (C18; 5 µm, 50 × 2 mm, Bischoff, Germany; http://www.bischoff-chrom.de) attached to a precolumn (C18, 4 × 2 mm, Phenomenex, USA). As mobile phases 0.05%/1% (v/v/v) formic acid/methanol/water (solvent A) and methanol (solvent B) were used in a gradient mode with the following conditions: time/concentration (min/%) for B: 0.0/15; 1.5/15; 4.5/98; 19.5/98; 20.5/15; 25.0/15; time/flow (min/mL): 0.0/0.4; 1.0/0.4; 1.5/0.2; 18.5/0.2; 19.5/0.4; 25/0.4. To minimize contaminations the solvent eluting from the column was injected into the mass spectrometer only between 1.5 and 18.5 min. Between 0 and 1.5 min and 18.5 and 25 min a mixture of 1/1 (v/v) methanol/water was injected to flush the MS/MS system.

The MS was used in ion positive mode and ions detected using multiple reaction monitoring (MRM) and their respective m/z transitions $[M+H]^+ > 92$ (Table 1) after collision induced fragmentation with argon gas under -25.5 V collision energy. For ionization, the needle was set at 5000 V and the drying gas (nitrogen) at 300 °C and 20 psi (housing 50 °C). The detector was set at 1800 V. Samples were kept at room temperature (RT) and separation was also performed at RT. Analysis of underivatized phytohormones from crude leaf extracts was performed as previously described [6].

Analysis of FFA by GC-MS

FFA extraction was performed according to [14]. Heptadecanoic acid (0.5 μg per sample) was added as internal standard for quantification. After extraction, samples were reconstituted in 0.2 mL of chloroform and lipids were separated on Partisil® K6 silica plates (Whatman, Dassel, Germany) which were developed with 70/30/1 (v/v/v) hexane/diethyl ether/acetic acid. Commercial FFAs were used as standards and plates were stained with 2% (v/v) 2'-7'-dichlorofluorescin/methanol and lipids were visualized under UV light. FFA were eluted from the silica with 3 mL of 2/1 (v/v) chloroform/methanol and methylated in 1% (v/v) H_2SO_4/methanol for 1 h at 75 °C. Fatty acid methyl esters were extracted with hexane and analyzed in a Varian CP-3800 GC coupled with a Varian Saturn 3800 ion trap MS in electron ionisation (EI; 70 eV) mode (Varian, Palo Alto, CA). One μl of the sample was injected in splitless mode on a DB-WAX column (30 m × 0.25 mm I.D., 0.25 μm film thickness, Agilent, Boeblingen, Germany) with helium at a constant flow of 1 mL min^{-1} as the carrier gas. The injector was at 230 °C. The oven temperature program was: 130 °C for 5 min, 220 °C at 3.0 °C/min, 5 °C/min ramp to 240 °C and hold for 1 min. EI spectra were recorded on Scan mode from 40 to 400 amu. Quantification was performed in the linear range of detection and based on calibration curves generated with increasing concentrations of commercial FAMES mixes (Matreya, Pleasant Gap, PA) and the IS (17:0).

List of abbreviations

GC-MS: gas chromatography-mass spectrometry; ESI: electrospray ionization; MRM: multi reaction monitoring; FFA: free fatty acids; IAA: indole-3-acetic acid; IBA: indole-3-butyric acid; ICA: indole-3-carboxylic acid; ABA: abscisic acid; JA: jasmonic acid; JA-Ile: jasmonyl-isoleucine; OPDA: 12-oxo-phytodienoic acid; dnOPDA: dinor-OPDA; SA: salicylic acid; Traumatic acid: 2E-dodecendioic acid; Traumatin: 12-oxo-10*E*-dodecenoic acid; Traumatol: 12-hydroxy-9Z-dodecenoic acid; Royal jelly acid: 10-hydroxy-*trans*-2-decenoic acid; GA: gibberellin.

Competing interests

The authors declare that they have no competing interests.

Authors' contributions

MK carried out the experiments and drafted the manuscript. ITB participated in the design and coordination of the study and helped to draft the manuscript. GB conceived of the study, participated in its design and coordination and helped to draft the manuscript. All authors read and approved the final manuscript.

Additional material

> **Additional file 1**
>
> *Table S1*: *Coefficients of variation (CV) of replicate measurements for standard mixtures at different concentrations and leaf sample.* **Table S2**. *Analysis of derivatized N.attenuata leaf extracts after multiple extractions and calculation of recovery rates.* **Table S3**: *Analysis of different amounts of N. attenuata leaf material.*
> Click here for file
> [http://www.biomedcentral.com/content/supplementary/1746-4811-5-17-S1.PDF]

References

1. Lima ES, Abdalla DSP: **High-performance liquid chromatography of fatty acids in biological samples.** *Analytica Chimica Acta* 2002, **465(1-2)**:81-91.
2. Johnson DW: **Contemporary clinical usage of LC/MS: Analysis of biologically important carboxylic acids.** *Clinical biochemistry* 2005, **38(4)**:351-361.
3. Nishikaze T, Takayama M: **Study of factors governing negative molecular ion yields of amino acid and peptide in FAB, MALDI and ESI mass spectrometry.** *International Journal of Mass Spectrometry* 2007, **268(1)**:47-59.
4. Forcat S, Bennett MH, Mansfield JW, Grant MR: **A rapid and robust method for simultaneously measuring changes in the phytohormones ABA, JA and SA in plants following biotic and abiotic stress.** *Plant Methods* 2008, **4**:16.
5. Pan XQ, Welti R, Wang XM: **Simultaneous quantification of major phytohormones and related compounds in crude plant extracts by liquid chromatography-electrospray tandem mass spectrometry.** *Journal of Phytochemistry* 2008, **69(8)**:1773-1781.
6. Diezel C, von Dahl CC, Gaquerel E, Baldwin IT: **Different Lepidopteran Elicitors Account for Cross-Talk in Herbivory-Induced Phytohormone Signaling.** *Plant Physiology* 2009, **150(3)**:1576-1586.
7. Valianpour F, Selhorst JJM, van Lint LEM, van Gennip AH, Wanders RJA, Kemp S: **Analysis of very long-chain fatty acids using electrospray ionization mass spectrometry.** *Molecular Genetics and Metabolism* 2003, **79(3)**:189-196.
8. Myher JJ, Kuksis A: **General strategies in chromatographic analysis of lipids.** *Journal of Chromatography B: Biomedical Sciences and Applications* 1995, **671(1-2)**:3-33.
9. Rezanka T: **Identification of very long chain fatty acids by atmospheric pressure chemical ionization liquid chromatography-mass spectroscopy from green alga Chlorella kessleri.** *Journal of Separation Science* 2002, **25(18)**:1332-1336.

Page 10 of 11
(page number not for citation purposes)

10. Christie WW: **Lipid Analysis; Isolation, Separation, Identifica-tion and Structural Analysis of Lipids.** *Volume 15.* 3rd edition. Bridgwater, England: The Oily Press; 2003.
11. Halitschke R, Schittko U, Pohnert G, Boland W, Baldwin IT: **Molec-ular interactions between the specialist herbivore Manduca sexta (Lepidoptera, Sphingidae) and its natural host Nico-tiana attenuata. III. Fatty acid-amino acid conjugates in her-bivore oral secretions are necessary and sufficient for herbivore-specific plant responses.** *Plant Physiology* 2001, **125(2):**711-717.
12. Kessler A, Baldwin IT: **Plant responses to insect herbivory: The emerging molecular analysis.** *Annual Review of Plant Biology* 2002, **53:**299-328.
13. Folch J, Lees M, Stanley GHS: **A Simple Method for the Isolation and Purification of Total Lipides from Animal Tissues.** *Journal of Biological Chemistry* 1957, **226(1):**497-509.
14. Conconi A, Miquel M, Browse JA, Ryan CA: **Intracellular levels of free linolenic and linoleic acids increase in tomato leaves in response to wounding.** *Plant Physiology* 1996, **111(3):**797-803.
15. Krugel T, Lim M, Gase K, Halitschke R, Baldwin IT: **Agrobacterium-mediated transformation of Nicotiana attenuata, a model ecological expression system.** *Chemoecology* 2002, **12(4):**177-183.

Table S1: Coefficients of variation (CV) of replicate measurements for standard mixtures at different concentrations and leaf sample.

Number	Substance	CV (calibration standards)*						CV (leaf sample)*	
		100 pg/μL	250 pg/μL	375 pg/μL	500 pg/μL	750 pg/μL	1000 pg/μL	Intial analysis	analysis after 2 days
1	$^{13}C_6$-jasmonic acid-isoleucine ($^{13}C_6$-JA-Ile)	0.091	0.068	0.054	0.041	0.039	0.031	0.043	0.061
2	Jasmonic acid-isoleucine (JA-Ile)	0.097	0.072	0.048	0.034	0.045	0.033	0.066	0.072
3	$^2H_4$-salicylic acid ($^2H_4$-SA)	0.092	0.037	0.035	0.035	0.04	0.025	0.027	0.045
4	Salicylic acid (SA)	0.091	0.089	0.056	0.031	0.043	0.022	0.043	0.059
5	$^2H_6$-abscisic acid ($^2H_6$-ABA)	0.058	0.047	0.036	0.036	0.06	0.019	0.048	0.051
8	Abscisic acid (ABA)	0.037	0.027	0.033	0.02	0.056	0.014	0.041	0.049
7	Indole-3-carboxylic acid (ICA)	0.094	0.093	0.066	0.052	0.041	0.017	-	-
8	Royal jelly acid (Tr IS)	0.088	0.076	0.031	0.026	0.063	0.037	0.045	0.047
9	Cinnamic acid (CA)	0.048	0.043	0.034	0.015	0.053	0.008	-	-
10	Jasmonic acid (JA)	0.04	0.071	0.031	0.018	0.047	0.006	0.017	0.015
11	Traumatol	0.097	0.091	0.061	0.013	0.01	0.018	-	-
13	Indole-3-acetic acid (IAA)	0.084	0.099	0.088	0.052	0.051	0.035	-	-
14	Traumatin	0.096	0.094	0.067	0.054	0.021	0.021	0.091	0.087
15	9,10-$^2H_2$-dihydro-jasmonic acid (D$_2$-JA)	0.048	0.06	0.032	0.025	0.046	0.009	0.021	0.022
16	Traumatic acid	0.081	0.073	0.055	0.046	0.039	0.023	0.062	0.068
17	Hexadecatrieonic acid (16:3)	0.051	0.09	0.014	0.018	0.05	0.006	0.087	0.082
18	(9S, 13S)-12-oxo-phytodienoic acid (OPDA)	0.048	0.074	0.062	0.045	0.044	0.021	0.045	0.098
19	Hexadecadienoic acid (16:2)	0.083	0.081	0.054	0.033	0.039	0.024	-	-
20	Gibberellin A$_3$ (GA$_3$)	0.086	0.068	0.059	0.047	0.043	0.034	-	-
12	$^2H_2$-OPC 8:0	0.098	0.096	0.068	0.052	0.052	0.021	0.018	0.024
21	Linolenic acid (18:3)	0.054	0.08	0.031	0.037	0.043	0.025	0.053	0.048
22	Hexadecenoic acid (16:1)	0.095	0.096	0.074	0.049	0.051	0.036	0.072	0.058
23	Heptadecenoic acid (17:1)	0.06	0.063	0.046	0.053	0.046	0.018	0.016	0.016
24	Linoleic acid (18:2)	0.087	0.081	0.069	0.061	0.051	0.038	0.05	0.043
25	Hexadecanoic acid (16:0)	0.089	0.011	0.05	0.031	0.061	0.03	0.021	0.024
26	Octadecenoic acid (18:1)	0.095	0.092	0.081	0.036	0.012	0.011	0.028	0.031
27	Heptadecanoic acid (17:0)	0.055	0.061	0.041	0.06	0.041	0.016	0.01	0.011
28	Stearic acid (18:0)	0.044	0.08	0.073	0.061	0.036	0.023	0.007	0.015

* CVs were calculated based on 10 injections for each sample.

Table S2. Analysis of derivatized *N.attenuata* leaf extracts after multiple extractions and calculation of recovery rates ($n =10$)

Substance	control ng gFW^{-1} (±SD)		W+FAC (60 min) ng gFW^{-1} (±SD)		Recovery rates [%]
JA-Ile	-		**114**	(± 9.8)	98.3
SA	**184**	(± 15)	**153**	(± 13)	98.2
ABA	**233**	(± 14)	**264**	(± 11)	98.7
ICA		-		-	
CA		-		-	
JA	**295**	(± 22)	**4380**	(± 67)	99.5
Traumatol		-		-	
dnOPDA		-		-	
IAA		-		-	
Traumatin	**11.3**	(± 0.6)	**17.7**	(± 0.9)	100
Tr. acid**		-	**25.2**	(± 1.8)	100
16:3	**29.6**	(± 2.4)	**41.4**	(± 3.5)	100
OPC-4:0		-	**13,1**	(± 1.0)	100
OPC-6:0		-	**18,9**	(± 1.5)	100
OPDA	**99.3**	(± 6.7)	**254**	(± 14)	97.6
16:2		-		-	
GA$_3$		-		-	
OPC-8:0		-		-	
GA$_4$		-		-	
18:3	**445**	(± 21)	**399**	(± 13)	99
16:1	**44**	(± 2.5)	**79**	(± 6)	100
18:2	**253**	(± 21)	**297**	(± 19)	98.4
16:0	**19300**	(± 1800)	**16800**	(± 1300)	99.3
18:1	**638**	(± 51)	**705**	(± 35)	98.6
18:0	**57600**	(± 2800)	**47200**	(± 1200)	

**: Traumatic acid

Table S3: Analysis of different amounts of *N. attenuata* leaf material (*n*=2)

Substance	5 mg		10 mg		30 mg		50 mg		100 mg		150 mg		200 mg	
	mass leaf tissue													
	Total amount obtained [ng]													
JA-Ile	-		-		-		9.14	(± 0.27)	17.5	(± 1.0)	24.8	(± 0.32)	35.6	(± 1.8)
SA	0.92	(± 0.15)	2.16	(± 0.28)	6.26	(± 0.69)	7.5	(± 0.19)	14.4	(± 0.6)	17.5	(± 2.0)	26.7	(± 0.3)
ABA	0.94	(± 0.003)	2.95	(± 0.15)	7.4	(± 0.58)	15.2	(± 1.6)	30.4	(± 3.6)	42.7	(± 1.7)	62.1	(± 5.7)
ICA	-		-		-		-		-		-		-	
CA	-		-		-		-		-		-		-	
JA	62.0	(± 0.2)	83.0	(± 18)	123	(± 13)	229	(± 21)	540	(± 4.5)	748	(± 8)	949	(± 15)
Traumatol	-		-		-		-		-		-		-	
dnOPDA	-		-		-		-		-		-		-	
IAA	-		-		-		-		-		-		-	
Traumatin	-		-		-		-		-		1.67	(± 0.08)	2.71	(± 0.18)
Tr. acid**	-		-		-		-		-		3.0	(± 0.14)	4.44	(± 0.47)
16:3	0.73	(± 0.10)	1.38	(± 0.07)	1.53	(± 0.05)	3.12	(± 0.19)	6.37	(± 0.11)	9.02	(± 1.22)	16.8	(± 0.98)
OPC-4:0	-										3.01	(± 0.13)	3.61	(± 0.09)
OPC-6:0	-										1.17	(± 0.10)	2.38	(± 0.15)
OPDA	1.32	(± 0.58)	2.96	(± 0.23)	9.21	(± 0.44)	13.1	(± 1.42)	33.0	(± 6)	49.2	(± 6.7)	65.1	(± 0.5)
16:2	-		-		-		-		-		-		-	
GA$_3$	-		-		-		-		-		-		-	
OPC-8:0	-		-		-		-		-		-		-	
GA$_4$	-		-		-		-		-		-		-	
18:3	5.16	(± 0.32)	7.13	(± 1.41)	9.92	(± 0.07)	21.1	(± 1.73)	39.3	(± 0.1)	60.9	(± 7.3)	79.1	(± 0.7)
16:1	1.5	(± 0.017)	3.26	(± 0.48)	4.34	(± 0.12)	6.82	(± 0.50)	12.7	(± 0.3)	18.9	(± 1.6)	25.6	(± 0.5)
18:2	5.35	(± 0.006)	9.33	(± 1.23)	16.5	(± 2.3)	19.2	(± 1.45)	36.4	(± 1.4)	56.7	(± 4.7)	71	(± 1.4)
16:0	57	(± 13)	140	(± 8)	470	(± 40)	868	(± 15)	1608	(± 151)	2258	(± 61)	2949	(± 131)
18:1	3.34	(± 0.56)	5.46	(± 0.51)	8.16	(± 0.91)	20.8	(± 2.5)	58	(± 4)	82.7	(± 3.8)	114	(± 8)
18:0	209	(± 37)	463	(± 12)	731	(± 2)	2178	(± 76)	4476	(± 168)	6070	(± 34)	8705	(± 69)

**: Traumatic acid

Nicotiana attenuata SIPK, WIPK, NPR1, and Fatty Acid-Amino Acid Conjugates Participate in the Induction of Jasmonic Acid Biosynthesis by Affecting Early Enzymatic Steps in the Pathway[1][W][OA]

Mario Kallenbach[2], Fiammetta Alagna[2], Ian Thomas Baldwin, and Gustavo Bonaventure*

Max Planck Institute for Chemical Ecology, Department of Molecular Ecology, Jena 07745, Germany

Wounding and herbivore attack elicit the rapid (within minutes) accumulation of jasmonic acid (JA) that results from the activation of previously synthesized biosynthetic enzymes. Recently, several regulatory factors that affect JA production have been identified; however, how these regulators affect JA biosynthesis remains at present unknown. Here we demonstrate that *Nicotiana attenuata* salicylate-induced protein kinase (SIPK), wound-induced protein kinase (WIPK), nonexpressor of PR-1 (NPR1), and the insect elicitor *N*-linolenoyl-glucose (18:3-Glu) participate in mechanisms affecting early enzymatic steps of the JA biosynthesis pathway. Plants silenced in the expression of SIPK and NPR1 were affected in the initial accumulation of 13-hydroperoxy-linolenic acid (13-OOH-18:3) after wounding and 18:3-Glu elicitation by mechanisms independent of changes in 13-lipoxygenase activity. Moreover, 18:3-Glu elicited an enhanced and rapid accumulation of 13-OOH-18:3 that depended partially on SIPK and NPR1 but was independent of increased 13-lipoxygenase activity. Together, the results suggested that substrate supply for JA production was altered by 18:3-Glu elicitation and SIPK- and NPR1-mediated mechanisms. Consistent with a regulation at the level of substrate supply, we demonstrated by virus-induced gene silencing that a wound-repressed plastidial glycerolipase (NaGLA1) plays an essential role in the induction of de novo JA biosynthesis. In contrast to SIPK and NPR1, mechanisms mediated by WIPK did not affect the production of 13-OOH-18:3 but were critical to control the conversion of this precursor into 12-oxo-phytodienoic acid. These differences could be partially accounted for by reduced allene oxide synthase activity in WIPK-silenced plants.

Jasmonic acid (JA) and some of its precursors and derivatives are signal molecules that function as essential mediators of the plant's wound, antiherbivore, and antipathogen responses, as well as in growth and development (Farmer, 1994; Creelman and Mullet, 1997; Turner et al., 2002). In unelicited mature leaves, JA is maintained at very low levels, however, upon specific stimulations, its biosynthesis is induced within a few minutes (Glauser et al., 2008). This rapid biosynthetic response must result from the activation of constitutively expressed JA biosynthesis enzymes in unelicited tissue by substrate availability and/or post-translational modifications. At present, little is known about the molecular mechanisms that activate JA biosynthetic enzymes.

According to the canonical mechanism for JA biosynthesis (Vick and Zimmerman, 1983), free α-linolenic acid ($18:3^{\Delta9,12,15}$, 18:3) forms 13(*S*)-hydroperoxyoctadecatrienoic acid [13S-(OOH)-18:3] by the action of 13-lipoxygenase (13-LOX) in plastids. 13S-(OOH)-18:3 is converted by allene oxide synthase (AOS) into a highly unstable allene oxide intermediate that is processed by allene oxide cyclase (AOC) to yield (9*S*,13*S*)-12-oxo-phytodienoic acid (OPDA). OPDA is transported from the plastid into the peroxisome where it is reduced by the action of OPDA reductase 3 (OPR3) and after three cycles of β-oxidation, (3*R*,7*S*)-JA is formed. Due to the large number of enzymes and different cellular compartments involved in JA biosynthesis, it is expected that the pathway is regulated at multiple steps. Resolution of the structures of the tomato (*Solanum lycopersicum*) OPR3 and Arabidopsis (*Arabidopsis thaliana*) AOC2 and ACX1 has provided insights into potential regulatory mechanisms for these enzymes (e.g. oligomerization and phosphorylation; Pedersen and Henriksen, 2005; Breithaupt et al., 2006; Hofmann et al., 2006).

The identification of two Arabidopsis plastidial glycerolipases, DAD1 and DGL (Ishiguro et al., 2001; Hyun et al., 2008), has provided genetic evidence for the importance of the release of trienoic fatty acids (FAs) from plastidial lipids in the activation of JA biosynthesis. Recently, some oxylipins have been

---

found esterified to galactolipids in Arabidopsis leaves and hence it is possible that in this species preformed precursors could also supply the JA biosynthesis pathway after their release from lipids (Stelmach et al., 2001; Hisamatsu et al., 2003; Buseman et al., 2006). However, lipid-bound oxylipins are not formed in the leaves of all plant families (Böttcher and Weiler, 2007).

In *Nicotiana attenuata*, wound-induced JA production is amplified by the application of lepidopteran larvae (e.g. *Manduca sexta*) oral secretions (OS) to mechanical wounds. Major elicitors of the OS-mediated response are FA-amino acid conjugates (FACs) that are sufficient to enhance JA production in leaves of this plant species (Halitschke et al., 2001). Recently, several regulatory factors with a potential function upstream of JA biosynthesis have been identified (Ludwig et al., 2005; Takabatake et al., 2006; Schweighofer et al., 2007; Takahashi et al., 2007); however, how these regulators affect JA biosynthesis is at present unknown. For example, wounding and herbivory in *Nicotina* spp. and tomato activate the mitogen-activated protein kinases salicylate-induced protein kinase (SIPK) and wound-induced protein kinase (WIPK; Seo et al., 1999; Kandoth et al., 2007; Wu et al., 2007). When SIPK and WIPK expression is silenced in tobacco (*Nicotiana tabacum*), the plants accumulate 60% to 70% less JA than wild type after wounding or OS elicitation (Seo et al., 2007; Wu et al., 2007). Another regulatory component that affects JA production in *N. attenuata* is Nonexpressor of PR-1 (NPR1), an essential component of the salicylic acid (SA) signal transduction pathway first identified in Arabidopsis (Cao et al., 1994). *N. attenuata* NPR1-silenced plants accumulate 60% to 70% lower JA levels after elicitation than wild type (Rayapuram and Baldwin, 2007). NPR1 interacts with the JA and ethylene signaling cascades, and a cytosolic role for this factor in the regulation of JA-dependent responses/biosynthesis has been proposed (Spoel et al., 2003).

In contrast to the mechanisms acting upstream of JA biosynthesis, the mechanisms mediating downstream JA responses are better characterized (Kazan and Manners, 2008; Browse, 2009). Among the best-characterized regulators of these responses is *CORONATIVE INSENSITIVE1* (*COI1*), a gene that participates in jasmonate perception (Xie et al., 1998) and regulates gene expression through its interaction with the JASMONATE ZIM-DOMAIN repressors (Chini et al., 2007; Thines et al., 2007).

To understand the early processes regulating the activation of JA biosynthesis by wounding and FAC elicitation in *N. attenuata* leaves, we quantified the initial rates of accumulation of plastid-derived JA precursors after these stimuli in wild type and four JA-deficient genotypes previously described: ir-sipk, ir-wipk, ir-npr1, and ir-coi1 (Rayapuram and Baldwin, 2007; Paschold et al., 2008; Meldau et al., 2009). We show that SIPK, WIPK, NPR1, and FACs contribute to the activation of de novo JA biosynthesis by affecting

diverse early enzymatic steps in this pathway. The identification of a plastidial glycerolipase A_1 type I family protein (GLA1) essential for JA biosynthesis pointed to this enzyme as one potential target of some of these activating mechanisms.

RESULTS

Analysis of the Initial Rates of Accumulation of JA Precursors after Wounding and FAC Elicitation

Wound- and FAC-inducible precursors of the JA biosynthetic pathway generated by the initial set of reactions in the plastid were profiled within short intervals after stimulation (0–10 min). Because JA accumulation occurs by de novo synthesis in *N. attenuata*, the rates of accumulation of these precursors within a few minutes of the wound response reflect the rapid and differential activation of specific JA biosynthetic steps when plants are subjected to different treatments. This activation therefore precedes the JA-induced transcriptional activation of JA biosynthesis genes. To study the mechanisms underlying the FAC-mediated induction of JA biosynthesis, synthetic *N*-linolenoyl-Glu (18:3-Glu) was applied onto the wounds as a single elicitor.

Because the release of trienoic FAs from membranes is considered one of the earliest regulated steps in JA biosynthesis, the absolute amounts and FA composition of four major leaf membrane glycerolipids, monogalactosyldiacylglycerol (MGDG), digalactosyldiacylglycerol, phosphatidylethanolamine, and phosphatidylcholine (PC) were first quantified within 20 min after wounding and FAC elicitation in leaves of wild-type plants. Within 10 and 20 min, JA already accumulated between 6 and 20 nmol g fresh weight $(FW)^{-1}$ (see below). Within 20 min, no significant changes in the absolute amounts of glycerolipids and their FA composition were detected (Supplemental Fig. S1a; Supplemental Table S1).

Second, levels of free FAs (FFAs) were quantified within 10 min after wounding and FAC elicitation in wild-type leaves. In unelicited tissue, total FFA accumulated to 156 ± 11 nmol g FW^{-1}, with approximately 90% of this value corresponding to saturated FFA (16:0 and 18:0) and 10% to unsaturated FFA. Saturated FFA are common constituents of epicuticular waxes and analysis of *N. attenuata* leaf waxes showed that at least 80% of total free 16:0 and 18:0 originated from the cuticle (50 ± 0.9 and 58 ± 1.3 nmol g FW^{-1}, respectively). Thus, further analysis was focused on detectable free unsaturated FA ($16:3^{\Delta 7,10,13}$, $18:1^{\Delta 9}$, $18:2^{\Delta 9,12}$, and $18:3^{\Delta 9,12,15}$). Within 10 min after the treatments, no significant changes in the levels of unsaturated FFAs were observed (Supplemental Fig. S1b), in particular of 18:3 (the major JA precursor; Fig. 1). Thus, similar to glycerolipid levels, levels of unsaturated FFA did not change significantly after wounding and FAC elicitation.
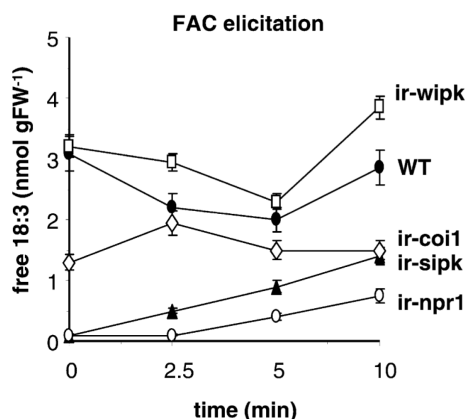
Kallenbach et al.

Figure 1. Levels of free 18:3 in FAC-elicited wild-type (WT) and RNAi-silenced leaves. Leaves of rosette stage wild-type, ir-sipk, ir-wipk, ir-npr1, and ir-coi1 plants were FAC elicited for different times, FFA isolated, and free 18:3 quantified. Bars = ±SE, $n = 4$. For statistical analysis, see text.

Levels of Unsaturated FFA Are Reduced in ir-sipk, ir-npr1, and ir-coi1 Plants

Total levels of unsaturated FFA were analyzed in leaves of ir-sipk, ir-wipk, ir-npr1, and ir-coi1 within 10 min after wounding and FAC elicitation. Changes in the levels of these molecules were similar between the two treatments and therefore data for FAC elicitation is only presented (Supplemental Fig. S2), and for clarity, the results corresponding to free 18:3 are presented in Figure 1. Basal levels of free 18:3 were similar to wild type in ir-wipk plants, however, reduced by approximately 10-fold in ir-sipk and ir-npr1 and by approximately 2-fold in ir-coi1 leaves (Fig. 1; $P < 0.05$, t test, wild type versus genotypes). Within 10 min after wounding and FAC elicitation, the levels of free 18:3 slowly increased in ir-sipk and ir-npr1 plants but remained nonetheless at approximately 50% and approximately 30% of wild-type levels, respectively (Fig. 1). In contrast, they remained approximately constant in ir-coi1 plants (Fig. 1). Importantly, the levels of all unsaturated FFAs were reduced in ir-sipk, ir-npr1, and ir-coi1 plants (Supplemental Fig. S2), suggesting a general alteration in FFA homeostasis in these genotypes. Quantification of MGDG, digalactosyldiacylglycerol, PC, and phosphatidylethanolamine and their FA composition in ir-sipk and ir-npr1 plants showed no significant variations compared to wild type (data not shown), suggesting that membrane glycerolipid homeostasis was not affected in these genotypes.

13-(OOH)-18:3 Production Is Differentially Induced by FAC Elicitation and Deficient in ir-sipk, ir-coi1, and ir-npr1 Plants

The levels of total free 13-(OOH)-18:3 were quantified within 10 min after wounding and FAC elicitation in wild-type and RNAi-silenced plants. In unelicited wild-type leaves, 13-(OOH)-18:3 accumulated at approximately 0.02 nmol g FW^{-1} and wounding induced a linear increase to 0.035 nmol g FW^{-1} after 5 min, the levels remaining constant for 10 min (Fig. 2A). Within 1.25 min after FAC elicitation, 13-(OOH)-18:3 levels peaked to approximately 0.07 nmol g FW^{-1} (a 2.5-fold induction compared to wounded levels at 1.25 min; $P < 0.05$, t test, wounding versus FAC elicitation) and remained at approximately 0.06 nmol g FW^{-1} within 10 min (Fig. 2A).

Similar to unsaturated FFA levels, the levels of 13-(OOH)-18:3 in ir-wipk were similar to wild type in both unelicited and elicited leaves (Fig. 2A). In contrast, basal levels of 13-(OOH)-18:3 were >2-fold lower in ir-sipk, ir-npr1, and ir-coi1 plants compared to unelicited wild-type plants (Fig. 2A; $P < 0.05$, t test, wild type versus genotypes). Moreover, after wounding, 13-(OOH)-18:3 levels were not induced in these silenced genotypes and at 10 min the levels remained >3-fold lower than in wild-type plants (Fig. 2A; $P < 0.05$, t test, wild type versus genotypes). After FAC elicitation, 13-(OOH)-18:3 levels were induced in ir-sipk, ir-npr1, and ir-coi1 plants, however, the maximum levels attained were still >2-fold lower than those in wild-type plants (Fig. 2A).

N. attenuata expresses two major 13-LOXs in leaves, LOX2 and LOX3. These two enzymes have been associated to C_6 volatile and JA biosynthesis, respectively (Halitschke et al., 2004). To quantify the fraction of total 13-(OOH)-18:3 (S + R enantiomers) originating from 13-LOX activity (S enantiomers), plants silenced in the expression of LOX3 (ir-lox3) and both LOX2 and LOX3 (ir-lox2/ir-lox3) were analyzed. ir-lox3 plants showed a significant approximately 50% reduction in basal levels of 13-(OOH)-18:3 compared to unelicited wild-type leaves (Fig. 2B; $P < 0.05$, t test, wild type versus ir-lox3) and within 10 min after wounding, the levels increased to wild-type levels (approximately 0.035 nmol g FW^{-1}), however, they were not enhanced by FAC elicitation (Fig. 2B). ir-lox2/ir-lox3 plants showed 3-fold-lower basal levels of 13-(OOH)-18:3 (approximately 0.007 nmol g FW^{-1}; $P < 0.01$, t test, wild type versus ir-lox2/ir-lox3) compared to wild type and the levels were not induced after wounding or FAC elicitation (Fig. 2B). The results indicated that LOX3 was responsible for most of the FAC-induced accumulation of 13-(OOH)-18:3 and that at least 60% to 70% of basal and almost all wound- and FAC-induced 13-(OOH)-18:3 derived from LOX2 and LOX3 activities.

OPDA Accumulation Is Compromised in ir-sipk, ir-wipk, ir-npr1, and ir-coi1 Plants

Initial changes in OPDA and dinorOPDA (dnOPDA) levels were quantified after wounding and FAC elicitation in wild-type plants and the four RNAi-silenced genotypes. In unelicited wild-type leaves, OPDA accumulated to levels <0.2 nmol g FW^{-1} and increased after 5 min of both stimuli to approximately
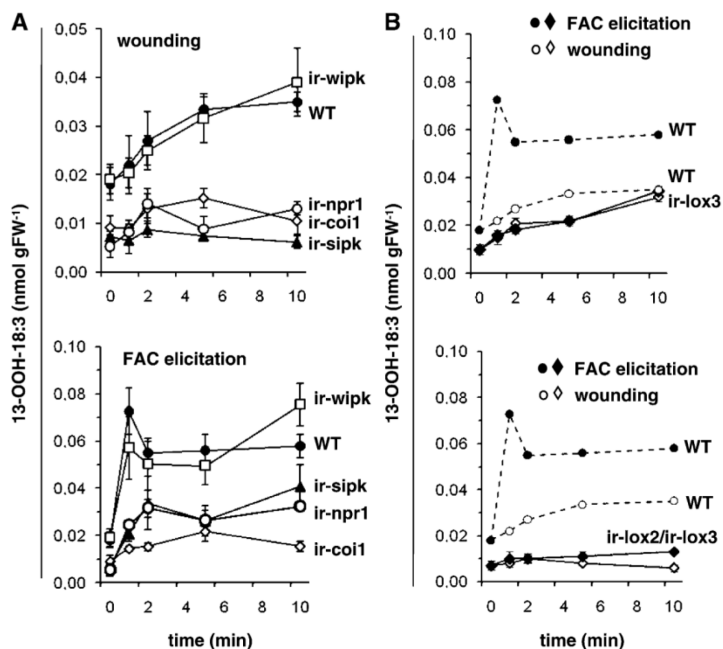
Figure 2. 13-(OOH)-18:3 levels in wild-type (WT) and RNAi-silenced plants. A, Leaves of rosette stage wild-type, ir-sipk, ir-wipk, ir-npr1, and ir-coi1 plants were wounded or FAC elicited, hydroperoxy-FA isolated, and free 13-(OOH)-18:3 quantified at different times. B, Leaves of rosette stage ir-lox3 and ir-lox2/ir-lox3 plants were treated and analyzed as above. Wild-type levels of 13-(OOH)-18:3 from A were also included (without SE) to ease the comparability. Bars = ±SE, $n = 5$. For statistical analysis, see text.

2 nmol g FW^{-1}. After wounding, the levels remained approximately constant for 10 min, however, FAC elicitation induced the accumulation of OPDA to 6 nmol g FW^{-1} at 10 min (Fig. 3A). dnOPDA could not be detected. Within 5 min after wounding or FAC elicitation, the rates of OPDA accumulation were >90% lower in ir-sipk, ir-wipk, ir-npr1, and ir-coi1 compared to wild type, and at 10 min its levels were on average 2- to 4-fold lower than in wild type (Fig. 3A; $P < 0.05$, t test, wild type versus genotypes).

We also determined whether OPDA accumulated as glycerolipid-esterified forms in *N. attenuata* leaves before and 15, 30, and 60 min after wounding and FAC elicitation. Neither OPDA nor dnOPDA could be detected in the glycolipid or polar lipid fractions whereas their levels in the neutral lipid fraction were similar to free levels in nonhydrolyzed samples (data not shown).

Quantification of JA levels within 10 min in wild-type plants showed that wounding and FAC elicitation stimulated an increase in its levels from approximately 0.25 nmol g FW^{-1} to approximately 6 nmol g FW^{-1} (Fig. 3B). Differential accumulation of JA upon FAC elicitation was detected only after 10 min (Supplemental Fig. S3) and was consistent with the sequential and differential accumulation of 13-(OOH)-18:3 and OPDA (Fig. 2A; Supplemental Fig. S3). Basal levels of JA in unelicited tissue were several-fold lower in the four silenced genotypes compared to wild type (Supplemental Fig. S4a) and within 10 min after wounding and FAC elicitation, JA accumulated at <3-fold-lower levels in the silenced genotypes (Fig. 3B; $P < 0.05$, t test, wild type versus genotypes). Basal and induced

levels of SA were also quantified in unelicited and stimulated tissue of ir-sipk, ir-wipk, ir-npr1, and ir-coi1. Basal SA levels were only significantly higher in ir-sipk and ir-coi1 plants (4.5- and 3-fold, respectively, $P < 0.05$, t test, wild type versus genotypes) compared to wild type (Supplemental Fig. S4b). Within 10 min after wounding and FAC elicitation, the SA levels in the different genotypes did not change significantly compared to its basal levels (Supplemental Fig. S4b).

ir-sipk, ir-wipk, and ir-npr1 Contain Similar Levels of LOX3 Protein and 13-LOX Activity But Have Reduced AOS Activity

To determine at which level of gene expression JA biosynthesis was affected in ir-sipk, ir-wipk, ir-npr1, and ir-coi1 plants, we first determined the transcript abundance of *LOX2*, *LOX3*, *AOS*, and *AOC* by real-time quantitative PCR (RT-qPCR) in unelicited leaves of wild type and the four silenced genotypes. The results showed no significant variations in the basal levels of these transcripts between all the genotypes, suggesting that basal transcription rates (or mRNA stability) of these genes were not affected (Supplemental Fig. S5a). Second, the levels of LOX3 protein were determined by immunoblotting using an anti-NaLOX3 antibody before and after FAC elicitation. LOX3 protein amounts were similar between all the genotypes before and after the treatment (Supplemental Fig. S5b). Finally, 13-LOX and AOS activities were quantified. Basal 13-LOX activity in ir-wipk, ir-sipk, and ir-npr1 was similar to wild type, however, reduced by approximately 40% in ir-coi1 plants (Fig. 4;

Figure 3. OPDA and JA levels in wild-type (WT) and RNAi-silenced plants. Leaves of rosette stage wild-type, ir-sipk, ir-wipk, ir-npr1, and ir-coi1 plants were wounded or FAC elicited for different times and OPDA (A) and JA (B) quantified. Bars = ±SE, n = 5. For statistical analysis, see text.
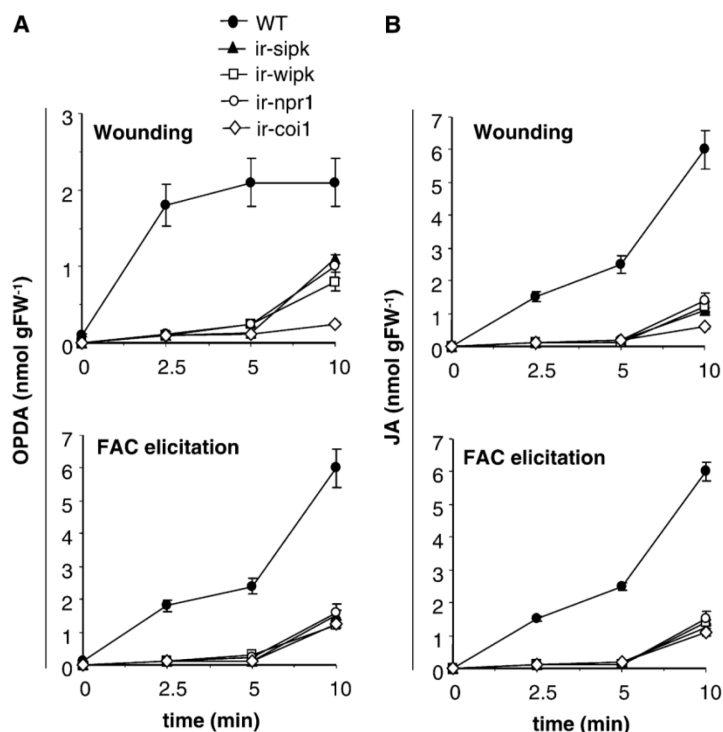
$P < 0.05$, t test, wild type versus genotype). AOS activity was, in contrast, significantly reduced in all silenced genotypes (by approximately 30% in ir-sipk, ir-wipk, and ir-npr1 and by 70% in ir-coi1 compared to wild type; Fig. 4; $P < 0.05$, t test, wild type versus genotype). After FAC elicitation, LOX and AOS activities remained similar to resting levels in the corresponding genotypes (Supplemental Fig. S5c).

Identification of a GLA₁-I Lipase Involved in JA Biosynthesis in *N. attenuata*

Based on the results presented above, one plausible scenario is that SIPK-, NPR1-, COI1-, and FAC-mediated mechanisms contribute to the release of 18:3 from membrane lipids and that free 18:3 is rapidly metabolized by the JA biosynthetic pathway. Thus far, only the Arabidopsis DGL and DAD1 lipases involved in wound-induced JA biosynthesis have been genetically characterized. To identify their functional homologs in *N. attenuata*, DAD1 and DGL amino acid sequences were used to search *Nicotiana* EST and UniGene databases in GenBank by basic local alignment (tblastn). Three *Nicotiana* spp. clones (DW004396, DV161431, and CK290998) gave hits with e values lower than $7e^{-22}$ when either DAD1 or DGL were used as the protein query. Based on these sequences, their respective homologs were identified in *N. attenuata*. DAD1 and DGL belong to the phospholipase-A₁ (PLA₁-I) family of phospholipases that is characterized by the presence of an N-terminal chloroplast transit peptide

and a conserved lipase-3 domain with a catalytic triad consisting of Glu-His-Ser (Ryu, 2004). The three *N. attenuata* homologs presented these domains together with additional conserved structures and were tentatively named glycerolipiase A1 (GLA1; homolog to DW004396), GLA2 (homolog to DV161431), and GLA3 (homolog to CK290998).

The transcript levels of *GLA1*, *GLA2*, and *GLA3* were quantified at 0, 30, 60, and 90 min after wounding in wild type, ir-sipk, ir-npr1, and ir-coi1. ir-wipk was excluded from this analysis because it contained wild-type levels of unsaturated FFAs and 13-(OOH)-18:3. Thirty minutes after wounding, *GLA1* mRNA levels were reduced by 3- to 4-fold in wild type and the four silenced genotypes and remained at lower levels for up to 90 min (Fig. 5A). In contrast, *GLA2* transcript levels were transiently induced by 2- to 3-fold in wild type and ir-npr1 after wounding (albeit with a different kinetic) whereas not induced in ir-coi1 and ir-sipk (Fig. 5B). *GLA3* mRNA levels did not change significantly upon wounding (Fig. 5C). The kinetic of induction for these three transcripts was also quantified after FAC elicitation in wild-type plants. *GLA2* transcript levels were induced by 10-fold at 60 min whereas *GLA1* and *GLA3* transcript levels were unaffected compared to wounding (Fig. 5D).

GLA1 Is Essential for JA Biosynthesis

Virus-induced gene silencing (VIGS) was used to investigate the involvement of the three putative
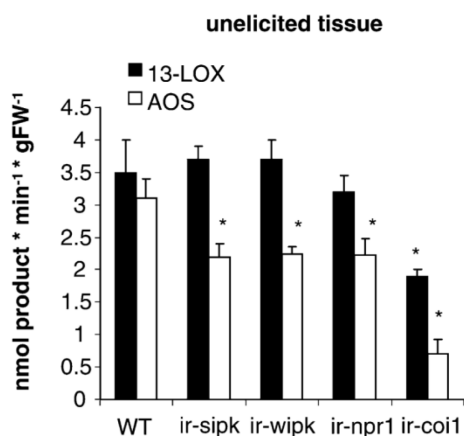
unelicited tissue

Figure 4. Analysis of 13-LOX and AOS activities. 13-LOX and AOS activities were quantified in unelicited leaves of wild-type (WT), ir-sipk, ir-wipk, ir-npr1, and ir-coi1 plants using $[1-{}^{14}C]$-18:3 or $[1-{}^{14}C]$-13-OOH-18:3 as substrates, respectively. Assays were performed in the linear phase of the reactions and ${}^{14}C$ products were extracted, separated by thin-layer chromatography, and quantified by densitometric scanning. Bars = ±SD, *n* = 3. *, See text.

GLAs in JA biosynthesis. Approximately 300 bp of their corresponding cDNAs were amplified and used for gene silencing. To ensure specific silencing, cDNA segments with low similarity between the three NaGLA cDNAs were selected (Supplemental Figure S6). Plants transformed with the empty vector (EV)

were used as controls. Gene-silencing efficiency was analyzed by qRT-PCR in unwounded leaves and 60 min after FAC elicitation. In GLA1 and GLA3 VIGS-silenced plants, the corresponding mRNA levels were reduced by more than 95% and in GLA2 VIGS-silenced plants by 85% compared to EV (Supplemental Fig. S7).

First, the levels of JA and JA-Ile were quantified in EV and GLA1-, GLA2-, and GLA3-silenced plants. Leaves of EV, GLA2-, and GLA3-silenced plants accumulated similar amounts of JA and JA-Ile after FAC elicitation (Supplemental Fig. S8). In contrast, GLA1-silenced plants showed reductions of >80% in JA and JA-Ile levels at 20 min and of 75% at 1 h after FAC elicitation (Fig. 6A; *P* < 0.01, *t* test, EV versus GLA1). Similar results were observed after wounding alone (Supplemental Fig. S9a). Consistent with the reductions in JA and JA-Ile levels, accumulation of 13-hydroperoxy-linolenic acid (13-OOH-18:3) and OPDA was also reduced in GLA1-silenced plants compared to EV (Supplemental Fig. S9b). In contrast, the levels of unsaturated FFA (and in particular 18:3) remained similar between GLA1-silenced and EV plants after the treatments and similar to the levels in wild-type plants (data not shown).

GLA1 Is a Plastidial Glycerolipid Acyl Hydrolase with sn1 Specificity

The full-length *GLA1* cDNA was obtained by 3' and 5' RACE (Supplemental Fig. S10). Alignment of the full predicted amino acid sequence of GLA1 with
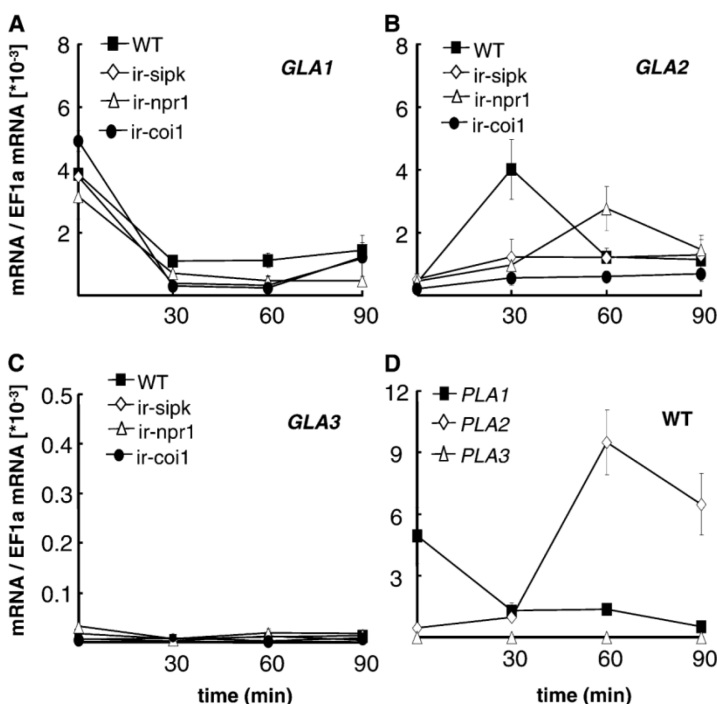
Figure 5. Analysis of GLA mRNA expression. GLA1 (A), GLA2 (B), and GLA3 (C) transcript levels were quantified by RT-qPCR in unelicited leaves of wild-type (WT), ir-sipk, ir-npr1, and ir-coi1 plants and at different times after wounding. Relative mRNA levels are expressed as the ratio of abundance of the queried mRNA over the standard (EF1a). D, Levels of all *GLA* mRNAs were quantified for different times after FAC elicitation in wild-type plants. Bars = ±SD, *n* = 3.

Kallenbach et al.
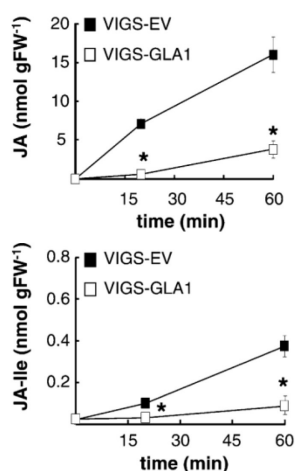
Figure 6. Quantification of JA and JA-Ile levels in plants silenced in GLA1 expression by VIGS. Control plants (VIGS-EV) and plants silenced in GLA1 expression by VIGS (VIGS-GLA1) were FAC elicited and JA and JA-Ile levels quantified in leaves after 20 and 60 min of the treatments. Bars = ±SE, n = 8. *, See text.

those from Arabidopsis DAD1 and DGL showed that GLA1 shared 46% identity/62% similarity and 37% identity/53% similarity with these proteins, respectively. Prediction of subcellular localization gave GLA1 a high score for plastid targeting with a predicted signal peptide of 53 residues (Supplemental Fig. S10).

To assess whether GLA1 encodes an active glycerolipid acyl hydrolase, we expressed GLA1 as a recombinant protein in bacteria and analyzed its activity toward different glycerolipid substrates. For the expression of recombinant GLA1, the predicted transit peptide was excluded to avoid the potential inhibition of lipase activity and the enzyme was fused by its N terminus to the maltose-binding protein (MBP) to promote stability (Ishiguro et al., 2001). To first evaluate if GLA1 encodes a glycerolipase type A_1, the specificity of purified MBP-GLA1 toward 1-palmitoyl-2-oleoyl-glycero-3-phosphorylcholine (POPC) was assayed. MBP-GLA1 released preferentially 16:0 from POPC whereas purified MBP showed no activity toward this substrate (Fig. 7A). MBP-GLA1 activity was also evaluated toward different glycerolipid classes, namely a phospholipid (PC), galactolipid (MGDG), and triacylglycerol (triolein). The purified enzyme hydrolyzed acyl groups at rates of approximately 2 μg h^{-1} μg protein^{-1} with MGDG and PC as substrates and at approximately 1.5 μg h^{-1} μg protein^{-1} with triolein as a substrate. Purified MBP did not present acyl-hydrolase activity (Fig. 7B).

To determine the subcellular localization of GLA1, the enzyme was fused to enhanced green fluorescent protein (EGFP) by its C terminus and cloned under regulation of the cauliflower mosaic virus 35S pro-

moter (P35S:GLA1-EGFP). As controls, P35S:EGFP and a fusion EGFP protein carrying the first 273 amino acids containing the predicted plastid transit peptide of LOX3 (P35S:pLOX3-EGFP) were used. *N. attenuata* leaves were infiltrated with *Agrobacteria* carrying the corresponding constructs and EGFP expression in mesophyll cells was analyzed by laser confocal microscopy (Fig. 7C). Prior to analysis, mesophyll protoplasts were released from leaves by cell wall digestion. Protoplast transformed with EGFP showed a diffused green fluorescence characteristic of cytosolic localization that did not overlap with chlorophyll red autofluorescence. In contrast, protoplasts expressing pLOX3-EGFP and GLA1-EGFP showed colocalization
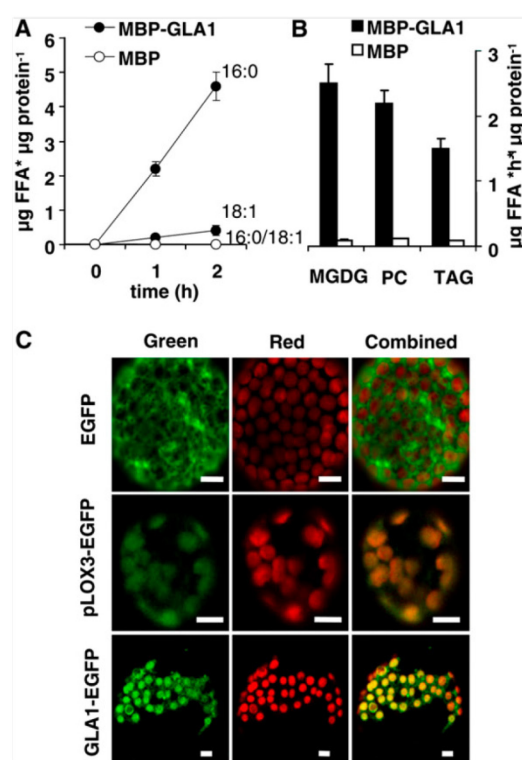
Figure 7. Characterization of GLA1 activity and subcellular localization. A, Recombinant MBP-GLA1 protein was expressed *Escherichia coli* cells and after induction and purification, enzyme activity toward POPC was assayed. Purified MBP was used as control. The assay was conducted at the optimal pH for this recombinant enzyme (pH: 6.5). Bars = ± SD, n = 3. B, MBP-GLA1 activity toward PC, MGDG, and triolein as substrates. Bars = ± SD, n = 3. C, Mesophyll protoplasts expressing P35S:EGFP, P35S:GLA1-EGFP, and P35S:pLOX3-EGFP were analyzed by laser confocal-scanning microscopy. Leaves of *N. attenuata* plants were *Agrobacteria* infiltrated and after protoplast release by cell wall digestion, mesophyll protoplasts were exited at 488 nm and emissions collected at 505 to 530 nm for EGFP and at 585 nm for chlorophyll red autofluorescence. Combined, Merged EGFP and chlorophyll autofluorescence. White scale bar: 10 μm.

of green and red fluorescences, consistent with their predicted plastidial localization.

DISCUSSION

GLA1 Participates in the Activation of JA Biosynthesis in *N. attenuata* Leaves

The absence of massive glycerolipid degradation and release of FFA after mechanical damage contrasted with some previous studies performed in other plant species where substantial breakdown of glycerolipids and release of FFA was detected after wounding (Conconi et al., 1996; Ryu and Wang, 1998). These differences are most likely a result of the different methods used to mechanically damage the leaf (crushing leaf tissue versus punctured wounds) and therefore differences in cell disruption and uncontrolled hydrolysis of membrane lipids. The absolute amounts of 18:3 in galactolipids were on average 1.3 μmol g FW^{-1}, more than 100-fold the amount of substrate needed to supply JA biosynthesis within 10 min (6–20 nmol g FW^{-1} g FW; Fig. 3B). Therefore, specific supply of 18:3 for JA biosynthesis within this time frame was not expected to cause substantial changes in the FA composition of major plastidial lipids. In contrast, however, significant changes in the total levels of free 18:3 (which accumulated to approximately 3 nmol g FW^{-1}; Fig. 1) were expected, since OPDA and JA accumulated to comparable levels (Fig. 3B) within 10 min after wounding and FAC elicitation, respectively. Unexpectedly, the levels of this FFA did not change significantly within this period. Consistent with this observation, plants silenced in GLA1 expression showed no significant changes in the levels of free 18:3 and other unsaturated FFAs compared to control EV plants after wounding and FAC elicitation, however, 13-OOH, OPDA, JA, and JA-Ile production was strongly reduced in these silenced plants (Fig. 6; Supplemental Fig. S9). These results, together with the localization of GLA1 in the chloroplasts, provided strong evidence for a rapid and specific supply of 18:3 for JA biosynthesis via GLA1. We cannot completely rule out, however, the possibility that the effect of GLA1 on JA biosynthesis is indirect.

Similar to Arabidopsis DGL and DAD1, GLA1 is a member of the lipase A_1-I family and is expressed in vegetative tissues in the absence of wounding (Ishiguro et al., 2001; Hyun et al., 2008). Also, similar to DAD1 and DGL, GLA1 hydrolyzed both PC and MGDG, however in contrast to DAD1 (which hydrolyzes PC more efficiently; Ishiguro et al., 2001) and DGL (which hydrolyzes galactolipids more efficiently; Hyun et al., 2008) the activity of GLA1 toward these substrates was similar. Because GLA1 localizes to the plastids, it is likely that galactolipids are the major in vivo substrates for this lipase. Whereas *DAD1* and *DGL* transcripts are induced by wounding (Ishiguro et al., 2001; Hyun et al., 2008), *GLA1* mRNA levels were repressed by this stimulus. This repression may reflect variations in the regulation of some JA biosynthetic genes in different plant species and underscore the fact that changes in transcript accumulation did not correlate with GLA1 function.

FAC Elicitation, SIPK, NPR1, and COI1 Regulate Early Enzymatic Steps in the JA Biosynthetic Pathway

Free 13-(OOH)-18:3 levels increased after wounding and more rapidly after FAC elicitation in wild-type plants (Fig. 2). The absolute amounts remained, however, low (0.01–0.08 nmol g FW^{-1}) in agreement with previous studies, suggesting a rapid utilization of this precursor (Weichert et al., 1999). After FAC elicitation, 13-LOX activity and LOX3 protein levels were not increased compared to unelicited tissue in wild-type plants (Fig. 4; Supplemental Fig. S5b), suggesting that the enhanced accumulation of 13-(OOH)-18:3 after this stimulus was the result of an increase in 18:3 supply rather than the differential activation of LOX3. One possible scenario is the differential activation of GLA1 via FAC-mediated mechanisms, however, this hypothesis requires further experimentation and is the focus of future studies.

Basal levels of FFA (including 18:3) were reduced >10-fold in ir-sipk and ir-npr1 plants compared to wild type (Fig. 1) and increased after wounding and FAC elicitation, remaining nonetheless lower than in wild type after the same treatments. These results suggested that homeostatic mechanisms that maintain wild-type levels of unsaturated FFA were affected in these silenced plants. Whether this global reduction in FFA levels was directly connected to a reduced supply of 18:3 for JA production in these genotypes is at present unknown. However, as the initial accumulation of 13-OOH-18:3 was strongly reduced after wounding and FAC elicitation in ir-sipk and ir-npr1 plants (Fig. 2A) independently of reductions in 13-LOX activity and LOX3 protein levels (Fig. 4; Supplemental Fig. S5b), we concluded that in ir-sipk and ir-npr1 plants, the supply of 18:3 for JA biosynthesis was affected. Thus, at present there are two potential explanations: (1) that a global suppression of FFA levels affects (by still unknown mechanisms) the supply of 18:3 for JA production in ir-sipk and ir-npr1 plants, or (2) that SIPK and NPR1 influences by independent mechanisms both, the regulation of homeostatic levels of FFA and the specific supply of 18:3 for JA production. Thus, although speculative at this point, we propose that the supply of 18:3 via NaGLA1 may be one regulatory step by which SIPK- and NPR1-mediated mechanisms contribute to the activation of JA biosynthesis.

ir-coi1 plants had approximately 50% reduced basal levels of FFAs compared to wild type (Supplemental Figs. S1b and S2) and in contrast to ir-sipk and ir-npr1 plants, FFA levels did not increase after wounding and FAC elicitation. ir-coi1 plants also accumulated lower levels of 13-OOH-18:3 after these treatments, however,

Kallenbach et al.

in contrast to ir-sipk and ir-npr1 plants, in ir-coi1 plants had 40% reduced levels of 13-LOX activity (Fig. 4). Thus, the results suggested that in the latter genotype, the initial 13-(OOH)-18:3 accumulation was primarily limited by reduced 13-LOX activity.

SIPK, WIPK, NPR1, and COI1-Mediated Mechanisms Participate in the Regulation of OPDA Synthesis

The mRNA levels of AOS and AOC in unelicited tissue of ir-sipk, ir-wipk, ir-npr1, and ir-coi1 were similar to those of wild-type plants, indicating that their rates of transcription/turnover were not affected (Supplemental Fig. S5a). However, AOS activity was reduced by 30% in ir-sipk, ir-npr1, and ir-wipk and by 70% in ir-coi1 plants, suggesting that these differences were the result of posttranscriptional processes.

Although ir-wipk plants contained wild-type levels of free 18:3 and accumulated wild-type levels of 13-(OOH)-18:3 after elicitation, the rate of OPDA synthesis was reduced by more than 90% within 5 min of the response (Fig. 3A). Thus, the reduced AOS activity in ir-wipk plants indicated that WIPK-mediated mechanisms are important to maintain basal AOS activity and suggested that this enzyme's activity limited OPDA accumulation after elicitation. However, since the reduction in the initial rates of OPDA accumulation were bigger than the expected by the 30% reduction in AOS activity, additional enzymatic steps may also be affected in ir-wipk plants. For example, evidence from the crystal structure of Arabidopsis AOC2 suggests that this enzyme is regulated posttranslationally by oligomerization (Hofmann et al., 2006). Thus, although speculative at this point, we do not rule out the possibility that AOC may also be a target of WIPK-mediated mechanisms.

CONCLUSION

Upon wounding and herbivory, cellular mechanisms quickly convey the signal to the plastid to activate constitutively expressed enzymes and to start the immediate production of JA. How plants convey the primary stress signal to activate these enzymes remain at present largely unknown. Due to the large number of enzymes and different cellular compartments involved in JA biosynthesis, it is expected that the pathway is regulated at multiple steps. Consistent with this hypothesis, recent evidence indicates that OPR3, AOC2, and ACX1 are subjected to regulation (Pedersen and Henriksen, 2005; Breithaupt et al., 2006; Hofmann et al., 2006). The recent identification of different regulatory factors that affect JA accumulation (Ludwig et al., 2005; Takabatake et al., 2006; Schweighofer et al., 2007; Takahashi et al., 2007) is also consistent with a complex network of signals inducing JA biosynthesis (Browse, 2009). In this study we demonstrated that signal transduction mechanisms involving SIPK, WIPK, NPR1, and the insect

elicitor 18:3-Glu affect different early JA biosynthetic steps. We propose that after wounding, FAC perception differentially stimulate the supply of 18:3 for JA biosynthesis and that SIPK- and NPR1-mediated mechanisms also stimulate this biochemical step. The identification of GLA1 as a lipase essential for JA biosynthesis suggested that the above-mentioned factors may exert their effects via the regulation of this enzyme's activity. In contrast, WIPK-mediated mechanisms operate in the control of the biosynthetic steps that convert 13-(OOH)-18:3 into OPDA. This control is at least partially executed by the regulation of AOS activity. Further elucidation of the mechanisms affecting enzyme activity would provide critical information on the understanding of how primary stress signals are translated into the activation of JA biosynthetic enzymes.

MATERIALS AND METHODS

Please refer to online Supplemental Experimental Procedures S1 for further details.

Plant Growth and Treatments

Seeds of the 22nd generation of an inbred line of *Nicotiana attenuata* plants were used as the wild-type genotype in all experiments. Plants were grown at 26°C to 28°C under 16 h of light. For all experiments, leaves at nodes +1, +2, and +3 of rosette stage (40-d-old) plants were used. Wounding was performed by rolling a fabric pattern wheel three times on each side of the midvein. The wounds were immediately supplied with either 10 μL of 0.02% (v/v) Tween 20/water (solvent control) or 10 μL of synthetic 18:3-Glu (0.03 nmol/μL in 0.02% [v/v] Tween 20/water). Tissue was collected and immediately frozen in liquid nitrogen for subsequent analysis.

Oxylipin Analysis

Hydroperoxy FAs were extracted with the chloroform-methanol method. Briefly, approximately 1 g of frozen leaf material was homogenized in 10 mL glass tubes containing 3.75 mL of ice-cold 2/1 (v/v) chloroform/methanol spiked with 5 ng of 15-hydroperoxy-eicosadienoic acid (Cayman Chemicals). After addition of 1.25 mL chloroform and 1 mL water, samples were vortexed and phases separated. The organic phase was collected and the water phase reextracted with 3 mL hexane. Hexane and chloroform fractions were combined, the solvent evaporated under a stream of nitrogen, and samples reconstituted in 70% (v/v) methanol/water and analyzed by liquid chromatography-(ESI)-tandem mass spectrometry (see online Supplemental Experimental Procedures S1). Commercial 13S-(OOH)-18:3 and 9(R/S)-OOH-18:3 were used as standards (Cayman Chemicals). For analysis of JA, JA-Ile, OPDA, and SA, approximately 0.1 g of frozen leaf material was homogenized in FastPrep tubes containing 1 g of FastPrep matrix (Bio 101) and 1 mL ethyl acetate spiked with 100 ng of [9,10-^{2}H]-dihydro-JA, [$^{13}C_4$]-SA, and [$^{13}C_6$]-JA-Ile. Homogenates were centrifuged for 10 min at 4°C, the organic phase collected, and plant material reextracted with 0.5 mL ethyl acetate. Organic phases were combined and the samples evaporated to dryness. The dry residue was reconstituted in 0.2 mL of 70% (v/v) methanol/water and analyzed by liquid chromatography-(ESI)-tandem mass spectrometry (see online Supplemental Experimental Procedures S1).

Identification of Homologs of DAD1 and DGL

The amino acid sequences from Arabidopsis (*Arabidopsis thaliana*) DAD1 (AtPLA$_1$-Iβ1) and DGL (AtPLA$_1$-Iα1) were used to search *Nicotiana* EST and RefSeq databases by basic local alignment (BLAST) in GenBank. Specific primers (Supplemental Table S2) were designed based on *Nicotiana* CK290998, DV161431, and DW004396 sequences to PCR amplify their respective homo-

logs in *N. attenuata*. PCR products were obtained using *N. attenuata* leaf cDNA as template and cloned into pGEM-T easy vector (Promega) and sequenced. The corresponding *N. attenuata* sequences were named GLA1 (homolog to DW004396), GLA2 (homolog to DV161431), and GLA3 (homolog to CK290998; see accession numbers listed below).

VIGS

A VIGS system based on *Tobacco rattle virus* was used (Ratcliff et al., 2001) adapted for *N. attenuata* according to Saedler and Baldwin (2004). cDNA fragments of GLA1, GLA2, and GLA3 (Supplemental Fig. S6) were amplified by PCR using plasmids carrying their respective cDNA sequences (see section above) as templates and specific primers (Supplemental Table S2). After digestion with *Bam*HI and *Sal*I and gel purification, the PCR products were subcloned into pTV100 to form pTV-LIP1, 2, and 3. *Agrobacterium tumefaciens* strain GV3101 carrying these gene-specific constructs were coinoculated with *Agrobacteria* carrying pBINTRA6 into *N. attenuata* leaves according to Saedler and Baldwin (2004). Plants were analyzed 15 d after inoculation.

In Vitro Quantification of GLA1 Activity

Soybean (*Glycine max*) PC, wheat (*Triticum aestivum*) MGDG, and triolein (Sigma) and POPC (Matreya) were used as substrates. Lipids were emulsified by sonication in 0.2% (v/v) Triton X-100 at 1 μg/μL. Reaction buffer (50 mM K-phosphate [pH 6.5], 0.2% [v/v] Triton X-100), 40 μg of substrate, and 16 μg of purified protein (either MBP or MBP-GLA1) in a final volume of 100 μL were used for the assays. The reaction was carried out at 30°C for 1 and 2 h and stopped by the addition of 2 mL of chloroform. Lipids were extracted twice with chloroform and FFA purification and analysis was performed by thin-layer chromatography and gas chromatography-mass spectrometry as described for plant material.

Subcellular Localization GLA1

N. attenuata leaves were infiltrated with *A. tumefaciens* GV3101 carrying pCAMBIA-1201 vectors expressing P35S:GLA1-EGFP, P35S:pLOX3-EGFP, and P35S:EGFP (see online Supplemental Experimental Procedures). Infiltration was performed as indicated in the VIGS section above. Four days after infiltration, leaves were collected and protoplast isolated by floating leaf strips on 0.2% (w/v) bovine serum albumin, 2% (w/v) cellulase, 1% (w/v) macerozyme, 400 mM mannitol, 8 mM CaCl$_2$, and 5 mM MES (pH 5.6) for 3 h at 25°C with gentle shaking. Protoplasts were collected by centrifugation (100g) for 5 min and immediately used for microscopy. Confocal laser-scanning microscopy was performed using a LSM 510 Meta microscope (Carl Zeiss) equipped with an argon laser. Samples were excited at 488 nm and emissions collected with 505 to 530 nm and 585 nm filters for EGFP and chlorophyll red autofluorescence, respectively. Images were processed using the image software supplied by the microscope manufacturer (Carl Zeiss).

Sequence data from this article can be found in the GenBank/EMBL data libraries under accession numbers: GLA1 (FJ821553), GLA2 (FJ821554), GLA3 (FJ821555), LOX3 (AY254349), LOX2 (AY254348), AOS (AJ295274), AOC (EF467332), DAD1 (Atg244810), and DGL (At1g05800).

Supplemental Data

The following materials are available in the online version of this article.

Supplemental Figure S1. Membrane glycerolipid and unsaturated FFA levels in wild-type leaves.

Supplemental Figure S2. Unsaturated FFA levels in RNAi-silenced plants.

Supplemental Figure S3. OPDA and JA levels in wild-type plants within 20 min of induction.

Supplemental Figure S4. Basal levels of JA and basal and induced levels of SA.

Supplemental Figure S5. RT-qPCR and LOX3 protein levels.

Supplemental Figure S6. Alignment of GLA sequences used for VIGS.

Supplemental Figure S7. Quantification of GLA mRNA levels in VIGS-silenced plants.

Supplemental Figure S8. Quantification of JA and JA-Ile levels in GLA2- and GLA3-silenced plants.

Supplemental Figure S9. Quantification of 13-OOH-18:3, OPDA, JA, and JA-Ile levels in GLA1-silenced plants.

Supplemental Figure S10. Full-length mRNA and amino acid sequences of GLA1.

Supplemental Table S1. FA composition of membrane glycerolipids in wild-type leaves.

Supplemental Table S2. Primer sequences.

Supplemental Experimental Procedures S1. Additional methods.

LITERATURE CITED

Böttcher C, Weiler E (2007) Cyclo-oxylipin-galactolipids in plants: occurrence and dynamics. Planta **226:** 629–637

Breithaupt C, Kurzbauer R, Lilie H, Schaller A, Strassner J, Huber R, MacHeroux P, Clausen T (2006) Crystal structure of 12-oxophytodienoate reductase 3 from tomato: self-inhibition by dimerization. Proc Natl Acad Sci USA **103:** 14337–14342

Browse J (2009) Jasmonate passes muster: a receptor and targets for the defense hormone. Annu Rev Plant Biol **60:** 183–205

Buseman CM, Tamura P, Sparks AA, Baughman EJ, Maatta S, Zhao J, Roth MR, Esch SW, Shah J, Williams TD (2006) Wounding stimulates the accumulation of glycerolipids containing oxophytodienoic acid and dinor-oxophytodienoic acid in Arabidopsis leaves. Plant Physiol **142:** 28–39

Cao H, Bowling SA, Gordon AS, Dong X (1994) Characterization of an *Arabidopsis* mutant that is nonresponsive to inducers of systemic acquired resistance. Plant Cell **6:** 1583–1592

Chini A, Fonseca S, Fernández G, Adie B, Chico J, Lorenzo O, García-Casado G, López-Vidriero I, Lozano F, Ponce M, et al (2007) The JAZ family of repressors is the missing link in jasmonate signalling. Nature **448:** 666–671

Conconi A, Miquel M, Browse JA, Ryan CA (1996) Intracellular levels of free linolenic and linoleic acids increase in tomato leaves in response to wounding. Plant Physiol **111:** 797–803

Creelman RA, Mullet JE (1997) Biosynthesis and action of jasmonates in plants. Annu Rev Plant Physiol Plant Mol Biol **48:** 355–381

Farmer EE (1994) Fatty-acid signaling in plants and their associated microorganisms. Plant Mol Biol **26:** 1423–1437

Glauser G, Grata E, Dubugnon L, Rudaz S, Farmer EE, Wolfender JL (2008) Spatial and temporal dynamics of jasmonate synthesis and accumulation in Arabidopsis in response to wounding. J Biol Chem **283:** 16400–16407

Halitschke R, Schittko U, Pohnert G, Boland W, Baldwin IT (2001) Molecular interactions between the specialist herbivore *Manduca sexta* (Lepidoptera, Sphingidae) and its natural host *Nicotiana attenuata*. III. Fatty acid-amino acid conjugates in herbivore oral secretions are necessary and sufficient for herbivore-specific plant responses. Plant Physiol **125:** 711–717

Halitschke R, Ziegler J, Keinanen M, Baldwin IT (2004) Silencing of hydroperoxide lyase and allene oxide synthase reveals substrate and defense signaling crosstalk in Nicotiana attenuata. Plant J **40:** 35–46

Hisamatsu Y, Goto N, Hasegawa K, Shigemori H (2003) Arabidopsides A and B, two new oxylipins from Arabidopsis thaliana. Tetrahedron Lett **44:** 5553–5556

Hofmann E, Zerbe P, Schaller F (2006) The crystal structure of *Arabidopsis thaliana* allene oxide cyclase: insights into the oxylipin cyclization reaction. Plant Cell **18:** 3201–3217

Kallenbach et al.

Hyun Y, Choi S, Hwang HJ, Yu J, Nam SJ, Ko J, Park JY, Seo YS, Kim EY, Ryu SB, et al (2008) Cooperation and functional diversification of two closely related galactolipase genes for jasmonate biosynthesis. Dev Cell **14:** 183–192

Ishiguro S, Kawai-Oda A, Ueda J, Nishida I, Okada K (2001) The DEFECTIVE IN ANTHER DEHISCIENCE gene encodes a novel phospholipase A1 catalyzing the initial step of jasmonic acid biosynthesis, which synchronizes pollen maturation, anther dehiscence, and flower opening in *Arabidopsis.* Plant Cell **13:** 2191–2209

Kandoth PK, Ranf S, Pancholi SS, Jayanty S, Walla MD, Miller W, Howe GA, Lincoln DE, Stratmann JW (2007) Tomato MAPKs LeMPK1, LeMPK2, and LeMPK3 function in the systemin-mediated defense response against herbivorous insects. Proc Natl Acad Sci USA **104:** 12205–12210

Kazan K, Manners J (2008) Jasmonate signaling: toward an integrated view. Plant Physiol **146:** 1459–1468

Ludwig AA, Saitoh H, Felix G, Freymark G, Miersch O, Wasternack C, Boller T, Jones JDG, Romeis T (2005) Ethylene-mediated cross-talk between calcium-dependent protein kinase and MAPK signaling controls stress responses in plants. Proc Natl Acad Sci USA **102:** 10736–10741

Meldau S, Wu JQ, Baldwin IT (2009) Silencing two herbivory-activated MAP kinases, SIPK and WIPK, does not increase Nicotiana attenuata's susceptibility to herbivores in the glasshouse and in nature. New Phytol **181:** 161–173

Paschold A, Bonaventure G, Kant MR, Baldwin IT (2008) Jasmonate perception regulates jasmonate biosynthesis and JA-Ile metabolism: the case of COI1 in Nicotiana attenuata. Plant Cell Physiol **49:** 1165–1175

Pedersen L, Henriksen A (2005) Acyl-CoA oxidase 1 from Arabidopsis thaliana: structure of a key enzyme in plant lipid metabolism. J Mol Biol **345:** 487–500

Ratcliff F, Martin-Hernandez AM, Baulcombe DC (2001) Technical advance: tobacco rattle virus as a vector for analysis of gene function by silencing. Plant J **25:** 237–245

Rayapuram C, Baldwin IT (2007) Increased SA in NPR1-silenced plants antagonizes JA and JA-dependent direct and indirect defenses in herbivore-attacked Nicotiana attenuata in nature. Plant J **52:** 700–715

Ryu SB (2004) Phospholipid-derived signaling mediated by phospholipase A in plants. Trends Plant Sci **9:** 229–235

Ryu SB, Wang X (1998) Increase in free linolenic and linoleic acids associated with phospholipase D-mediated hydrolysis of phospholipids in wounded castor bean leaves. Biochim Biophys Acta **1393:** 193–202

Saedler R, Baldwin IT (2004) Virus-induced gene silencing of jasmonate-induced direct defences, nicotine and trypsin proteinase-inhibitors in Nicotiana attenuata. J Exp Bot **55:** 151–157

Schweighofer A, Kazanaviciute V, Scheikl E, Teige M, Doczi R, Hirt H,

Schwanninger M, Kant M, Schuurink R, Mauch F, et al (2007) The PP2C-type phosphatase AP2C1, which negatively regulates MPK4 and MPK6, modulates innate immunity, jasmonic acid, and ethylene levels in *Arabidopsis.* Plant Cell **19:** 2213–2224

Seo S, Katou S, Seto H, Gomi K, Ohashi Y (2007) The mitogen-activated protein kinases WIPK and SIPK regulate the levels of jasmonic and salicylic acids in wounded tobacco plants. Plant J **49:** 899–909

Seo S, Sano H, Ohashi Y (1999) Jasmonate-based wound signal transduction requires activation of WIPK, a tobacco mitogen-activated protein kinase. Plant Cell **11:** 289–298

Spoel SH, Koornneef A, Claessens S, Korzelius JP, Van Pelt JA, Mueller MJ, Buchala AJ, Metraux JP, Brown R, Kazan K, et al (2003) NPR1 modulates cross-talk between salicylate-and jasmonate-dependent defense pathways through a novel function in the cytosol. Plant Cell **15:** 760–770

Stelmach B, Müller A, Hennig P, Gebhardt S, Schubert-Zsilavecz M, Weiler E (2001) A novel class of oxylipins, sn1-O-(12-oxophytodienoyl)-sn2-O-(hexadecatrienoyl)-monogalactosyl diglyceride, from Arabidopsis thaliana. J Biol Chem **276:** 12832–12838

Takabatake R, Seo S, Ito N, Gotoh Y, Mitsuhara I, Ohashi Y (2006) Involvement of wound-induced receptor-like protein kinase in wound signal transduction in tobacco plants. Plant J **47:** 249–257

Takahashi F, Yoshida R, Ichimura K, Mizoguchi T, Seo S, Yonezawa M, Maruyama K, Yamaguchi-Shinozaki K, Shinozaki K (2007) The mitogen-activated protein kinase cascade MKK3-MPK6 is an important part of the jasmonate signal transduction pathway in *Arabidopsis.* Plant Cell **19:** 805–818

Thines B, Katsir L, Melotto M, Niu Y, Mandaokar A, Liu GH, Nomura K, He SY, Howe GA, Browse J (2007) JAZ repressor proteins are targets of the SCFCO11 complex during jasmonate signalling. Nature **448:** 661–665

Turner JG, Ellis C, Devoto A (2002) The jasmonate signal pathway. Plant Cell **14:** S153–S164

Vick BA, Zimmerman DC (1983) The biosynthesis of jasmonic acid: a physiological role for plant lipoxygenase. Biochem Biophys Res Commun **111:** 470–477

Weichert H, Stenzel I, Berndt E, Wasternack C, Feussner I (1999) Metabolic profiling of oxylipins upon salicylate treatment in barley leaves-preferential induction of the reductase pathway by salicylate. FEBS Lett **464:** 133–137

Wu JQ, Hettenhausen C, Meldau S, Baldwin IT (2007) Herbivory rapidly activates MAPK signaling in attacked and unattacked leaf regions but not between leaves of *Nicotiana attenuata.* Plant Cell **19:** 1096–1122

Xie DX, Feys BF, James S, Nieto-Rostro M, Turner JG (1998) COI1: an Arabidopsis gene required for jasmonate-regulated defense and fertility. Science **280:** 1091–1094

Table SI. Fatty acid composition of glycerolipids in local leaf sections of WT plants (mol%)

	16:0	16:1[3]	16:2[7,10]	16:3[7,10,13]	18:0	18:1[9]	18:2[9,12]	18:3[9,12,15]
Time (min) after wounding								
MGDG								
0	5.1 ± 0.2	nd	1.3 ± 0.3	30.6 ± 1.7	1.0 ± 0.1	0.4 ± 0.1	1.9 ± 0.1	59.5 ± 2.2
2.5	4.2 ± 0.8	nd	0.7 ± 0.2	29.3 ± 4.5	0.8 ± 0.2	0.3 ± 0.1	1.8 ± 0.0	62.9 ± 8.3
5	3.7 ± 0.1	nd	0.8 ± 0.3	29.4 ± 4.5	0.5 ± 0.1	0.3 ± 0.1	1.9 ± 0.1	63.4 ± 3.0
10	3.6 ± 0.4	nd	0.6 ± 0.1	27.8 ± 2.0	0.5 ± 0.0	0.2 ± 0.0	2.0 ± 0.3	65.3 ± 4.1
20	3.7 ± 0.1	nd	1.1 ± 0.0	25.0 ± 2.4	0.7 ± 0.2	0.4 ± 0.0	1.7 ± 0.2	67.4 ± 0.8
DGDG								
0	32.0 ± 2.2	nd	nd	1.9 ± 0.2	6.0 ± 0.3	1.3 ± 0.2	4.9 ± 0.3	51.2 ± 1.7
2.5	29.4 ± 1.7	nd	nd	2.1 ± 0.1	5.4 ± 0.3	0.9 ± 0.2	4.6 ± 1.0	56.3 ± 1.2
5	27.5 ± 1.1	nd	nd	2.0 ± 0.3	4.9 ± 0.6	0.8 ± 0.1	4.2 ± 0.7	60.6 ± 2.7
10	26.5 ± 0.3	nd	nd	1.7 ± 0.1	4.7 ± 0.3	1.0 ± 0.1	4.3 ± 0.4	59.6 ± 4.3
20	26.8 ± 2.5	nd	nd	1.7 ± 0.2	5.6 ± 1.3	0.9 ± 0.2	3.5 ± 0.1	61.1 ± 4.3
PE								
0	35.0 ± 2.6	nd	nd	0.5 ± 0.2	8.0 ± 1.5	1.4 ± 0.3	29.9 ± 3.7	25.2 ± 2.2
2.5	34.4 ± 9.5	nd	nd	nd	8.5 ± 2.3	2.5 ± 1.2	23.1 ± 6.5	31.6 ± 6.0
5	34.1 ± 5.1	nd	nd	0.8 ± 0.2	5.1 ± 0.6	1.1 ± 0.2	29.9 ± 3.9	29.0 ± 3.4
10	33.4 ± 4.3	nd	nd	0.7 ± 0.2	5.3 ± 1.1	1.0 ± 0.2	30.1 ± 5.5	29.5 ± 2.3
20	29.6 ± 2.7	nd	nd	0.7 ± 0.2	6.5 ± 1.6	1.6 ± 0.4	32.4 ± 5.7	29.2 ± 4.3
PC								
0	34.4 ± 5.2	nd	nd	0.3 ± 0.3	9.8 ± 1.1	3.3 ± 1.0	25.3 ± 5.5	26.9 ± 4.1
2.5	34.2 ± 3.3	nd	nd	nd	8.7 ± 1.6	nd	26.4 ± 4.8	30.7 ± 2.9
5	31.8 ± 2.6	nd	nd	0.2 ± 0.2	7.4 ± 0.1	2.5 ± 0.9	24.9 ± 3.4	33.2 ± 3.4
10	32.1 ± 1.7	nd	nd	0.2 ± 0.2	7.1 ± 0.7	1.6 ± 0.4	24.8 ± 5.6	34.2 ± 2.7
20	30.1 ± 3.8	nd	nd	0.2 ± 0.2	9.2 ± 1.2	3.0 ± 0.4	27.8 ± 2.9	29.7 ± 0.5
Time (min) after FAC elicitation								
MGDG								
0	5.3 ± 0.4	nd	1.3 ± 0.1	31.0 ± 4.5	0.8 ± 0.1	0.5 ± 0.1	3.1 ± 0.5	58.0 ± 6.4
2.5	3.9 ± 0.3	nd	0.6 ± 0.1	28.8 ± 3.3	0.6 ± 0.1	0.3 ± 0.0	1.8 ± 0.1	64.0 ± 5.4
5	3.4 ± 0.4	nd	0.6 ± 0.1	28.5 ± 6.5	0.4 ± 0.1	0.3 ± 0.0	1.7 ± 0.2	65.1 ± 10.3
10	3.7 ± 0.8	nd	0.6 ± 0.3	27.8 ± 5.1	0.7 ± 0.1	0.3 ± 0.1	1.7 ± 0.3	65.2 ± 11.0
20	3.6 ± 0.1	nd	0.7 ± 0.2	29.8 ± 2.5	0.6 ± 0.1	0.3 ± 0.0	1.8 ± 0.2	63.2 ± 3.2
DGDG								
0	32.2 ± 1.5	nd	nd	2.0 ± 0.3	4.8 ± 0.3	1.3 ± 0.1	6.9 ± 0.3	49.5 ± 1.3
2.5	28.1 ± 5.1	nd	nd	2.0 ± 0.2	5.0 ± 0.7	0.7 ± 0.2	4.0 ± 0.8	60.1 ± 8.1
5	28.6 ± 1.8	nd	nd	2.0 ± 0.3	4.4 ± 0.3	0.7 ± 0.1	3.7 ± 0.1	59.9 ± 4.8
10	28.8 ± 2.5	nd	nd	1.8 ± 0.4	4.7 ± 1.0	0.7 ± 0.1	3.6 ± 0.3	60.3 ± 2.4
20	29.1 ± 3.8	nd	nd	1.9 ± 0.3	4.9 ± 0.9	0.7 ± 0.1	3.4 ± 0.6	59.8 ± 4.5
PE								
0	32.9 ± 3.2	nd	nd	0.5 ± 0.1	5.8 ± 0.8	1.4 ± 0.2	36.9 ± 4.0	22.5 ± 2.2
2.5	33.1 ± 4.6	nd	nd	0.7 ± 0.2	6.3 ± 1.7	1.2 ± 0.3	29.4 ± 4.5	29.3 ± 3.7
5	33.9 ± 3.4	nd	nd	0.7 ± 0.1	4.9 ± 0.9	0.9 ± 0.2	30.4 ± 5.5	29.2 ± 3.8
10	32.8 ± 6.1	nd	nd	0.3 ± 0.2	7.9 ± 1.1	2.0 ± 1.0	22.5 ± 6.6	34.5 ± 5.5
20	33.0 ± 1.8	nd	nd	0.6 ± 0.2	5.6 ± 0.7	1.3 ± 0.1	31.2 ± 3.9	28.3 ± 3.6
PC								
0	30.7 ± 5.0	nd	nd	2.3 ± 2.3	7.2 ± 1.1	3.2 ± 1.1	31.8 ± 6.7	24.8 ± 4.3
2.5	33.5 ± 5.2	nd	nd	0.5 ± 0.2	8.0 ± 1.0	2.4 ± 0.5	22.2 ± 2.4	33.4 ± 3.5
5	33.1 ± 0.8	nd	nd	0.5 ± 0.2	6.4 ± 0.4	2.2 ± 0.4	23.9 ± 2.4	33.9 ± 2.7
10	32.6 ± 3.1	nd	nd	nd	7.8 ± 0.6	2.1 ± 0.2	28.2 ± 1.9	29.3 ± 4.9
20	33.6 ± 2.8	nd	nd	0.3 ± 0.1	6.9 ± 0.6	2.4 ± 0.5	24.4 ± 3.0	32.4 ± 2.0

1

Table SII. Fatty acid composition of glycerolipids in distal leaf sections of WT plants (mol%)

	16:0	16:1[3]	16:2[7,10]	16:3[7,10,13]	18:0	18:1[9]	18:2[9,12]	18:3[9,12,15]
Time (min) after wounding								
MGDG								
0	5.1 ± 0.2	nd	1.3 ± 0.3	30.6 ± 1.7	1.0 ± 0.1	0.4 ± 0.1	1.9 ± 0.1	59.5 ± 2.2
2.5	4.5 ± 0.5	nd	0.8 ± 0.2	28.2 ± 4.7	1.8 ± 1.7	0.4 ± 0.1	1.9 ± 0.1	62.4 ± 5.6
5	4.1 ± 0.5	nd	0.9 ± 0.1	27.6 ± 4.7	0.6 ± 0.1	0.3 ± 0.1	2.3 ± 0.2	64.2 ± 5.5
10	4.0 ± 0.5	nd	0.9 ± 0.1	29.0 ± 2.0	0.8 ± 0.0	0.4 ± 0.1	2.0 ± 0.1	62.9 ± 3.6
20	3.3 ± 0.5	nd	1.5 ± 0.2	26.9 ± 1.6	0.8 ± 0.2	0.5 ± 0.2	2.4 ± 0.6	64.6 ± 6.3
DGDG								
0	32.0 ± 2.2	nd	nd	1.9 ± 0.2	6.0 ± 0.3	1.3 ± 0.2	4.9 ± 0.3	51.2 ± 1.7
2.5	27.4 ± 2.1	nd	nd	2.0 ± 0.3	5.5 ± 0.4	0.9 ± 0.1	4.0 ± 0.3	60.0 ± 4.0
5	30.1 ± 2.3	nd	nd	1.5 ± 0.2	5.3 ± 1.2	1.0 ± 0.1	4.7 ± 0.5	54.6 ± 1.5
10	28.8 ± 1.6	nd	nd	2.1 ± 0.3	5.4 ± 0.4	0.9 ± 0.1	4.2 ± 0.2	58.2 ± 0.9
20	26.9 ± 1.8	nd	nd	1.8 ± 0.2	5.7 ± 1.1	1.1 ± 0.2	3.7 ± 0.8	60.1 ± 6.8
PE								
0	35.0 ± 2.6	nd	nd	0.5 ± 0.2	8.0 ± 1.5	1.4 ± 0.3	29.9 ± 3.7	25.2 ± 2.2
2.5	31.8 ± 1.9	nd	nd	0.3 ± 0.3	9.0 ± 1.0	3.1 ± 0.8	24.0 ± 1.5	31.8 ± 0.4
5	32.3 ± 6.0	nd	nd	0.6 ± 0.2	5.6 ± 1.2	1.3 ± 0.4	30.4 ± 4.4	29.8 ± 2.6
10	31.4 ± 3.3	nd	nd	0.2 ± 0.2	8.1 ± 1.0	3.1 ± 0.1	25.7 ± 1.0	31.5 ± 3.0
20	30.6 ± 5.6	nd	nd	0.5 ± 0.1	6.7 ± 1.1	1.7 ± 0.4	32.1 ± 3.2	28.4 ± 4.7
PC								
0	34.4 ± 5.2	nd	nd	0.3 ± 0.3	9.8 ± 1.1	3.3 ± 1.0	25.3 ± 5.5	26.9 ± 4.1
2.5	34.9 ± 4.3	nd	nd	0.2 ± 0.1	9.1 ± 1.0	2.9 ± 0.6	23.5 ± 0.7	29.4 ± 3.8
5	31.8 ± 6.4	nd	nd	0.3 ± 0.0	7.7 ± 0.8	2.5 ± 0.3	24.5 ± 1.1	33.2 ± 3.6
10	30.3 ± 9.3	nd	nd	0.3 ± 0.1	8.1 ± 1.3	2.5 ± 0.7	27.3 ± 3.4	31.5 ± 2.7
20	28.8 ± 3.6	nd	nd	0.2 ± 0.2	9.0 ± 0.7	3.8 ± 0.9	29.7 ± 3.5	28.5 ± 3.3
Time (min) after FAC elicitation								
MGDG								
0	5.3 ± 0.4	nd	1.3 ± 0.1	31.0 ± 4.5	0.8 ± 0.1	0.5 ± 0.1	3.1 ± 0.5	58.0 ± 6.4
2.5	3.9 ± 0.5	nd	0.9 ± 0.1	27.7 ± 2.4	0.7 ± 0.2	0.3 ± 0.0	2.1 ± 0.1	64.3 ± 3.7
5	3.8 ± 0.6	nd	1.0 ± 0.4	30.2 ± 1.2	0.6 ± 0.1	0.3 ± 0.1	2.1 ± 0.3	62.0 ± 6.6
10	4.3 ± 0.5	nd	0.6 ± 0.1	27.2 ± 2.9	0.8 ± 0.1	0.3 ± 0.1	2.0 ± 0.3	64.9 ± 8.6
20	4.8 ± 1.0	nd	1.0 ± 0.4	30.6 ± 9.3	0.9 ± 0.3	0.3 ± 0.1	1.9 ± 1.0	60.5 ± 2.2
DGDG								
0	32.2 ± 1.5	nd	nd	2.0 ± 0.3	4.8 ± 0.3	1.3 ± 0.1	6.9 ± 0.3	49.5 ± 1.3
2.5	27.2 ± 1.9	nd	nd	1.9 ± 0.4	5.5 ± 0.7	0.9 ± 0.3	4.2 ± 0.7	60.3 ± 6.1
5	27.6 ± 2.8	nd	nd	2.1 ± 0.4	4.8 ± 0.2	1.0 ± 0.2	4.8 ± 0.6	58.4 ± 7.7
10	29.7 ± 2.1	nd	nd	1.7 ± 0.2	5.6 ± 0.4	0.8 ± 0.0	4.1 ± 0.3	57.9 ± 4.9
20	31.4 ± 4.1	nd	nd	1.7 ± 0.3	5.5 ± 1.0	0.8 ± 0.1	3.5 ± 0.5	57.0 ± 11.7
PE								
0	32.9 ± 3.2	nd	nd	0.5 ± 0.1	5.8 ± 0.8	1.4 ± 0.2	36.9 ± 4.0	22.5 ± 2.2
2.5	31.5 ± 2.1	nd	nd	0.5 ± 0.1	6.2 ± 0.7	1.3 ± 0.3	30.5 ± 2.2	30.1 ± 1.7
5	33.2 ± 2.2	nd	nd	0.5 ± 0.2	5.5 ± 0.3	1.4 ± 0.4	30.8 ± 3.3	28.5 ± 2.1
10	33.8 ± 5.0	nd	nd	0.4 ± 0.0	6.6 ± 1.1	1.0 ± 0.3	28.7 ± 6.0	29.5 ± 5.9
20	34.0 ± 10.3	nd	nd	0.6 ± 0.3	6.5 ± 2.6	1.2 ± 0.6	30.7 ± 11.3	26.9 ± 7.3
PC								
0	30.7 ± 5.0	nd	nd	2.3 ± 2.3	7.2 ± 1.1	3.2 ± 1.1	31.8 ± 6.7	24.8 ± 4.3
2.5	30.2 ± 6.5	nd	nd	0.3 ± 0.3	8.8 ± 1.3	3.1 ± 1.3	25.1 ± 6.3	32.5 ± 6.4
5	31.3 ± 5.8	nd	nd	0.3 ± 0.1	6.8 ± 1.2	3.2 ± 1.7	26.5 ± 9.1	31.9 ± 6.7
10	34.5 ± 4.3	nd	nd	0.2 ± 0.0	7.9 ± 1.3	2.0 ± 0.6	21.8 ± 2.3	33.6 ± 3.8
20	32.4 ± 4.4	nd	nd	0.1 ± 0.1	8.9 ± 1.4	2.9 ± 1.3	24.8 ± 7.2	31.0 ± 7.0

2

Table SIII. Amounts of oxylipins recovered from wounded and FAC elicited *N. attenuata* leaves after lipid fractionation and hydrolysis (n=3).

oxylipins	Fractions	0 min (resting)	15 min	30 min	60 min
		nmol gFW^{-1} (standard deviation)			
OPDA	Neutral lipids	<0.1	1.2 (0.2)	<0.1	<0.1
(wounded)	Non-hydrolyzed total extract	<0.1	1.0 (0.2)	<0.1	<0.1
dnOPDA (C$_{16}$-OPDA)	Neutral lipids	-	-	-	-
(wounded)	Non-hydrolyzed total extract	-	-	-	-
OPDA	Neutral lipids	<0.1	5.1 (0.4)	0.5 (0.1)	<0.1
(FAC elicited)	Non-hydrolyzed total extract	<0.1	4.9 (0.5)	0.6 (0.1)	<0.1
dnOPDA (C$_{16}$-OPDA)	Neutral lipids	-	-	-	-
(FAC elicited)	Non-hydrolyzed total extract	-	-	-	-

3

Table SIV. Fatty acid composition of major glycerolipids in ir-sipk and ir-npr1 unelicited leaves (mol%)

	16:0	16:1[3]	16:2[7,10]	16:3[7,10,13]	18:0	18:1[9]	18:2[9,12]	18:3[9,12,15]
ir-sipk								
MGDG	3.8 ± 0.2	nd	nd	29.9 ± 3.5	0.8 ± 0.1	0.6 ± 0.1	2.2 ± 0.2	62.7 ± 6.3
DGDG	24.9 ± 2.0	nd	nd	2.4 ± 0.3	5.6 ± 0.3	1.2 ± 0.1	3.7 ± 0.5	62.1 ± 6.3
PE	31.4 ± 2.2	nd	nd	0.8 ± 0.1	7.1 ± 0.7	1.7 ± 0.1	29.7 ± 3.3	29.3 ± 1.7
PC	28.6 ± 1.0	nd	nd	0.4 ± 0.1	9.8 ± 1.0	4.2 ± 0.6	28.4 ± 4.1	28.6 ± 1.5
ir-npr1								
MGDG	4.3 ± 0.2	nd	nd	26.7 ± 1.2	0.9 ± 0.1	0.4 ± 0.1	1.8 ± 0.1	65.9 ± 3.2
DGDG	27.6 ± 1.9	nd	nd	1.2 ± 0.1	7.7 ± 0.4	1.2 ± 0.1	3.5 ± 0.3	58.7 ± 4.8
PE	31.4 ± 1.4	nd	nd	0.6 ± 0.1	8.0 ± 0.3	1.9 ± 0.2	27.0 ± 1.6	31.1 ± 1.2
PC	30.2 ± 5.7	nd	nd	0.3 ± 0.1	9.3 ± 0.8	3.5 ± 0.3	27.1 ± 3.0	29.6 ± 6.8

4

Table SV. Sequences of primers used for cloning and RT-qPCR

Primers used for RT-qPCR

	Forward	Reverse
NaAOC[*]	CTATATACCGGAGACCTAAAGAAGA	AGTATCCTCGTAAGTCAAGTACGAT
NaAOS[*]	GACGGCAAGAGTTTTCCCAC	TAACCGCCGGTGAGTTCAGT
NaEF1a	ACACTTCCCACATTGCTGTCA	AAACGACCCAATGGAGGGTAC
NaPLA1	AGTAGCAGATGATGTTAGTACATGTA	ACATGTGAATATGCCCATGGCATACT
NaPLA2	CGAGATTAAGTGCTAGAGCACAGCT	GCTTTGTTCCCTACTTGTGGACTAC
NaPLA3	TAGCCTAGGTGCATCACTTGCAAC	TATTTCGGAACAATGTCCAGTAGGT
NaLOX2[*]	TTAGTAGAAAATGAGCACCACAA	TTGCACTTGGTGTTTGAGATGGT
NaLOX3[*]	GGCAGTGAAATTCAAAGTAAGAG	CCCAAAATTTGAATCCACAACA

*: Described in Paschold et al (2008), Halitschke et al (2004).

Primers used to clone the homologues of Arabidopsis DAD1 and DGL in *N. attenuata*

	Forward	Reverse
NaPLA1	CAAGCTTAGCTGAATCTGTG	ACATGTGAATATGCCCATGG
NaPLA2	TCGTGGTACAACGAGAAATTATGA	TAATGAGTTATAAGATCAATCTTG
NaPLA3	GCGAGGAACGATTCAGACACTGGA	TATTTCGGAACAATGTCCAGTAGG

Primers used for construction of VIGS vectors

	Forward	Reverse
NaPLA1	GCGGCGGTCGACACAGGACATAGTCTTGGTGC	GCGGCGGGATCCGCCCATGGCATACTATTGTC
NaPLA2	GCGGCGGTCGACGCGCCTAAAGTAATGAATGG	GCGGCGGGATCCGAAACTCCTTTAGCCTTTCG
NaPLA3	GCGGCGGTCGACTAATCAGGCTAGTGCCAGAG	GCGGCGGGATCCTCGGAACAATGTCCAGTAGG

Primers used to evaluate gene silencing in VIGS-silenced plants

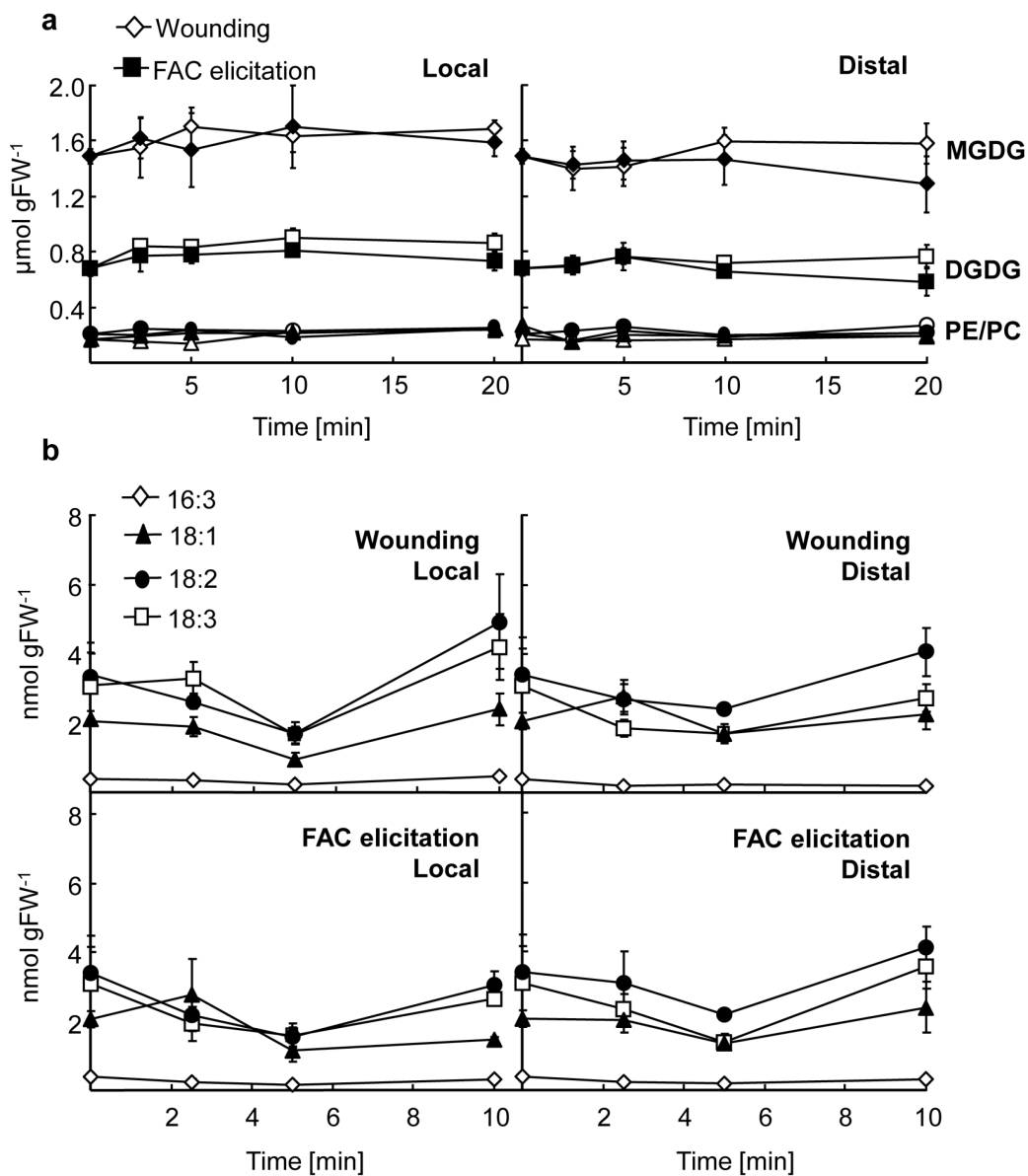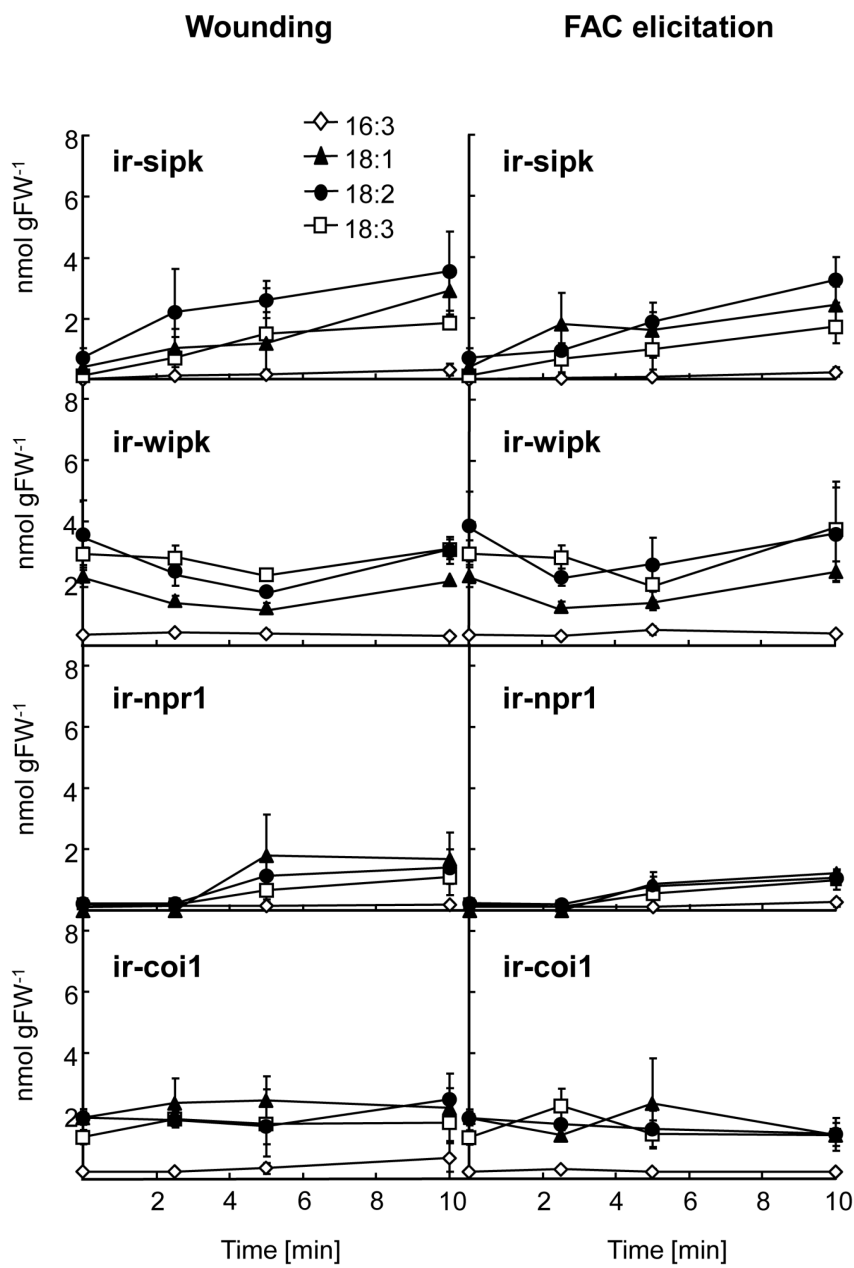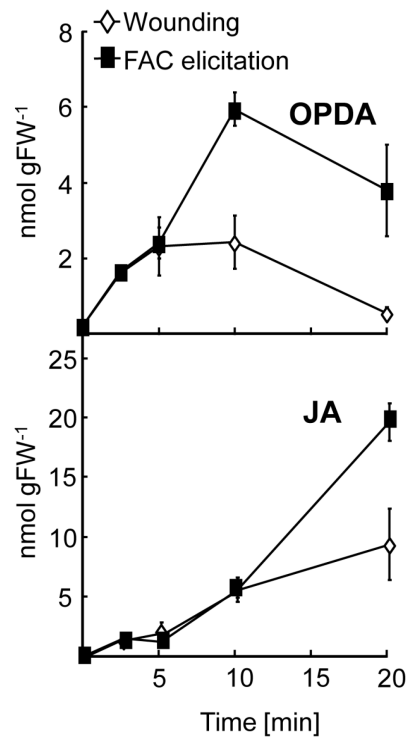|	Forward	Reverse
NaPLA1	GTGGGTTTTTGAGCTTATACCAAAC	ACATGTGAATATGCCCATGGCATACT
NaPLA2	GATCCATTAAACCTCCATCTCCGG	TTGTAATCTGAAGCCGATTCGAACA
NaPLA3	ACTTGACCCACTCAAGTATAAAGTA	TCCAGTGTCTGAATCGTTCCTCGC

Figure S1

Wounding   FAC elicitation

Figure S2

Figure S3

a

b

Figure S4

a

b

c

Figure S5

Figure S6

Figure S7

a

b

Figure S8

A

NaPLA1 full length cDNA

ATAATTCAGCTGATTTTAACACATTGACTTTTTCTCTCTCTAAATAACACAACTTTCCTCCTCTCTCTCTCTCTAAGAAAATC<u>ATG</u>CAGGTGGCA
GTGGCAACTA**ATGTTCATTTTTTTCAGGCACGTCGATCCAGTTTCAAGTACTGTAATGGTTCAYCTCCATTAAACCCTATACCTAGAGCTACTGC
TGTAAATGTACAATGTTTAAAAACAGTAGCAACACCACCAACTTCTACAACAGAGATGACAAAAAAACATCTTTCAAATCTTGAAATGCTTTTAC
AAAAGCAATCTCAGCCACATCCAATGGATTCAGCAGAGCCAATTATTCAAGAAATAAAACAGAGGAAAACAGGGGAAAACAGGGGAAGGAATATG
TTGGAAGGGCTAAATTTGGCAAGAATTTGGCCAGAAATGAAAGCAGCTGAAGAATATTCTCCTAGGCATTTGGTTAAATTACACAGGATGTTATC
ATCAAAATCAATGGAATATTCTCCTAGAAATAATCTTGGGACTAGGTGGAGAGAGTACCACGGGTGCAAAGATTGGTTAGGACTTATTGATCCAT
TGGATGAGAATCTCCGGCGAGAGTTAGTCCGATATGGTGAGTTTATTCAAGCAGCTTACCATTGTCTTCATTCCAACCCCGCCACGTCAGAAAAA
GAAAATGCTGACGTGGCGAGGAACGTGTCGTTACCTGATAGGTCTTACAAGGTGACTAAGAGCCTTTATGCCACGTCATCCGTTGGCCTGCCTAA
ATGGGTGGATGACGTGGCACCGGATCTTGGGTGGATGACCCAAAGGTCCAGTTGGATCGGGTACGTCGCTGTGTGCGACGACAAAACCGAGATCC
AACGGATGGGAAGGAGGGATATTGTCATCGCGTTACGTGGTACTGCCACGTGTCTAGAATGGGGCGAAAATTTTCGCGACGTGCTAGTTCAAATG
CCAGGAAAAAATGATTCAGTTGAAGGACAACCAAAAGTAGAATGTGGGTTTTTGAGCTTATACCAAACAGGTGGAAATAAAATTCCAAGCTTAGC
TGAAYCTGTGGTGAATGAAGTGAAAAGACTCATTGAAATGTACAAAGGTGAGAGTCTAAGTATAACAGTAACAGGACATAGTCTTGGTGCTGCTT
TAGCTTTATTAGTAGCAGATGATGTTAGTACATGTACACCAGATTCACCACCAGTTGCTGTTTTTACATTTGGAGGTCCTAGGGTAGGCAACAAA
GGCTTTGCCAATCGACTCGAATCGAAAAATGTTAAGGTCTTACGTATCGTGAACAAACAAGATGTGATTACTAAAGTTCCAGGAATGTTTGTGAG
CGAAGCGCTTGACAAAAAACTAAGGGAAAAAGGCGCTGCGGGGGTGTTAAAATTTGCTTGACAATAGTATGCCATGGGCATATTCACATGTTGGTA
CTGAATTAAGAGTTGACACAACGAAGTCTCCGTTTTTAAAACCAGATGCAGATGTCGCATGTTGTCATGATTTGGAAGCATATTTGCATTTGGTG
GATGGGTATTTGGGATCAAATGAATCATTTAGACCAAATGCAAAGAGAAGCCTTGTTAAGTTATTGACTGAACAAAGGACTAATATCAAAAAATT
GTACAATAGTAAGGGGAAAGATTTGAGTAGTCTTAATCTTAATAGTGAATTTAATTTTCCTAGACCTAGTTGTTTGCCTAGTCCTAGTGTCTTGC
CTAGTCCTTCAGCT**<u>TGA</u>**AATTGTTGGACAGGAGATGTATGCTTCTTGTACAAATTTAASAAGTAATGAGAAGTATATGTTTTCTAGT<u>AAAAAAAA
AAAAAAAAAAAAAAAAAAAA</u>**

B

NaPLA1 complete protein sequence

<u>MQVAVATNVHFFQARRSSFKYCNGSXPLNPIPRATAVNVQCLKTVATPPTSTTEM</u>TKKHLSNLEMLLQKQSQPHPMDSAEPIIQEIKQRKTGENR
GRNMLEGLNLARIWPEMKAAEEYSPRHLVKLHRMLSSKSMEYSPRNNLGTRWREYHGCKDWLGLIDPLDENLRRELVRYGEFIQAAYHCLHSNPA
TSEKENADVARNVSLPDRSYKVTKSLYATSSVGLPKWVDDVAPDLGWMTQRSSWIGYVAVCDDKTEIQRMGRRDIVIALRGTATCLEWGENFRDV
LVQMPGKNDSVEGQPKVECGFLSLYQTGGNKIPSLAEXVVNEVKRLIEMYKGESLSITVTGHSLGAALALLVADDVSTCTPDSPPVAVFTFGGPR
VGNKGFANRLESKNVKVLRIVNKQDVITKVPGMFVSEALDKKLREKGAAGVLNLLDNSMPWAYSHVGTELRVDTTKSPFLKPDADVACCHDLEAY
LHLVDGYLGSNESFRPNAKRSLVKLLTEQRTNIKKLYNSKGKDLSSLNLNSEFNFPRPSCLPSPSVLPSPSA
Underlined : predicted plastid transit peptide (53 aa)

C

Protein alignment of NaPLA1 with Arabidopsis DAD1 and DGL
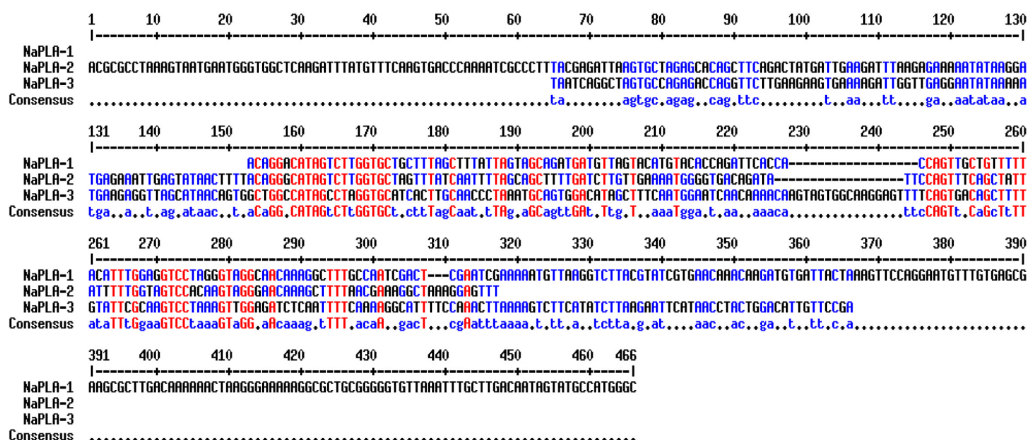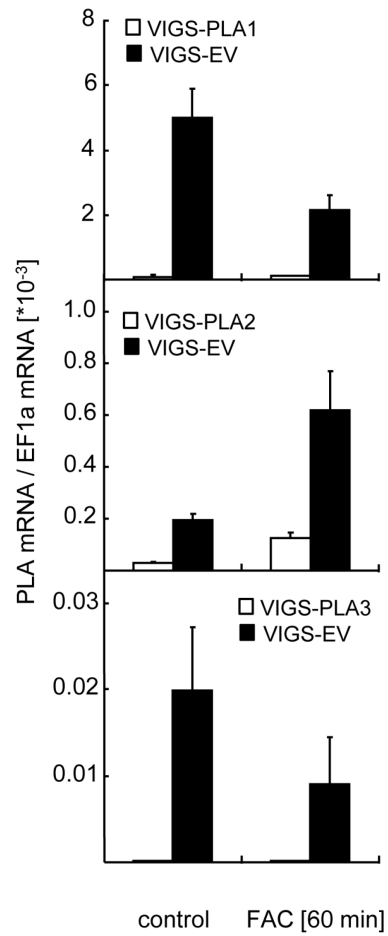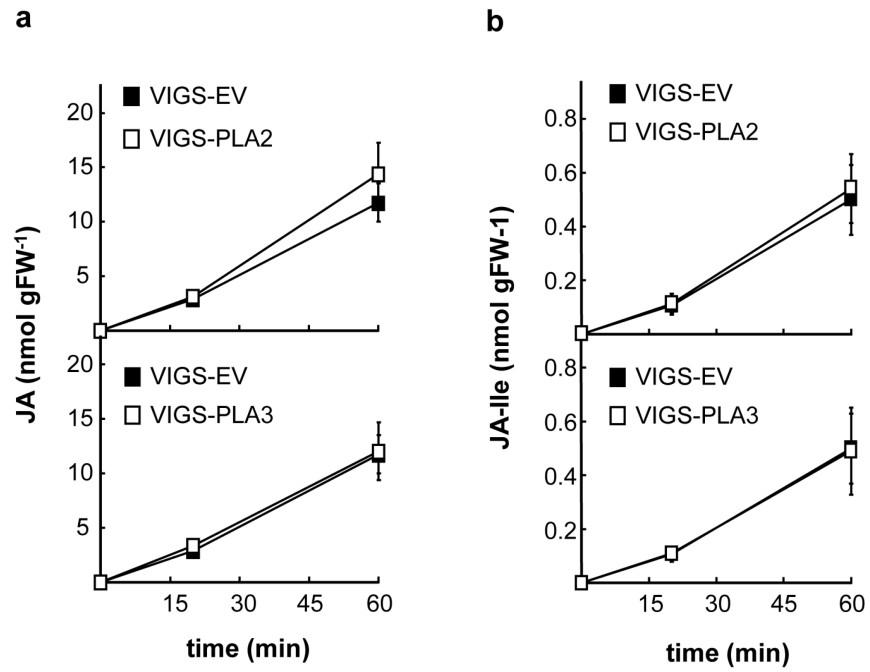

Figure S9

14

LEGENDS FOR SUPPLEMENTARY FIGURES

Figure S1. Membrane glycerolipid and unsaturated FFA levels in WT plants

(a) Leaves of rosette stage WT plants were wounded or FAC elicited, glycerolipid classes isolated and quantified from local and distal leaf sections at different times. Lipid classes: MGDG, DGDG, PC, PE. Bars (±SE, n=4). **(b)** Leaves of rosette stage WT plants were wounded or FAC elicited, FFA isolated and quantified from local and distal leaf sections at different times. Bars (±SE, n=4). **Note**: The data corresponding to free 18:3 levels in local FAC elicited leaves has been used in Fig. 1 and it has been included here for comparison with the other FFA.

Figure S2. Unsaturated FFA levels in RNAi-silenced plants

Leaves of rosette stage ir-sipk, ir-wipk, ir-npr1 and ir-coi1 plants were wounded or FAC elicited for different times, FFA isolated and quantified from local leaf sections. Bars (±SE, n=4). **Note**: The data corresponding to free 18:3 levels in FAC elicited leaves has been used in Fig. 1 and it has been included here for comparison with the other FFA.

Figure S3. OPDA and JA levels in WT plants within 20 min of induction

Leaves of rosette stage WT plants were wounded or FAC elicited for different times and OPDA and JA quantified in local leaf sections. Bars (±SE, n=5). **Note**: The data between time 0 and 10 min is presented in Fig. 3 and it has been included here for comparison with time 20 min.

15

Figure S4. Basal levels of JA and basal and induced levels of SA in leaves

(a) Basal levels of JA in unelicited leaves of WT and RNAi-silenced genotypes. **(b)** Levels of SA in unelicited, wounded and FAC elicited (10 min after the treatments) leaves from WT and RNai-silenced genotypes. Bars (±SD, n=5). *see text.

Figure S5. RT-qPCR, LOX3 protein levels and protein activities in elicited leaves

(a) Basal transcript levels were quantified in resting leaves of WT, ir-sipk, ir-wipk, ir-npr1 and ir-coi1 plants. Relative transcript abundance was quantified by RT-qPCR and expressed as the ratio of abundance of the queried mRNA over the standard (EF1a). Bars (±SD, n=3). **(b)** LOX3 protein levels were analyzed by immuno-blotting using a purified anti-NaLOX3 antibody. Total proteins were extracted from resting (control) and FAC elicited (20 min), separated by SDS-PAGE and NaLOX3 detected by immuno-chemoluminescence. Gel loading was evaluated by coomasie-blue staining. **(c)** Leaf 13-LOX and AOS activities were quantified after 20 min of FAC elicitation in WT and ir-sipk, ir-wipk, ir-npr1, ir-coi1 by using, respectively, $[1-^{14}C]$-18:3 or $[1-^{14}C]$-13-hydroperoxy-18:3 as substrates. Assays were performed in the linear phase of the reactions and ^{14}C products were extracted, separated and quantified by densitometric scanning. Bars (±SD, n=3). *P<0.05, Students t-test, WT vs genotypes.

Figure S6. Alignment of PLA sequences used for VIGS

DNA alignments were performed using the MultiAlign sofware (Symbol comparison table: dna Gap weight: 5 Gap length weight: 0) as described (F. Corpet (1988) Multiple sequence alignment with hierarchical clustering. Nucl. Acids Res., 16, 10881-10890).

16

Figure S7. Quantification of PLA mRNA levels in VIGS-silenced plants

VIGS vectors carrying specific sequences in antisense orientation of PLA1, PLA2 and PLA3 cDNAs were generated and used for specific gene silencing. The efficiency of gene silencing was evaluated by quantification of PLA1, PLA2 and PLA3 transcript levels by RT-qPCR in unelicited leaves and 60 min after elicitation. mRNA levels are expressed as the ratio of abundance of the queried mRNA over the standard (EF1a). Control plants were empty vector (EV) plants. Bars (±SD, n=4).

Figure S8. Quantification of JA and JA-Ile levels in PLA2 and PLA3 VIGS-silenced plants

JA and JA-Ile levels were quantified in unelicited leaves and at 20 and 60 min after FAC elicitation. VIGS-PLA silenced plants (white), VIGS-EV plants (black). Bars (±SE, n=8).

Figure S9. Full length mRNA and AA sequences of PLA1

(a) Full length PLA1 mRNA sequence showing the ORF in blue letters (start and stop codons uunderlined); **(b)** Full length PLA1 protein sequence with predicted transit peptide underlined; **(c)** Alignment of PLA1, DAD1 and DGL protein sequences. Protein alignments were performed with ClustalW2 using protein gap open penalty = 10.0, protein gap extension penalty = 0.2, Protein matrix = Gonnet, Protein/DNA ENDGAP = -1, and Protein/DNA GAPDIST = 4.

17

SUPPLEMETAL EXPERIMENTAL PROCEDURES

Glycerolipid extraction

Leaf material (0.5 g) was ground in liquid nitrogen, transferred into 10 mL glass tubes, 2 mL of 2-propanol were added and the solution was heated for 10 min at 80°C to inactivate lipases. After cooling, 3 mL of hexane and 2 mL 6.7% (w/v) Na_2SO_4/water were added. After centrifugation, the organic phase was collected and the aqueous phase re-extracted with 3 mL of 3/2 (v/v) 2-propanol/hexane. The organic phases were combined, the solvent evaporated under nitrogen and the samples reconstituted in 200 μL 10/1 (v/v) chloroform/methanol.

Glycerolipid and FFA analyses

Glycerolipid classes were separated on Partisil$^®$ K6 silica plates (Whatman, Dassel, Germany) impregnated with 0.15 M aqueous NH_4SO_4 and activated for 3 h at 110°C. The plates were developed three times with 91/30/8 (v/v/v) acetone/toluene/water and lipids were detected after spraying with 2% (w/v) 2'-7'-dichlorofluorescin/methanol and visualization under UV light. Commercial PC, PG, MGDG, DGDG (Matreya, Pleasant Gap, PA) standards were used to identify the different lipid classes. Glycerolipids were eluted from the silica with 3 mL of 2/1 (v/v) chloroform/methanol. 5 μg of heptadecanoic acid (17:0) were added as internal standard and lipids were trans-methylated in 1% (v/v) H_2SO_4/methanol for 1 h at 75°C. Fatty acid methyl esters were extracted with hexane and analyzed by GC-MS (see below).

FFA extraction was performed according to (Conconi et al., 1996). Heptadecanoic acid (0.5 μg per sample) was added as internal standard for quantification. After extraction, samples were reconstituted in 0.2 mL of chloroform and lipids separated on Partisil® K6 silica plates (Whatman, Dassel, Germany) developed with 70/30/1 (v/v/v) hexane/diethyl ether/acetic acid. Commercial FFAs were used as standards and plates were stained with 2% (v/v) 2'-7'-dichlorofluorescin/methanol and lipids visualized under UV light. FFA were eluted from the silica with 3 mL of 2/1 (v/v) chloroform/methanol and methylated in 1% (v/v) H_2SO_4/methanol for 1 h at 75°C. Fatty acid methyl esters were extracted with hexane and analyzed by GC-MS (see below).

18

To evaluate whether wounding and FAC elicitation caused differential leaf water loss during the 20 min of the experiments, the ratio between gDW and gFW was determined at the beginning (T0) and end (20 min) of this interval for both treatments. Leaf gDW/gFW ratios remained constant and similar to T0 values (0.10 ± 0.03) for WT leaves and the four additional genotypes tested, indicating no substantial water loss within this time frame.

Analysis of FA in leaf waxes

Leaf surface waxes were extracted by dipping leaves (~0.5 g of leaf material) in either 20 mL of hexane or chloroform for 1 and 2 min. 10 µg of 17:0 were added as internal standard. The samples were evaporated under nitrogen and methylated in 1% (v/v) H_2SO_4/methanol for 1h at 70°C. After extraction of FAMES with hexane the samples were analyzed by GC-MS (see below).

GC-MS analysis

Fatty acid methyl esters were analyzed in a Varian CP-3800 GC coupled with a Varian Saturn 3800 ion trap MS in electron ionisation (EI; 70 eV) mode (Varian, Palo Alto, CA). 1 µl of the sample was injected in splitless mode on a DB-WAX column (30m×0.25mm I.D., 0.25 µm film thickness, Agilent, Boeblingen, Germany) with helium at a constant flow of 1 mL min^{-1} as the carrier gas. The injector was at 230°C. The oven temperature program was: 130°C for 5 min, 220°C at 3.0°C/min, 5°C/min ramp to 240°C and hold for 1 min. EI spectra were recorded on Scan mode from 40 to 400 amu. Quantification was performed in the linear range of detection and based on calibration curves generated with increasing concentrations of commercial FAMES mixes (Matreya, Pleasant Gap, PA) and the IS (17:0).

LC-(ESI)-MS/MS

JA, JA-Ile, OPDA and 13-OOH-18:3 were quantified on a LC-(ESI)-MS/MS system (Varian 1200 Triple-Quadrupole-LC-MS system; Varian, Palo Alto, CA). 10 µL of the sample were injected onto a ProntoSIL® column (C18; 5 µm, 50 × 2 mm, Bischoff, Leonberg, Germany) connected to a precolumn (C18, 4x2mm, Phenomenex, USA). As mobile phases 0.05%/1%

19

(v/v/v) formic acid/acetonitrile/water (solvent A) and 0.05% (v/v) formic acid/acetonitrile (solvent B) were used in a gradient mode with the following conditions: time/concentration (min/%) for B: 0.0/5; 3.0/5; 10.0/98; 17.5/98; 20.5/5; 27.0/5; time/flow (mL/min): 0.0/0.4; 0.5/0.2; 17.5/0.2; 19.5/0.4; 27.0/0.4. Compounds were detected in the ESI negative mode and multiple reaction monitoring (MRM). For 13-OOH-18:3 and 15-OOH-20:2 (Cayman Chemicals, Ann Arbor, MI) the specific precursor-product ion transitions used for detection and quantification were m/z = 309>291 and 339>321 (fragmented under 5V collision energy). Commercial 13S-(OOH)-18:3 and 9(R/S)-OOH-18:3 were used as standards (Cayman Chemicals, Ann Arbor, MI). For OPDA, the specific precursor-product ion transitions used was m/z = 291>165 (fragmented under 12V collision energy). For JA and [9, 10-^{2}H]dihydro-JA, the specific precursor-product ion transitions were m/z =209>59 and 213>59 (fragmented under 18V collision energy). For JA-Ile and [^{13}C$_6$]-JA-Ile, the specific precursor-product ion transitions were m/z = 322>130 and 328>136 (fragmented under 19V collision energy). For SA and [^{13}C$_4$]-SA, the precursor-product ion transitions used were m/z = 137>93 and 141>97 (fragmented under 19V collision energy).

Analysis of lipid-bound OPDA

Total lipids were extracted by the hexane-isopropanol method (see Glycerolipid extraction above). Rosette-stage resting, wounded or FAC elicited leaves were analyzed. Times after treatments were 15, 30 and 60 min. After extraction, lipids were reconstituted in chloroform. To separate neutral lipids, glycolipids and phospholipids, 1 mL of the extract was used for solid phase extraction (SPE) on silica Sep Pak cartridges (Millipore, Schwalbach/Ts, Germany) according to (Cahoon and Ohlrogge, 1994) with some modifications. Briefly, lipid extracts dissolved in 1 mL chloroform were transferred to the cartridge and after the sample had entered the packing, two 5 mL chloroform washes were used to elute neutral lipids. Glycolipids were eluted by the sequential addition of two 5 mL acetone washes. Phospholipids were eluted with two 5 mL 100/50/40 (v/v/v) methanol/chloroform/water washes. Purification was evaluated by TLC separation of lipid classes according to Bonaventure *et al* (2004).

One mL of the extract was evaporated under nitrogen and trans-methylated by vortexing in 2 M KOH in methanol (0.6 mL) plus hexane (4 mL) for 5 min at room temperature. The reaction was quenched by adding 4 mL of 1 M aqueous acetic acid. The hexane phase was

20

removed and the acidified aqueous phase was extracted with 2/1 (v/v) and then 1/2 (v/v) chloroform/methanol. The organic phases were combined and evaporated to dryness under nitrogen. OPDA-ME was analyzed by GC-MS on a DB-Wax column as described above. Commercial 12-oxo-phytodienoic acid (Cayman Chemicals, Ann Arbor, MI) was methylated with diazomethane and used as a standard.

Total lipids and lipid fractions were also subjected to alkaline hydrolysis with 1 mL methanol and 1 mL 15% (v/v) aqueous KOH for 1h at 60°C. 2 mL of 1M citric acid were added and FA extracted twice with 3 mL 1/1 (v/v) hexane/di-ethyl ether. The solvent was evaporated under nitrogen and the dry residue reconstituted in 70% (v/v) methanol/water for OPDA analysis by LC-(ESI)-MS/MS (see above).

Analysis of esters and amides of JA in resting tissue

To rule out the possibility that at least a fraction of JA originated from a preformed JA pool in resting *N. attenuata* leaves, the total content of JA was analyzed after ester and amide bond hydrolysis. Total lipid extracts were spiked with $^{13}C_2$-JA as internal standard and hydrogenated before hydrolysis to prevent oxidation of double bonds in the strong alkaline conditions used to cleave amide bonds. After hydrolysis, the level of dihydro-JA (produced from endogenous JA) was similar to the endogenous basal levels of JA (0.25 ± 0.05 nmol gFW^{-1}) in non-hydrolyzed samples. These results indicated that no pre-formed pools of JA were present in resting leaves and therefore that JA must originate from the *de novo* synthesis. For this experiment, 0.3 g frozen leaf tissue was extracted by homogenization in FastPrep® tubes containing 1 g of FastPrep® matrix (Bio 101, La Jolla, CA) and 1 mL ethyl-acetate spiked with 0.5 nmol [1,2-^{13}C]JA. Homogenates were centrifuged for 10 min at 4 °C, supernatants collected into fresh tubes and plant material re-extracted with 0.5 mL ethyl-acetate. Supernatants from both extractions were pooled and evaporated until dryness. For esters of JA, the dry residue was reconstituted in 1 mL methanol and ester bonds hydrolyzed by adding 1 mL 15% (v/v) KOH/water and heating for 1 h at 60°C. Afterwards, 2 mL 1M citric acid were added and the mixture extracted twice with 3 mL chloroform, evaporated under nitrogen and resuspended in 70% (v/v) methanol/water for JA analysis by LC-(ESI)-MS/MS (see above). For total JA analysis (amides plus esters of JA), the dry residue was re-suspended in 1 mL THF (dried over molecular sieve), and hydrogenated with 5 mg PtO$_2$, by stirring under a hydrogen atmosphere for 24 h. The

21

catalyst was removed by centrifugation, THF evaporated under nitrogen and the pellet was re-suspended in 2 mL dioxane and heated for 12 h with 10% (w/v) aqueous Ba(OH)$_2$ at 110 °C. After saponification the aqueous phase was washed with 2 mL chloroform, acidified to pH 4.0 with HCL and extracted twice with 2 mL ethyl-acetate. The ethyl-acetate was evaporated under nitrogen and the sample re-suspended in 70% (v/v) methanol/water for analysis by LC-(ESI)-MS/MS (see above).

13-LOX and AOS activity assays

The method was adapted from Bonaventure *et al* (2007). One leaf disc of 5 mm diameter was punched out from the leaf and ground thoroughly with a pestle in 50 μl reaction buffer (40 mM MOPS/KOH, pH 7.0, 10% (v/v) glycerol, 0.01% (v/v) Tween-20). After a 10 sec spin, 1.5 μl of the supernatant were added into 1.7 mL of reaction buffer containing 20,000 DPM of either [1-^{14}C]-9,12,15-linolenic acid (51.7 mCi/mmol, Perkin-Elmer, Rodgau, Germany) or synthesized [1-^{14}C]13-OOH-18:3 (see below), vortexed briefly and incubated at room temperature for 1, 2 and 4 min (linear range of substrate conversion). Reactions were stopped by the addition of 1 mL of chloroform. After vortexing and centrifugation, the organic phase was kept, samples re-extracted with 1 mL of chloroform, the organic phases pooled and evaporated under a stream of nitrogen and samples reconstituted in 20 μL of chloroform and loaded onto a TLC plate (silica gel 60; Merck, Darmstadt, Germany). The plates were developed with diethyl ether/toluene/formic acid 70/30/1 (v/v/v), exposed to ^{14}C sensitive screens for different times and screens scanned with an FLA-3000 densitometric scanner and band intensities quantified with the Aida Image Analyzer v3.11 software (Fujifilm, Duesseldorf, Germany). Bands corresponding to 13-(OOH)-18:3, 13-OH-18:3 and α and β ketols were quantified as products dependent on 13-LOX activity for their formation.

[1-^{14}C]13-OOH-18:3 was synthesized using 10 μL of 80,000 units/mL of LOX1-B (Sigma, Taufkirchen, Germany; prepared in 50 mM sodium borate buffer, pH 9.0) in 1 mL Tris-HCl buffer (40 mM Tris, 1mM CaCl$_2$, adjust to pH 8.9 with 0.5M HCl) containing 20 μL of [1-^{14}C]-9,12,15-linolenic acid (51.7 mCi/mmol, Perkin-Elmer, Rodgau, Germany) . The reaction was carried out for 60 min at room temperature. The radiolabeled hydroperoxy-18:3 was recovered after chloroform extraction and the synthesis checked by TLC separation using diethyl ether/toluene/formic acid 70/30/1 (v/v/v) as the solvent system. Immediately before usage, the

22

chloroform was removed under a stream of argon and the ^{14}C-labeled hydroperoxy-18:3 dissolved in 0.5 mL of reaction buffer (see above). Bands corresponding to α and β ketols were quantified as AOS products.

Quantitative real time-PCR (qRT-PCR)

After different treatments, leaf material was immediately frozen in liquid nitrogen. Total RNA was extracted from ~0.1 g of tissue with TRIzol® (Invitrogen, Karlsruhe, Germany), DNase-I treated and 5 μg reverse-transcribed using oligo(dT)$_{18}$ and the SuperScript-II Reverse Transcriptase kit (Invitrogen, Karlsruhe, Germany) according to commercial instructions. Quantitative real-time PCR was performed on an ABI PRISM 7700 sequence detection system according to the manufacturer's instructions (Applied Biosystems, Foster City, CA), using the Core Reagent kit for SYBR Green analysis (Eurogentec, Koeln, Germany) and gene-specific primers (Suppl. Table SV). All reactions were performed with 3 biological replicates. The EF1a (Elongation Factor 1a) was used as an internal standard for cDNA normalization. Standard calibration curves were generated for all primers with a cDNA of known concentration. The relative amounts of all mRNAs were calculated using the calibration curves and the comparative threshold cycle method as described in User Bulletin No. 2 from PE-Applied Biosystems (Applied Biosystems, Foster City, CA).

Cloning of the full length PLA1 cDNA and construction of MBP and EGFP fusion proteins

For cloning of full length PLA1 cDNA, total RNA was extracted from 0.1 g of leaf material with TRIzol® (Invitrogen, Karlsruhe, Germany) and DNase-I treated according to commercial instructions. 5´RACE was performed using 5´RACE System for Rapid Amplification of cDNA Ends (Invitrogen, Karlsruhe, Germany). 5 μg of total RNA were reverse-transcribed with SuperScript-II reverse transcriptase and gene specific primer CCGCAGCGCCTTTTTCCCT according to commercial instructions. PCR amplification was performed using the AUAP primer and the gene specific primer TCGAGTCGATTGGCAAAGCCTT. 3´RACE was performed using the 3´RACE System for Rapid Amplification of cDNA Ends (Invitrogen, Karlsruhe, Germany). Five μg of total RNA were reverse-transcribed with SuperScript-II reverse transcriptase and

23

primer AP according to commercial instructions. PCR amplification was performed using the AUAP primer and the gene specific primer ACTCGAATCGAAAAATGTTAAGGTC. The PCR products were purified, subcloned into pGEM-T easy vector (Promega, Madison, WI) and sequenced. Analysis of the full length amino acid sequence of PLA1 by ChloroP gave a score of 0.557 cTP/Y/CS-score 2.553 and by TargetP of cTP 0.655 for plastid localization.

The PLA1 cDNA was cloned in frame to the maltose binding protein (MBP) in the vector pMAL-c4X (New England Biolabs, Beverly, MA). In this case, the putative plastid signal peptide was excluded to avoid activity inhibition (Fig. S4). For PCR amplification, the primers GGCCGAATTCATGAAAGCAGCTGAAGAATA and CCGGCTGCAGTTATCAAGCTGAAGGACTAGGCA were used and the amplicon was digested with EcoRI and PstI for subcloning into pMAL-c4X. *E.coli* BL21(DE3) cells were transformed and used for recombinant protein expression. MBP-PLA1 and MBP (control) were induced with 1mM of IPTG for 16 h at 25°C in LB media in the presence of ampicillin (100 µg/mL). The proteins were purified by amylose column chromatography (New England Biolabs, Beverly, MA) and washed and concentrated with Microcon YM-3 centrifugal filter units (Millipore, Schwalbach/Ts, Germany) according to commercial instructions. Protein amounts were quantified using the Bio-Rad Protein Assay kit (Bio-Rad, München, Germany) and BSA as a standard. SDS-PAGE and staining with Bio-Safe^{TM} Commasie (Bio-Rad, München, Germany) were used to evaluate protein purification.

For generation of EGFP fusion proteins, the full length PLA1 was PCR amplified from total cDNA using the primers GGCCCTGCAGATGCAGGTGGCAGTGGCAAC and CCGGGGTACCGCAGCTGAAGGACTAGGCAAGA. After purification, the PCR product was digested with PstI and KpnI and subcloned into the pEGFP vector (Clontech, Mountain View, CA). The PLA1-EGFP fusion construct was PCR amplified using the primers GGCCCTCGAGATGCAGGTGGCAGTGGCAAC and CCGGGAGCTCTCATTACTTGTACAGCTCGTCCAT and cloned into the pCAMBIA-1201 downstream of CaMV35S. The first 273 bp of the LOX3 coding region were PCR amplified from total cDNA with the primers GGCCCTGCAGATGGCACTAGCTAAAGAAATTAT and CCGGGGTACCGCTTCCTTGTTCTTGTTCCTCACTG. After purification, the PCR product was digested with PstI and KpnI and subcloned into pEGFP. The pLOX3-EGFP fusion product was amplified using the primers GGCCCTCGAGATGGCACTAGCTAAAGAAATTAT and CCGGGAGCTCTCATTACTTGTACAGCTCGTCCAT and subcloned into pCAMBIA-1201

24

downstream of CaMV35S. EGFP gene was PCR amplified from the pEGFP vector with primers
GGCCCTCGAGATGGTGAGCAAGGGCGAGGA and
CCGGGAGCTCTCATTACTTGTACAGCTCGTCCAT and subcloned into the pCAMBIA-1201
downstream of CaMV35S.

Generation of anti-NaLOX3 antibodies and Western blot analysis.

A purified rabbit polyclonal antibody against *N. attenuata* LOX3 was obtained
commercially (Eurogentec, Seraing, Belgium) and was induced by inoculation of the synthetic
peptides DWSKKSNLKTERVNY and SSEIRRIEKEIDDRN. Purification was performed by
affinity chromatography against the specific peptides coupled on the affinity column
(Eurogentec, Seraing, Belgium). Total protein extraction was performed as described
(Bonaventure et al., 2004) and SDS-PAGE and protein transfer to nitrocellulose membranes was
performed using standard conditions. Western blot analysis was performed using the
WesternBreeze® kit from Invitrogen (Invitrogen, Karlsruhe, Germany) following commercial
instructions. A 1/2000 (v/v) dilution of the anti-NaLOX3 antibody was used. Membranes were
exposed for different times to Blue X-Ray films (CL-XPosure™ Film, Thermo Scientific,
Rockford, IL) and developed using standard conditions. For gel staining, Bio-Safe™ Coomasie
(Bio-Rad, München, Germany) was used following commercial instructions.

ADDITIONAL REFERENCES

Bonaventure G, Ba XM, Ohlrogge J, Pollard M (2004) Metabolic responses to the reduction in
    palmitate caused by disruption of the FATB gene in Arabidopsis. Plant Physiology **135:**
    1269-1279

**Bonaventure G, Gfeller A, Proebsting WM, Hortensteiner S, Chetelat A, Martinoia E,
    Farmer EE** (2007) A gain-of-function allele of TPC1 activates oxylipin biogenesis after
    leaf wounding in Arabidopsis. Plant J **49:** 889-898

Cahoon EB, Ohlrogge JB (1994) Metabolic Evidence for the Involvement of a Delta(4)-
    Palmitoyl-Acyl Carrier Protein Desaturase in Petroselinic Acid Synthesis in Coriander
    Endosperm and Transgenic Tobacco Cells. Plant Physiology **104:** 827-837

25

Classification:

Biological Science, Ecology

Title:

Empoasca leafhoppers attack wild tobacco plants in a jasmonate-dependent manner and identify jasmonate mutants in natural populations

Author affiliation:

Mario Kallenbach, Gustavo Bonaventure, Paola A. Gilardoni, Antje Wissgott, and Ian T. Baldwin

Max-Planck-Institute for Chemical Ecology, Hans-Knoell-Strasse 8, D-07745 Jena, Germany

Corresponding author:

Ian T. Baldwin

Email: baldwin@ice.mpg.de

Fax: +49-3641-571102

Tel: +49-3641-571100

Abstract

Choice of host plants by phytophagous insects is essential for their survival and reproduction. This choice involves complex behavioral responses to a variety of physical and chemical characteristics of potential plants for feeding. For insects of the order Hemiptera, these behavioral responses involve a series of steps including labial dabbing and probing using their piercing mouthparts. These initial probing and feeding attempts also elicit a rapid accumulation of phytohormones such as jasmonic acid (JA) and the induced defense metabolites they mediate. When *Nicotiana attenuata* plants are rendered JA deficient by silencing the initial committed step of the JA biosynthesis pathway, they are severely attacked in nature by hemipteran leafhoppers of the genus *Empoasca*. By

producing *N. attenuata* plants silenced in multiple steps in JA biosynthesis, perception and the biosynthesis of the plant's three major classes of JA-inducible insecticidal defenses, we demonstrate that the choice of plants for feeding by *Empoasca* leafhoppers in both nature and the glasshouse is independent of the accumulation of major insecticidal molecules, the presence of *Candidatus* Phytoplasma spp and were not associated with detectable changes in plant volatiles, but depends on the plant´s capacity to mediate JA signaling. We exploited this trait and used *Empoasca* leafhoppers to discover genetic variation in JA accumulation and signaling hidden in *N. attenuata* natural populations.
\body

Introduction

Plants provide a variety of resources, such as food, mating and oviposition sites, and shelter for a majority of phytophagous insect species. Host plant selection by insects involves complex behavioral responses to a variety of physical and chemical characteristics of the host plant that operate at different spatial scales and include long-range olfactory (*e.g.*, plant derived volatiles perceived by odor-receptors) and visual cues (*e.g.*, plant shape, size and color) and short-range chemotactic and gustatory cues (*e.g.*, surface metabolites perceived by chemo-receptors) (1-3). The physical and chemical characteristics of plants that insects use for host selection depend on the feeding guild and the dietary behavior (*e.g.,* polyphagy or oligophagy) of the insect species (4). For example, *Drosophila melanogaster* flies (order Diptera) use a wide range of olfactory cues such as methyl-, ethyl- and propyl-esters of short chain fatty acids generated by microorganisms growing on decaying fruit (5) while *D. seychella* flies use a specific molecule (methyl-hexanoate) emitted by its exclusive foodplant, *Morinda citrifolia* (6). Insects with mouthparts capable of piercing plant tissues and sucking out liquids (*e.g.*, order Hemiptera) use labial dabbing and probing to perceive chemical cues (*e.g.* waxes, terpenoids, acylsugars and alkaloids) on tissue surfaces or internal cellular layers (1-3,7). Interestingly, it has been shown that insects can also perceive phytohormones. *Helicoverpa zea* (order Lepidoptera) larvae can perceive jasmonic acid (JA) (8) which accumulates in the foodplants during attack and induces *de novo* synthesis of plant defense metabolites (9,10). Thus, one possible scenario is that insects can select plants for feeding based on the plant's

capacity to produce JA (or to signal JA-mediated responses) as a means of eavesdropping on the defensive capacity of a potential host plant.

In some cases insects can suppress the accumulation of plant defense metabolites as a mechanism of foodplant selection (11,12). These suppression mechanisms are often associated with the alteration of phytohormone biosynthesis or signaling pathways and may involve specific enzymes (*e.g.*, glucose oxidase) produced by the insect (13) or vectored microorganisms (14,15). Leafhoppers of the genus *Empoasca* are hemipterans (family *Cicadellidae)* that feed on phloem and cell contents of a broad range of host plants (16,17). During feeding, the leafhoppers may induce a "hopper burn" in the plant tissue; damage that is characterized by the yellowing of the tissue around the feeding site (18). *Empoasca* leafhoppers can also vector viruses, bacteria and fungi and efficiently transmit them to plants as a consequence of their ingestion-egestion feeding behavior (18). For example, cell wall-lacking bacteria of the species *Candidatus* Phytoplasma can be transmitted by *Empoasca* leafhoppers (19,20). Interestingly, the transmission of *Ca.* Phytoplasma spp into the plant can affect the interaction of the plant with the transmitting insect via the modification of direct or indirect plant defenses. It has been shown that *Malus domestica* trees infected by *Ca.* Phytoplasma mali emit larger amounts of the volatile, ß-caryophyllene, compared to non-infected trees, a volatile that lures insect vectors to infected plants (14). A recent laboratory study performed with *Arabidopsis thaliana* and *Macrosteles quadrilineatus* leafhoppers*,* has shown that effector proteins produced by *Ca.* Phytoplasma asteris interfere with the activation of JA biosynthesis in the plant and thereby reduce the induction of JA-mediated defense responses (15).

Nicotiana attenuata (Solanaceae), an annual tobacco plant native to the Southwestern US, germinates after fires from long-lived seed banks to form monocultures and has to cope with an unpredictable insect community (21). Populations of *N. attenuata* plants are known to harbor significant genetic diversity among individuals and the genetic diversity within populations is frequently larger than among populations (22), likely due to the plant's fire-chasing germination behavior and long-lived seed banks (21). In their natural environment as well as in the glasshouse, *N. attenuata* plants respond strongly and specifically to the attack of insects from different feeding guilds (23,24). A large number of these responses is governed by a strong burst of JA which is amplified by elicitors in the

insect's oral secretions (OS) (10,25-27). The initial steps of JA biosynthesis involve the release of trienoic fatty acids (*e.g.*, α-linolenic acid [18:3]) from membrane lipids in the chloroplast by the action of glycerolipases (GLA1 in *N. attenuata*; (28,29)). The released trienoic fatty acids are oxidized by 13-lipoxygenases (LOX3 in *N. attenuata*) to form (13S)-hydroperoxy-18:3 (30). This molecule is the substrate for allene oxide synthase (AOS) that forms (9Z, 13S, 15Z)-12, 13-epoxy-18:3 which is subsequently cyclized to an isomeric mixture of 12-oxo-phytodienoic acid (OPDA) by allene oxide cyclase (AOC) (31). OPDA is transported into the peroxisome where the C_{10}-C_{11} double bond in (9S, 13S)-OPDA is reduced by an OPDA reductase (OPR) (32). The reduced OPDA (OPC-8:0) undergoes three cycles of ß-oxidation, involving acyl-CoA transferase (ACX) (33) and finally forming (3R, 7S)-jasmonic acid (JA). JA can be modified, for example, by jasmonyl-O-methyl transferase (JMT) to form methyl-jasmonic acid (MeJA) (34) or by JASMONATE RESISTANT (JAR) that conjugates isoleucine to form JA-Ile (35,36). JA-Ile activates the SCF^{COI1}-JAZ complex (37) which transcriptionally activates genes involved in the biosynthesis of defense molecules among other responses (38,39).

Previously, we have reported that *N. attenuata* plants rendered deficient in JA biosynthesis by silencing Na*LOX3* (as-*lox3*) are heavily damaged by *Empoasca* leafhoppers in nature (40). Here, we used a set of eleven *N. attenuata* transgenic lines deficient in specific steps of JA biosynthesis and perception and deficient in the accumulation of major insecticidal molecules to disentangle the mechanisms underlying the selection of plants for feeding by *Empoasca* leafhoppers. In addition, we used these insects to discover genetic variation in JA accumulation and signaling in natural *N. attenuata* populations.

Results

Candidatus Phytoplasma spp is not found in Empoasca leafhoppers or the plants they attack in the field

A previous study has shown that *Ca.* Phytoplasma asteris transmitted by *Macrosteles quadrilineatus* leafhoppers can affect JA biosynthesis in infected *A. thaliana* plants in the laboratory (15). Thus, we first examined whether the interaction between

Empoasca leafhoppers and *N. attenuata* plants involved *Ca*. Phytoplasma species. For this purpose we carried out two different sets of experiments. In the 2009 field season, we observed that *N. attenuata* plants silenced in the expression of *COI1* (ir-*coi1*) were severely attacked by adult *Empoasca* leafhoppers. These adult leafhoppers originated from *Cucurbita foetidissima* plants growing adjacent to our field plot and they are referred to as *Empoasca* spp hereafter. *Empoasca* spp adults and leaves from *Empoasca* spp damaged and undamaged ir-*coi1* plants were collected for analysis (first set). In parallel, adult *Empoasca* leafhoppers were collected and used to establish a colony in our glasshouse (see Materials and Methods for details). This colony was composed of a single *Empoasca* species and is referred to as *Empoasca* sp hereafter. Adult leafhoppers from this in-house colony were used to challenge ir-*coi1* plants for seven days under glasshouse conditions. Adult leafhoppers and attacked and unattacked (control) leaves were collected and used for analysis (set 2). The presence of *Ca.* Phytoplasma spp was analyzed in adult *Empoasca* leafhoppers and leaf samples from both sets. A PCR approach using universal primers for the amplification of 16S rRNA (Table S1) (14,41,42) was used for *Ca*. Phytoplasma spp detection (Fig. S1). *Ca*. Phytoplasma spp were detected in the positive control samples (isolated genomic DNA from *Ca*. Phytoplasma asteris and *Callistephus chinensis* leaves infected with *Ca*. Phytoplasma asteris) but not in the negative control samples and in samples collected from field and glasshouse experiments (Fig. S1; see supporting materials and methods for details). These results demonstrate that the interaction between *Empoasca* leafhoppers and *N. attenuata* plants was independent of the presence of *Ca*. Phytoplasma spp.

Generation of a toolbox of transformed plants to examine Empoasca leafhopper plant choice mechanisms

To examine the mechanisms underlying *Empoasca* leafhopper plant choice, we transformed *N. attenuata* plants with RNAi inverted repeat (ir) constructs to silence: (i) specific steps of JA biosynthesis (ir-*lox3* (43), ir-*aos*, ir-*aoc*, ir-*opr3*; ir-*acx1* (see supporting materials and methods for details)), (ii) JA perception (ir-*coi1*) (44), and (iii) accumulation of JA-dependent defense molecules: nicotine (ir-*pmt*), trypsin proteinase inhibitor (PI, ir-*pi*), nicotine and PIs (ir-*pmt/pi*) (45), and diterpene glycosides (ir-*ggpps*)

(46) (Fig. 1A). Additionally, we ectopically expressed the JA methyl transferase 1 (JMT1; 35S-*jmt1*) to metabolically deplete jasmonate accumulation by redirecting the flux of JA into methyl-JA (MeJA) (47). Compared to control plants, 35S-*jmt1* plants have reduced levels of JA-Ile after simulated herbivory and they are therefore reduced in their COI1-mediated JA-signaling capacity (47).

Plants silenced in the expression of the *AOS* (ir-*aos*), *AOC* (ir-*aoc*), *OPR3* (ir-*opr3*) and *ACX1* (ir-*acx1*) genes were newly generated for this study and two homozygous independently transformed lines harboring a single T-DNA insertion (Fig. S2) were selected for each genotype. In unelicited leaves, the transcript levels of Na*AOS*, Na*AOC*, Na*OPR3* and Na*ACX1* were silenced by 10- to 100-fold in the respective lines compared to WT (Fig. 1B). In leaves elicited with synthetic fatty acid-amino acid conjugate (FAC), to amplify the induction of the JA biosynthesis pathway (28), the target transcripts were reduced by 5- to 100-fold in the respective lines compared to WT at 60 min after elicitation (Fig. 1C). Consistent with the reduced expression of the JA biosynthesis genes, all lines showed significantly reduced levels of JA and JA-Ile after FAC elicitation (Fig. S3). ir-*acx1* plants lost their capacity to suppress JA accumulation in the 3rd generation and one line was therefore used as an additional control (line A466) to the plants transformed with the empty vector (EV) construct.

This set of transgenic lines, deficient in JA-accumulation, JA-perception and JA-dependent defense molecules, allowed us to study in detail the steps of the JA biosynthesis and signaling pathways that are responsible for feeding choice decisions of *Empoasca* leafhoppers.

Defense molecules or volatiles do not direct initial Empoasca leafhopper feeding in nature

To examine *Empoasca* leafhopper plant choice in nature, all of the transgenic *N. attenuata* lines mentioned above were grown in a fully randomized design in a field plot in the Great Basin Desert during the 2009 field season (Fig. 2A-B). ir-*aos* plants did not survive transplantation to the field and were not included in the analysis. An adjacent *Medicago sativa* (alfalfa) field served as a source of *Empoasca* spp adults that were encouraged to move into the *N. attenuata* plantation by mowing the alfalfa field (Fig. 2C).

Eight days after mowing, we quantified *Empoasca* spp attack as the percentage of total canopy area damaged (Fig. 2D). Importantly, although the degree of damage was expressed per total canopy area for normalization, we observed that 80 to 90% of the canopy damage inflicted by *Empoasca* leafhoppers occurred on stem leaves.

ir-*lox3*, ir-*aoc*, 35S-*jmt1* and ir-*coi* plants were heavily damaged by *Empoasca* spp (Fig. 2D). Interestingly, *opr3* plants had wild type levels of *Empoasca* spp damage (Fig. 2D) even though the levels of JA and JA-Ile in these plants were strongly reduced (Fig. S3). The reduced levels of *Empoasca* spp damage on ir-*opr3* plants can be explained however by their reduced number of stem leaves due to decelerated growth in the field (Fig. S4). Thus, when the experiment was conducted, the canopy of ir-*opr3* plants was dominated by rosette leaves. An alternative explanation for these observations is the possibility that OPDA plays a role in the mechanisms underlying the interaction between *Empoasca* leafhoppers and *N. attenuata* plants. This possibility was however ruled out with additional experiments (see below). The damage to plants with reduced levels of JA-dependent defense molecules (ir-*pmt*, ir-*pi,* ir-*pmt*/*pi* and ir-*ggpps*) was not distinguishable from that of control plants (Fig. 2D). These results demonstrated that *Empoasca* leafhoppers feed preferentially on plants with reduced jasmonate accumulation and perception capacities for feeding rather than plants with reduced accumulation of nicotine, PIs and DTGs (ir-*pmt*, ir-*pi,* ir-*pmt*/*pi* and ir-*ggpps*).

To test whether *Empoasca* leafhopper feeding choice in nature was driven by constitutively emitted volatiles from *N. attenuata* plants, we first trapped leaf volatiles from unattacked ir-*lox3*, ir-*aoc*, ir-*opr3*, 35S-*jmt1*, ir-*coi1*, ir-*pmt*, ir-*ggpps*, EV and A466 plants grown in the field. Ultra-high resolution GC analysis detected 197 volatiles constitutively released from these plants. These 197 volatiles were subjected to principal component analysis (PCA) (48) for which the genotypes were grouped in two classes based on their significant differences in *Empoasca* spp damage (Fig. 2D). Principal components (PCs) 1 and 2 explained 44% of the variation but did not separate the two plant classes (Fig. S4C). Secondly, we tested whether herbivory-induced plant volatiles (HIPVs) –which consist of green leaf volatiles (GLVs) released immediately upon insect attack and terpenoids released during the following photoperiod (48)– affected *Empoasca* spp feeding choices. For this, we caged three adult *Empoasca* leafhoppers on leaves of the

genotypes mentioned above and trapped HIPVs for 4 h during two different periods: i) immediately after caging the leafhoppers (0-4 h) and, ii) 24 h after caging the leafhoppers (24-28 h). HIPVs differentially emitted by *Empoasca* spp feeding from the different transgenic lines were defined as compounds with a fold change (FC) of 1.5 ≤FC ≤0.66 and a *P*-value <0.05 when compared to unattacked plants of the same genotype. A total of 83 HIPVs of 197 volatiles detected were identified as differentially accumulating among all the genotypes (Table S2). These 83 HIPVs were used for PCA analysis (48) in which the two volatile trapping periods were individually analyzed and, as mentioned above, the genotypes were grouped in two classes based on their significant differences in *Empoasca* spp damage (Fig. 2D). PCs 1 and 2 explained 50% of the variation within the first trapping period and 52% of the variation within the second trapping period but for both trapping periods, PC1 and PC2 did not separate the two plant classes (Fig. 2E-F). Thus, in summary, these results demonstrate that with an ultra-high resolution analysis of plant volatiles neither the detectable constitutively released volatiles nor HIPVs were associated with *Empoasca* spp feeding preferences in the field.

Empoasca leafhopper damage correlates with reduced levels of OPDA and JA accumulation

The field observations showed clearly that *Empoasca* spp preferentially attacked plants with reduced jasmonate accumulation and signaling capacity. To more directly evaluate the association between the *Empoasca* leafhopper feeding preferences observed in the field (Fig. 2D) with the jasmonate producing capacities (OPDA, JA and JA derivatives) of the transgenic *N. attenuata* lines used, we first assessed the capacity of EV, A466, ir-*lox3*, ir-*aoc*, ir-*opr3*, ir-*coi1*, 35S-*jmt1*, ir-*ggpps*, ir-*pi*, ir-*pmt* and ir-*pmt/pi* plants to accumulate jasmonates after a standardized mechanical wounding under glasshouse conditions (Fig. 3A). Principal component analysis (PCA) separated the transgenic *N. attenuata* lines deficient in JA accumulation and perception from controls and lines deficient in JA-dependent defense molecules (Fig. 3B). PC 1 explained almost all (99.7%) variance present in the data and was positively influenced by jasmonate levels (loading factors between 0.2 and 0.4) but negatively by *Empoasca* spp damage (loading factor: -0.34) (Fig. 3B). A correlation analysis between the amount of *Empoasca* spp damage

quantified in the field and the capacity of the plants to accumulate jasmonates after standardized mechanical wounding revealed that damage correlated negatively with the capacity of the plants to accumulate OPDA and JA (JA vs. damage: Pearson's R^2= 0.36, P= 0.03; OPDA vs. damage: Pearson's R^2=0.50, P=0.01, Figs. 3C-D). We therefore hypothesized that the extent of initial *Empoasca* leafhopper feeding on *N. attenuata* plants depended either on OPDA or JA accumulation or on their respective signaling capacities.

Empoasca leafhopper feeding preferences depend on the plants' capacity to mediate JA signaling

To examine which jasmonate triggers initial feeding of *Empoasca* leafhoppers on *N. attenuata* plants, we first analyzed the induction of jasmonate biosynthesis in WT leaves after *Empoasca* sp feeding. For this experiment, twenty-five adult *Empoasca* sp from the glasshouse colony were caged on single leaves of *N. attenuata* wild type (WT) plants. After 24h, the levels of OPDA, JA, JA derivatives and methyl-JA (MeJA) were quantified. The levels of OPDA, JA, JA-Ile, 11/12-hydroxy-JA-Ile and 11/12-carboxy-JA-Ile were significantly increased (3- to 8-fold) in leaves attacked by *Empoasca* sp compared to control leaves (Figs. 4A-B, Table S3A). 11/12-hydroxy-JA, MeJA and JA-amino acid conjugates other than JA-Ile were not detected in leaves. Thus, the induction of OPDA and JA accumulation by *Empoasca* sp feeding is consistent with a potential role of these two jasmonates in the plant selection process.

To determine the predominant factor influencing plant selection by *Empoasca* sp (*i.e.* OPDA or JA accumulation or mediated signaling) we performed choice experiments using *N. attenuata* WT (control), ir-*lox3*, ir-*coi1* and 35S-*jmt1* plants in the glasshouse. Leaves were treated either with lanolin (control treatment) or with lanolin containing MeJA. Two days after the treatment, the plants were challenged with 150 adult *Empoasca* sp and the percentage of leaf damage was determined after 7 days (Fig. S5A). Lanolin treated ir-*lox3*, ir-*coi1* and 35S-*jmt1* plants were damaged significantly more by *Empoasca* sp than lanolin-treated WT plants (Fig. 4C). Treatment of ir-*lox3* plants with MeJA decreased *Empoasca* sp damage significantly by 8-fold compared to the lanolin treatment, whereas it did not decrease damage in ir-*coi1* and 35S-*jmt1* plants (Fig. 4C).

To evaluate the accumulation of jasmonates after external MeJA application, the levels of OPDA, JA, JA derivatives and MeJA were quantified in unchallenged WT, ir-*lox3*, ir-*coi1* and 35S-*jmt1* plants treated with lanolin or MeJA (Table S3B). None of the jasmonates analyzed were detected in lanolin-treated leaves. JA levels accumulated to 2.5 to 4.6 nmol g^{-1} FM in MeJA-treated leaves of WT, ir-*lox3*, ir-*coi1* and 35S-*jmt1* plants (Fig. 4D, Table S3B) indicating that the levels of JA did not affect *Empoasca* sp feeding damage. JA-Ile was detected in low amounts (0.01-0.02 nmol g^{-1} FM) in MeJA-treated leaves of WT, ir-*lox3* and 35S-*jmt1* plants, but in significantly higher amounts in MeJA-treated ir-*coi1* leaves (0.14 nmol g^{-1} FM), consistently with the lower metabolism of JA-Ile in ir-coi1 plants (44,49,50). Thus, since *Empoasca* sp feeding damage was similar on lanolin and MeJA treated ir-*coi1* plants, JA-Ile levels did not directly affect *Empoasca* sp feeding choice. In MeJA-treated leaves, MeJA was only detected in leaves of 35S-*jmt1* plants (1 nmol g^{-1} FM) (Fig. 4D, Table S3B) but also did not directly affect *Empoasca* sp feeding. OPDA was detected in similar amounts in MeJA-treated leaves of control and 35S-*jmt1* plants (0.01-0.02 nmol g^{-1} FM) (Fig. 4D) but was not detected in ir-*lox3* and ir-*coi1* plants consistent with the activation of the JA biosynthetic pathway by exogenous MeJA (23). Although OPDA levels in MeJA treated 35S-*jmt1* plants were similar to those of MeJA treated WT leaves, *Empoasca* sp feeding on 35S-*jmt1* was not affected by MeJA treatment. This demonstrated that OPDA or its associated signaling cascade was not involved in the plant selection process by *Empoasca* sp. The results revealed that *Empoasca* sp feeding on *N. attenuata* can be reduced by external MeJA application to lines silenced in JA biosynthesis but not in lines silenced in JA perception (ir-*coi1*) or in plants in which the flux of JA is redirected to an inactive jasmonate (35S-*jmt1*).

To provide independent evidence of the deficiency in JA-mediated defense signaling in ir-*coi1* and 35S-*jmt1* plants, the induction of trypsin proteinase inhibitor (PI) activity (as an indicator of induced defenses mediated by JA-mediated COI1 signaling (51)), was quantified in WT, ir-*lox3*, ir-*coi1* and 35S-*jmt1* plants elicited with MeJA. Compared to lanolin-treated leaves, PI activity was induced to an activity of 2-2.5 nmol mg protein^{-1} in MeJA treated leaves of control and ir-*lox3* plants, not induced in leaves of ir-*coi1* and was reduced by 60% (0.9 nmol mg protein^{-1}) in 35S-*jmt1* plants (Fig. 4E). Although MeJA treatment of 35S-*jmt1* plants partially induced JA-mediated defenses (*i.e.*

PI activity), damage by *Empoasca* sp on MeJA treated 35S-*jmt1* plants was similar to that on lanolin-treated 35S-*jmt1* plants. These experiments demonstrated that MeJA treatment induced defense responses (*i.e.* PI activity) in *N. attenuata* and were consistent with the results obtained from the field with *N. attenuata* ir-*pi* lines (Fig. 2D) (*i.e.* the choice of plants for feeding by *Empoasca* leafhoppers is independent of PI levels).

Finally, to evaluate if the *Empoasca* sp in-house colony used for these experiments was free of *Ca.* Phytoplasma spp, we analyzed the presence of *Ca.* Phytoplasma spp in severely *Empoasca* sp-damaged leaves from WT, ir-*lox3*, ir-*coi1* and 35S-*jmt1* plants and ten adult *Empoasca* leafhoppers from the colony. Phytoplasma was not detected in either leaf or leafhopper samples (Fig. 5B; see supporting materials and methods for details).

Empoasca leafhopper attack identified variations in JA accumulation in nature

The work presented above demonstrated that *Empoasca* spp damage could be used to identify genetically modified *N. attenuata* plants deficient in JA accumulation and signaling in the field and glasshouse. We next asked: could *Empoasca* spp attack also identify natural variation in JA accumulation and signaling? During the 2009 field season, a natural population of 100 *N. attenuata* plants was screened using *Empoasca* spp (collected from *C. foetidissima* plants) to discover genetic variation in JA accumulation hidden in natural populations. Two of the plants in the population showed *Empoasca* spp damage, and after leaf elicitation with *Manduca sexta* oral secretions (OS) in the field, these plants accumulated less JA than neighboring unattacked plants of the same population (Fig. 6A-B). OS-elicitation provides a standard method to assess the maximal capacity of the plants to produce JA after an insect-associated response. Moreover since the OS was collected from *M. sexta* larvae, the analysis allowed us to exclude the possibility that factors (in addition to phytoplasma) introduced by *Empoasca* spp attack were responsible for the suppression of the JA burst. Self-pollinated seeds from the two plants showing *Empoasca* spp damage and their closest undamaged neighbors were collected and grown in the glasshouse. Consistent with the field results, elicitation of leaves with *M. sexta* OS elicited smaller JA bursts in the progeny of the two plants previously showing *Empoasca* spp damage compared to the progeny of previously unattacked plants (Fig. 6C-D).

A second screening of native *N. attenuata* populations was carried out during the 2011 field season. In this case and in contrast to 2009, we used natural infestations of *Empoasca* spp originating from *C. foetidissima* plants growing within natural *N. attenuata* populations. We screened two populations consisting of approximately 400 and 200 *N. attenuata* plants (Fig. 6E) and found three and two plants, respectively, that were highly damaged by *Empoasca* spp compared to neighboring plants at similar growth stages (Fig. S5C). Undamaged leaves from the five plants showing *Empoasca* spp damage and from undamaged neighbor plants were *M. sexta* OS-elicited and harvested 60 min after the treatment. All five plants showing *Empoasca* spp damage accumulated significantly lower JA levels than their undamaged neighbors within a population but not between populations (Fig. 6F). The analysis of phytoplasma in leaves and *Empoasca* spp collected in both plant populations was again negative (Fig. S5D; see supporting materials and methods for details). These results demonstrated that the initial *Empoasca* leafhopper feeding choice can be used to identify variations of JA accumulation or signaling in *N. attenuata* populations. In addition, these experiments allowed us to exclude any role of *Empoasca* spp feeding in the suppression of the JA signaling in these plants.

Discussion

Volatile release is not associated with Empoasca leafhopper damage

Plant selection by *Empoasca* leafhoppers can be guided by perceiving non-volatile molecules during the first feeding but also by perceiving specific volatile cues released from plants appropriate for feeding. Several studies have highlighted the fundamental role of plant volatiles in plant selection by herbivore insects (52,53). For example, *Manduca* moths can distinguish *N. attenuata* plants already infested by *M. sexta* larvae and preferably lay eggs on uninfested plants (54). Furthermore, *Empoasca fabae* leafhoppers are more arrested by volatiles emitted from an alfalfa genotype susceptible to *E. fabae* than from a resistant alfalfa genotype (55). Additionally, phytopathogen infections can cause dramatic changes in volatile emissions and these emissions can lure insect vectors to infected plants (14). Our studies were focused on the initial selection of plants for feeding

by *Empoasca* leafhoppers. We therefore analyzed *N. attenuata* volatile emissions before and during the first stages of leafhopper attack rather than tracking long term changes. Changes in plant volatiles released from both unattacked and *Empoasca* spp-attacked plants and analyzed by ultra-high resolution GCxGC-ToF mass spectrometry were not associated with *Empoasca* spp feeding preferences. While we cannot exclude the possibility that unmeasured volatiles might play a role, our results are consistent with the conclusion that the choice of plants for feeding by *Empoasca* leafhoppers is based on plant characteristics perceived during the initial probing process (see below).

Empoasca leafhopper plant choice is not associated with the presence of Ca. phytoplasma spp in nature and the glasshouse

Recent laboratory studies have shown that *Ca.* Phytoplasma asteris infection reduces JA biosynthesis in *A. thaliana* plants (15) and that *Ca.* Phytoplasma mali infections induces *Malus domestica* to emit higher amounts of ß-caryophyllene to lure insect vectors (14). In nature, the proportion of *Ca.* Phytoplasma spp infected leafhoppers is low (approximately 2%, (56)) and in our study the choice of *N. attenuata* plants by *Empoasca* leafhoppers was not associated with the presence of *Ca.* Phytoplasma spp in both natural and laboratory environments.

The major defense molecules of N. attenuata do not affect initial Empoasca leafhopper feeding

Since Fraenkel (57) first argued for a defensive function of plant secondary metabolites, many laboratory studies have described defensive metabolites induced by herbivore attack (7). We demonstrate that *Empoasca* leafhopper feeding on *N. attenuata* plants is independent of the accumulation of the three major classes of insecticidal compounds in *N. attenuata* (*i.e.* nicotine, trypsin proteinase inhibitors (PIs) and diterpene glycosides (DTGs)). The biosynthesis of these molecules is regulated by JA signaling, and they are known to strongly influence the herbivore community on *N. attenuata* in field experiments (45,46,58). Although the total herbivore damage on ir-*pmt*, ir-*pi*, ir-*pmt/pi* and ir-*ggpps* plants was significantly higher compared to control plants (Fig. S4D), damage by *Empoasca* spp were similar to that on control plants (Fig. 2D) in the field. Furthermore, in

the glasshouse, MeJA treatment of 35S-*jmt1* plants significantly induces the activity of PIs but these plants were similarly attacked by *Empoasca* leafhoppers to lanolin treated 35S-*jmt1* plants. *Empoasca* leafhopper performance may be affected by nicotine, PIs or DTGs but the initial feeding choice of *Empoasca* leafhoppers (as reflected by the initial feeding damage) is clearly not affected by these molecules.

JA signaling mediates Empoasca leafhopper plant choice

In nature, *Empoasca* leafhoppers preferentially select *N. attenuata* plants for feeding when they are rendered deficient in JA accumulation or JA perception (Fig. 2D). Eleven ir-lines deficient in JA accumulation, perception and JA regulated defense molecules were analyzed in the field to disentangle the mechanisms responsible for feeding preferences of *Empoasca* leafhopper. We also re-assessed as-*aos* plants which were previously shown to be similarly attacked by *Empoasca* spp compared to WT (Fig. S6A (40)). We found that the wound-induced accumulation of JA was similar to that of EV control plants (Fig. S6B): a likely explanation for why *Empoasca* spp did not attack as-*aos* plants in the 2003 field season (40). Our results demonstrate that initial *Empoasca* spp feeding on *N. attenuata* plants in the field negatively correlates with the accumulation of jasmonates (Fig. 3). To examine these correlations, wound-induced jasmonate accumulation rather than *Empoasca* spp induced JA accumulation was used because (i) *Empoasca* spp feed differentially on the different genotypes analyzed and (ii) *Empoasca* spp feed at irregular times. Therefore we used a single wounding elicitation to provide rigorous quantitative measures for comparisons of JA bursts amongst genotypes.

The results demonstrated that in the glasshouse and in the field, the capacity to induce defense responses mediated by JA signaling dictates the initial feeding choice of *Empoasca* spp. Treatment with MeJA elicits the accumulation of JA in ir-*coi1* but not JA-mediated defenses and therefore, did not decrease *Empoasca* spp feeding damage compared to lanolin treated plants (Fig. 4). MeJA treatment induces JA-mediated defenses in 35S-*jmt1* but attack from *Empoasca* spp was not decreased (Fig. 4). Thus, initial *Empoasca* spp feeding can be either directly mediated by the plant's JA signaling capacity or most likely by JA-dependent responses via COI1. The identification of single molecules or a combination of molecules (including signaling complexes) that *Empoasca* spp

perceives in the plant will require experiments in which the response of *Empoasca* spp to the exposure of these molecules can be determined. These responses can range from behavioral responses (e.g., attraction, repulsion) to the recording of electrical signals from the precibarial sensilla (60) that are likely used by Cicadellidae leafhoppers in assessing the JA bursts elicited by their ingestion-egestion mode of feeding. Imaging techniques commonly used to study, for example, calcium signaling in *Drosophila melanogaster* neurons upon excitation with specific molecules can be developed for *Empoasca* spp (5). These experiments will have to be coupled with the isolation of molecules from the plant and, in later steps, with the generation of transgenic plants deficient in the accumulation of specific molecules.

JA is a chemical and functional analog of eicosanoids in animals, and during the divergence of plants and animals, the function of these oxygenated derivatives of fatty acids in mediating defense responses against sucking insects has been conserved. Hematophagous insects induce the accumulation of eicosanoids in the bite zone that elicits inflammation and defensive behavioral responses in the host (61). Thus, as for blood-feeding dipterans, the responses induced by phytophagous hemipterans are associated with the production of oxygenated forms of fatty acids. During the course of evolution, *Empoasca* spp have acquired the capacity to select appropriate hosts with diminished defensive response by indirectly perceiving JA signaling (*e.g.* the SCF^{COI1}-JA-Ile complex) after feeding. As an evolutionary counter-response, animal and plant hosts may have amplified their attack-elicited signaling to function as an aposematic signal, warning of impending defense responses to these eavesdropping potential grazers.

In summary, we demonstrate that *Empoasca* spp leafhoppers select plants for feeding in nature by eavesdropping on JA-mediated signaling. Given their high mobility, *Empoasca* spp leafhoppers may probe plants at random in the field and settle on those with lower levels of JA-mediated signaling for sustained feeding. This behavior can be used to identify natural variation in JA accumulation in native populations. This native tobacco uses fires to synchronize its germination from long-lived seed banks to grow in dense populations characterized by intense intraspecific competition and variable herbivore pressures (21). Hence, we hypothesize that growth-defense tradeoffs are likely severe for this plant, and these tradeoffs likely provide the selective pressure to maintain these JA-

signaling mutants in native populations, despite the clear disadvantages of being defense-impaired. Once we have completed the sequencing of the *N. attenuata* genome, we will characterize in greater detail these JA-signaling mutants that *Empoasca* leafhoppers have identified for us from natural populations.

Material and Methods

Plant material and growth

Seeds of the 30th and 31st generations of an inbred line of *Nicotiana attenuata* were used as the wild-type (WT) genotype in all experiments. The inbred line originated from seeds collected in 1988 from a natural population at the DI ranch in southwestern Utah, USA. Seeds were germinated and plants were grown as described (62).

We used plants harboring an empty vector construct (EV, line A-03-9-1 (63)) as controls in all field experiments, stably transformed lines: ir-*lox3* line A-03-562-2 (43), ir-*aos*, ir-*aoc*, ir-*opr3*, ir-*acx1*, ir-*coi1* line A-04-249-A-1 (44) and 35S-*jmt1* line A-07-291-2 (47) as plants that are silenced to various degrees in their JA production, signaling and perception capabilities and lines silenced in the expression of JA-mediated direct defenses: diterpene glycosides (DTGs, ir-*ggpps* line A-07-231-3 (46)), nicotine (ir-*pmt* line A-03-108-3 (45)), proteinase inhibitors (PIs; ir-*pi* line A-04-186-1 (45)) and nicotine and PIs together (ir-*pmt/pi* line A-04-103-3 (45)).

Plant treatments

In the glasshouse, tissue was collected from the first fully elongated leaf at nodes +1 (64) of rosette stage (~30 day old) *N. attenuata* plants. Wounding was performed by rolling a fabric pattern wheel three times on each side of the midvein. To analyze differences in jasmonate accumulation between plants, leaves were treated with water (W), synthetic fatty acid-amino acid conjugate (FAC) or *Manduca sexta* oral secretions (OS). For FAC elicitation, the wounds were supplied immediately with 0.6 pmol of synthetic N-linolenoyl-glutamic acid (18:3-Glu; 20 μL of a 0.03 nmol/mL solution in 0.02% (v/v) Tween 20/water). For OS elicitation we used *M. sexta* OS, stored under argon at -20°C

immediately after collection until usage. The wounds were supplied with 20 µL of 1:5 (v/v) diluted OS. Leaf tissue was collected at different times and immediately frozen in liquid nitrogen for subsequent analysis.

For the screening of native *N. attenuata* plants in the field, the least damaged non-senescing leaves available on each plant were used. The leaves were randomly chosen as either control or elicited leaves. Wounding and OS elicitation was performed as described above for the glasshouse treatments. Tissue was collected 60 min after elicitation and immediately frozen between dry ice blocks.

For methyl jasmonate (MeJA) treatment, 34.6 µL of pure MeJA (Sigma-Aldrich, Taufkirchen, Germany) were dissolved in 5 mL of pure lanolin (Roth, Karlsruhe, Germany) to attain a final concentration of 7.5 µg µL^{-1}. 20 µL of either pure lanolin or MeJA-containing lanolin were applied to the abaxial-side of leaf bases of the first three fully elongated leaves (positions +1, +2, +3) (64) of rosette-stage plants. Choice experiments were performed 2 days after treatments. For jasmonate and PI activity analysis, tissue was collected from the untreated leaf portion 3 days after the treatment and immediately frozen in liquid nitrogen.

To analyze the changes in jasmonate levels after *Empoasca* sp attack, 25 adult leafhoppers were caged onto WT leaves with two 50 mL plastic containers (Huhtamaki, Bad Bertricher, Germany) or two empty 50 mL plastic containers were placed onto WT leaves as controls. After 24 h, the plastic container together with leaf and insects were removed from the plant and flushed with CO_2 for 15 s to anaesthetize the leafhoppers. All *Empoasca* sp were removed and the leaves immediately frozen in liquid nitrogen. Control leaves were treated similarly in the absence of *Empoasca* sp.

Insect collection and treatment

For all experiments in the field, *Empoasca* leafhoppers were collected from infested *Cucurbita foetidissima* plants growing adjacent to the field plot at the Lytle Ranch Preserve in SW Utah during the 2009 and 2011 field seasons, respectively. For field experiments, we collected *Empoasca* spp adults on the day of the experiments, between 4 AM and 6 AM, when the leafhoppers are relatively immobile and easier to collect. Leafhopper adults were kept in plastic containers until the start of the experiment.

To establish a glasshouse colony of *Empoasca* sp, approximately 400 adults were collected from *C. foetidissima* growing at the Lytle Ranch Preserve on May 30th 2009 and on June 16th 2011, respectively, and placed in an adapted Plexiglas container (1 x 2 x 1.5 m^3) in the glasshouse and reared on *C. moschata*, *C. maxima* and *C. pepo* plants, which were replaced weekly. So far, we have not been able to identify the *Empoasca* species used in this study because of their poorly understood phylogeny of the genus (18). We assume that the species is *Empoasca fabae* but further corroboration is required to ascertain the actual species. We would greatly appreciate expert knowledge regarding the identity of the leafhopper species. We can provide males as voucher specimens, stored in 80% ethanol, as well as living individuals as long as our in-house colony remains viable. For the glasshouse experiments, *Empoasca* sp adults were collected from the colony immediately before use, anaesthetized with CO_2 for 15 s and separated in 50 mL plastic containers in different numbers according to the experiment.

Field experiments

Seeds of the following *N. attenuata* genotypes: empty vector (EV), ir-*lox3*, ir-*aos*, ir-*aoc*, ir-*opr3*, A466 (ir-*acx1*), ir-*coi1*, 35S-*jmt1*, ir-*ggpps*, ir-*pi*, ir-*pmt* and ir-*pmt/pi*, were imported under APHIS notification number 07-341-101n and the field experiments were conducted under notification number 06-242-3r-a2. All transformed *N. attenuata* genotypes mentioned above were used for experiments in the experimental field plot at the Lytle Ranch Preserve near Santa Clara, Utah in 2009.

For germination, seeds were treated with 1 mM gibberellic acid (GA_3) in 1:50 (v/v) diluted liquid smoke (House of Herbs, Passaic, NJ), germinated on agar plates containing Gamborg's B5 medium (Duchefa, Haarlem, The Netherlands) and grown in a shade house. After 2 weeks, young seedlings were transplanted into Jiffy 703 pots (Jiffy Products, Shippegan, New Brunswick, Canada), fertilized with approximately 300 µg Borax (7.5 mg L^{-1} Na$_2$[B$_4$O$_5$(OH)$_4$]*8 H$_2$O in water) and grown outdoors for 2 weeks. At 28-30 days after germination, plants were planted into the field plot and a plastic label carrying the APHIS identification number of each genotype was buried under the roots of each plant to ensure unambiguous genotype identifications. A 10 cm bamboo stick with the APHIS identification code was placed in the soil by each plant. The field plot consisted of 26 rows

separated by open irrigation troughs which allowed plants to be watered every second day until they were established rosette-stage plants.

Size matched EV, ir-*pi*, ir-*pmt*, ir-*pmt/pi* and ir-*ggpps* plants (10 to 15 plants per genotype) were planted in a fully randomized design. A466, ir-*lox3*, ir-*aos*, ir-*aoc*, ir-*opr3* and ir-*coi1* plants were planted in a randomized design, each paired with a size-matched EV plant (15 pairs per genotype). 35S-*jmt1* plants were planted pairwise with a size-matched EV plant (26 pairs). All plants were monitored daily during reproductive growth and all flowers of each genotype were removed before their corollas opened and could release pollen. Rosette diameter and stem length was determined continuously between 15th and 29th of May 2009 (24 to 38 days after plantation).

An alfalfa field adjacent to the field plot provided a source of *Empoasca* spp leafhoppers. We mowed this field on May 27th 2009 to encourage movement of leafhoppers to the *N. attenuata* plantation. We quantified the damage caused by *Empoasca* spp feeding as a percentage of the leaf area damaged normalized to the total plant area 8 days after the mowing of the alfalfa field (44 days after transplantation).

Jasmonate analysis

The analysis of OPDA, JA, JA-Ile, MeJA, JA-Val, 11/12-hydroxy-JA, 11/12-hydroxy-JA-Ile and 11/12-carboxy-JA-Ile was performed as previously described (29,47). The principal component analysis (PCA, Fig. 3B) was performed using the Metaboanalyst software (65,66). The grouping of the transgenic *N. attenuata* lines, necessary for PCA analysis, was done by separating lines deficient in JA accumulation and perception from controls and lines deficient in JA dependent defense molecules. For this analysis levels of jasmonates and *Empoasca* spp damage were normalized using autoscaling.

Analysis of PI activity

Leaf tissue from 40-day-old ir-*lox3*, ir-*coi1*, 35S-*jmt1* and WT plants was harvested 2 days after treatment with either lanolin or MeJA containing lanolin. The analysis of PI activity was performed as previously described (67).

Empoasca sp choice experiments

Six leaves of each three plants of WT, ir-*lox3*, ir-*coi1* and 35S-*jmt1* were treated with either pure lanolin or MeJA containing lanolin (7.5 µg µL^{-1}) as described above. Two days after the treatment, the plants were placed in a fully randomized design within a containment cage and challenged with 150 *Empoasca* sp adults. After 7 days, the percentage of canopy leaf area damaged by *Empoasca* sp of treated leaves (Fig. 5A) was determined.

Identification of natural variation of JA accumulation capacities in native populations of N. attenuata

Native *N. attenuata* plants growing in the Great Basin desert, southwestern Utah, were selected for analysis (22). In 2009, we selected one population consisting of approximately 100 plants (Fig. 5A) and in 2011, we selected two populations consisting of approximately 200 and 400 plants (Fig. 5E).

In 2009, all plants in the population were carefully inspected and plants showed no evidence of *Empoasca* spp feeding damage or the presence of *Empoasca* spp adults or nymphs on the plants. Fifty *Empoasca* spp adults were collected from infested *C. foetidissima* plants growing adjacent to our field plot and released into the native population. Two days after this release, the plants were re-screened for *Empoasca* spp damaged leaves and two plants were found that had been attacked. Leaves from these two plants and an unattacked control plant were OS elicited as described, harvested 60 min after elicitation and immediately frozen on dry ice for subsequent jasmonate analysis. Flowers from these plants were bagged to exclude flower visitors, and seed capsules from these self-pollinated flowers were collected from both *Empoasca* spp attacked plants and their closest undamaged neighbors. Seeds from each plant and 30x inbred WT plants were grown in the glasshouse. Leaves were either left unelicited (control) or were OS-elicited as described above and harvested after 60 min for jasmonate analysis.

In 2011, we screened all 600 plants of the two populations and five plants with visible *Empoasca* spp damage were found. Leaves from these plants and their nearest undamaged neighbors were either unelicited or OS elicited as described, harvested 60 min after elicitation and immediately frozen on dry ice for subsequent jasmonate analysis.

Acknowledgements

References

1. Thorsteinson AJ (1960) Host selection in phytophagous insects. *Ann Rev Entomol* 5:193-218.
2. Bernays EA, Chapman RF (1994) *Host-plant selection by phytophagous insects* (New York, Chapman and Hall). 312 p.
3. Powell G, Tosh CR, Hardie J (2006) Host plant selection by aphids: Behavioral, evolutionary, and applied perspectives. *Ann Rev Entomo* 51:309-330.
4. Prokopy RJ Owens ED (1978) Visual generalist with visual specialist phytophagous insects – host selection behavior and application to management. *Ent exp and appl* 24:609-620.
5. Hansson B, Knaden M, Sachse S, Stensmyr M, Wicher D (2010) Towards plant-odor-related olfactory neuroethology in *Drosophila*. *Chemoecology* 20:51 - 61
6. Dekker T, Ibba I, Siju KP, Stensmyr MC, Hansson BS (2006) Olfactory shifts parallel superspecialism for toxic fruit in *Drosophila melanogaster* sibling, *D. sechellia*. *Current Biology* 16:101-109.
7. Dicke M (2000) Chemical ecology of host-plant selection by herbivorous arthropods: a multitrophic perspective. *Biochem Syst Ecol* 28:601-617.
8. Li XC, Schuler MA, Berenbaum MR (2002) Jasmonate and salicylate induce expression of herbivore cytochrome P450 genes. *Nature* 419:712-715.
9. Dicke M, Baldwin IT (2010) The evolutionary context for herbivore-induced plant volatiles: beyond the 'cry for help'. *Trends Plant Sci* 15:167-175.
10. Howe GA, Jander G (2008) Plant immunity to insect herbivores. *Ann Rev Plant Biol* 59:41-66.
11. Will T, Tjallingii WF, Thönnessen A, vanBel AJE (2007) Molecular sabotage of plant defense by aphid saliva. *Proc Natl Acad Sci USA* 104:10536-10541
12. Mutti NS, *et al*. (2008) A protein from the salivary glands of the pea aphid, Acyrthosiphon pisum, is essential in feeding on a host plant. *Proc Natl Acad Sci USA* 105:9965-9969.
13. Musser RO, et al. (2002) Herbivory: Caterpillar saliva beats plant defences - A new weapon emerges in the evolutionary arms race between plants and herbivores. *Nature* 416:599-600.
14. Mayer CJ, Vilcinskas A, Gross J (2008) Phytopathogen lures its insect vector by altering host plant odor. *J Chem Ecol* 34:1045-1049.
15. Sugio A, Kingdom HN, MacLean AM, Grieve VM, Hogenhout SA (2011) Phytoplasma protein effector SAP11 enhances insect vector reproduction by manipulating plant development and defense hormone biosynthesis. *Proc Natl Acad Sci USA* 108:1254–1263.
16. Gyrisco GG (1958) Forage insects and their control. *Ann Rev Entomo* 3:421-448.
17. Carter W (1952) Injuries to plants caused by insect toxins 2. *Bot Rev* 18:680-721.
18. Backus EA, Serrano MS, Ranger CM (2005) Mechanisms of hopperburn: an overview of insect taxonomy, behavior, and physiology. *Ann Rev Entomo* 50:125-151.
19. Pérez KA, Piñol B, Rosete YA, Wilson M, Boa E, Lucas J (2010) Transmission of the Phytoplasma Associated with Bunchy Top Symptom of Papaya by Empoasca papayae Oman. *J Phytopathol* 158: 194-196
20. Galetto L, Marzachì C, Demichelis S, Bosco D (2011), Host Plant Determines the Phytoplasma Transmission Competence of Empoasca decipiens (Hemiptera: Cicadellidae). *J Econ Entomol* 104: 360-366

---

21. Preston CA, Baldwin IT (1999) Positive and negative signals regulate germination in the post-fire annual, *Nicotiana attenuata*. *Ecology* 80:481-494.

22. Bahulikar RA, Stanculescu D, Preston CA, Baldwin IT (2004) ISSR and AFLP analysis of the temporal and spatial population structure of the post-fire annual, *Nicotiana attenuata*, in SW Utah. *BMC Ecology* 4:12.

23. Voelckel C, Baldwin IT (2004) Herbivore-induced plant vaccination. Part II. Array-studies reveal the transience of herbivore-specific transcriptional imprints and a distinct imprint from stress combinations. *Plant J* 38:650-663.

24. Diezel C, von Dahl C, Gaquerel E, Baldwin I (2009) Different lepidopteran elicitors account for cross-talk in herbivory-induced phytohormone signaling. *Plant Physiol* 150:1576-1586.

25. Halitschke R, Schittko U, Pohnert G, Boland W, Baldwin IT (2001) Molecular interactions between the specialist herbivore *Manduca sexta* (*Lepidoptera*, *Sphingidae*) and its natural host *Nicotiana attenuata*. III. Fatty acid-amino acid conjugates in herbivore oral secretions are necessary and sufficient for herbivore-specific plant responses. *Plant Physiol* 125:711-717.

26. Stork W, Diezel C, Halitschke R, Galis I, Baldwin IT (2009) An ecological analysis of the herbivory-elicited JA burst and its metabolism: plant memory processes and predictions of the moving target model. *PlosOne* 4 (3):e4697.

27. Schmelz EA, Engelberth J, Alborn HT, Tumlinson JH, 3rd, Teal PE (2009) Phytohormone-based activity mapping of insect herbivore-produced elicitors. *Proc Natl Acad Sci USA* 106:653-657.

28. Kallenbach M, Alagna F, Baldwin IT, Bonaventure G (2010) *Nicotiana attenuata* SIPK, WIPK, NPR1, and fatty acid-amino acid conjugates participate in the induction of jasmonic acid biosynthesis by affecting early enzymatic steps in the pathway. *Plant Physiol* 152:96-106.

29. Bonaventure G, Schuck S, Baldwin IT (2011) Revealing complexity and specificity in the activation of lipase-mediated oxylipin biosynthesis: a specific role of the *Nicotiana attenuata* GLA1 lipase in the activation of JA biosynthesis in leaves and roots. *Plant Cell Environ* 34(9):1507-20.

30. Halitschke R, Baldwin IT (2003) Antisense LOX expression increases herbivore performance by decreasing defense responses and inhibiting growth-related transcriptional reorganization in *Nicotiana attenuata*. *Plant Journal* 36:794-807.

31. Schaller F (2001) Enzymes of the biosynthesis of octadecanoid-derived signalling molecules. *J Exp Bot* 52:11-23.

32. Breithaupt C, Kurzbauer R, Lilie H, Schaller A, Strassner J, et al. (2006) Crystal structure of 12-oxophytodienoate reductase 3 from tomato: self-inhibition by dimerization. *Proc Natl Acad Sci USA* 103:14337-14342.

33. Pedersen L, Henriksen A (2005) Acyl-CoA Oxidase 1 from *Arabidopsis thaliana*. Structure of a key enzyme in plant lipid metabolism. *J Mol Biol* 345:487-500.

34. Seo HS, Song JT, Cheong JJ, Lee YH, Lee YW, et al. (2001) Jasmonic acid carboxyl methyltransferase: a key enzyme for jasmonate-regulated plant responses. *Proc Natl Acad Sci USA* 98:4788-4793.

35. Suza WP, Staswick PE (2008) The role of JAR1 in Jasmonoyl-L: -isoleucine production during *Arabidopsis* wound response. *Planta* 227:1221-1232.

36. Wang L, Halitschke R, Kang JH, Berg A, Harnisch F, et al. (2007) Independently silencing two JAR family members impairs levels of trypsin proteinase inhibitors but not nicotine. *Planta* 226:159-167.

37. Fonseca S, Chini A, Hamberg M, Adie B, Porzel A, et al. (2009) (+)-7-iso-Jasmonoyl-L-isoleucine is the endogenous bioactive jasmonate. *Nat Chem Biol* 5:344-350.

38. Chini A, Fonseca S, Fernández G, Adie B, Chico J, et al. (2007) The JAZ family of repressors is the missing link in jasmonate signalling. *Nature* 448:666-671.

39. Thines B, Katsir L, Melotto M, Niu Y, Mandaokar A, et al. (2007) JAZ repressor proteins are targets of the SCFCO11 complex during jasmonate signalling. *Nature* 448:661-662.

40. Kessler A, Halitschke R, Baldwin IT (2004) Silencing the jasmonate cascade: induced plant defenses and insect populations. *Science* 305:665-668.

41. Lorenz KH, Schneider B, Ahrens U, Seemuller E (1995) Detection of the apple proliferation and pear decline phytoplasma by PCR amplification of ribosomal and nonribosomal DNA. *Phytopathology* 85:771-776.

42. Lee IM, Bartoszyk IM, Gundersen DE, Mogen B, Davis RE (1996) Nested-PCR assays for ultrasensitive detection of potato ring rot bacterium, *Clavibacter michiganensis* subsp. *sepedonicus*. *Phytopathology* 86:S96.

---

43. Allmann S, Halitschke R, Schuurink R, Baldwin I (2010) Oxylipin channelling in *Nicotiana attenuata*: lipoxygenase 2 supplies substrates for green leaf volatile production. *Plant Cell Environ* 33:2028-2040.
44. Paschold A, Halitschke R, Baldwin I (2007) Co(i)-ordinating defenses: NaCOI1 mediates herbivore-induced resistance in *Nicotiana attenuata* and reveals the role of herbivore movement in avoiding defenses. *Plant J* 51:79-91.
45. Steppuhn A, Baldwin IT (2007) Resistance management in a native plant: nicotine prevents herbivores from compensating for plant protease inhibitors. *Ecol Lett* 10:499-511.
46. Heiling S, Schuman MC, Schoettner M, Mukerjee P, Berger B, et al. (2010) Jasmonate and ppHsystemin regulate key malonylation steps in the biosynthesis of 17-hydroxygeranyllinalool diterpene glycosides, an abundant and effective direct defense against herbivores in *Nicotiana attenuata*. *Plant Cell* 22:273-292.
47. Stitz M, Gase K, Baldwin IT, Gaquerel E (2011) Ectopic expression of AtJMT in *Nicotiana attenuata*: creating a metabolic sink has tissue-specific consequences for the jasmonate metabolic network and silences downstream gene expression. *Plant Physiol* 157:341-354.
48. Gaquerel E, Weinhold A, Baldwin IT (2009) Molecular interactions between the specialist herbivore *Manduca sexta* (*Lepidoptera*, *Sphigidae*) and its natural host *Nicotiana attenuata*. VIII. An unbiased GCxGC-ToFMS analysis of the plant's elicited volatile emissions. *Plant Physiol* 149:1408-1423.
49. VanDoorn A, Bonaventure G, Schmidt D, Baldwin IT (2011) Regulation of jasmonate metabolism and activation of systemic signaling in Solanum nigrum: COI1 and JAR4 play overlapping yet distinct roles. *New Phytol* 190:640-652.
50. Koo AJK, Cooke TF, Howe GA (2011) Cytochrome P450 CYP94B3 mediates catabolism and inactivation of the plant hormone jasmonoyl-L-isoleucine. *Proc Natl Acad Sci USA* 108:9298-9303.
51. van Dam NM, Baldwin IT (2003) Heritability of a quantitative and qualitative protease inhibitor polymorphism in *Nicotiana attenuata*. *Plant Biol* 5:179-185.
52. Baldwin IT (2010) Plant volatiles. *Curr Biol* 20:392-397.
53. Bruce TJA, Wadhams LJ, Woodcock CM (2005) Insect host location: a volatile situation. *Trends Plant Sci* 10:269-274.
54. Allmann S, Baldwin IT (2010) Insects betray themselves in nature to predators by rapid isomerization of green leaf volatiles. Science 329:1075-1078.
55. Ranger CM, Winter REK, Backus EA, Rottinghaus GE, Ellersieck MR, et al. (2005) Discrimination by the potato leafhopper (*Hemiptera* : *Cicadellidae*) of host volatiles from resistant and susceptible alfalfa, *Medicago sativa* L. *Environ Entomol* 34:271-280.
56. Hill GT, Sinclair WA (2000) Taxa of leafhoppers carrying phytoplasmas at sites of ash yellows occurrence in New York state. *Plant Dis* 84:134-138.
57. Fraenkel GS (1959) Rasion detre of secondary plant substances. *Science* 129:1466-1470.
58. Ussuf KK, Laxmi NH, Mitra R (2001) Proteinase inhibitors: Plant-derived genes of insecticidal protein for developing insect-resistant transgenic plants. *Current Sci India* 80:847-853.
59. Zavala JA, Patankar AG, Gase K, Baldwin IT (2004) Constitutive and inducible trypsin proteinase inhibitor production incurs large fitness costs in *Nicotiana attenuata*. *Proc Natl Acad Sci USA* 101: 1607-1612.
60. Backus EA, McLean DL (1983) The sensory systems and feeding behavior of leafhoppers. II. A comparison of the sensillar morphologies of several species *(Homoptera*: *Cicadellidae*). *J Morphol* 176:3-14.
61. Alvarenga PH, Francischetti IMB, Calvo E, Sá-Nunes A, Ribeiro JMC, et al. (2010) The function and three-dimensional structure of a thromboxane A_2 cysteinyl leukotriene-binding protein from the saliva of a mosquito vector of the malaria parasite. *PLoS Biol* 8:e1000547.
62. Krügel T, Lim M, Gase K, Halitschke R, Baldwin IT (2002) *Agrobacterium*-mediated transformation of *Nicotiana attenuata*, a model ecological expression system. *Chemoecology* 12:177-183.
63. Bubner B, Gase K, Berger B, Link D, Baldwin IT (2006) Occurrence of tetraploidy in *Nicotiana attenuata* plants after *Agrobacterium*-mediated transformation is genotype specific but independent of polysomaty of explant tissue. *Plant Cell Rep* 25:668-675.
64. Pluskota WE, Qu N, Maitrejean M, Boland W, Baldwin IT (2007) Jasmonates and its mimics differentially elicit systemic defence responses in *Nicotiana attenuata*. *J Exp Bot* 58:4071-4082.

---

65.   Xia J, Psychogios N, Young N, Wishart DS (2009) MetaboAnalyst: a web server for metabolomic data analysis and interpretation. *Nucleic Acids Res* 37:652-660.
66.   Xia J, Wishart DS (2011) Web-based inference of biological patterns, functions and pathways from metabolomic data using MetaboAnalyst. *Nat Protoc* 6:743-760.
67.   Gilardoni PA, Hettenhausen C, Baldwin IT, Boneventure G (2011) *Nicotiana attenuata* LECTIN RECEPTOR KINASE1 suppresses the insect-mediated inhibition of induced defense responses during *Manduca sexta* herbivory. *Plant Cell* 23:3512-3532.

Figure legends

Fig. 1. Lines of transformed plants generated to dissect the mechanisms of *Empoasca* spp feeding choice. (**A**) Enzymes of the jasmonate biosynthetic and signaling pathway and of jasmonate-regulated direct defenses in *N. attenuata.* All enzymes in red font were silenced by RNAi while *JMT* (blue font) was ectopically expressed to generate a toolbox of transformed plants to examine *Empoasca* spp feeding choice in nature. (**B**) RNAi lines were generated by transforming *N. attenuata* plants with constructs harboring an inverted repeat (ir) fragment of each gene. Silencing efficiency of two independently transformed homozygous ir-lines with a single T-DNA insertion was determined in unelicited leaves and leaves harvested 60 min after fatty-acid amino-acid (FAC) elicitation by qPCR analysis. Transcript levels were quantified by comparing the levels of corresponding genes to the eukaryotic elongation factor 1A-α (NaEF1A-α) (average ± SE, *n*=3, asterisks indicate statistically significant differences, Student *t*-test with Welch correction, WT versus ir-line, *: P< 0.05, **: P< 0.01, ***: P< 0.001).

Fig. 2. *Empoasca* spp select plants deficient or modified in JA accumulation or perception for feeding in the field, independently of released herbivory induced volatiles (HIPVs). (**A**) Timeline of experimentation during the 2009 Utah field season. (**B**) Design of the field plot and the location of the different *N. attenuata* genotypes within the field plot. (**C**) In the field, *N. attenuata* plants were grown adjacent to a *Medicago sativa* (alfalfa) field, a source of *Empoasca* spp. *Empoasca* spp damage (white circles) on *N. attenuata* was determined as the percentage of canopy area exhibiting the characteristic damage resulting from *Empoasca* spp attack. (**D**) Eight days after the mowing of the alfalfa field, damage was quantified on: empty vector (EV) and A466 controls, lines silenced in JA biosynthesis (ir-*lox3*, ir-*aoc*, ir-*opr3*) and perception (ir-*coi1*), lines silenced in JA-dependent defense molecules: diterpene glycosides (ir-*ggpps*), trypsin proteinase inhibitors (PIs; ir-*pi*),

nicotine (ir-*pmt*) and both nicotine and PIs,(ir-*pmt/pi*), and lines ectopically expressing a jasmonic acid methyl transferase (35S-*jmt1*). Asterisks represent significant differences compared to control plants, *n*= 7-10, Student *t*-test, *: P<0.05, **: P<0.01, ***: P<0.001, a: P=0.07). (**E-F**) After caging *Empoasca* leafhopper on single leaves, HIPVs were collected for 4 h during two different periods: i) immediately after caging the leafhoppers (0-4 h) and, ii) 24 h after caging the leafhoppers (24-28 h). A total of 83 HIPVs of 197 detected emitted by *Empoasca* spp feeding with a fold change (FC) of 1.5 ≤FC ≤0.66 (*P*-value <0.05) when compared to volatiles released from unattacked plants of the same genotype. These 83 HIPVs were used for principal component analysis (PCA) analysis in which the two volatile trapping periods were individually analyzed. *N. attenuata* plants were grouped in two classes based on *Empoasca* spp damage (black: no significant differences in *Empoasca* spp damage compared to controls; red: significant differences) and principal components (PCs) 1 and 2 of the transgenic lines were plotted against each other.

Fig. 3. Wound-elicited JA and OPDA levels correlate with *Empoasca* spp damage. (**A**) All lines analyzed in the field were grown in the glasshouse and jasmonate accumulations in treated leaves were analyzed 1 h after wounding (numbers represent average ±SE, *n*=5, *: The damage data is the same as shown in Fig. 2D and it has been included here for comparison and to assist with the understanding of the results in this figure). (**B**) Principal component analysis (PCA) separated the transgenic *N. attenuata* lines deficient in JA accumulation and perception from controls and lines deficient in JA-dependent defense molecules. (**C-D**) *Empoasca* spp damage observed in the field negatively correlated with the wound-induced JA and OPDA levels observed in the glasshouse (Pearson correlation; JA vs. damage: Pearson's R²= 0.36, P= 0.03; OPDA vs. damage: R²= 0.50, P= 0.01).

Fig. 4. Initial *Empoasca* sp feeding induces jasmonate accumulation and is triggered by JA signaling capacities. (**A-B**) 25 *Empoasca* sp were caged on *N. attenuata* WT leaves jasmonate accumulation was measured. OPDA and JA levels were measured 24 h after *Empoasca* sp feeding in control and attacked leaves (bars represent average ± SE, *n*= 4, Asterisks represent significant differences compared to control plants, Student *t*-test, **: P < 0.01; ***: P < 0.001). In glasshouse bioassays, MeJA treatment of leaves enhances the

resistance to *Empoasca* sp attack of WT (control) and ir-*lox3* plants, but not of ir-*coi1* and 35S-*jmt1* plants. Leaves of WT, ir-*lox3,* ir-*coi1* and 35S-*jmt1* plants were either treated with lanolin or lanolin containing MeJA. (**C**) Two days after the treatment, plants were challenged with 150 *Empoasca* sp adults and damage was recorded after 7 days (damage is shown as the percentage of canopy area; average ±SE; *n*=15-18, different letters indicate statistically significant differences, Student *t*-test, P <0.05). (**D**) Levels of MeJA, JA, JA-Ile and OPDA were quantified in MeJA-treated leaves of WT, ir-*lox3,* ir-*coi1* and 35S-*jmt1* plants 3 days after the treatment (Table S3; average ±SE; *n*= 4-9; different letters indicate statistical significance among lines and within analytes, Student *t*-test, P < 0.05, nd: not detected). (**E**) To analyze JA signaling capacities, we determined the levels of trypsin proteinase inhibitor (PI) activity in lanolin and MeJA-treated leaves 3 days after the treatment (average ±SE; *n*= 6, different letters indicate statistically significant differences, Student *t*-test, P <0.05, nd: not detected).

Fig. 5. *Empoasca* spp identified natural variation in JA accumulation in genetically diverse native *N. attenuata* populations. (**A**) During the 2009 field season, approximately 50 *Empoasca* spp were released into a native *N. attenuata* population (ca. 100 plants) and *Empoasca* spp damage on all plants was determined after 2 days. (**B**) Two plants with detectable *Empoasca* spp damage were found. Leaves from both plants and a non-attacked control plant were elicited with *M. sexta* oral secretion (OS) and harvested for jasmonate analysis after 60 min. Both plants showing *Empoasca* spp damage had lower OS-elicited amounts of JA compared to control plants (average ±SE, *n*= 3-4; bars sharing same the letters are not significantly different, Student *t*-test, P<0.05). (**C**) Selfed seeds from these plants and neighboring undamaged plants (N1, N2) were grown in the glasshouse, OS-elicited and harvested for jasmonate analysis after 60 min. (**D**) JA accumulations in plants from two accessions showing *Empoasca* spp damage in the field were significantly lower than those plants derived from undamaged neighbors (average ±SE, *n*= 4; bars sharing same the letters are not significantly different, Student *t*-test, P<0.05). (**E**) During the 2011 field season, two areas with approximately 400 and 200 native *N. attenuata* plants were surveyed to identify *Empoasca* spp damaged plants. We found five plants with increased *Empoasca* spp damage compared to neighboring plants in the same developmental stage.

(**F**) Leaves of these 5 plants and undamaged neighbor plants were OS elicited and harvested for JA analysis after 60 min. All plants with *Empoasca* spp damage had lower elicited JA values compared to their undamaged neighbors (average ±SE, *n*= 3; asterisks are indicating statistical significance of the *Empoasca* spp attacked plant compared to their respective neighbors, Student *t*-test, *: $P < 0.05$; ***: $P < 0.001$).

Conflict of interest statements:

The authors declare no conflict of interest.

Author contributions:

M.K., G.B. and I.T.B. designed research; M.K., G.B., P.A.G., A.W. and I.T.B. performed research; M.K., P.A.G. and A.W. analyzed data; and M.K., G.B., and I.T.B. wrote the paper.
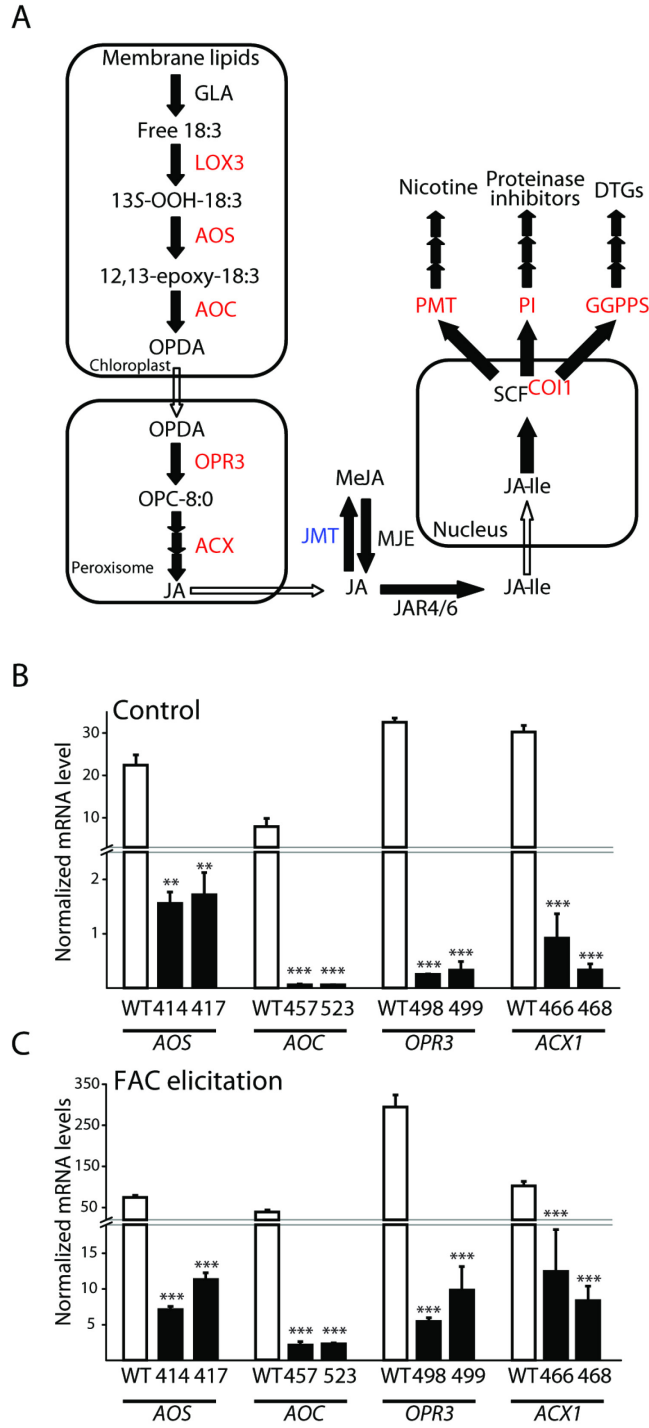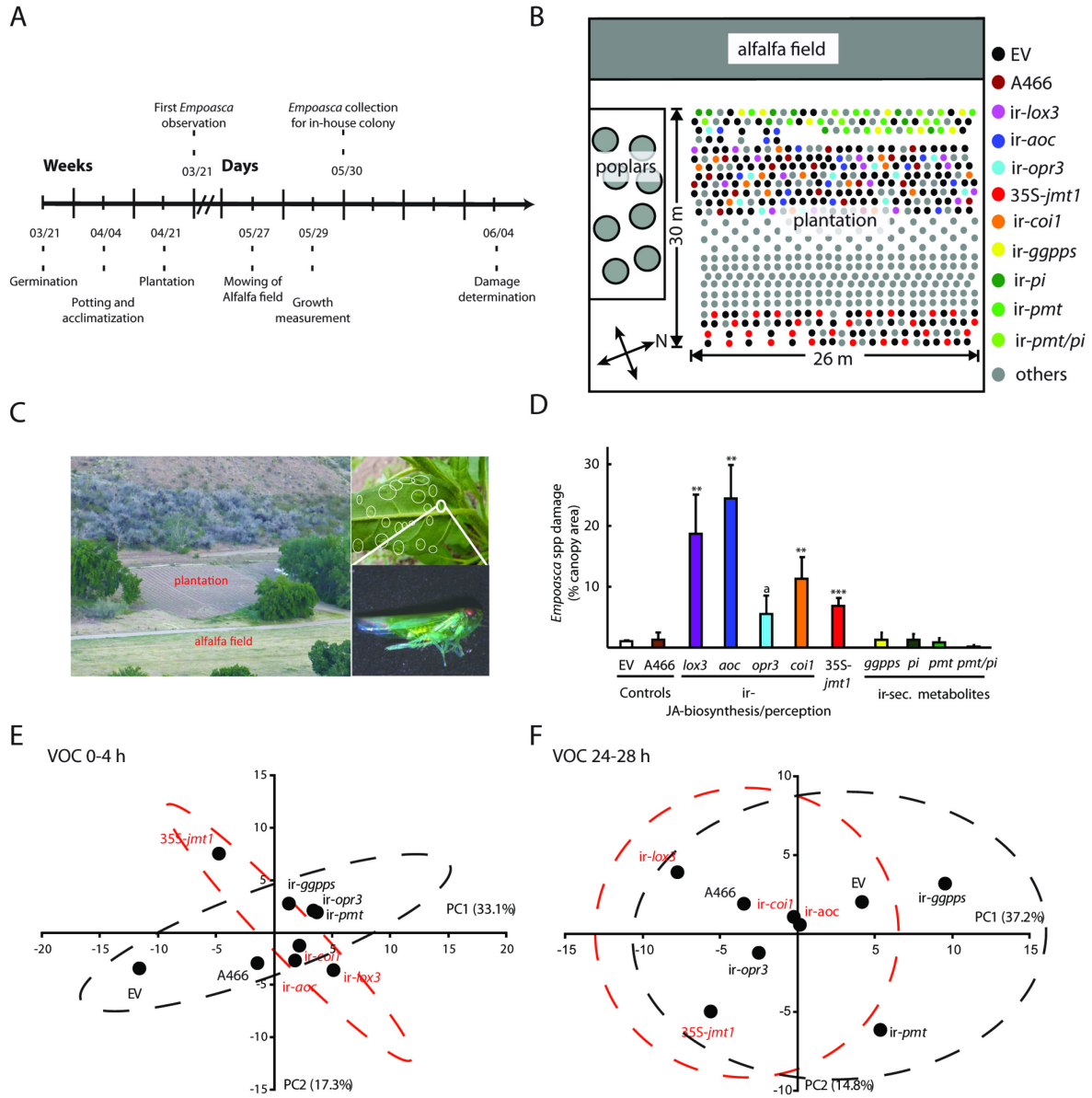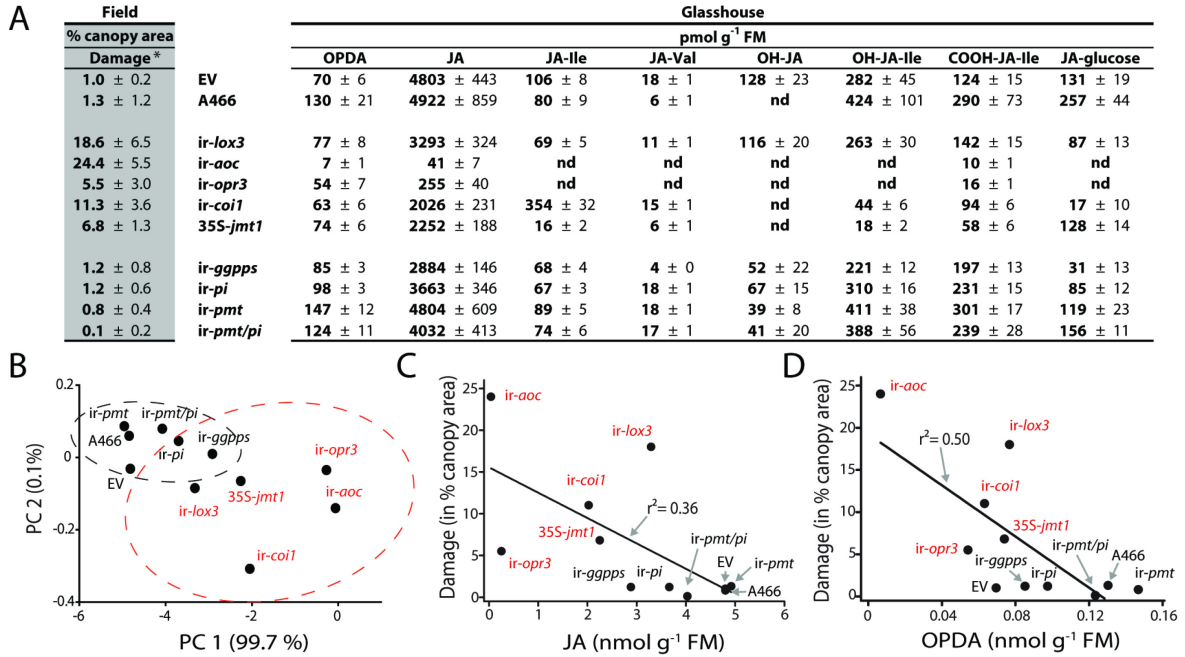
A

B

C

Figure 1

A

B

C

D

E

VOC 0-4 h

F

VOC 24-28 h

Figure 2

A

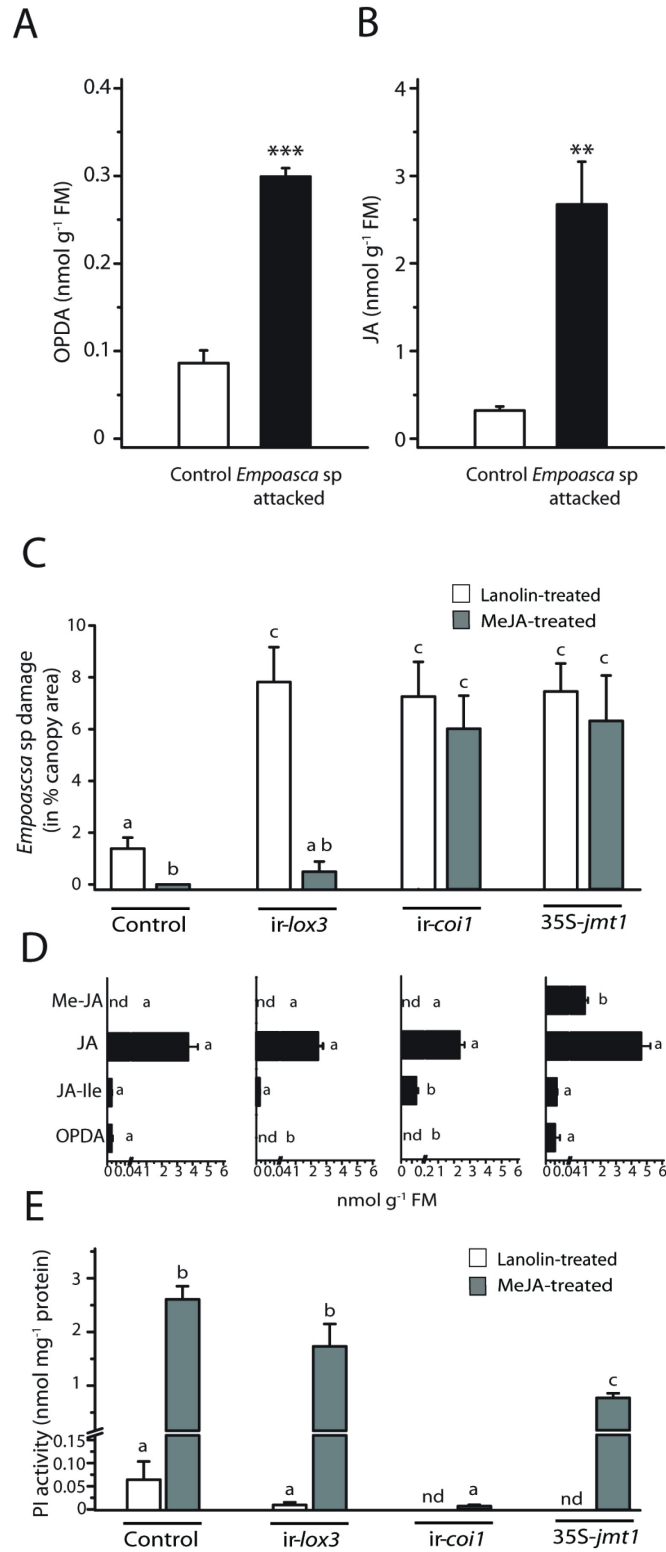| Field | | Glasshouse | | | | | | | |
% canopy area					pmol g^{-1} FM			
Damage*		OPDA	JA	JA-Ile	JA-Val	OH-JA	OH-JA-Ile	COOH-JA-Ile	JA-glucose
1.0 ± 0.2	EV	70 ± 6	4803 ± 443	106 ± 8	18 ± 1	128 ± 23	282 ± 45	124 ± 15	131 ± 19
1.3 ± 1.2	A466	130 ± 21	4922 ± 859	80 ± 9	6 ± 1	nd	424 ± 101	290 ± 73	257 ± 44
18.6 ± 6.5	ir-*lox3*	77 ± 8	3293 ± 324	69 ± 5	11 ± 1	116 ± 20	263 ± 30	142 ± 15	87 ± 13
24.4 ± 5.5	ir-*aoc*	7 ± 1	41 ± 7	nd	nd	nd	nd	10 ± 1	nd
5.5 ± 3.0	ir-*opr3*	54 ± 7	255 ± 40	nd	nd	nd	nd	16 ± 1	nd
11.3 ± 3.6	ir-*coi1*	63 ± 6	2026 ± 231	354 ± 32	15 ± 1	nd	44 ± 6	94 ± 6	17 ± 10
6.8 ± 1.3	35S-*jmt1*	74 ± 6	2252 ± 188	16 ± 2	6 ± 1	nd	18 ± 2	58 ± 6	128 ± 14
1.2 ± 0.8	ir-*ggpps*	85 ± 3	2884 ± 146	68 ± 4	4 ± 0	52 ± 22	221 ± 12	197 ± 13	31 ± 13
1.2 ± 0.6	ir-*pi*	98 ± 3	3663 ± 346	67 ± 3	18 ± 1	67 ± 15	310 ± 16	231 ± 15	85 ± 12
0.8 ± 0.4	ir-*pmt*	147 ± 12	4804 ± 609	89 ± 5	18 ± 1	39 ± 8	411 ± 38	301 ± 17	119 ± 23
0.1 ± 0.2	ir-*pmt/pi*	124 ± 11	4032 ± 413	74 ± 6	17 ± 1	41 ± 20	388 ± 56	239 ± 28	156 ± 11

Figure 3

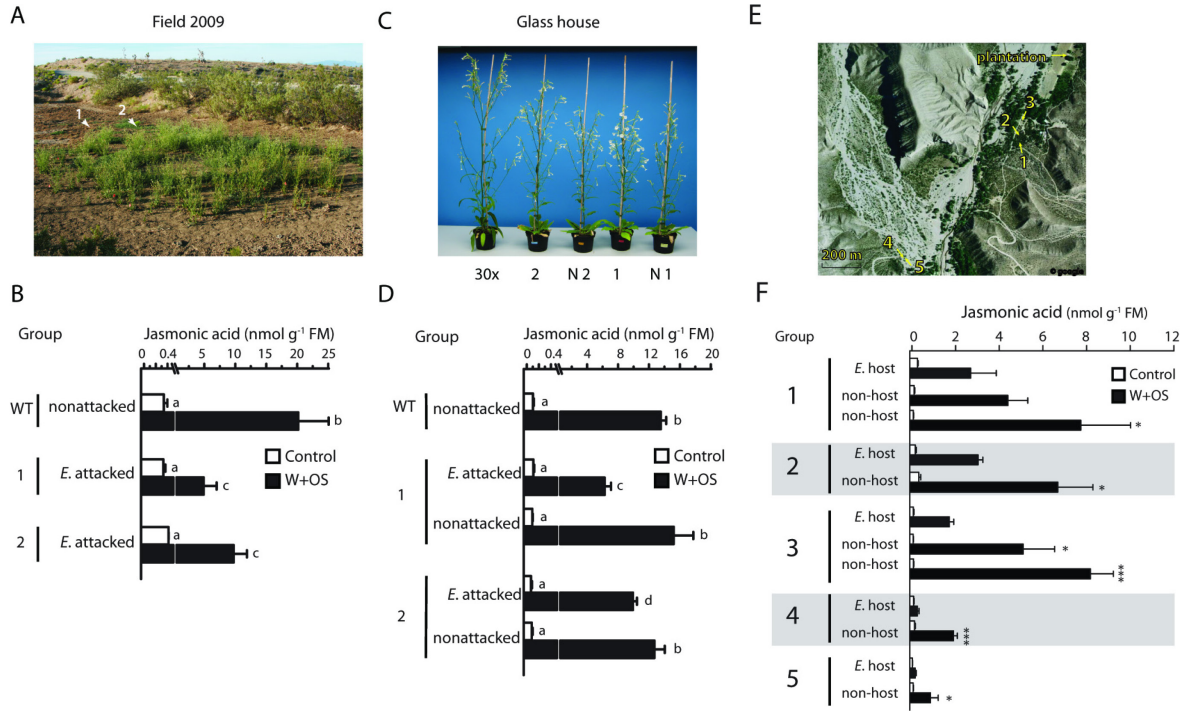**Figure 4**

Figure 5

Supporting information

Supporting Materials and Methods

Generation of ir-aos, ir-aoc, ir-opr3 and ir-acx1 plants

N. attenuata plants silenced in the expression of the *AOS*, *AOC*, *OPR3* and *ACX1* genes by inverted repeat gene silencing (ir) were generated using *Agrobacterium*-mediated transformation as previously described (1). Partial sequences of Na*AOS* (240 bp), Na*AOC* (258 bp), Na*OPR3* (277 bp) and Na*ACX1* (369 bp) cDNAs were PCR amplified using the primers listed in Table S4 and cloned in pSOL and pRESC vectors as inverted repeat (IR) constructs, respectively (2,3). At least 10 independent transgenic lines per genotype were selected for homozygosity on agar plates supplemented with hygromycin (3). Homozygous plants were selected for the identification of lines efficiently silenced in either *AOS*, *AOC*, *OPR3* or *ACX1* mRNA accumulation and carrying one T-DNA insertion as described below.

To determine the silencing efficiency of the transformed lines, total RNA was extracted from ~0.1 g of leaf tissue with TRIzol® (Invitrogen, Karlsruhe, Germany), DNase-I (Fermentas, St. Leon-Rot, Germany) treated according to the manufacturer's instructions and 5 µg of total RNA were reverse-transcribed using oligo(dT)18 and the SuperScript-II Reverse Transcriptase kit (Invitrogen, Karlsruhe, Germany) according to the manufacturer's instructions. Quantitative real-time PCR was conducted using the core reagent kit (qPCR Core Kit for SYBR Green I; Eurogentec, Köln, Germany) and gene specific primer pairs (Table S4) in a Stratagene 500 Mx3005P (Stratagene, Waldbronn, Germany) instrument. All qPCR reactions were performed with 3 biological replicates. The eukaryotic elongation factor 1A-α (NaEF1A-α) was used as an internal standard for data normalization. The relative amounts of all mRNAs were calculated using the comparative threshold cycle method as described in User Bulletin No. 2 from PE-Applied Biosystems (Applied Biosystems, Foster City, CA).

For determination of the T-DNA insertion number (Fig. S2), genomic DNA from the stably silenced lines and WT *N. attenuata* plants was isolated by the cetyltrimethylammoniumbromide (CTAB) method. DNA samples (10 µg) were digested

with Xbal (New England Biolabs, Ipswich, MA) overnight at 37°C according to the manufacturer's instructions and separated on a 0.8% (w/v) agarose gel using standard conditions. DNA was blotted onto Gene Screen Plus Hybridization-Transfer membranes (Perkin Elmer Life and Analytical Sciences, Boston, MA) using the capillary transfer method. A gene-specific probe for the hygromycin resistance gene hptII was generated by PCR using the primer pairs HYG1-18 (5′-CCGGATCGGACGATTGCG-3′) and HYG3-20 (5′-CGTCTGTCGAGAAGTTTCTG-3′). The probe was labeled with [α-^{32}P]dCTP (Perkin Elmer) using the RediprimeII kit (GE Healthcare, Freiburg, Germany) according to the manufacturer's instruction. For each construct, we chose two independently transformed homozygous lines harboring a single insertion for the transgene and exhibiting the strongest silencing of the expression of the endogenous targeted gene for further experimentation. These lines corresponded to: ir-*aos*, lines A-04-414-3, A-04-417-3; ir-*aoc*, lines A-07-457-1, A-04-523-2; ir-*opr3*, lines A-07-498-3, A-04-499-3 and ir-*acx1*, lines A-07-466-1, A-07-468-3.

Volatile Collection and Analysis

In 2009, volatiles from *Empoasca* spp attacked plants were collected from the following genotypes: EV, A466, ir-*lox3*, ir-*aoc*, ir-*opr3*, ir-*coi1*, 35S-*jmt1*, ir-*ggpps* and ir-*pmt*. Three adult leafhoppers were caged onto the leaves between two 50 mL plastic containers (Huhtamaki, Bad Bertricher, Germany, www.polarcup.de). Leaves used were labeled with cotton string and the *Empoasca* sp damage caused by this experiment was determined afterwards and subtracted from following damage determinations. Volatiles were collected on charcoal traps (OrboM32, Sigma-Aldrich) by drawing air through the cage with a vacuum pump. To avoid UV-mediated oxidation of the emitted volatiles, charcoal traps were covered with aluminum foil. The constitutive volatile emission of each leaf used for the experiment was collect for 2h before the start of the experiment. Herbivory induced plant volatiles were trapped between 0 and 4h and between 24 and 28 h after the start of the experiment. Charcoal traps were spiked with 400 ng of tetralin (Sigma-Aldrich, Germany, www.sigma-aldrich.com) and eluted into a GC vial with 500 µL of dichloromethane. Samples were analyzed on an GCxGC-ToF-MS (Agilent 6890N GC, Agilent Technologies, Böblingen, Germany) coupled with an LECO Pegasus III Tof-MS

(LECO, Mönchengladbach, Germany) and data processing was performed as described in (4). Sample mixes from each trapping period, containing an aliquot of all samples collected, were analyzed by GCxGC-ToF-MS. Raw data obtained after analysis were first deconvoluted using the LECO ChromaToF software (version 2.21). Known artifact peaks and contaminants were removed and peak lists combined to create a reference peak file containing 197 analytes. All samples were processed against the reference peak file using LECO ChromaToF software. Peak areas were corrected against the peak area of tetralin and the mean of 3 independent replicates was normalized by autoscaling for statistical analysis. All analytes with a fold change (FC) of 1.5 ≤FC ≤0.66 and a *P*-value <0.05 when compared to untreated plants of the same genotype were considered as induced after *Empoasca* spp feeding, resulting in a matrix of 83 different analytes (Table S2). The Metaboanalyst software (5,6) was used to perform principal component analysis (PCA). The grouping of the transgenic *N. attenuata* lines, necessary for PCA analysis, was done by separating lines similarly damaged by *Empoasca* spp in the field compared to controls from lines damaged significantly more by *Empoasca* spp.

Detection of Ca. Phytoplasma spp

In 2009, when the first *Empoasca* spp individuals were observed on *Curcubita foetidissima* plants growing adjacent to the field plot, the first signs of *Empoasca* spp feeding damage were observed on ir-*coi1* plants in the field plot. Several *Empoasca* spp adults from *C. foetidissima* plants were collected to test for the presence of *Ca.* Phytoplasma spp in the first generation of leafhoppers of the 2009 field season. In parallel, leaves from field-grown ir-*coi1* and EV control plants without previous *Empoasca* spp damage were collected as putative phytoplasma-free plants (control for negative infected plants). After one day, three *Empoasca* spp per plant (6 replicate plants in total) were caged on leaves without previous herbivore damage of EV and ir-*coi1* plants between two 50 mL plastic containers (Huhtamaki, Bad Bertricher, Germany) to force *Empoasca* spp to feed on these plants. After 3 days, the insects were removed and frozen on dry ice. Cages remained on the leaves for another 5 days. Five days after the initial *Empoasca* spp caging, we caged another 3 *Empoasca* spp adults on 3 replicates of previously attacked EV and ir-*coi1* leaves. All leaf tissues and *Empoasca* spp from the second caging were collected 8

days after the initial feeding and frozen on dry ice. Additionally, ir-*coi1* plants were placed either inside the cage of the *Empoasca* sp glasshouse colony or in an empty cage (to control for any cage effects). After 7 days, more than 80% of ir-*coi1* leaves on plants inside the colony showed the characteristic signs of *Empoasca* sp feeding and adult *Empoasca* sp were collected and leaf material was harvested from *Empoasca* sp-damaged and control leaves.

To determine the presence of *Ca*. Phytoplasma spp in the choice assay (Fig. 4) ten *Empoasca* sp adults and leaf material from the most damaged leaves of WT, ir-*lox3*, ir-*coi1* and 35S-*jmt1* plants were collected.

During 2011 field season, leaf material from the 5 native *N. attenuata* showing *Empoasca* spp damage was collected for phytoplasma detection. Additionally, *Empoasca* spp adults were collected from the native *N. attenuata* populations that were screened.

For the detection of phytoplasma, DNA was isolated from leaf material and leafhoppers using the Agentcourt® Cholopure Kit (Agencourt Bioscience Corporation, Beverly, MA, USA) following the manufacturer's instructions. As controls, we included DNA material from uninfected (negative control for phytoplasma infection) and infected China aster (*Callistephus chinensis*, positive control for *Ca*. Phytoplasma spp infection) and from the phytoplasma strain Aster Yellow- Witches' broom (AY-WB, *Candidatus* Phytoplasma asteris), kindly provided by Dr. Saskia Hogenhout (John Innes Center, Norwich Research Park, Norwich, UK).

We used different group-specific and universal primers for the detection of phytoplasma based on the 16S rRNA sequence (Table S1A) using either direct or nested PCR according as described in previous studies (7-9). The PCRs were performed in a final volume of 50 μL containing 100-200 ng of template, 1x PCR buffer (Sigma-Aldrich, Taufkirchen, Germany), 0.5 μM of each primer, 100 μM of the four dNTPs (Invitrogen, Karlsruhe, Germany) and 1U JumpStart™ Taq DNA Polymerase (Sigma-Aldrich). All primer pair combinations and PCR conditions are listed in Table S1B. For nested PCR, a 1:50 (v/v) dilution in water of the products of the preceding direct PCR was used as a template. All PCR products were resolved in 1% (w/v) agarose gels and the extracted bands were cloned into the pGEM-T easy vector (Promega, Madison, WI) and sequenced on an ABI Prism 377 XL DNA sequencer using the BigDye terminator kit (PE-Applied

Biosystems, Weiterstadt, Germany). Sequence data were analyzed using the Lasergene software package (DNASTAR, Madison, WI). Sequence similarity searches were performed in both GenBank using the BLAST algorithms and in The Ribosomal Database Project (RDP; http://rdp.cme.msu.edu/).

Supporting Figures

Fig. S1. *Empoasca* spp collected in Utah during the 2009 field season do not harbor or transmit *Ca*. Phytoplasma spp to *N. attenuata* plants during feeding. *Ca*. Phytoplasma spp detection assays were performed with different combinations of PCR conditions and primers (Table S2B): (1) direct PCR using fU5/rU3 primer pairs, (2) direct PCR using P1/P7 primer pairs followed by nested PCR using R16F2n/R16R2 primer pairs, (3) direct PCR using R16mF2/R16R1 primer pairs followed by nested PCR using R16F2n/R16R2 primer pairs, (4) direct PCR using R16F2n/R16R2 primer pairs and (5) direct PCR using R16mF2/R16R1 primer pairs. Sample reference: lane 1 (no template sample, mock); lane 2 (DNA extracted from uninfected China aster (*Callistephus chinensis*) leaves, leaf control); lane 3 (DNA extracted from Aster Yellow- Witches' broom (AY-WB, *Candidatus* phytoplasma *asteris*), AY-WB); lane 4 (DNA extracted from AY-WB-infected China aster leaves, AY-WB infected leaves); lane 5 (DNA extracted from ir-*coi1* plants grown in Utah showing no signs of *Empoasca* spp feeding, ir-coi1 control); lane 6 (DNA extracted from ir-coi1 plants grown in Utah and enclosed with 3 *Empoasca* spp adult leafhoppers, ir-coi1); lane 7 (DNA extracted from ir-*coi1* plants grown in Utah and twice subjected to *Empoasca* spp leafhopper feeding over 8 days, ir-*coi1* damaged); lane 8 (DNA extracted from 1 *Empoasca* spp adult fed on sample 6, E1); lane 9 (DNA extracted from 1 adult *Empoasca* spp fed on ir-*coi1* leaves which had been previously attacked by leafhoppers [sample 7], E2); lane 10 (DNA extracted from undamaged ir-coi1 plants grown in the glasshouse, ir-*coi1* control); lane 11 (DNA extracted from ir-*coi1* plants grown in glasshouse on which 3 adult *Empoasca* sp leafhoppers were clip-caged for 7 days, ir-*coi1*); lane 12 (DNA extracted from 3 adult *Empoasca* sp collected from the glasshouse colony, E3). All PCR products were purified from the gel and sequenced. Only the bands labeled in samples 3 and 4 (positive controls) matched *Ca*. phytoplasma spp 16S-ribosomal DNA sequences.

Fig. S2. Southern blot analysis of stably transformed ir-lines. The number of T-DNA insertions in the genomic DNA of stably silenced *N. attenuata* plants was assessed by digesting 10 μg of genomic DNA extracted from plants of the T2 generation with Xbal and separation of the digested DNA fragments on a 0.8 % (w/v) agarose gel. The DNA was blotted onto Gene Screen Plus Hybridization Transfer membranes using the capillary transfer method. A gene-specific probe for the hygromycin resistance gene hptII was generated by PCR using the primer pairs HYG1-18 (5′-CCGGATCGGACGATTGCG-3′) and HYG3-20 (5′-CGTCTGTCGAGAAGTTTCTG-3′). The probe was labeled with [α-32P] dCTP using the Rediprime II kit according to the manufacturer's instructions.

Fig. S3. Kinetics of OPDA, JA and JA-Ile accumulations in stably transformed ir-lines and WT plants after FAC-elicitation. We examined the consequences of silencing the different genes of the JA biosynthetic pathway in plants of the T2 generation of RNAi silenced lines by comparing the accumulation of OPDA, JA and JA-Ile with those in WT in FAC-elicited leaves at different times after elicitation (average ± SE, *n*=4, stars indicate statistically significant differences, Student *t*-test WT versus line, *: $P < 0.05$, **: $P < 0.01$, ***: $P < 0.001$ for lines with bold font, +: $P < 0.05$, ++: $P < 0.01$, +++: $P < 0.001$ for lines presented in regular font). One independently transformed line of each construct was used for further experiments (bold font: ir-*aos* line 417, ir-*aoc* line 457, ir-*opr3* line 498 and ir-*acx1* line 466).

Fig. S4. Growth parameters, analysis of volatiles released from unattacked leaves and total herbivore damage of plants deficient in JA biosynthesis and perception in the 2009 field season. (**A-B**) The rosette diameter and stem length of empty vector (EV), ir-*lox3*, ir-*aoc*, ir-*opr3* and ir-*coi1* plants were measured between 15th and 29th of May 2009 (24 to 38 days after transplanting plants into the field plantation). (**C**) Leaf volatiles were collected for 2 h from unattacked leaves (Table S2). *N. attenuata* plants were grouped in two classes based on *Empoasca* spp damage (black: no significant differences in *Empoasca* spp damage compared to controls; red: significant differences). 197 volatiles were detected and analyzed by principal component analysis (PCA) and principal components (PCs) 1 and 2

of the transgenic lines were plotted against each other. (**D**) Total herbivore damage was quantified on: empty vector (EV) and A466 controls, lines silenced in JA biosynthesis (ir-*lox3*, ir-*aoc*, ir-*opr3*) and perception (ir-*coi1*), lines silenced in JA-dependent defense molecules: diterpene glycosides (ir-*ggpps*), trypsin proteinase inhibitors (PIs; ir-*pi*), nicotine (ir-*pmt*) and both nicotine and PIs,(ir-*pmt/pi*), and lines ectopically expressing a jasmonic acid methyl transferase (35S-*jmt1*). Asterisks represent significant differences compared to control plants, *n*= 7-10, Student *t*-test, *: $P<0.05$, **: $P<0.01$, ***: $P<0.001$.

Fig. S5. *Empoasca* sp feeding preferences are independent of *Ca*. Phytoplasma spp in the glasshouse and on five jasmonate-deficient accessions identified by *Empoasca* spp damage during the 2011 field season. (**A**) During choice assays, severely *Empoasca* sp damaged *N. attenuata* leaves were used to analyze for the presence of *Ca*. phytoplasma spp. Examples of leaves showing 1, 7, 15 and 30% canopy area damaged are shown. (**B**) *Empoasca* sp did not harbor or transmit *Ca*. Phytoplasma spp to *N. attenuata* plants. *Ca*. Phytoplasma spp detection assays were performed with different combinations of PCR conditions and primers: (1) direct PCR using fU5/rU3 primer pairs, (2) direct PCR using P1/P7 primer pairs followed by nested PCR using R16F2n/R16R2 primer pairs, (3) direct PCR using R16mF2/R16R1 primer pairs followed by nested PCR using R16F2n/R16R2 primer pairs and (4) direct PCR using R16F2n/R16R2 primer pairs. Sample reference (left to right): lane 1 (no template sample, mock); lane 2 (DNA extracted from ir-*coi1* plants grown in Utah showing no signs of *Empoasca* sp feeding, leaf control); lane 3 (DNA extracted from Aster Yellow- Witches' broom (AY-WB, *Candidatus* Phytoplasma *asteris*, AY-WB); lane 4 (DNA extracted from AY-WB-infected China aster leaves, AY-WB infected leaf); lane 5 (DNA extracted from leafhopper damaged WT leaves, WT); lane 6 (DNA extracted from leafhopper damaged ir-*lox3* leaves, ir-*lox3*); lane 7 (DNA extracted from leafhopper damaged ir-*coi1* leaves, ir-*coi1*); lane 8 (DNA extracted from leafhopper damaged 35S-*jmt1* leaves, 35S-*jmt1*); lane 9 (DNA extracted from 10 adult *Empoasca* sp collected from the in-house colony, GH).

Empoasca spp damage to plants in native populations provides a rapid visual screening tool for plants deficient in jasmonate signaling and identified 5 plants with reduced JA accumulations among approximately 600 plants in native populations during

the 2011 field season (Figure 5E-F). (**C**) For all *Empoasca* spp attacked plants (E), their location, their characteristic *Empoasca* spp damage and the distance to the non-damaged neighboring plants, which served as controls, were recorded (n/a: quantification of *Empoasca* spp damage was not possible because plants had been extensively damaged by other herbivore species, particularly *Tupiochorus notatus*). (**D**) *Ca*. Phytoplasma spp detection in these plants and adult *Empoasca* spp from the corresponding areas were performed by different combinations of PCR conditions and primers: (1) direct PCR using fU5/rU3 primer pairs, (2) direct PCR using P1/P7 primer pairs followed by nested PCR using R16F2n/R16R2 primer pairs, (3) direct PCR using R16mF2/R16R1 primer pairs followed by nested PCR using R16F2n/R16R2 primer pairs and (4) direct PCR using R16F2n/R16R2 primer pairs. Sample reference: lane 1 (no template sample, mock); lane 2 (DNA extracted from ir-*coi1* plants grown in Utah showing no signs of *Empoasca* spp feeding, leaf control); lane 3 (DNA extracted from Aster Yellow- Witches' broom (AY-WB, *Candidatus* Phytoplasma *asteris*), AY-WB); lane 4 (DNA extracted from AY-WB-infected China aster leaves, AY-WB infected leaf); lane 5 (DNA extracted from native plant 1 leaves (P1); lane 6 (DNA extracted from native plant 2 leaves (P2); lane 7 (DNA extracted from native plant 3 leaves (P3); lane 8 (DNA extracted from native plant 4 leaves (P4); lane 9 (DNA extracted from native plant 5 leaves (P5); lane 10 (DNA extracted from 10 adult *Empoasca* spp collected in the area around native plants 1-3 (Pop1); lane 11 (DNA extracted from 10 adult *Empoasca* spp collected in the area around native plants 4-5 (Pop2).

Fig. S6. Previously published levels of *Empoasca* spp leaf damage quantified on as-lox3 and as-*aos* plants during the 2003 field season and wound-elicited JA accumulation in as-*aos* leaves. (**A**) Previous research in our group demonstrated that *Empoasca* spp leafhoppers only fed on plants silenced by antisense RNA in Na*LOX3* expression (as-*lox3*) but not on plants silenced by antisense RNA in Na*AOS* expression (as-*aos*) (10). (**B**) We re-assessed as-*aos* plants and found that silencing of *AOS* expression in as-*aos* plants was not sufficient to reduce the wound-elicited JA burst (average ± SE, *n*= 5; asterisks represent significant difference compared to EV leaves, Student *t*-test, ***: P<0.001).

Supporting tables

Table S1. List of primers and PCR conditions used for *Ca*. Phytoplasma spp analysis.

Table S2. Constitutive and *Empoasca* spp feeding induced volatile emission on transgenic *N. attenuata* lines in the field. Volatiles emitted from untreated plants were collected for 2h prior the start of the experiment. Herbivory induced plant volatiles (HIPVs) were collected for 4 h (0-4 h; immediately after the start of leafhopper feeding) and for 4 h after the following photoperiod (24 h after the start of the experiment). Volatiles analysis was performed on a GCxGC-ToF-MS instrument. Numbers represent the average of the normalized peak area (*n*=3, nd: not detected, the relative standard deviation is below 40% and not shown for clarity). A total of 83 HIPVs emitted by *Empoasca* spp feeding with a fold change (FC) of 1.5 ≤FC ≤0.66 (*P*-value <0.05) when compared to untreated plants of the same genotype.

Table S3. *Empoasca* spp feeding and MeJA treatment induce jasmonate accumulation. (**A**) 25 *Empoasca* spp were caged on *N. attenuata* WT leaves to elicit jasmonate accumulation. Jasmonate levels were measured levels 24 h after *Empoasca* spp feeding in control and attacked leaves (*Emp*. fed). Values represent average ± SE, *n*= 4, nd: not detected. (**B**) Leaves of WT, ir-*lox3*, ir-*coi1* and 35S-*jmt1* plants were treated by exogenous MeJA application. Jasmonates levels were measured 2 d after MeJA treatment (average ± SE, *n*= 6, nd: not detected).

Table S4. List of primers used for cDNA synthesis to generate constructs for Na*AOS*, Na*AOC*, Na*OPR3* and Na*ACX1* and to quantify silencing efficiency.

Supporting references

1. Krügel T, Lim M, Gase K, Halitschke R, Baldwin IT (2002) *Agrobacterium*-mediated transformation of *Nicotiana attenuata*, a model ecological expression system. *Chemoecology* 12:177-183.
2. Bubner B, Gase K, Berger B, Link D, Baldwin IT (2006) Occurrence of tetraploidy in *Nicotiana attenuata* plants after *Agrobacterium*-mediated transformation is genotype specific but independent of polysomaty of explant tissue. *Plant Cell Rep* 25:668-675.

3. Gase K, Weinhold A, Bozorov T, Schuck S, Baldwin IT (2011) Efficient screening of transgenic plant lines for ecological research. *Mol Ecol Resour* 11:890-902.
4. Gaquerel E, Weinhold A, Baldwin IT (2009) Molecular interactions between the specialist herbivore *Manduca sexta* (*Lepidoptera*, *Sphigidae*) and its natural host *Nicotiana attenuata*. VIII. An unbiased GCxGC-ToFMS analysis of the plant's elicited volatile emissions. *Plant Physiol* 149:1408-1423.
5. Xia J, Psychogios N, Young N, Wishart DS (2009) MetaboAnalyst: a web server for metabolomic data analysis and interpretation. *Nucleic Acids Res* 37:652-660.
6. Xia J, Wishart DS (2011) Web-based inference of biological patterns, functions and pathways from metabolomic data using MetaboAnalyst. *Nat Protoc* 6:743-760.
7. Mayer CJ, Vilcinskas A, Gross J (2008) Phytopathogen lures its insect vector by altering host plant odor. *J Chem Ecol* 34:1045-1049.
8. Lorenz KH, Schneider B, Ahrens U, Seemuller E (1995) Detection of the apple proliferation and pear decline phytoplasma by PCR amplification of ribosomal and nonribosomal DNA. *Phytopathology* 85:771-776.
9. Lee IM, Bartoszyk IM, Gundersen DE, Mogen B, Davis RE (1996) Nested-PCR assays for ultrasensitive detection of potato ring rot bacterium, *Clavibacter michiganensis* subsp. *sepedonicus*. *Phytopathology* 86:S96.
10. Kessler A, Halitschke R, Baldwin IT (2004) Silencing the jasmonate cascade: induced plant defenses and insect populations. *Science* 305:665-668.
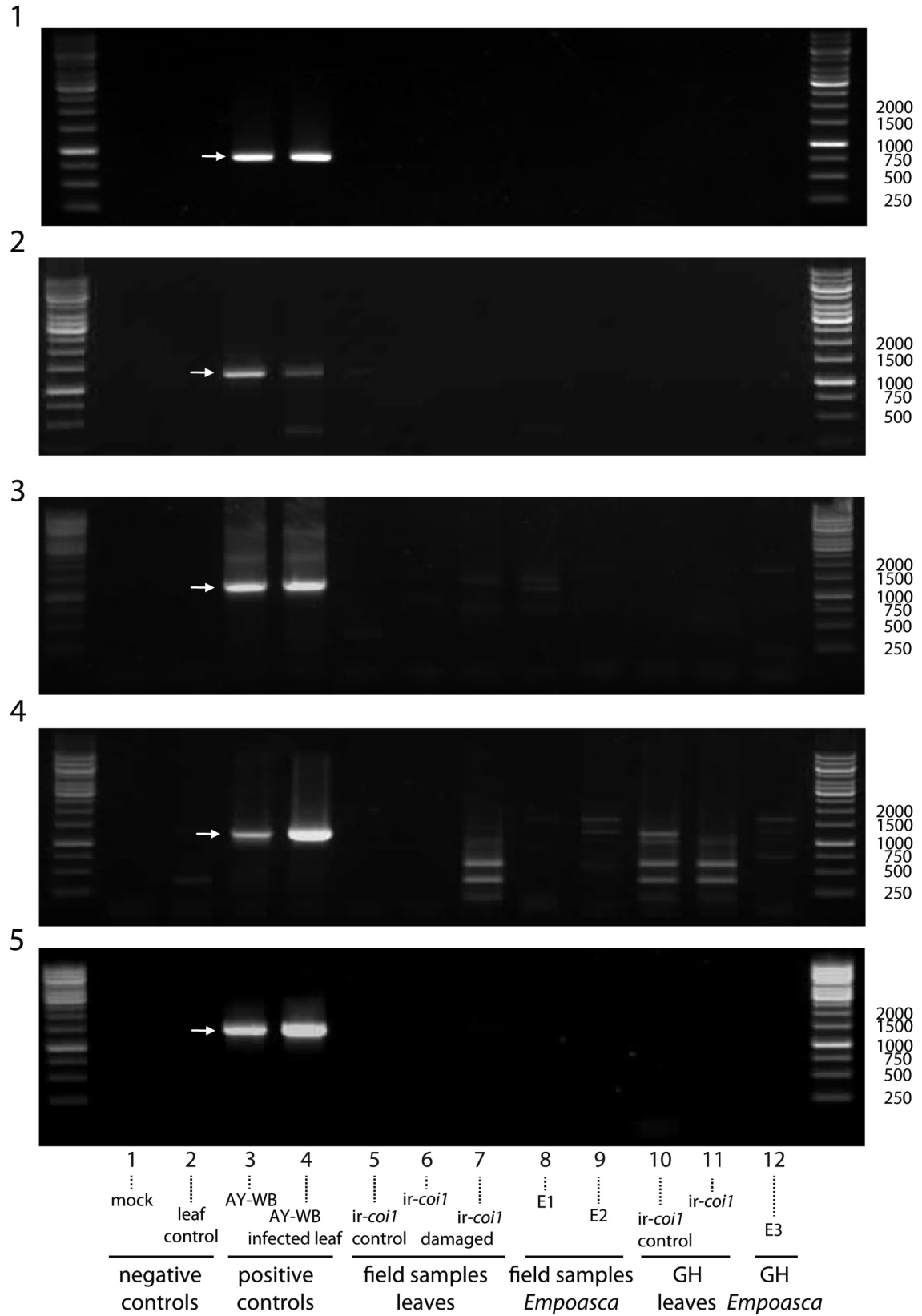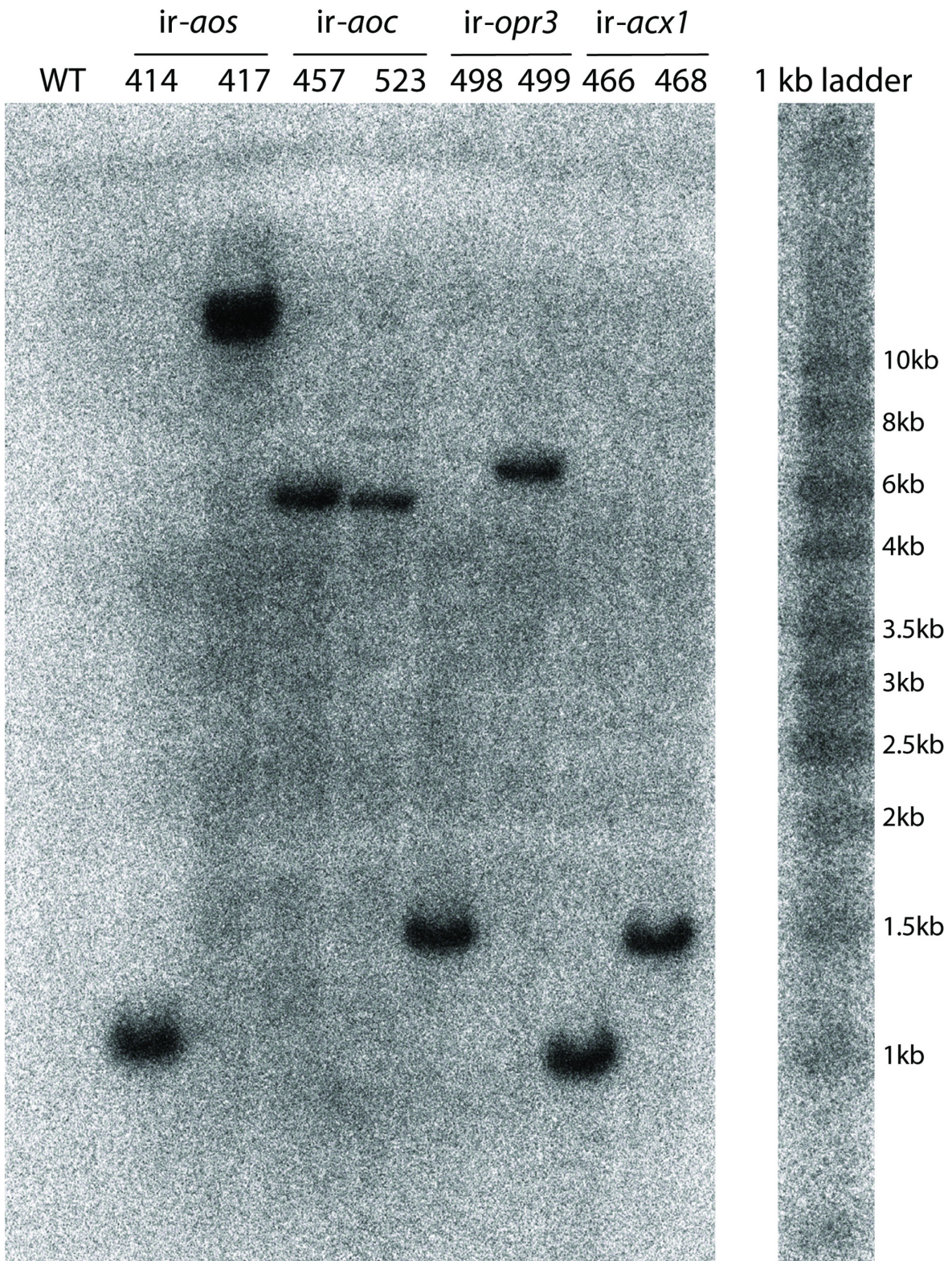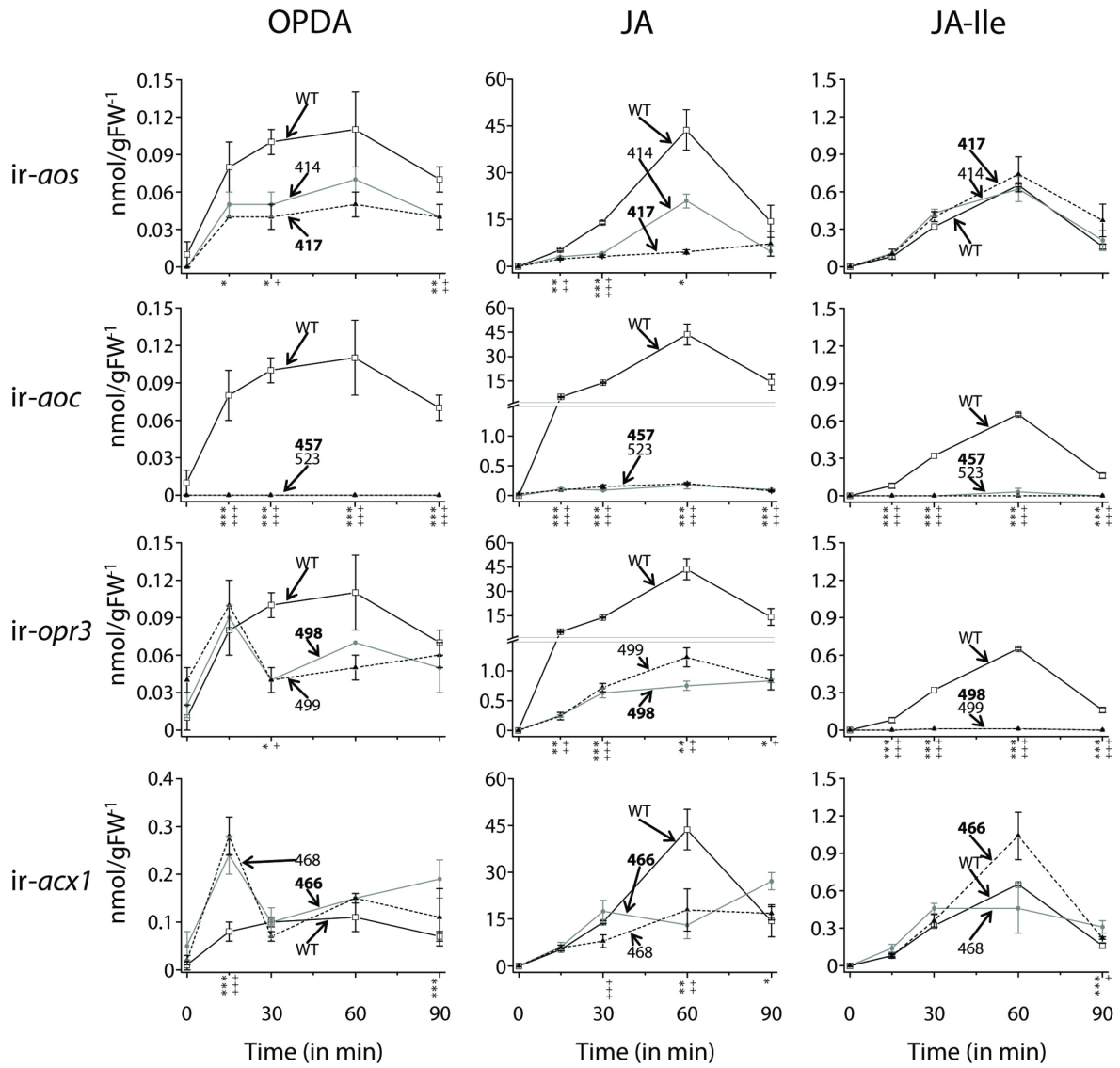
Figure S1

Figure S2

Figure S3

Figure S4

A

1 %

7 %

15 %

30 %

C

Plant	Location	Neighbors	Damage (%)	Distance to E (cm)
1	N 37.14363 W 114.01902		n/a	
		N1	0	32
		N2	0	35
2	N 37.14346 W 114.01902		1	
			0	28
3	N 37.14391 W 114.01879		10	
		N1	1	770
		N2	3	280
4	N 37.13770 W 114.02616		5	
		N1	0.5	143
5	N 37.13770 W 114.02612		5	
		N1	n/a	80

B

D
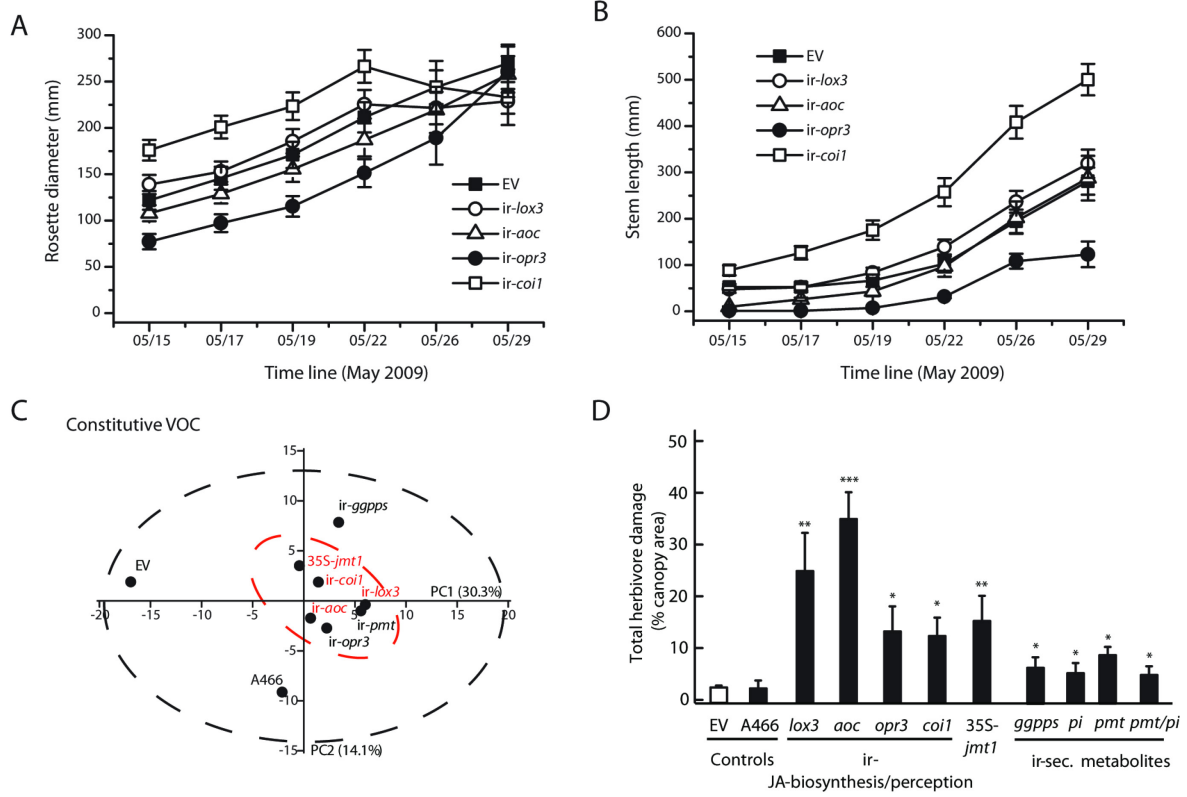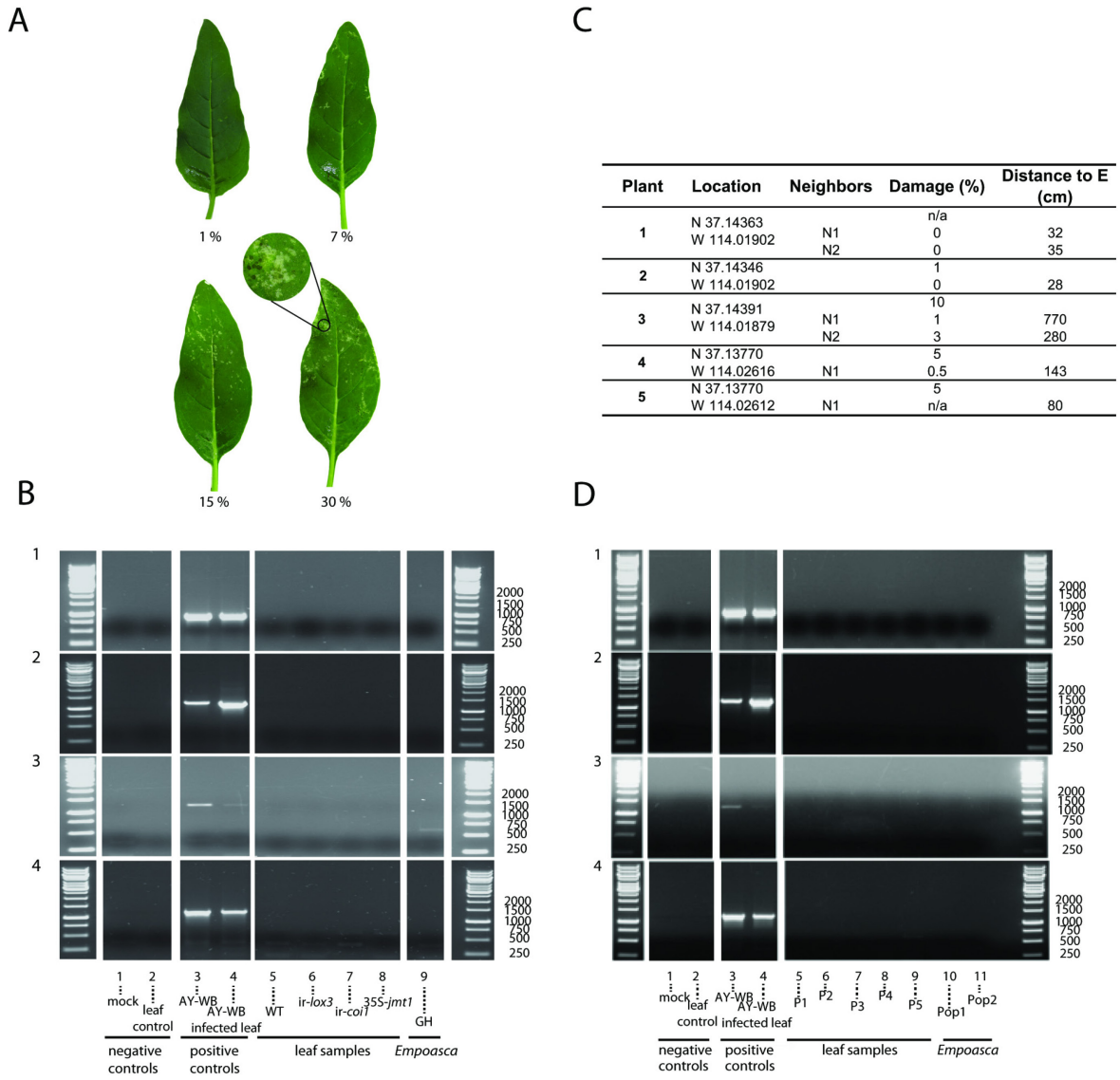
Figure S5

Table S1

A

Primers used for *Ca.* Phytoplasma spp detection

fu5	CGGCAATGGAGGAAACT
ru3	TTCAGCTACTCTTTGTAACA
R16mF2	CATGCAAGTCGAACGGA
R16mR1	CTTAACCCCAATCATCGAC
P1	AAGAGTTTGATCCTGGCTCAGGATT
P7	CGTCCTTCATCGGCTCTT
R16F2n	GAAACGACTGCTAAGACTGG
R16R2	TGACGGGCGGTGTGTACAAACCCCG

B

PCR conditions used for *Ca.* Phytoplasma spp detection

PCR	Primers used	Direct PCR PCR conditions	Primers used	Nested PCR PCR conditions
1	Fw: fU5 Rev: rU3	2 min at 95°C; 35 cycles of: 0.5 min at 94°C, 1.2 min at 60°C, 5 min at 72°C		
2	Fw: P1 Rev: P7	2 min at 95°C; 35 cycles of: 0.5 min at 94°C, 1 min at 53°C, 1.5 min at 72°C; 5 min at 72°C	Fw: R16Fn2 Rev: R16R2	2 min at 94°C; 35 cycles of: 1 min at 94°C, 2 min at 55°C, 3 min at 72°C; 5 min at 72°C
3	Fw: R16mF2 Rev: R16R1	2 min at 94°C; 35 cycles of: 1 min at 94°C, 2 min at 60°C, 3 min at 72°C; 5 min at 72°C	Fw: R16Fn2 Rev: R16R2	2 min at 94°C; 35 cycles of: 1 min at 94°C, 2 min at 55°C, 3 min at 72°C; 5 min at 72°C
4	Fw: R16Fn2 Rev: R16F2	2 min at 94°C; 35 cycles of: 1 min at 94°C, 2 min at 55°C, 3 min at 72°C; 5 min at 72°C		
5	Fw: R16mF2 Rev: R16R1	2 min at 94°C; 35 cycles of: 1 min at 94°C, 2 min at 60°C, 3 min at 72°C; 5 min at 72°C		

Table S2

Class	RT1	RT2	Substance	EV	A466	ir-*lox3*	ir-*aoc*	ir-*opr3*	ir-*coi1*	35S-*jmt*	ir-*ggpps*	ir-*pmt*
							Constitutive volatile release					
GLVs	246	2.63	(Z)-3-hexenol	295.4	117.4	nd	39.5	62.6	21.5	51.2	21.4	29.8
	570	2.92	(Z)-3-hexenyl acetate	27.7	14.7	3.6	5.8	8.4	11.3	7.5	8.9	3.9
	588	2.47	**unknown**	nd	nd	5.6	8.8	18.7	3.4	nd	nd	5.3
	594	2.38	**unknown**	201.1	166.6	97.6	89.7	105.7	73.1	104.8	66.5	56.1
	756	2.67	(Z)-3-hexenyl propionate	92.9	38.2	28.4	65.7	25.4	71.7	437.7	416.7	217.9
	912	2.70	(Z)-3-hexenyl butyrate	nd	1.1	nd	nd	0.8	3.0	nd	nd	nd
C9 compounds	858	2.83	(E)-2-nonenal	nd	nd	nd	nd	nd	nd	2.4	nd	nd
	882	2.47	1-nonanol	5.1	1.3	nd	1.8	4.1	nd	nd	nd	nd
	144	1.65	**unknown**	11.0	17.1	nd	20.2	3.8	nd	0.3	0.8	nd
	228	2.16	**unknown**	12.9	6.2	nd	2.5	0.9	nd	2.8	nd	12.1
	438	2.69	**unknown**	18.7	4.3	nd	2.2	nd	0.8	1.0	nd	nd
	450	2.68	**unknown**	5.3	5.8	nd	3.0	2.4	1.9	3.2	2.5	nd
	492	2.68	**unknown**	3.6	nd	30.4	2.1	56.9	nd	54.9	38.5	63.9
	510	2.61	**unknown**	2.9	3.0	10.8	nd	11.9	1.4	14.8	11.3	8.1
Oxidized Hydrocarbons	612	2.52	**2-ethyl-1-hexanol**	120.0	50.6	3.5	75.3	2.3	49.3	5.1	4.6	3.5
	1236	1.84	(E)-9-hexadecenol	15.2	9.9	3.2	12.3	2.6	12.8	61.1	76.0	26.0
	1386	1.85	**tridecanol**	7.5	5.0	5.9	5.4	9.4	5.0	3.3	4.9	4.0
	336	3.03	**heptanal**	20.0	6.9	0.7	15.4	0.8	7.6	35.4	19.1	14.6
	456	2.99	**unknown**	10.6	11.2	3.6	13.0	3.2	8.2	4.6	4.1	3.4
	942	2.57	**decanal**	9.7	2.5	nd	5.4	nd	7.0	nd	nd	nd
	1524	1.88	(E)-14-hexadecenal	3.7	3.7	10.2	3.2	8.4	4.6	21.5	nd	8.0
	150	1.47	**unknown**	nd	nd	1.2	0.7	1.1	nd	20.7	nd	7.2
Monoterpenes	390	2.06	α-pinene	223.3	105.0	nd	24.2	17.1	12.9	3.0	4.5	0.7
	480	2.36	ß-pinene	174.7	91.4	nd	15.9	nd	4.6	nd	nd	nd
	528	2.24	ß-myrcene	69.0	37.8	nd	7.0	0.8	1.8	nd	nd	nd
	600	2.69	1,8-cineole	nd	nd	nd	nd	19.0	nd	3.4	3.4	2.4
	720	2.59	unknown monoterpene	6.1	nd	nd	nd	3.5	6.1	3.4	2.8	1.9
	906	3.09	α-terpineol	104.8	83.4	nd	5.0	2.0	1.6	0.3	nd	nd
Sesqui-terpenes	1248	2.61	**longifolene**	5.5	2.7	22.8	3.1	1.7	nd	101.4	90.6	44.7
	1488	1.49	**unknown sesquiterpene**	nd	nd	nd	1.0	nd	nd	3.1	nd	nd
	1272	2.59	**(E)-ß-caryophyllene**	27.4	14.2	14.3	12.4	18.7	1.2	55.8	8.7	9.1
Aromatic compounds	678	4.76	**acetophenone**	41.7	87.8	nd	30.2	3.6	7.0	1.0	nd	nd
	774	4.46	**phenylethanol**	43.2	nd	nd	nd	nd	1.0	nd	nd	nd
	780	4.36	**unknown**	2.1	9.1	nd	0.8	1.4	nd	2.0	nd	nd

Table S2 (continued)

Category	ID		Name									
Hydrocarbons	252	1.40	unknown	9.3	11.4	7.5	15.6	8.4	11.3	10.9	4.7	10.6
	324	1.61	unknown	18.4	11.6	9.4	15.4	8.0	13.8	12.8	3.1	11.7
	606	1.59	trimethyl decan	48.4	5.2	6.9	2.4	4.9	51.3	11.1	6.4	3.9
	702	1.72	dimethyl decene	11.5	8.5	1.6	8.4	2.5	18.5	3.1	16.8	3.2
	714	1.71	trimethyl octene	15.9	5.4	155.6	9.9	154.8	16.1	114.7	166.3	132.3
	1080	1.81	2-methyl tetradecene	8.2	1.4	nd	3.1	4.4	4.6	9.2	nd	nd
Short-term inducible	138	1.52	unknown	173.6	164.7	2.5	166.7	8.3	142.6	14.6	18.6	9.9
	300	2.81	unknown	36.6	10.4	nd	4.4	8.8	nd	9.6	5.8	4.2
	462	4.75	unknown	22.8	1.2	11.9	15.6	12.4	2.5	15.5	nd	6.1
	528	3.24	unknown	20.3	6.0	5.1	7.0	1.0	9.0	3.0	2.2	8.1
	564	1.55	unknown	nd	8.9	1.6	15.0	1.1	21.5	nd	nd	0.9
	612	2.31	unknown	1.3	11.5	30.6	3.8	25.7	nd	28.6	29.8	28.6
	732	1.75	unknown	nd	nd	3.0	2.2	4.4	1.6	8.0	2.6	7.9
	750	1.61	unknown	8.3	26.4	nd	18.5	nd	25.7	nd	nd	nd
	774	1.60	unknown	2.5	4.4	1.9	4.0	14.8	3.9	11.2	5.6	6.1
	810	1.46	unknown	nd	0.8	nd	nd	52.2	0.5	63.8	nd	20.6
	1164	1.65	unknown	9.9	6.9	1.1	15.1	2.2	nd	0.9	nd	6.2
Induced at next photoperiod	150	1.63	unknown	173.9	81.7	1.5	91.8	2.2	38.5	2.0	nd	nd
	678	1.97	unknown	1.0	nd	nd	3.3	3.7	0.8	0.6	nd	nd
	1416	3.25	unknown	1.5	nd	nd	2.6	2.5	7.7	3.1	3.1	nd
	1470	3.38	unknown	11.4	2.4	17.6	nd	19.3	nd	14.2	7.0	23.3
	162	1.76	unknown	nd	4.6	nd	5.4	44.2	2.5	7.1	9.1	2.1
	216	1.83	unknown	12.3	13.2	3.9	22.2	5.9	21.3	3.5	25.7	9.8
	216	2.03	unknown	143.2	53.9	4.1	18.1	65.0	6.8	47.4	76.7	23.9
	570	1.58	unknown	21.2	3.1	nd	5.1	5.6	nd	11.3	2.6	1.7
	678	4.66	unknown	118.8	52.9	4.9	82.8	7.5	15.0	10.7	3.3	8.8
Long-term inducible	696	2.56	unknown	19.5	7.4	8.7	13.8	8.0	2.4	9.2	8.4	7.0
	1134	1.66	unknown	12.6	11.4	2.1	11.3	12.5	9.8	16.3	12.3	5.2
	1206	2.92	unknown	8.9	6.5	nd	8.2	7.8	8.3	3.6	nd	2.0
	1248	1.74	unknown	30.6	13.8	nd	2.1	2.7	13.0	2.5	nd	nd
	1476	3.32	unknown	9.2	nd	8.2	11.1	3.6	nd	7.7	2.1	2.3
	1602	4.08	unknown	17.9	58.1	172.4	16.3	187.4	21.3	165.8	184.4	137.1
	156	1.54	unknown	4.5	2.4	3.2	5.1	5.8	2.3	50.6	45.9	27.4
Unknown regulation	240	1.98	unknown	110.9	198.1	26.7	166.9	19.4	123.7	32.8	28.5	22.5
	558	2.78	unknown	24.7	8.8	nd	18.2	26.0	10.5	24.7	nd	22.0
	660	1.59	unknown	35.0	35.8	3.3	25.3	3.2	32.1	4.4	4.3	2.5
	744	1.67	unknown	83.7	72.1	1.2	31.9	4.1	106.8	5.0	4.7	2.3

Table S2 (continued)

Group							HIPVs immediately released after *Empoasca* sp feeding					
GLVs	912	1.82	unknown	3.6	4.0	3.2	4.1	2.5	3.8	0.9	0.7	1.4
	1116	1.74	unknown	3.6	4.4	0.5	3.7	1.2	4.0	1.2	1.7	0.6
	1332	2.63	unknown	1.3	1.5	nd	0.5	0.8	0.9	2.2	nd	1.8
	1344	2.66	unknown	0.9	1.8	1.8	0.6	3.3	0.9	2.5	nd	4.2
	1452	1.68	unknown	2.6	0.8	1.4	1.6	0.9	1.7	2.6	nd	0.9
	1590	3.82	unknown	1.7	2.0	14.8	4.0	10.1	2.7	12.3	23.0	18.5
	1590	5.73	unknown	2.7	1.4	13.0	4.7	7.3	1.7	17.5	16.1	13.3
	1626	2.66	unknown	13.6	11.4	1.8	14.3	6.2	14.8	4.2	3.0	6.0
	1632	2.28	unknown	13.7	11.0	6.9	13.6	4.9	15.2	10.4	6.0	6.5
	1650	3.93	unknown	4.9	5.2	0.6	4.6	0.7	3.6	2.0	2.6	1.4
	1656	1.90	unknown	8.8	7.5	nd	7.3	nd	7.9	nd	nd	nd
	1698	2.45	unknown	2.0	1.4	nd	1.5	nd	1.2	nd	nd	nd
	246	2.63	(*Z*)-3-hexenol	448.2	269.8	51.9	194.1	23.8	83.5	38.1	27.1	45.2
	570	2.92	(*Z*)-3-hexenyl acetate	48.4	40.9	10.2	41.8	5.0	20.2	8.1	5.2	5.2
	588	2.47	unknown	18.7	nd	nd	4.0	nd	3.8	2.1	nd	14.7
	594	2.38	unknown	165.3	52.1	109.9	141.9	106.4	75.2	80.3	138.9	109.3
	756	2.67	(*Z*)-3-hexenyl propionate	104.9	155.3	115.1	143.4	328.6	237.4	113.0	237.0	386.0
	912	2.70	(*Z*)-3-hexenyl butyrate	6.6	14.4	nd	nd	nd	nd	0.5	nd	nd
C9 compounds	858	2.83	(*E*)-2-nonenal	0.5	nd	nd	nd	nd	10.7	nd	nd	nd
	882	2.47	1-nonanol	5.6	1.2	2.4	0.9	3.0	5.4	nd	1.8	nd
	144	1.65	unknown	6.8	2.6	5.2	1.5	1.8	0.7	nd	nd	1.7
	228	2.16	unknown	18.1	4.4	nd	nd	nd	1.5	nd	1.8	nd
	438	2.69	unknown	17.5	6.5	1.7	nd	0.8	0.9	nd	nd	0.4
	450	2.68	unknown	nd	nd	1.9	3.8	1.8	3.2	nd	1.6	0.5
	492	2.68	unknown	1.9	nd	1.7	nd	75.1	76.0	41.2	57.1	53.9
	510	2.61	unknown	4.6	nd	nd	1.5	9.7	11.2	9.1	14.1	8.6
Oxidized Hydrocarbons	612	2.52	2-ethyl-1-hexanol	88.8	64.0	68.7	69.9	4.9	4.6	2.8	4.4	3.5
	1236	1.84	(*E*)-9-hexadecenol	10.0	10.5	7.0	8.7	57.2	45.1	8.7	39.8	46.8
	1386	1.85	tridecanol	4.1	3.4	2.6	3.7	6.1	10.7	1.7	6.3	nd
	336	3.03	heptanal	16.0	17.9	19.8	14.0	33.5	32.0	7.9	34.9	37.7
	456	2.99	unknown	6.9	4.8	3.8	5.3	3.5	3.5	3.6	5.5	2.6
	942	2.57	decanal	23.4	21.2	18.3	23.5	nd	1.8	nd	nd	nd
	1524	1.88	(*E*)-14-hexadecenal	3.2	3.6	2.5	3.3	5.2	20.8	5.4	18.6	13.0
	150	1.47	unknown	1.8	1.4	nd	0.4	16.4	21.7	nd	15.0	7.3
Monoterpenes	390	2.06	α-pinene	74.6	39.9	7.7	6.9	4.4	1.8	1.2	1.3	4.4
	480	2.36	β-pinene	54.6	22.5	3.1	3.9	nd	nd	nd	nd	nd
	528	2.24	β-myrcene	9.3	9.5	1.3	0.8	nd	nd	nd	nd	nd
	600	2.69	1,8-cineole	4.2	nd	nd	2.0	3.2	1.2	nd	1.4	2.9

Table S2 (continued)

Category			Compound									
	720	2.59	**unknown monoterpene**	0.7	3.0	0.4	nd	3.0	5.3	nd	nd	2.7
	906	3.09	**α-terpineol**	22.2	1	1.2	nd	nd	0.6	0.6	0.6	nd
Sesqui-terpenes	1248	2.61	**longifolene**	4.7	3.1	3.3	2.8	27.2	50.5	59.5	47.8	31.5
	1488	1.49	**unknown sesquiterpene**	0.5	nd	nd	nd	nd	6.2	0.6	nd	1.2
	1272	2.59	**(E)-ß-caryophyllene**	15.4	4.0	7.7	3.3	38.1	33.4	62.9	71.0	36.2
Aromatic compounds	678	4.76	**acetophenone**	50.0	69.3	84.0	86.1	nd	1.2	nd	nd	nd
	774	4.46	**phenylethanol**	18.6	7.6	1.0	2.0	nd	1.4	nd	nd	nd
	780	4.36	**unknown**	2.5	nd	nd	0.2	1.3	3.0	nd	nd	0.7
Hydrocarbons	252	1.40	**unknown**	25.1	14.2	15.5	19.6	11.4	3.8	20.1	2.2	5.7
	324	1.61	**unknown**	44.7	10.6	36.2	1.7	16.9	20.0	12.6	12.5	13.7
	606	1.59	**trimethyl decan**	20.5	18.0	4.6	12.7	4.4	5.1	9.5	9.8	11.9
	702	1.72	**dimethyl decene**	16.3	15.4	11.9	9.8	4.7	4.2	5.0	1.9	2.2
	714	1.71	**trimethyl octene**	9.1	12.2	9.5	6.7	110.8	171.4	122.2	174.0	36.3
	1080	1.81	**2-methyl tetradecene**	3.1	3.2	1.8	0.8	nd	58.3	nd	nd	nd
Short-terminducible	138	1.52	**unknown**	141.0	139.6	122.1	127.5	17.5	16.2	4.3	10.7	3.1
	300	2.81	**unknown**	27.5	3.4	nd	nd	31.6	85.9	3.6	30.5	25.1
	462	4.75	**unknown**	21.1	17.9	8.5	3.7	16.5	22.5	23.8	7.5	nd
	528	3.24	**unknown**	147.5	39.9	35.1	11.3	3.5	26.8	3.2	6.1	6.2
	564	1.55	**unknown**	28.2	27.3	5.6	8.5	nd	0.6	nd	1.1	1.2
	612	2.31	**unknown**	8.0	9.9	4.7	10.4	55.9	14.1	40.8	40.2	48.1
	732	1.75	**unknown**	5.4	0.5	2.2	nd	9.6	5.0	9.0	10.4	7.8
	750	1.61	**unknown**	31.8	39.0	32.4	37.3	nd	1.0	0.8	0.8	1.4
	774	1.60	**unknown**	19.9	13.9	7.0	3.3	14.2	13.7	3.7	3.5	7.0
	810	1.46	**unknown**	0.6	nd	nd	0.7	15.7	61.3	1.6	3.4	1.5
	1164	1.65	**unknown**	14.0	10.3	6.2	9.7	nd	0.4	2.4	2.2	nd
Induced at next photoperiod	150	1.63	**unknown**	38.5	17.2	24.5	18.1	6.8	2.5	nd	5.5	nd
	678	1.97	**unknown**	nd	nd	1.5	3.0	nd	nd	nd	nd	nd
	1416	3.25	**unknown**	0.7	3.3	3.5	1.2	1.6	4.5	nd	1.7	nd
	1470	3.38	**unknown**	0.4	nd	1.7	nd	29.3	10.4	22.4	24.9	21.0
	162	1.76	**unknown**	1.7	0.9	0.7	1.3	20.8	43.3	3.1	8.1	19.5
	216	1.83	**unknown**	42.5	29.4	29.0	30.3	9.8	14.5	nd	23.5	22.2
	216	2.03	**unknown**	129.9	28.2	7.4	6.2	38.9	32.2	18.7	26.9	27.7
	570	1.58	**unknown**	7.4	13.8	22.3	nd	7.2	18.0	0.9	6.7	11.2
Long-term inducible	678	4.66	**unknown**	61.7	31.0	30.4	49.7	9.4	15.3	6.0	8.0	13.2
	696	2.56	**unknown**	6.1	6.5	2.2	4.8	7.9	12.1	11.2	6.9	10.9
	1134	1.66	**unknown**	4.0	4.1	6.0	7.1	8.6	19.7	4.8	1.3	10.1
	1206	2.92	**unknown**	11.3	13.3	9.6	7.5	nd	6.9	nd	2.4	3.6
	1248	1.74	**unknown**	19.6	14.3	10.3	9.8	nd	2.4	nd	nd	nd
	1476	3.32	**unknown**	4.4	0.3	1.5	0.5	12.7	5.9	5.0	nd	8.8
	1602	4.08	**unknown**	40.9	56.0	35.2	36.9	250.2	152.8	139.3	271.3	200.9

Table S2 (continued)

Category	ID	RT	Compound	3.3	2.4	1.6	5.6	59.6	55.1	16.2	41.5	67.6
	156	1.54	unknown									
	240	1.98	unknown	346.6	240.3	138.2	150.0	41.0	38.9	29.4	39.1	48.6
	558	2.78	unknown	27.0	31.2	26.6	25.9	30.9	90.2	nd	23.5	36.2
	660	1.59	unknown	35.8	39.8	30.0	32.1	3.7	4.4	3.3	4.5	3.6
	744	1.67	unknown	56.2	39.4	21.7	19.7	5.9	5.4	3.9	5.1	7.5
	912	1.82	unknown	3.4	3.7	3.3	3.5	1.4	2.8	2.0	4.0	1.9
	1116	1.74	unknown	4.7	5.4	4.8	5.0	1.8	1.0	1.3	1.8	2.5
	1332	2.63	unknown	2.4	0.7	3.2	4.3	1.9	3.0	0.3	1.6	nd
Unknown	1344	2.66	unknown	0.7	0.6	0.7	0.8	nd	0.6	0.9	nd	1.0
regulation	1452	1.68	unknown	1.0	0.8	2.3	2.2	2.0	2.6	3.4	2.4	2.3
	1590	3.82	unknown	nd	0.1	0.9	0.9	6.1	9.0	10.9	11.8	7.0
	1590	5.73	unknown	2.2	3.8	3.2	0.9	14.1	17.4	18.4	24.8	14.0
	1626	2.66	unknown	8.1	16.3	6.7	7.2	1.4	3.1	1.9	3.4	nd
	1632	2.28	unknown	12.9	20.3	10.4	14.0	4.7	7.6	5.5	8.4	5.6
	1650	3.93	unknown	2.7	1.3	1.1	2.0	nd	0.8	0.8	2.7	1.1
	1656	1.90	unknown	6.6	7.8	2.9	5.8	nd	nd	nd	nd	nd
	1698	2.45	unknown	0.4	1.9	0.9	1.4	nd	nd	nd	nd	nd

HIPVs released the following photoperiod after Empoasca sp feeding

Category	ID	RT	Compound	3.3	2.4	1.6	5.6	59.6	55.1	16.2	41.5	67.6
	246	2.63	(Z)-3-hexenol	617.4	371.3	77.4	284.6	12.0	267.8	451.8	215.0	122.9
	570	2.92	(Z)-3-hexenyl acetate	65.3	65.0	29.6	37.3	3.1	25.0	79.2	32.5	17.5
GLVs	588	2.47	unknown	3.4	nd	nd	nd	4.0	3.8	7.9	nd	4.2
	594	2.38	unknown	66.5	78.3	47.8	51.7	60.7	110.1	78.6	80.7	67.6
	756	2.67	(Z)-3-hexenyl propionate	83.5	621.0	385.1	291.5	93.0	567.8	526.2	570.6	296.2
	912	2.70	(Z)-3-hexenyl butyrate	2.2	nd	nd	2.3	nd	4.1	nd	0.8	4.0
C9 compounds	858	2.83	(E)-2-nonenal	nd	1.7	1.6	0.6	nd	34.7	10.5	0.7	nd
	882	2.47	1-nonanol	5.3	6.4	2.8	3.7	nd	12.6	8.4	4.4	0.6
	144	1.65	unknown	nd	nd	5.7	0.6	1.8	8.5	14.8	8.1	4.2
	228	2.16	unknown	7.8	5.7	2.9	7.5	1.0	7.2	16.4	10.8	4.1
	438	2.69	unknown	7.4	13.0	7.1	10.3	0.3	2.6	5.9	2.5	0.4
	450	2.68	unknown	1.4	4.5	7.4	9.7	1.4	7.6	12.6	2.9	1.3
	492	2.68	unknown	1.2	3.9	3.6	2.3	68.6	128.5	153.4	121.0	73.2
	510	2.61	unknown	nd	2.9	4.2	6.1	11.1	18.3	20.3	18.3	15.3
Oxidized	612	2.52	2-ethyl-1-hexanol	64.9	116.5	117.2	106.8	4.7	8.2	9.7	7.3	8.3
Hydrocarbons	1236	1.84	(E)-9-hexadecenol	14.4	17.0	15.0	14.9	19.9	120.1	130.6	120.9	50.4
	1386	1.85	tridecanol	6.1	7.8	9.2	7.3	5.6	11.2	9.6	7.7	7.0
	336	3.03	heptanal	12.6	119.8	84.0	81.4	8.5	51.8	47.7	49.2	31.5
	456	2.99	unknown	6.1	10.2	7.7	12.5	3.7	6.1	4.4	4.6	4.9
	942	2.57	decanal	8.8	61.4	29.2	20.6	nd	7.8	6.7	5.2	4.0
	1524	1.88	(E)-14-hexadecenal	4.7	5.0	4.4	4.4	14.3	22.9	33.6	28.7	15.7
	150	1.47	unknown	7.3	0.9	5.2	1.5	15.5	50.6	59.2	25.0	11.5

Table S2 (continued)

Group	Code	RI	Compound									
Monoterpenes	390	2.06	**α-pinene**	35.2	70.5	44.6	33.2	2.9	3.5	10.0	6.3	3.9
	480	2.36	**ß-pinene**	20.2	39.6	27.9	24.8	nd	5.3	8.7	9.1	nd
	528	2.24	**ß-myrcene**	6.2	6.8	4.6	4.3	nd	nd	0.9	nd	nd
	600	2.69	**1,8-cineole**	1.2	6.3	6.5	7.4	4.6	4.6	10.4	5.0	3.3
	720	2.59	**unknown monoterpene**	0.8	2.1	2.1	1.6	1.0	5.1	3.7	2.3	0.8
	906	3.09	**α-terpineol**	12.1	14.0	nd	2.6	0.8	0.8	0.7	nd	nd
Sesqui-terpenes	1248	2.61	**longifolene**	2.2	5.0	3.8	3.1	nd	53.0	114.0	65.8	52.8
	1488	1.49	**unknown sesquiterpene**	nd	1.5	nd	0.4	0.7	13.6	25.6	31.2	4.1
	1272	2.59	**(E)-ß-caryophyllene**	9.0	6.0	12.3	7.0	17.3	19.7	9.6	18.5	19.7
Aromatic compounds	678	4.76	**acetophenone**	32.6	16.6	nd	nd	nd	5.1	13.1	nd	0.5
	774	4.46	**phenylethanol**	40.4	30.8	1.0	20.4	nd	nd	3.3	2.7	nd
	780	4.36	**unknown**	2.3	nd	3.8	3.1	1.8	4.2	8.9	4.9	1.7
Hydrocarbons	252	1.40	**unknown**	13.0	19.9	30.9	8.2	5.0	18.4	9.3	15.0	2.1
	324	1.61	**unknown**	24.3	70.0	37.7	26.2	5.9	6.6	10.7	14.0	26.0
	606	1.59	**trimethyl decan**	5.9	6.6	2.2	13.9	5.8	9.0	7.5	9.1	4.5
	702	1.72	**dimethyl decene**	6.9	5.6	7.9	8.2	2.9	5.8	5.2	4.1	2.5
	714	1.71	**trimethyl octene**	6.3	6.3	6.2	5.8	117.0	293.8	184.8	251.8	152.1
	1080	1.81	**2-methyl tetradecene**	1.9	5.4	4.0	3.8	nd	94.3	3.9	nd	nd
Short-term inducible	138	1.52	**unknown**	175.7	233.6	220.4	202.6	15.7	31.0	29.0	25.9	16.8
	300	2.81	**unknown**	1.6	nd	nd	nd	12.3	46.0	51.3	28.6	22.5
	462	4.75	**unknown**	17.2	16.5	29.3	26.1	4.6	5.6	5.5	14.6	3.7
	528	3.24	**unknown**	26.3	49.0	38.0	33.3	nd	9.3	3.5	9.4	3.1
	564	1.55	**unknown**	4.7	3.7	nd	13.8	nd	3.3	1.9	nd	nd
	612	2.31	**unknown**	1.4	1.9	2.1	0.7	7.0	13.2	nd	13.7	21.5
	732	1.75	**unknown**	2.6	nd	1.1	nd	4.2	13.4	10.0	4.5	146.2
	750	1.61	**unknown**	14.2	23.6	10.8	nd	0.5	1.1	1.6	0.9	0.9
	774	1.60	**unknown**	5.1	6.8	6.6	1.7	6.2	7.6	5.8	10.9	8.7
	810	1.46	**unknown**	nd	nd	1.5	0.7	3.4	127.5	66.7	19.1	8.2
	1164	1.65	**unknown**	7.2	12.2	2.5	12.1	4.0	0.7	3.5	0.5	0.6
Induced at next photoperiod	150	1.63	**unknown**	15.0	23.1	66.5	59.4	nd	nd	3.4	10.9	2.2
	678	1.97	**unknown**	3.2	0.4	0.6	1.2	nd	2.2	1.1	nd	0.4
	1416	3.25	**unknown**	9.2	9.6	2.9	3.0	3.0	5.9	nd	23.5	4.0
	1470	3.38	**unknown**	nd	0.4	3.3	2.9	26.7	40.8	43.2	34.4	21.8
Long-term inducible	162	1.76	**unknown**	5.9	17.5	4.5	9.5	5.8	54.8	53.6	31.4	13.7
	216	1.83	**unknown**	34.0	31.4	35.4	38.6	6.3	3.1	15.0	2.4	2.7
	216	2.03	**unknown**	46.9	28.3	14.9	32.4	45.6	66.1	97.1	67.7	13.5
	570	1.58	**unknown**	2.0	14.1	13.1	3.6	3.8	17.7	33.2	18.3	11.0
	678	4.66	**unknown**	43.8	90.5	125.9	71.4	2.3	8.5	3.4	11.2	4.0
	696	2.56	**unknown**	8.0	34.7	21.2	14.8	8.9	11.4	16.3	16.5	14.0
	1134	1.66	**unknown**	5.5	9.5	4.5	10.4	9.3	13.4	20.4	10.1	22.0

Table S2 (continued)

1206	2.92	**unknown**	11.3	15.3	15.1	11.7	1.3	10.2	5.6	5.4	5.9
1248	1.74	**unknown**	13.5	19.8	22.9	20.1	nd	6.6	0.7	1.0	1.7
1476	3.32	**unknown**	nd	4.5	3.3	1.9	2.5	4.7	5.2	4.9	2.4
1602	4.08	**unknown**	15.5	16.8	11.7	12.0	176.6	331.0	288.9	285.9	205.6
156	1.54	**unknown**	2.1	4.8	2.5	4.1	20.7	110.0	122.7	106.9	48.1
240	1.98	**unknown**	279.1	284.4	247.7	306.0	13.6	32.5	32.6	31.3	58.5
558	2.78	**unknown**	18.4	123.2	83.8	74.5	26.0	80.5	93.3	65.4	16.3
660	1.59	**unknown**	22.2	22.0	24.8	26.3	3.3	5.7	6.7	5.5	5.9
744	1.67	**unknown**	31.5	55.0	56.0	67.0	1.8	4.5	3.8	3.7	8.3
912	1.82	**unknown**	4.1	5.5	4.5	4.2	1.0	2.2	0.7	2.0	1.4
1116	1.74	**unknown**	3.0	3.2	4.2	3.2	nd	2.4	2.6	2.5	2.0
1332	2.63	**unknown**	nd	3.0	0.8	1.8	0.7	3.1	4.4	4.4	5.7
Unknown regulation 1344	2.66	**unknown**	1.7	2.1	1.7	1.6	nd	nd	0.3	1.0	0.1
1452	1.68	**unknown**	2.4	5.0	4.1	4.0	2.2	2.3	4.8	7.2	7.3
1590	3.82	**unknown**	nd	nd	nd	nd	12.2	15.9	14.0	13.7	17.4
1590	5.73	**unknown**	4.8	4.5	6.4	7.6	15.6	25.0	25.6	22.9	25.2
1626	2.66	**unknown**	15.6	14.5	14.9	14.6	nd	nd	1.0	nd	nd
1632	2.28	**unknown**	20.2	19.1	23.0	24.2	6.2	15.5	12.4	13.0	16.3
1650	3.93	**unknown**	1.4	nd	nd	nd	1.8	3.8	2.0	2.6	3.8
1656	1.90	**unknown**	9.8	13.7	12.2	11.8	nd	nd	nd	nd	nd
1698	2.45	**unknown**	2.2	1.9	2.1	2.4	nd	nd	nd	nd	nd

Table S3

A

	OPDA	JA	JA-Ile	nmol g^{-1} FM 11/12-OH-JA	11/12-OH-JA-Ile	11/12-COOH-JA-Ile	Me-JA
Control	**0.086** ± 0.015	**0.322** ± 0.048	nd	nd	**0.001** ± 0.001	nd	nd
Emp. **fed**	**0.264** ± 0.033	**2.674** ± 0.488	**0.017** ± 0.003	nd	**0.009** ± 0.001	**0.040** ± 0.005	nd

B

	OPDA	JA	JA-Ile	nmol g^{-1} FM 11/12-OH-JA	11/12-OH-JA-Ile	11/12-COOH-JA-Ile	Me-JA
WT	**0.01** ± 0.003	**3.71** ± 0.633	**0.01** ± 0.001	**1.31** ± 0.057	nd	nd	nd
ir-*lox3*	nd	**2.46** ± 0.325	**0.01** ± 0.001	**1.03** ± 0.128	nd	nd	nd
ir-*coil*	nd	**2.36** ± 0.309	**0.14** ± 0.018	**0.27** ± 0.055	nd	nd	nd
35S-*jmt1*	**0.02** ± 0.011	**4.63** ± 0.595	**0.02** ± 0.002	**0.89** ± 0.125	nd	nd	**0.99** ± 0.190

Table S4

Na*AOS*	
AOS N1-32	GCGGCGCTGCAGCCATACCCGTTTAGCAAACG
AOS N2-32	GCGGCGCCATGGTTGCAAATGGTTGGTACCCG
AOS N3-31	GCGGCGGAGCTCCATACCCGTTTAGCAAACG
AOS N4-32	GCGGCGCTCGAGTTGCAAATGGTTGGTACCCG
Na*AOC*	
AOC3-32	GCGGCGCTGCAGCCTGCTTATCTTCGCTTGAG
AOC4-31	GCGGCGCCATGGCCGGTAACAGCAAGATAAG
AOC5-31	GCGGCGGAGCTCCTGCTTATCTTCGCTTGAG
AOC6-31	GCGGCGCTCGAGCCGGTAACAGCAAGATAAG
Na*OPR3*	
OPR33-34	GCGGCGCTGCAGCTGAAGGCACTATGATTTCTCC
OPR34-34	GCGGCGCCATGGCTCTTGGTTTTGGATAAATAGC
OPR35-33	GCGGCGGAGCTCTGAAGGCACTATGATTTCTCC
OPR36-35	GCGGCGCTCGAGGCTCTTGGTTTTGGATAAATAGC
Na*ACX1*	
ACX13-32	GCGGCGCTGCAGAGTCAAGGACTGGCTGAAAC
ACX14-31	GCGGCGCCATGGCTGGGAATATAAGGCTCTG
ACX15-32	GCGGCGGAGCTCAGTCAAGGACTGGCTGAAAC
ACX16-31	GCGGCGCTCGAGCTGGGAATATAAGGCTCTG

Primers used to evaluate gene silencing	
Na*AOS*	Fw GACGGCAAGAGTTTTCCCAC
	Rev TAACCGCCGGTGAGTTCAGT
Na*AOC*	Fw ATCGTACTTGACTTACGAGGATACT
	Rev TCACAAGCTTTAGACTTCAGGTGCTT
Na*OPR3*	Fw ATGCCAGATGGAACTCATGCTATTT
	Rev TATCAAACTTGCCAAGATTCTGAGC
Na*ACX1*	Fw ATGTCGTGCTACTACTACAGGTTG
	Rev TATCAAACTTGCCAAGARRCRGAGC
Na*EF1A-a*	Fw ACACTTCCCACATTGCTGTCA
	Rev AAACGACCCAATGGAGGGTAC

C$_{12}$ derivatives of the hydroperoxide lyase pathway are produced by product recycling through lipoxygenase-2 in *Nicotiana attenuata* leaves

Mario Kallenbach, Paola A. Gilardoni, Silke Allmann, Ian T. Baldwin and Gustavo Bonaventure

Department of Molecular Ecology, Max Planck Institute of Chemical Ecology, Hans Knöll Str. 8, D-07745 Jena, Germany

Summary

Author for correspondence:
Gustavo Bonaventure
Tel: +49 3641 571118
Email: gbonaventure@ice.mpg.de

- In response to diverse stresses, the hydroperoxide lyase (HPL) pathway produces C$_6$ aldehydes and 12-oxo-(9Z)-dodecenoic acid ((9Z)-traumatin). Since the original characterization of (10E)-traumatin and traumatic acid, little has been added to our knowledge of the metabolism and fluxes associated with the conversion of (9Z)-traumatin into diverse products in response to wounding and herbivory.
- A liquid chromatography–mass spectrometry/mass spectrometry (LC-MS/MS) method was developed to quantify C$_{12}$ derivatives of the HPL pathway and to determine their metabolism after wounding and simulated herbivory in *Nicotiana attenuata* leaves.
- Ninety-eight per cent of the (9Z)-traumatin produced was converted to 9-hydroxy-(10E)-traumatin (9-OH-traumatin); two-thirds by product recycling through lipoxygenase-2 (NaLOX2) activity and one-third by nonenzymatic oxidation. Thirty-eight per cent of the *de novo* produced 9-OH-traumatin was conjugated to glutathione, consistent with this oxylipin being a reactive electrophile species. 12-OH-(9Z)-dodecenoic and dodecenedioic acids also showed rapid increases after wounding and simulated herbivory and a role for C$_{12}$ derivatives as signals in these processes was consistent with their ability to elicit substantial changes in gene expression.
- These results underscore the importance of metabolite reflux through LOX2, an insight which creates new opportunities for a functional understanding of C$_{12}$ derivatives of the HPL pathway in the regulation of stress responses.

Abbreviations: (10E)-traumatin, 12-oxo-(10E)-dodecenoic acid; (9Z)-traumatin, 12-oxo-(9Z)-dodecenoic acid; 13S-HPODE, 13S-hydroperoxy-(9Z,11E)-octadecadienoic acid; 13S-HPOTE, 13S-hydroperoxy-(9Z,11E)-octadecatrienoic acid; 4-OH-traumatic acid, 4-hydroxy-(2E)-dodecenedioic acid; 9,12-hydroxy-(10E)-dodecenoic acid, 9,12-OH-(10E)-dodecenoic acid; 9,12-OH-(10E)-dodecanoic acid, 9,12-hydroxy-(10E)-dodecanoic acid; 9-OH-traumatin, 9-hydroxy-12-oxo-(10E)-dodecenoic acid; traumatic acid, (2E)-dodecenedioic acid.

Introduction

In plants, the production of oxylipins from polyunsaturated fatty acids (PUFAs) is immediately induced in response to diverse stresses including wounding, and insect and pathogen attacks (Turner *et al.*, 2002; Farmer *et al.*, 2003; Mueller, 2004; Taki *et al.*, 2005; Matsui, 2006; Browse, 2009; Mosblech *et al.*, 2009). Oxylipins are diverse in structure and they play essential roles as signaling molecules during the plant's responses to these environmental stresses.

For example, jasmonic acid is essential for the induction of defense responses against pathogens and insect herbivores (Farmer *et al.*, 2003; Kessler *et al.*, 2004; Browse, 2005), C$_6$ aldehydes are important signals acting during pathogenesis and plant–insect communication (Croft *et al.*, 1993; Matsui, 2006; Baldwin, 2010), C$_{12}$ diacids and ω-oxo-acids were originally described as wound-associated hormones (Bonner & English, 1937; Zimmerman & Coudron, 1979), divinyl ethers inhibit mycelial growth and spore germination of some oomycete species (Prost *et al.*,

2005) and phytoprostanes play diverse roles in biotic stress responses (Loeffler *et al.*, 2005).

13-lipoxygenases (13-LOXs) initiate the enzymatic biosynthesis of oxylipins by di-oxygenating PUFAs such as linoleic ($18{:}2^{\Delta 9,12}$; 18:2) and α-linolenic ($18{:}3^{\Delta 9,12,15}$; 18:3) acids to generate 13S-hydroperoxy dienoic (13S-HPODE) and trienoic (13S-HPOTE) acids, respectively. Hydroperoxide lyase (HPL) cleaves 13S-HPODE and -HPOTE to generate the green leaf volatiles (GLVs) hexanal and (3*Z*)-hexenal, respectively, and 12-oxo-(9*Z*)-dodecenoic acid ((9*Z*)-traumatin; compound 1a in Fig. 1) (Vick & Zimmerman, 1976). In *Nicotiana attenuata* leaves, the supply of 13S-HPODE and 13S-HPOTE for the biosynthesis of hexanal and (3*Z*)-hexenal requires the activity of the lipoxygenase-2 gene (*NaLOX2*); plants with reduced expression of this gene have a greatly reduced production of GLVs (Allmann *et al.*, 2010). *Nicotiana attenuata* plants with reduced expression of *NaHPL* have similarly reduced production of GLVs (Halitschke *et al.*, 2004 and this study).

Hexanal, (3*Z*)-hexenal and (9*Z*)-traumatin undergo rapid modifications by diverse enzymatic and nonenzymatic reactions, generating multiple potential chemical signals. These modifications involve, among others, the isomerization of double bonds (*Z* to *E*), the oxidation of the aldehyde groups to carboxyl groups, their reduction to alcohols and their esterification (Grechkin, 2002). These modifications change the physicochemical properties of the molecules, and in some cases their importance in biological processes has been demonstrated (Zimmerman & Coudron, 1979; Ivanova *et al.*, 2001; Allmann & Baldwin, 2010). In the case of (9*Z*)-traumatin, the *Z* double bond isomerizes to *E* to form 12-oxo-(10*E*)-dodecenoic acid ((10*E*)-traumatin; compound 1b in Fig. 1), and the aldehyde group can auto-oxidize to form (3*Z*)- or (2*E*)-dodecenedioic acid ((3*Z*)- or (2*E*)-traumatic acid; compounds 2a and 2b in Fig. 1) (Zimmerman & Coudron, 1979) or be reduced to form (9*Z*)- or (10*E*)-12-hydroxy-dodecenoic acid (12-OH-dodecenoic acid; compounds 3a and 3b in Fig. 1) (Grechkin, 2002). (9*Z*)-traumatin can be oxidized to 9-hydroxy-12-oxo-(10*E*)-dodecenoic acid (9-OH-traumatin; compound 4 in Fig. 1) either enzymatically by a LOX-mediated mechanism (Gardner, 1998) or nonenzymatically (Noordermeer *et al.*, 2000). A recent study showed that 9-OH-traumatin can be subsequently converted into 4-hydroxy-(2*E*)-dodecenedioic acid (4-OH-traumatic acid; compound 5 in Fig. 1), 9,12-hydroxy-(10*E*)-dodecenoic acid (9,12-OH-(10*E*)-dodecenoic acid; compound 6 in Fig. 1) and 9,12-hydroxy-(10*E*)-dodecanoic acid (9,12-OH-(10*E*)-dodecanoic acid; compound 7 in Fig. 1) in pea (*Pisum sativum*) seedlings (Mukhtarova *et al.*, 2011). 9-OH-traumatin belongs to a class of oxylipins defined as oxylipin-reactive electrophile species (RES) based on their chemical reactivity, which in turn results from an α-β unsaturated carbonyl group (Gardner, 1998;

Farmer & Davoine, 2007; Mueller & Berger, 2009) (Fig. 1). Moreover, the presence of the hydroxyl group at C-4 of the α-β unsaturated carbonyl group increases the reactivity of C-3 to nucleophiles such as thiols and amines (Esterbauer *et al.*, 1976; Uchida, 2003).

In the case of C_{12} derivatives of the HPL pathway, early experiments have shown that (10*E*)-traumatin and (2*E*)-traumatic acid have growth-stimulating and wound-healing activities in plants (Bonner & English, 1937, 1938; English & Bonner, 1937; Zimmerman & Coudron, 1979) and, more recently, 12-OH-(9*Z*)-dodecenoic acid has been shown to act as a potent stimulator of the mitotic cycle (Ivanova *et al.*, 2001). In recent years, research has been focused primarily on the biochemical and functional characterization of GLVs during herbivore and pathogen attacks, and less attention has been paid to the metabolism and signal capacities of the C_{12} derivatives of the HPL pathway. As a result, the metabolic fluxes and fates of these molecules under these stress conditions are largely unknown in plants. These shortcomings hamper the development of new hypotheses concerning the potential roles of these molecules as signals. Hence, in this study we present a detailed analysis of the fluxes and metabolism of C_{12} derivatives of the HPL pathway in *N. attenuata* plants induced by wounding and simulated herbivory. Part of this analysis is based on a new liquid chromatography–mass spectrometry/mass spectrometry (LC-MS/MS) method developed for the quantification of these metabolites. We reveal new aspects of the biogenesis of C_{12} derivatives of the HPL pathway and open new perspectives for possible roles of these metabolites in the regulation of stress responses.

Materials and Methods

Plant growth and treatments

Seeds of *Nicotiana attenuata* Torr. ex S. Watson wild-type (WT), ir-lox2 (line 52-2) (Allmann *et al.*, 2010), ir-lox2/ir-lox3 (Kallenbach *et al.*, 2010) and ir-hpl (line 428-8; Supporting Information Methods S1) plants were germinated on agar plates containing Gamborg's B5 medium as previously described (Krügel *et al.*, 2002). Plates were maintained in a growth chamber (Snijders Scientific, Tilburg, the Netherlands) at 26°C : 16 h (155 µmol s^{-1} m^{-2} light), 24°C : 8 h dark for 10 d. Ten-day-old seedlings were transferred to TEKU pots (Pöppelmann GmbH & Co. KG, Lohne, Germany) with Klasmann plug soil (Klasmann-Deilmann GmbH, Geesten, Germany). After 10 d, seedlings were transferred to soil in 1-l pots and grown in the glasshouse under high-pressure sodium lamps (200–300 µmol s^{-1} m^{-2}) with a day : night ratio of 16 h (26–28°C) : 8 h (22–24°C) and 45–55% humidity.

Leaf wounding was performed by rolling a fabric pattern wheel three times on each side of the midvein of the leaves

New
Phytologist
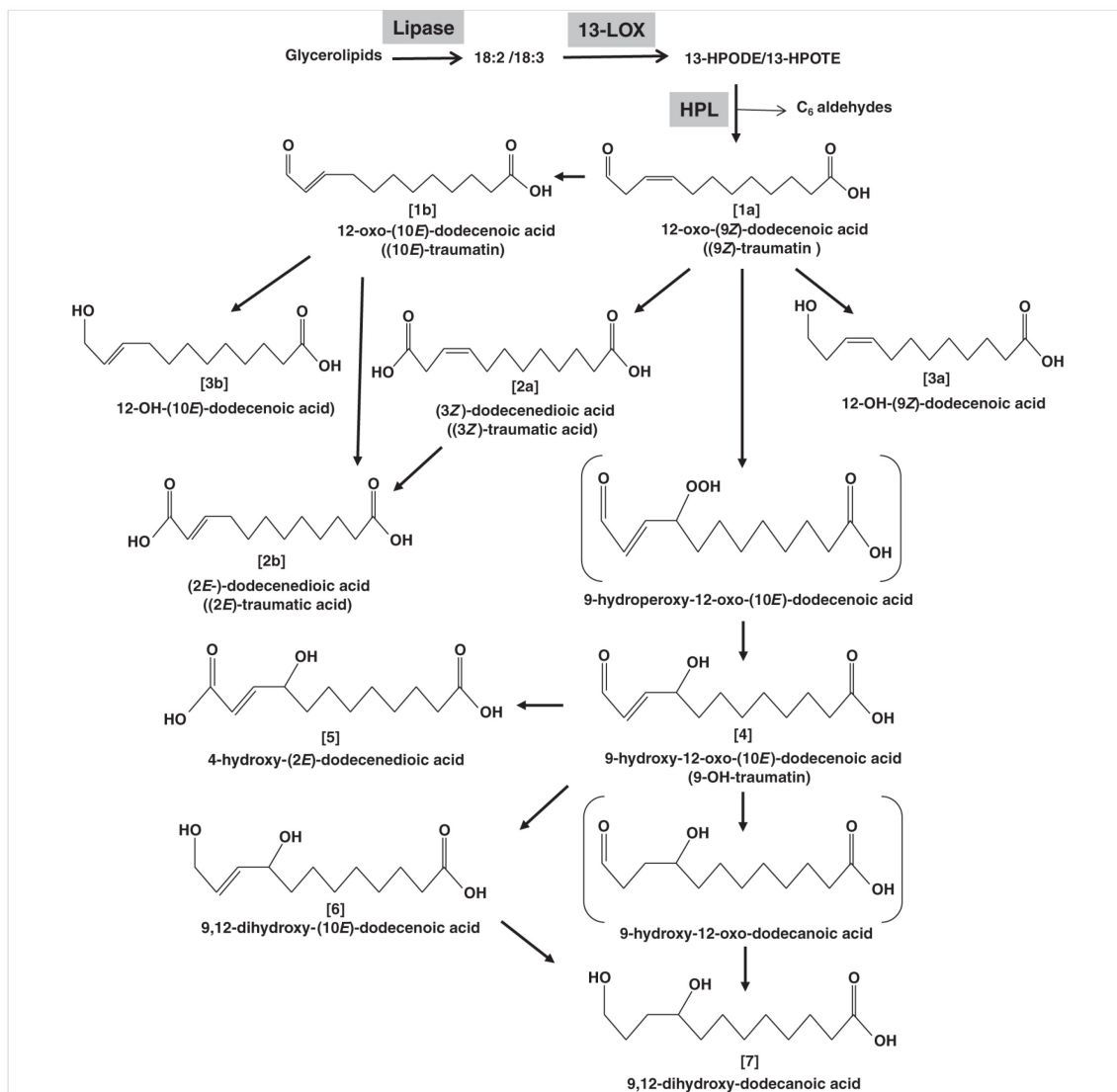
Fig. 1 Schematic representation of the hydroperoxide lyase (HPL) pathway in plants and the generation of derivatives of 12-oxo-(9*Z*)-dodecenoic acid ((9*Z*)-traumatin). In leaves, 18:2 and 18:3 fatty acids are released from membranes and dioxygenated by 13-lipoxygenases (13-LOXs) to generate 13S-hydroperoxides (13-HPODE and 13-HPOTE, respectively). These molecules are substrates of HPL and are cleaved to produce C$_6$ aldehydes and (9*Z*)-traumatin (compound 1a). This molecule can undergo several enzymatic and nonenzymatic modifications to be converted into the products (10*E*)-traumatin (compound 1b), (3*Z*)-traumatic acid (compound 2a), (2*E*)-traumatic acid (compound 2b), 12-OH-(9*Z*)-dodecenoic acid (compound 3a), 12-OH-(10*E*)-dodecenoic acid (compound 3b) and 9-OH-traumatin (compound 4). The latter compound can be converted into 4-OH-traumatic acid (compound 6), 9,12-OH-(10*E*)-dodecenoic acid (compound 5) and 9,12-OH-(10*E*)-dodecanoic acid (compound 4) according to Mukhtarova *et al.* (2011). The formation of 9-OH-traumatin by LOX-mediated activity has been proposed by Gardner (1998), whereas its nonenzymatic formation has been proposed by Noordermeer *et al.* (2000).

of 40-d-old rosette-stage plants, and the wounds were immediately supplemented with water. For fatty acid–amino acid conjugate (FAC) elicitation, the wounds were immediately supplemented with 20 μl of synthetic *N*-linolenoyl-glutamic acid (18:3-Glu; 0.03 nmol μl^{-1}). Leaf tissue was collected at different times after the treat-

ments and was frozen immediately in liquid nitrogen (N) for subsequent analysis. For C$_{12}$ treatments, leaves from ir-lox2/ir-lox3 plants were wounded as described above and a 1 : 1 mixture of (9*Z*)-traumatin:9-OH-traumatin (1 μg each per leaf dissolved in 0.02% aqueous Tween-20) or solvent (control treatment) was immediately applied to the wounds.

Purchased chemicals and synthesis of C_{12} derivatives of the HPL pathway

(9*Z*)-traumatin and (10*E*)-traumatin were purchased from Larodan (Malmö, Sweden); (2*E*)-traumatic acid was purchased from Sigma (Taufkirchen, Germany). 12-OH-(9*Z*)-dodecenoic acid and 12-OH-(10*E*)-dodecenoic acid were synthesized by reduction of 25 μg of (9*Z*)-traumatin or (10*E*)-traumatin, respectively, with excess NaBH$_4$ in 1 ml of ethanol for 4 h at 0°C. After acidification with HCl to pH 4, the products were purified by reverse solid-phase extraction (SPE) on a C18 column (Vac C18 3cc; Waters, Eschborn, Germany) by washing with water and eluting with methanol. 9-OH-traumatin was generated *in vitro* by two different methods: nonenzymatic oxidation (Noordermeer *et al.*, 2000); and processing of *N. attenuata* leaf extracts using the protocol described in the section 'In vitro assays with leaf extracts'. 9-OH-traumatin was fractionated by reverse-phase HPLC on a Gemini-NX® column (C18; 3 μm, 150 × 2 mm; Phenomenex, Aschaffenburg, Germany) using methanol and water as running solvents in a gradient mode in a Dionex UPLC system (Dionex, Germering, Germany) equipped with a fraction collector (WPS3000-FC; Dionex). The structures of the synthetic 12-OH-dodecenoic acids and 9-OH-traumatin were confirmed by gas chromatography–mass spectrometry (GC-MS) analysis: the carboxyl group of 12-OH-dodecenoic acids was transmethylated with diazomethane and the terminal hydroxyl group was silylated (trimethylsilyloxy ether (OTMSi)) by N-methy-N-(trimethylsilyl) trifluoroacetamide (MSTFA) (Machery-Nagel, Düren, Germany); the aldehyde group in 9-OH-traumatin was reduced with excess NaBH$_4$, the carboxyl group transmethylated with diazomethane and the hydroxyl groups finally silylated (OTMSi) with MSTFA. GC-MS analyses were performed on a Varian CP-4000 GC coupled to a Varian Saturn 4000 ion trap MS in electron ionization (EI; 70 eV) mode (Varian, Palo Alto, CA, USA). One microliter of the sample was injected using a 1 to 10 split ratio on a DB-5 column (30 m × 0.25 mm i.d.; 0.25-μm film thickness; Agilent, Boeblingen, Germany) with helium at a constant flow of 1 ml min^{-1} as the carrier gas. The injector was at 260°C. The oven temperature program was: 140°C for 2 min, 180°C at 6.0°C min^{-1}, 20°C min^{-1} ramp to 240°C and hold for 1 min. Electron impact (EI) spectra were recorded in scan mode from 40 to 400 *m/z*.

The glutathione (GSH) adduct of 9-OH-traumatin was synthesized by mixing 10 μg of HPLC-purified 9-OH-traumatin with 13 μg of GSH in 1 ml of buffer (10 mM MOPS and 0.02% (v/v) Tween-20; pH 7.0) for 4 h at room temperature. The solution was reduced to *c.* 50 μl in an Eppendorf SpeedVac® (Eppendorf, Wesseling-Berzdorf, Germany) connected to a high-vacuum membrane pump (Varian SH100; Varian). Then 200 μl of methanol was added to the sample and the 9-OH-traumatin–GSH conju-gate was purified by reverse-phase HPLC using a Dionex UPLC system as described for the purification of 9-OH-traumatin.

Analysis of synthetic standards, and detection and isomeric separation of C_{12} derivatives of the HPL pathway in leaves

Optimization of the multiple reaction monitoring (MRM) parameters for LC-(electrospray ionization (ESI))-MS/MS analysis was carried out by direct injection of single analytes (1 ng μl^{-1} in 70% (v/v) methanol/water) into the ESI–MS interface. Ionization was performed in the negative mode and the first quadrupole was set on their corresponding [M-H]$^-$ masses (Table S1). The third mass analyzer was set in the scan mode, ranging from 50 to 350 *m/z*. The MS/MS fragmentation patterns of the analytes were obtained by collision-induced dissociation (CID) with argon gas in the second quadrupole with increasing collision energies. The parent > daughter (*m/z*) ion transitions that gave the highest intensities were used to optimize the separation and detection of the analytes, and the final parameters used are listed in Table S1.

For the chromatographic separation of the C_{12} analytes and their *Z*/*E* isomers, 10 μl of standard solutions (1 ng μl^{-1}) was injected onto a Gemini-NX® column (C18; 3 μm, 50 × 2 mm; Phenomenex) connected to a pre-column (Gemini-NX; C18, 4 × 2 mm; Phenomenex). As mobile phases, 0.05% : 1% (v/v/v) formic acid : acetonitrile : water (solvent A) and methanol (solvent B) were used. The solvent gradient of the mobile phases was 5% of B for 2 min (pre-run), followed by a linear gradient to 45% of B to 6 min, 45% of solvent B to 22 min, a linear gradient to 98% of solvent B to 24 min, 98% of B to 27 min, a linear gradient to 5% of B to 28 min, and 5% of solvent B to 32 min. The total flow rates were 0.4 ml min^{-1} for 0.5 min, 0.2 ml min^{-1} from 0.5 to 26 min and 0.4 ml min^{-1} to 32 min.

Extraction and quantification of C_{12} derivatives of the HPL pathway in leaf extracts

For extraction, 0.3 g of frozen leaf material was homogenized in 2-ml tubes containing two steel beads (ASK, Korntal-Muenchingen, Germany) by shaking the tubes in a Genogrinder (SPEX Certi Prep, Metuchen, NJ, USA) for 30 s at 1300 strokes min^{-1}. One milliliter 2 : 1 (v/v) methanol : chloroform spiked with 200 ng of 10-hydroxy-(2*E*)-decenoic acid (internal standard (IS)) and containing 1% (w/v) butylhydroxytoluene (BHT) as a radical scavenger was added and the samples were vortexed for 10 min. After centrifugation for 10 min at 4°C (16 100 *g*), the organic phase was collected and the residual plant material was re-extracted with 0.5 ml of 2 : 1 (v/v) methanol : chloroform. The organic phases were combined and the solvent

was evaporated under reduced pressure avoiding complete dryness. The samples were reconstituted in 0.2 ml of 70% (v/v) methanol : water for analysis.

Analysis was performed on an LC-(ESI)-MS/MS system (Varian 1200 Triple-Quadrupole-LC-MS system; Varian). Ten microliters of the sample was injected onto a ProntoSIL® column (C18; 5 μm, 50 × 2 mm; Bischoff, Leonberg, Germany) connected to a precolumn (C18; 4 × 2 mm; Phenomenex). As mobile phases, 0.05% : 1% (v/v/v) formic acid : acetonitrile : water (solvent A) and methanol (solvent B) were used in a gradient mode with the following conditions: time : concentration (min:%) for B: 0.0 : 5; 1.0 : 5; 8.0 : 98; 16.0 : 98; 17.0 : 5; 20.0 : 5; time : flow (min:ml min^{-1}): 0.0 : 0.4; 0.5 : 0.2; 15.5 : 0.2; 16.0 : 0.4; 20.0 : 0.4. Compounds were detected in the ESI negative mode and MRM (Table S2).

The response curves of the synthetic or purified C_{12} analytes vs the IS (10-hydroxy-(2E)-decenoic acid) were determined and used to calculate the response factors (Fig. S4). For quantification of endogenous C_{12} derivatives, the corresponding peak areas obtained in the LC chromatogram were integrated and divided by the peak area of the IS, and the values were corrected by the respective response factor. For determination of the linearity and the sensitivity of the method, the standards of all C_{12} analytes were dissolved at different concentrations in a leaf matrix derived from unelicited ir-lox2 plants. Linearity (as expressed by the correlation coefficient (r)) was calculated by the method of least squares and sensitivity was calculated by determining the limit of detection according to the calibration curve method (Fig. S2).

In vitro assays with leaf extracts

Per assay, one 50-mm^2 leaf disc was cut from rosette-stage *N. attenuata* plants with a cork borer and was gently and thoroughly crushed with a pestle in a 1.5-ml tube containing 0.2 ml of reaction buffer (10 mM MOPS and 15% (w/v) glycerol; pH 6.8). The sample was centrifuged at 4°C for 5 min at 2300 g to pull down tissue debris and the supernatant was kept on ice. The amount of protein in the extract was quantified using the Bio-Rad Protein Assay kit (Bio-Rad, München, Germany) and BSA as a standard. One microgram of either (9Z)-traumatin or (10E)-traumatin (dissolved in 10 μl of 0.02% (v/v) Tween-20 : water) was added to 200 μl of reaction buffer containing 100 μg of total protein and the reaction was carried out at room temperature for different times. The reaction was stopped by the addition of 1 ml of 2 : 1 (v/v) chloroform : methanol containing 1 μg of 10-hydroxy-(2E)-decenoic acid (IS) and 1% (w/v) BHT. After centrifugation (1 min at 16 100 g), the supernatant was collected and concentrated under a stream of N, avoiding complete dryness, and the samples were reconstituted in 1 ml of 70% (v/v) methanol : water for LC-MS/MS analysis as

described previously in the section 'Extraction and quantification of C_{12} derivatives of the HPL pathway in leaf extracts'.

For LOX activity inhibition, a final concentration of 10 mM 3,4-dihydroxy-phenylethanol (DHPE; Sigma) was used in the reaction. Leaf extracts were heat-inactivated by incubation at 95°C for 5 min.

Analysis of surface-deposited C_{12} derivatives of the HPL pathway

Unelicited and elicited leaves from rosette-stage *N. attenuata* plants were cut at the base of the petiole, weighed, and washed for 1 min in 8 ml of methanol. Then 500 ng of 10-hydroxy-(2E)-decenoic acid (IS) and 1% (w/v) BHT were added to the 8-ml wash. The remaining leaf material was extracted with 2 : 1 (v/v) methanol : chloroform containing 500 ng of 10-hydroxy-(2E)-decenoic acid (IS) and 1% (w/v) BHT. The solvent was evaporated under a stream of N, avoiding complete dryness, and both leaf wash and leaf samples were reconstituted in 0.5 ml of 70% (v/v) methanol : water for analysis by LC-MS/MS as described above in Extraction and quantification of C_{12} derivatives of the HPL pathway in leaf extracts.

Microarray analysis

Total RNA was extracted based on the method of Kistner & Matamoros (2005) and its quality checked by spectrophotometry (NanoDrop, Wilmington, DE, USA). Genomic DNA was removed by DNAse treatment following commercial instructions (Turbo DNase; Ambion), RNA was cleaned up using RNeasy MinElute columns (Qiagen, Hilden, Germany) and the RNA quality was checked with the RNA 6000 Nano kit (Agilent, Santa Clara, CA, USA) using an Agilent 2100 Bioanalyzer. Total RNA was used to generate labeled cRNA with the Quick Amp labeling kit (Agilent) and the yield was determined spectrophotometrically (NanoDrop). Labeled cRNA was hybridized using the Gene Expression Hybridization kit (Agilent) onto 44 K custom-designed 60-mer *N. attenuata* Agilent microarrays (sequences available upon request) containing 43 533 sequences. Microarrays were hybridized overnight at 65°C and slides were washed with the Gene Expression Wash Buffer kit (Agilent) as outlined in the One-Color Microarray-Based Gene Expression Analysis manual (Agilent). Three biological replicates were used per treatment with a total of six arrays. Arrays were scanned with an Agilent G2565BA scanner and image data were acquired with the Agilent SCAN CONTROL software (version A.7.0.1 for the B scanner). Data were extracted using the Agilent FEATURE EXTRACTION software (version 9.5) and analyzed with the SIGNIFICANCE ANALYSIS OF MICROARRAYS (SAM) software (Tusher *et al.*, 2001). The *q*-values for each gene corresponded to a computed false discovery rate (FDR) of

3.3%. Significant changes in gene expression were considered when the $\log_2$(fold change; treatment vs control) was > 1 or < −1 and *q*-values < 0.035 (according to the FDR value calculated by SAM).

Statistical analysis

Statistics were calculated using the SPSS software version 17.0 (SPSS, Chicago, IL, USA).

Results

Development of a method for the analysis of C_{12} derivatives of the HPL pathway by LC-MS/MS

The standards (9*Z*)-traumatin, (10*E*)-traumatin, 12-hydroxy-(9*Z*)-dodecenoic acid, 12-hydroxy-(10*E*)-dodecenoic acid, 9-OH-traumatin, (2*E*)-traumatic acid, (3*Z*)-traumatic acid and 10-hydroxy-(2*E*)-decenoic acid (used as internal standard) were either purchased or synthesized (see the Materials and Methods section). These standards were first directly injected into the ESI–MS interface to determine their [M-H]⁻ parent ion and their parent > daughter (*m*/*z*) ion transitions by collision-induced dissociation (CID) using increasing voltage energies. The parent > daughter (*m*/*z*) ion transitions giving the strongest intensity at fixed collision energies were selected (Tables S1,S2) for MRM during the chromatographic separation of the standards by LC. This separation was performed by reverse-phase LC and the method was first established for the separation of the *E* and *Z* stereoisomers of the standards (Fig. 2a).

Next, to determine the C_{12} derivatives of the HPL pathway that accumulated endogenously in leaves of *N. attenuata* plants, the method was applied to the analysis of leaf extracts from unelicited and wounded WT plants. (9*Z*)-traumatin, 9-OH-traumatin, (2*E*)-traumatic acid, (3*Z*)-traumatic acid, and 12-OH-(9*Z*)-dodecenoic acid were detected while (10*E*)-traumatin, 12-OH-(10*E*)-dodecenoic acid, 4-OH-traumatic acid, 9,12-OH-(10*E*)-dodecenoic acid and 9,12-OH-(10*E*)-dodecanoic acid were either absent or below the limit of detection (LoD; Table S2).

Based on these results, a shorter method that did not discriminate between the dodecenedioic acid isomers ((2*E*)- and (3*Z*)-traumatic acids) was developed for the quantification of C_{12} derivatives in a large number of samples. When this method was used, all C_{12} analytes eluted from the column within 13 min (Fig. 2b). The C_{12} analytes presented a linear response, with an *r* value of 0.99 and LoD values of *c*. 1 ng in the column (Fig. S2). The extraction method was validated by performing 10 biological replicates of *N. attenuata* unelicited and wounded leaves after 60 min of the treatment. For each replicate, 0.3 g of leaf tissue was extracted and analyzed by LC-MS/MS. The standard deviations of the calculated amounts were below 10% of the

average values for all detectable compounds. To determine the extraction recovery rate, the residual leaf material obtained after the extraction protocol was re-extracted and analyzed for the presence of C_{12} derivatives. The recovery rates were > 98% for all the molecules tested.

To corroborate the endogenous production of 9-OH-traumatin, leaf extracts from *N. attenuata* plants were supplied with (9*Z*)-traumatin and the products of the reaction were analyzed by GC-MS. Fig. 2(c) shows a chromatogram and the MS spectrum corresponding to 9-OH-traumatin. Formation of 11-OH-traumatin could not be detected in leaf extracts; however, it was detected when (9*Z*)-traumatin was subjected to auto-oxidation *in vitro* (Fig. S1), as previously described (Noordermeer *et al.*, 2000).

9-OH-traumatin is the most abundant C_{12} derivative accumulating after wounding and FAC elicitation in *N. attenuata* leaves

The endogenous accumulation of C_{12} molecules was first quantified in leaves of WT *N. attenuata* after wounding and simulated herbivory. For the latter treatment, wounds were supplemented with the fatty acid–amino acid conjugate (FAC) *N*-linoleyl-glutamic acid (18:3-Glu), a major elicitor of herbivore responses in this plant species (Halitschke *et al.*, 2001). The accumulation of C_{12} molecules was quantified in both treated (local) and distal (systemic) leaves.

In unelicited leaf tissue of early rosette-stage *N. attenuata* plants (40 d old), 9-OH traumatin accumulated to *c*. 2 nmol g⁻¹ FW while (9*Z*)-traumatin, 12-OH-(9*Z*)-dodecenoic acid and dodecenedioic acids accumulated to < 0.1 nmol g⁻¹ FW (Fig. 3). Fifteen minutes after wounding and FAC elicitation, 9-OH-traumatin concentrations increased on average to 8 and 10 nmol g⁻¹ FW, respectively, and then decreased to reach on average 3 nmol g⁻¹ FW after 8 h (Fig. 3). The concentrations of dodecenedioic acids and 12-OH-(9*Z*)-dodecenoic acid also increased several-fold rapidly after wounding and FAC elicitation; however, the absolute amounts remained below 0.25 nmol g⁻¹ FW (Fig. 3). Analysis of earlier time-points (within 5 min) failed to show a rapid burst of (9*Z*)-traumatin after induction by wounding and FAC elicitation (data not shown), suggesting that this HPL product is rapidly utilized after production. In systemic leaves, no significant changes in the concentrations of these molecules were detected (data not shown).

NaLOX2 and NaHPL supply the substrates for the biosynthesis of (9*Z*)-traumatin

To validate the analysis of the C_{12} derivatives of the HPL pathway in *N. attenuata* leaves, ir-lox2 plants with reduced expression of *NaLOX2* (Allmann *et al.*, 2010) and ir-hpl plants with reduced expression of *NaHPL* (Methods S1,
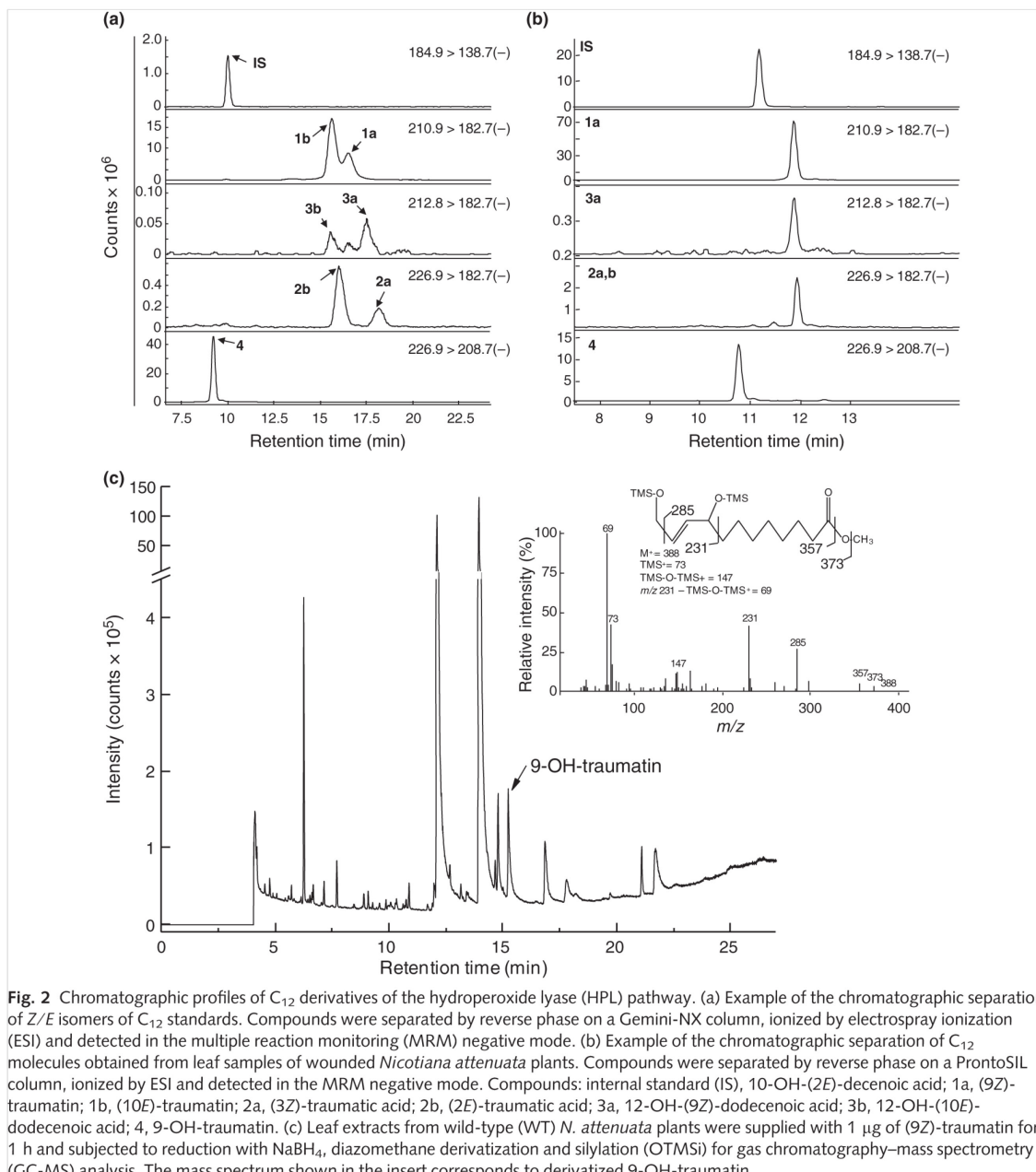
Fig. 2 Chromatographic profiles of C_{12} derivatives of the hydroperoxide lyase (HPL) pathway. (a) Example of the chromatographic separation of *Z/E* isomers of C_{12} standards. Compounds were separated by reverse phase on a Gemini-NX column, ionized by electrospray ionization (ESI) and detected in the multiple reaction monitoring (MRM) negative mode. (b) Example of the chromatographic separation of C_{12} molecules obtained from leaf samples of wounded *Nicotiana attenuata* plants. Compounds were separated by reverse phase on a ProntoSIL column, ionized by ESI and detected in the MRM negative mode. Compounds: internal standard (IS), 10-OH-(*2E*)-decenoic acid; 1a, (*9Z*)-traumatin; 1b, (*10E*)-traumatin; 2a, (*3Z*)-traumatic acid; 2b, (*2E*)-traumatic acid; 3a, 12-OH-(*9Z*)-dodecenoic acid; 3b, 12-OH-(*10E*)-dodecenoic acid; 4, 9-OH-traumatin. (c) Leaf extracts from wild-type (WT) *N. attenuata* plants were supplied with 1 µg of (*9Z*)-traumatin for 1 h and subjected to reduction with $NaBH_4$, diazomethane derivatization and silylation (OTMSi) for gas chromatography–mass spectrometry (GC-MS) analysis. The mass spectrum shown in the insert corresponds to derivatized 9-OH-traumatin.

Figs S5, S6 and Table S4) were also analyzed. In unelicited leaves of ir-lox2 plants, 9-OH-traumatin accumulated to < 0.2 nmol g^{-1} FW (Fig. 4). Moreover, after wounding and FAC elicitation, the concentrations of this C_{12} metabolite remained largely unchanged and the absolute concentrations were below 0.2 nmol g^{-1} FW (Fig. 4). (*9Z*)-traumatin, 12-OH-(*9Z*)-dodecenoic acid and dodecene-

dioic acids were either not detected or accumulated to very low concentrations in leaves of ir-lox2 plants (Fig. S3).

Analysis of ir-hpl plants showed that the concentrations of 9-OH-traumatin were reduced to *c.* 50% of WT concentrations in unelicited leaves and that they were increased twofold after wounding (Fig. 4a). After FAC elicitation, the concentrations of this metabolite increased but at lower
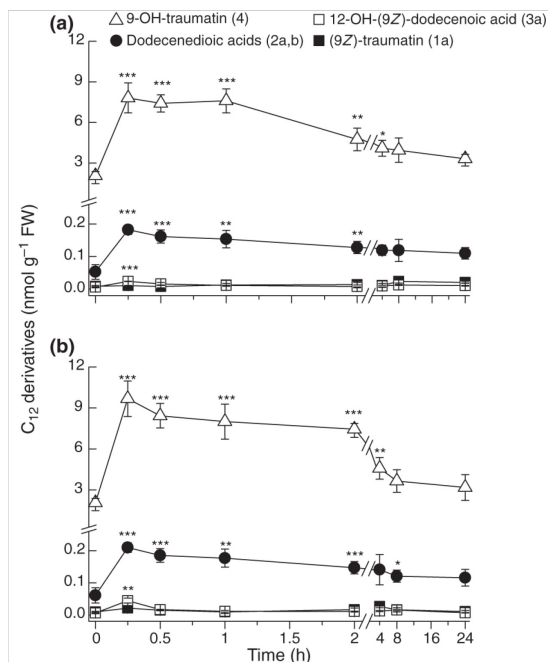
Fig. 3 Accumulation of C_{12} metabolites in leaves of wild-type (WT) *Nicotiana attenuata* plants after wounding and fatty acid–amino acid conjugate (FAC) elicitation. Leaves from WT plants were either wounded with a fabric pattern wheel (a) or subjected to wounding plus the addition of 18:3-Glu (b; FAC elicitation). Leaf samples were harvested at different times, extracted and the amounts of C_{12} derivatives of the hydroperoxide lyase (HPL) pathway (Fig. 1) were quantified by liquid chromatography–mass spectrometry/mass spectrometry (LC-MS/MS) (*, $P < 0.05$; **, $P < 0.01$; ***, $P < 0.001$; Student's *t*-test (T0 vs different times); $n = 3$; bars indicate ± SE).

Fig. 4 Accumulation of 9-OH-traumatin in leaves of *Nicotiana attenuata* wild-type (WT; triangles), ir-lox2 (closed circles) and ir-hpl (open circles) plants after wounding and fatty acid–amino acid conjugate (FAC) elicitation. Leaves from WT, ir-lox2 and ir-hpl plants were either wounded with a fabric pattern wheel (a) or subjected to wounding plus the addition of 18:3-Glu (b; FAC elicitation). Leaf samples were harvested at different times, extracted and the amounts of 9-OH-traumatin were quantified by liquid chromatography–mass spectrometry/mass spectrometry (LC-MS/MS) (*, $P < 0.05$; **, $P < 0.01$; ***, $P < 0.001$; Student's *t*-test (WT vs transgenic line at the same time-point); $n = 3$; bars indicate ± SE).

rates than in WT, and attained WT concentrations after 2 h of treatment (Fig. 4b). These results were consistent with a 50% reduction in green leaf volatile production in ir-hpl plants (Table S4) and therefore with residual HPL activity in these plants. The concentrations of the remaining C_{12} derivatives were also reduced in leaves of ir-hpl plants compared with the WT (Fig. S3).

The majority of 9-OH-traumatin is formed from (9Z)-traumatin via NaLOX2 activity

The mechanism of 9-OH-traumatin formation from (9*Z*)-traumatin in plants has been a matter of controversy, with some results supporting the enzymatic (Gardner, 1998) and others the nonenzymatic biogenesis of this metabolite (Noordermeer *et al.*, 2000). To investigate the mechanism of 9-OH-traumatin formation in *N. attenuata*, equal amounts of proteins from leaf extracts of WT and ir-lox2 plants were incubated with either (9*Z*)-traumatin or (10*E*)-traumatin and the reaction products were analyzed by LC-MS/MS.

Consistent with the nonenzymatic formation of 9-OH-traumatin from (9*Z*)-traumatin (Noordermeer *et al.*, 2000), approximately one-third of *de novo* produced 9-OH-traumatin in WT leaf extracts was generated immediately (first phase: T0) after supplying the substrate; however, the remaining two-thirds required an incubation period of at least 15 min (second phase; Fig. 5a). When leaf extracts of ir-lox2 plants were supplied with (9*Z*)-traumatin, the amount of 9-OH-traumatin produced immediately was similar to that in WT leaf extracts; however, the second phase of accumulation was suppressed (Fig. 5a). Consistent with the formation of the major fraction of 9-OH-traumatin by enzymatic mechanisms, the heat inactivation of WT leaf extracts suppressed the accumulation of 9-OH-traumatin (Fig. 5b) and co-incubation of WT leaf extracts with the LOX inhibitor 3,4-dihydroxy-phenylethanol (DHPE) also suppressed its accumulation during the second phase of the reaction (Fig. 5b). When (10*E*)-traumatin was used as the substrate, *de novo* formation of 9-OH-traumatin in WT
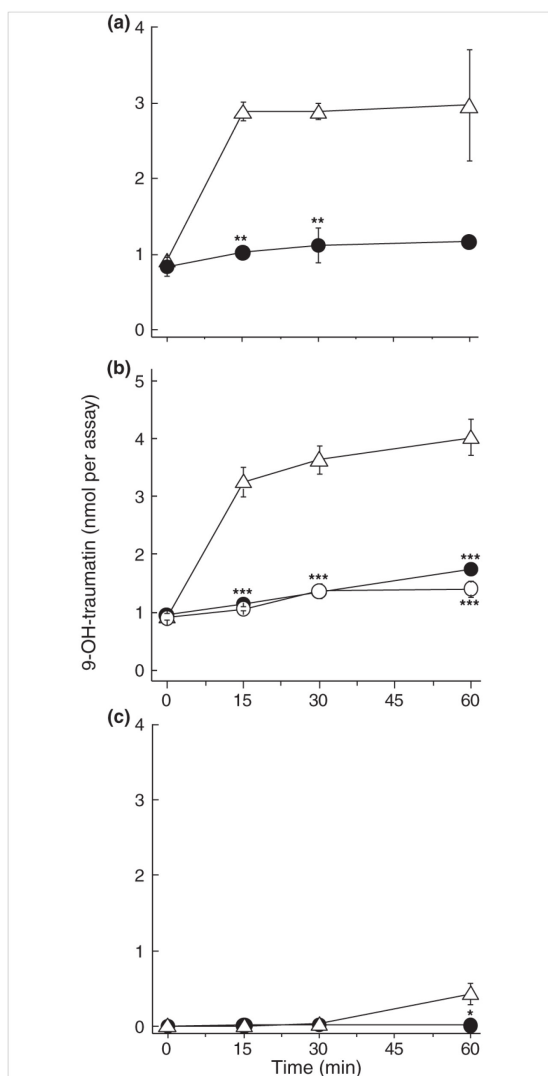
Fig. 5 Analysis of the mechanisms of 9-OH-traumatin formation in leaves of *Nicotiana attenuata* plants. (a) 100 μg of total protein from wild-type (WT; triangles) and ir-lox2 (circles) leaf extracts was incubated in 0.2 ml of reaction buffer supplied with 1 μg of (9Z)-traumatin. (b) 100 μg of total protein from WT leaf extracts were incubated in 0.2 ml of reaction buffer supplied with 1 μg of (9Z)-traumatin. Heat inactivation was achieved by incubating the leaf extracts for 5 min at 95°C before the addition of the substrate. The lipoxygenase inhibitor dihydroxyphenylethanol (DHPE) was added to obtain a final concentration of 10 mM. Triangles, control; closed circles, heat-inactivated; open circles, 10 mM DHPE. (c) 100 μg of total protein from WT (triangles) and ir-lox2 (circles) leaf extracts was incubated in 0.2 ml of reaction buffer supplied with 1 μg of (10E)-traumatin. In all cases the reactions were carried out at room temperature and stopped by the addition of chloroform : methanol. After extraction, 9-OH-traumatin was quantified by liquid chromatography–mass spectrometry/mass spectrometry (LC-MS/MS) (*, $P < 0.05$; **, $P < 0.01$; ***, $P < 0.001$; Student's *t*-test (WT vs genotype or treatment at same time point); $n = 3$; bars indicate ± SE).

and ir-lox2 leaf extracts was 10 times lower compared with its formation from (9Z)-traumatin (Fig. 5c).

It has been previously shown that the co-incubation of soybean (*Glycine max*) LOX-1 *in vitro* with (3Z)-nonenal and C_{18} hydroperoxides stimulated the activity of this enzyme toward formation of 4-OH-(2E)-nonenal (4HNE) (Gardner & Grove, 1998). To evaluate whether the oxidation of (9Z)-traumatin by NaLOX2 was indirect and depended on the accumulation of C_{18}-hydroperoxides, equimolar amounts of (9Z)-traumatin and C_{18}-hydroperoxides were added to leaf extracts of WT and ir-lox2 plants. The accumulation of 9-OH-traumatin was not affected by the added C_{18}-hydroperoxides (data not shown).

9-OH-traumatin forms conjugates with GSH during the wound and FAC elicitation response

9-OH-traumatin is an oxylipin-RES (Gardner, 1998) and as a soft electrophile it is liable to form Michael-type adducts with, for example, the sulfhydryl groups of abundant nucleophilic targets, such as reduced glutathione (GSH) (Farmer & Davoine, 2007; Mueller & Berger, 2009). GSH is an important intracellular redox buffer that accumulates at 1–5 mM in leaves and controls the concentrations of reactive molecules (Mueller & Berger, 2009). To first evaluate whether 9-OH-traumatin forms adducts with GSH, purified 9-OH-traumatin was incubated *in vitro* with commercial GSH and the reaction products were analyzed by LC-MS/MS. Formation of the 9-OH-traumatin–GSH conjugate occurred *in vitro* and, after 4 h of reaction at room temperature, > 50% of the initial amount of 9-OH-traumatin reacted with GSH (data not shown). To analyze the endogenous formation of this adduct, leaves of WT and ir-lox2 *N. attenuata* plants were wounded and the levels of 9-OH-traumatin-GSH accumulation were quantified (Fig. 6a). In WT plants, 9-OH-traumatin-GSH adducts were < 0.05 nmol g^{-1} FW in unelicited leaves; however, their concentrations increased rapidly after the treatments to reach *c.* 9 nmol g^{-1} FW within 1 h (Fig. 6a). In ir-lox2 plants, 9-OH-traumatin-GSH was undetected in unelicited leaves and accumulated at < 0.3 nmol g^{-1} FW after wounding (Fig. 6a).

9-OH-traumatin is not deposited on the leaf surfaces of *N. attenuata* plants

In addition to conjugation, cells can control the effects of reactive molecules by depositing them outside cells; for example, on the leaf surface. To investigate whether this was the case for 9-OH-traumatin, the surfaces from unelicited and wounded leaves were washed with methanol and both the washes and the surface-washed leaves were analyzed (Fig. 6b). In unelicited leaves, 9-OH-traumatin and 9-OH-traumatin-GSH accumulated primarily in the surface-
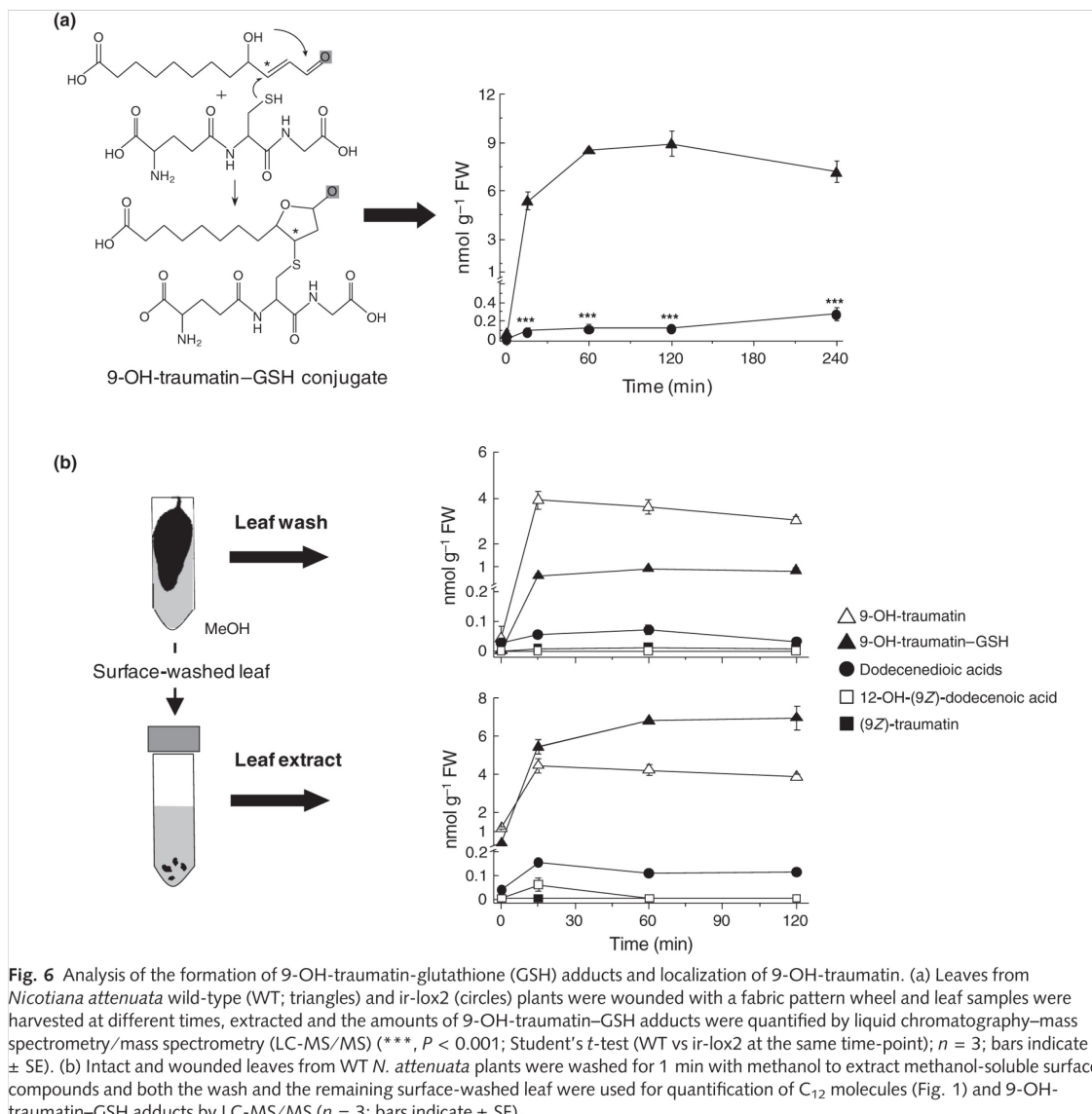
Fig. 6 Analysis of the formation of 9-OH-traumatin-glutathione (GSH) adducts and localization of 9-OH-traumatin. (a) Leaves from *Nicotiana attenuata* wild-type (WT; triangles) and ir-lox2 (circles) plants were wounded with a fabric pattern wheel and leaf samples were harvested at different times, extracted and the amounts of 9-OH-traumatin–GSH adducts were quantified by liquid chromatography–mass spectrometry/mass spectrometry (LC-MS/MS) (***, $P < 0.001$; Student's *t*-test (WT vs ir-lox2 at the same time-point); $n = 3$; bars indicate ± SE). (b) Intact and wounded leaves from WT *N. attenuata* plants were washed for 1 min with methanol to extract methanol-soluble surface compounds and both the wash and the remaining surface-washed leaf were used for quantification of C_{12} molecules (Fig. 1) and 9-OH-traumatin–GSH adducts by LC-MS/MS ($n = 3$; bars indicate ± SE).

washed leaf, with lower amounts in the wash (time 0; Fig. 6b), while the remaining C_{12} derivatives were detected at very low levels (< 0.1 nmol g^{-1} FW) in both fractions (Fig. 6b). At 15 min after wounding, 9-OH-traumatin was recovered from the wash and the surface-washed leaf extract in comparable amounts (*c.* 4 nmol g^{-1} FW) whereas 9-OH-traumatin-GSH was detected in higher amounts (6 vs 1 nmol g^{-1} FW) in the surface-washed leaf (Fig. 6b). The remaining C_{12} derivatives were *c.* 2 times more abundant in the leaf extract than in the wash (Fig. 6b). These results suggested that 9-OH-traumatin was retained in the cells and that after wounding it probably became accessible

to methanol through the damaged tissue during the leaf wash.

Formation of 9-OH-traumatin by NaLOX2 activity establishes a major flux for the production of reactive C_{12} derivatives of the HPL pathway

Calculation of the rates of accumulation of the C_{12} derivatives of the HPL pathway within 15 min of the wound response showed that on average 1 g of leaf converted 850 pmol min^{-1} of (9Z)-traumatin to 9-OH-traumatin, with approximately two-thirds of this conversion being
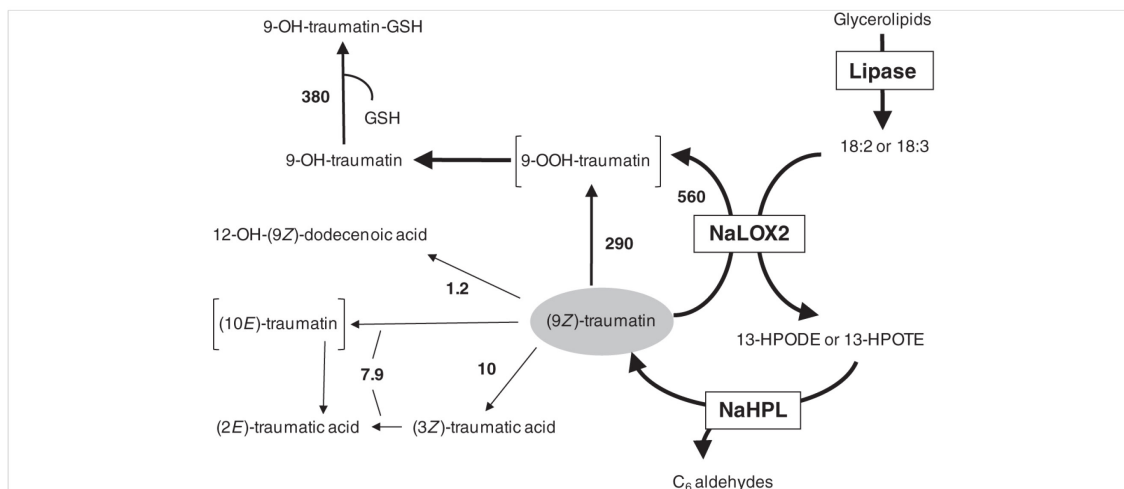
Fig. 7 Proposed model for the biosynthesis and metabolism of C_{12} derivatives of the hydroperoxide lyase (HPL) pathway in *Nicotiana attenuata* leaves. Upon wounding and fatty acid–amino acid conjugate (FAC) elicitation, 18:2 and 18:3 are released from membrane glycerolipids and dioxygenated by lipoxygenase-2 (NaLOX2) to generate 13-hydroperoxides (13-HPODE and 13-HPOTE, respectively). These molecules are substrates for NaHPL which produces C_6 aldehydes and (9Z)-traumatin. Formation of 9-OH-traumatin determines the major flux of C_{12} derivatives in leaves (850 pmol min^{-1} g^{-1} FW) and recycling NaLOX2 activity determines two-thirds of this flux (560 pmol min^{-1} g^{-1} FW) while the remaining third is determined by the nonenzymatic oxidation of (9Z)-traumatin (290 pmol min^{-1} g^{-1} FW). Formation of (2E)-traumatic acid may occur via (10E)-traumatin (not detected) auto-oxidation or isomerization of (3Z)-traumatic acid. The rates of accumulation were calculated based on the amounts of C_{12} molecules generated *de novo* within 15 min of the wound response.

catalyzed by NaLOX2 activity and the remaining one-third nonenzymatically (Fig. 7). It was found that 380 pmol min^{-1} of the 9-OH-traumatin was conjugated to GSH and the remaining (9Z)-traumatin was converted to (2E)-traumatic acid (7.9 pmol min^{-1}), (3Z)-traumatic acid (2.1 pmol min^{-1}) and 12-OH-(9Z)-dodecenoic acid (1.2 pmol min^{-1}; Fig. 7).

C_{12} derivatives of the HPL pathway induce changes in gene expression

To evaluate the signaling capacity of the C_{12} derivatives of the HPL pathway during the wound response, leaves of plants with reduced expression of *NaLOX2* and *NaLOX3* (ir-lox2/ir-lox3; Kallenbach *et al.*, 2010) were used. In this case, doubly silenced lines were chosen to minimize the effects of endogenously produced C_{12} derivatives and jasmonates after wounding. Thus, ir-lox2/ir-lox3 plants were wounded with a fabric pattern wheel, and either a 1 : 1 mixture of (9Z)-traumatin : 9-OH-traumatin or solvent (control treatment) was immediately applied to the wounds. In this case, 1 µg of each component was applied per leaf; amounts that corresponded to the endogenous amounts produced by leaves after wounding (Fig. 3). Total RNA was extracted from leaves at 120 min after the treatments and used for analysis of gene expression by microarray hybridization (see the Materials and Methods section).

The results of the analysis showed that, after the treatment with C_{12} derivatives, 320 genes showed significant changes in expression ($-1 > \log_2(\text{fold change}) > 1$; *q*-value < 0.035; FDR 3.3%) compared with the control treatment, with five genes down-regulated and the remainder up-regulated. A subset of these genes is presented in Table 1 and the complete list of genes in Table S3. Among the genes with known function that were most strongly up-regulated were *N. attenuata* homologs of glutathione *S*-transferase (GST), serine incorporator 1 (SERC1), mono-dehydroascorbate reductase (MDAR), protein disulfide isomerase (PDI) and a thioredoxin domain-containing protein; genes associated with oxidative stress responses in plants and animals (Table 1; see the Discussion section). Among the up-regulated genes were also four homologs of basic-helix-loop-helix (bHLH)-containing domain transcription factors and homologs of the defense-associated genes *PATHOGENESIS-RELATED PROTEIN 5* (*PR5*), proteinase inhibitor (*PI*) and a disease resistance response gene (Table 1). Among the signaling components, homologs of *ETHYLENE RECEPTOR 1* (*ETR1*), receptor-like protein kinase BRASSINOSTEROID INSENSITIVE 1 (BRI1)-like 3 (*BRL3*) and *MITOGEN-ACTIVATED KKK3* (*MKKK3*) were also up-regulated (Table 1). Among the down-regulated genes was BAK1 (BRASSINOSTEROID INSENSITIVE 1-associated receptor kinase 1; Table S3).

Discussion

Understanding the biosynthesis and function of the C_{12} derivatives of the HPL pathway has been a challenge in

Table 1 Example of genes up-regulated by C_{12} treatment of wounded leaves from ir-lox2/ir-lox3 *Nicotiana attenuata* plants

Gene ID	$\log_2$(FC)	SD	*q*-value	Gene annotation
Na_30516	3.3	0.92	< 0.001	Unknown function
Na_24874	3.1	0.84	< 0.001	IQ7REH6IGST Glutathione *S*-transferase (*Plasmodium yoelii*)
Na_11850	2.8	0.61	0.013	Unknown function
Na_26610	2.8	0.43	0.009	Unknown function
Na_21166	2.6	0.52	< 0.001	IQ8WW36.1IZCH13 Zinc finger CCHC domain-containing protein 13 (*Homo sapiens*)
Na_11915	2.5	0.19	< 0.001	IP40561.1ISGN1 RNA-binding protein Salivary gland transcription factor 1 (SGN1) (*Saccharomyces cerevisiae*)
Na_28441	2.5	0.60	0.017	IQ3MHV9ISERC1 Serine incorporator 1 (*Bos taurus*)
Na_22608	2.3	0.48	0.005	IBAB13708.1I Elicitor inducible protein (*Nicotiana tabacum*)
Na_17639	2.2	0.30	< 0.001	IQ9FFT9.1IRH32 DEAD-box ATP-dependent RNA helicase 32 (*Arabidopsis thaliana*)
Na_09481	2.1	0.18	0.004	IQ9LK94IMDAR2 Monodehydroascorbate reductase (*Arabidopsis thaliana*)
Na_29882	2.1	0.41	0.017	IQ9FF55.1IPDI14 Protein disulfide isomerase-like 1-4 (*Arabidopsis thaliana*)
Na_11459	2.0	0.30	0.017	IQ9CQ79.1ITXND9 Thioredoxin domain-containing protein 9 (*Mus musculus*)
Na_15649	1.9	0.21	0.006	splQ9SEL7.3IDEGP5 Protease Do-like 5 (*Arabidopsis thaliana*)
Na_20636	1.9	0.16	0.004	IQ6J163.1I5NG4 Auxin-induced protein 5NG4 (*Pinus taeda*)
Na_05174	1.8	0.23	< 0.001	IQ9LJF3IBRL3 Receptor-like protein kinase BRASSINOSTEROID INSENSITIVE 1 (BRI1)-like 3 (*Arabidopsis thaliana*)
Na_01467	1.5	0.15	0.013	IQ9C5M8.2IPEL18 Pectate lyase 18 (*Arabidopsis thaliana*)
Na_21450	1.4	0.04	0.017	IQ9C670I Transcription factor basic-helix-loop-helix (bHLH) 76 (*Arabidopsis thaliana*)
Na_09136	1.4	0.14	0.021	IP28493IPR5 Pathogenesis-related protein 5 (*Arabidopsis thaliana*)
Na_15178	1.4	0.09	< 0.001	IP83241IIP23 Proteinase inhibitor PSI-1.2 (*Capsicum annuum*)
Na_30583	1.4	0.04	0.006	IQ08080IHSP7S Stromal 70-kDa heat shock-related protein (*Spinacia oleracea*)
Na_09273	1.4	0.11	0.021	IQ9ZWL6IETR1 Ethylene receptor (*Pinus edulis*)
Na_18991	1.3	0.13	< 0.001	IQ9FLI1I Transcription factor bHLH36 (*Arabidopsis thaliana*)
Na_09028	1.3	0.12	0.017	IP13240IDR206 Disease resistance response protein 206 (*Pisum sativum*)
Na_32575	1.3	0.05	0.006	IO81893.3IITPK3 Inositol-tetrakisphosphate 1-kinase 3 (*Arabidopsis thaliana*)
Na_17734	1.3	0.03	0.013	IO22042IMKKK3 Mitogen-activated protein kinase kinase kinase 3 (*Arabidopsis thaliana*)
Na_13278	1.2	0.07	0.006	IQ9XEF0I Transcription factor bHLH51 (*Arabidopsis thaliana*)
Na_39624	1.1	0.05	0.031	IQ8S3D5IBH069 Transcription factor bHLH69 (*Arabidopsis thaliana*)

FC, fold change (treatment vs control); SD, standard deviation.

plant biology, and efforts initiated to this end a few decades ago have not been pursued with the same impetus as those associated with the C_6 derivatives of this pathway. With the opportunity to use reverse genetic approaches in the unraveling of the biosynthesis and signaling capacities of these molecules, the requirement for a suitable method for their analysis is self-evident. Here, we have described an LC-MS/MS-based approach to quantify C_{12} derivatives of the HPL pathway and have shown its application in the detection of changes induced by wounding and FAC elicitation in WT plants and by genetic deficiencies of biosynthetic enzymes (i.e. NaLOX2 and NaHPL).

Generation of 9-OH-traumatin in *N. attenuata* leaves

9-OH-traumatin was initially isolated as a product of 13-HPODE in extracts of soybean and alfalfa (*Medicago sativa*) seedlings, and it has been suggested that (9*Z*)-traumatin is converted to 9-OH-traumatin by LOX activity (Gardner, 1998). A subsequent study showed, however, that 9-OH-traumatin is formed preferentially nonenzymatically

and perhaps indirectly via 13-HPODE formation and not directly by LOX activity towards (9*Z*)-traumatin (Noordermeer *et al.*, 2000). We observed that approximately one-third of the *de novo* synthesized 9-OH-traumatin was formed nonenzymatically. However, consistent with the proposed LOX-mediated biogenesis of this oxylipin, the production of the remaining two-thirds depended either directly or indirectly on NaLOX2 activity. The reduced capacity of ir-lox2 leaf extracts to produce 9-OH-traumatin after exogenous addition of (9*Z*)-traumatin, the sensitivity of its production to heat inactivation and to the LOX inhibitor DHPE, and the independence of its accumulation to the presence of C_{18} hydroperoxides strongly suggested that NaLOX2 directly acts on (9*Z*)-traumatin to form 9-OH-traumatin. Although it is unlikely, we cannot completely rule out the possibility that the formation of 9-OH-traumatin by this enzyme is indirect via the generation of an oxidative metabolite other than C_{18} hydroperoxides. We have previously shown that NaLOX2 also oxidizes the fatty acid moiety of the FAC 18:3-Glu to form 13-OOH-18:3-Glu and its derivatives (Vandoorn

et al., 2010). Thus, the range of substrates that this enzyme can use is not restricted to free 18:2 and 18:3 and may include (9*Z*)-traumatin to generate 9-OH-traumatin, as previously proposed in other systems (Gardner, 1998).

Generation of other low-abundance C_{12} derivatives of the NaHPL pathway and systemic accumulation

Alcohol dehydrogenase activity reduces the aldehyde groups of (9*Z*)-traumatin to form 12-OH-(9*Z*)-dodecenoic acid (Grechkin *et al.*, 1990). The low amounts of this derivative accumulating in wounded and FAC-elicited *N. attenuata* leaves suggest that either this enzymatic activity is very low in this tissue or the rapid oxidation of (9*Z*)-traumatin to 9-OH-traumatin outcompetes its reduction. The low levels of accumulation of dodecenedioic acids in wounded and FAC-elicited leaves were consistent with the rapid exchange of (9*Z*)-traumatin from NaHPL to NaLOX2, as the accumulation of dodecenedioic acids remained below 0.02 nmol g^{-1} FW (Fig. S3).

Even though the concentrations of dodecenedioic acids and 12-OH-(9*Z*)-dodecenoic acid were much lower than those of 9-OH-traumatin, their accumulation increased rapidly and transiently upon wounding and FAC elicitation (Fig. 3b). Thus, a possible scenario is that, as previously demonstrated for different plant responses (English & Bonner, 1937; Bonner & English, 1938; Ivanova *et al.*, 2001), these molecules may work as signals during the responses of *N. attenuata* to wounding and herbivory.

In distal leaves, the concentrations of the C_{12} metabolites did not change significantly within 2 h after wounding and FAC elicitation; however, we cannot exclude the possibility that some of these derivatives are vascularly transported in small amounts to distal leaves. It has been recently shown that azelaic acid, a saturated C_9 dicarboxylic acid, accumulates in the sap of *Arabidopsis thaliana* and confers local and systemic resistance against *Pseudomonas syringae* (Jung *et al.*, 2009).

The role of C_{12} derivatives as potential signaling molecules acting during the response to wounding and herbivory

9-OH-traumatin accumulated to *c.* 2 nmol g^{-1} FW in unelicited WT leaves, probably reflecting a basal flux of 18:2 and 18:3 through NaLOX2 and NaHPL in this tissue and the cellular tolerance to small amounts of this oxylipin RES. This basal flux was also reflected in the basal production of C_6 volatiles in WT plants (Table S4). The effect of oxylipin RES in cellular processes has been well documented in both plants and animals. For example, they can negatively affect cellular metabolism by the chemical modification of enzymes or by reducing photosynthetic rates (Almeras *et al.*, 2003; Mueller & Berger, 2009). At the level of gene expression,

oxylipin RES can induce the transcription of genes related to detoxification, stress responses and secondary metabolism (Bate & Rothstein, 1998; Vollenweider *et al.*, 2000; Almeras *et al.*, 2003; Weber *et al.*, 2004; Mueller *et al.*, 2008). Thus, one possibility is that 9-OH-traumatin plays a role in the wound and herbivore responses through its RES properties; for example, by the activation of cell protection genes (Farmer & Davoine, 2007). After wounding, 38% of *de novo* synthesized 9-OH-traumatin conjugated to GSH, indicative of a strict control of its accumulation above certain levels, probably to prevent cytotoxic effects. The formation of oxylipin RES conjugates with GSH has been observed during the hypersensitive response (HR) induced by cryptogein elicitation in tobacco leaves (Davoine *et al.*, 2006) and it has been proposed that the generation of these conjugates may play a direct role in signaling; for example, by the alteration of the cellular redox balance (Meyer & Hell, 2005; Mullineaux & Rausch, 2005; Ogawa, 2005; Davoine *et al.*, 2006). Thus, an additional possibility is that the conjugation of 9-OH-traumatin to GSH plays a signaling role during the responses of *N. attenuata* to wounding and herbivory.

Consistent with the potential signaling roles of C_{12} derivatives of the HPL pathway during the wound response, gene expression analysis by microarrays showed that these derivatives have the capacity to exert changes in the expression of 320 genes. Among the top 12 most up-regulated transcripts (> 4-fold at 120 min) were several involved in responses to oxidative stress and protein chemical modification; a result consistent with 9-OH-traumatin being sensed as an RES by cells. These transcripts corresponded to GST (an enzyme that conjugates GSH to electrophilic centers on a wide variety of substrates, including peroxidized lipids and RES), MDAR (a component of the GSH-ascorbate antioxidant system; Dinakar *et al.*, 2010), PDI (an enzyme involved in the formation of disulfide bonds in chloroplasts; Wittenberg & Danon, 2008) and SERC1 (an enzyme involved in the protein mis-folding response in the ER-Golgi system; Aoki *et al.*, 2002). Interestingly, the expression of four transcription factors (TFs) corresponding to the bHLH family were induced by C_{12} derivatives (Table 1). This family of TFs contains the well-characterized Myelocytomatosis transcription factor (MYC)2, 3 and 4 which are involved in the regulation of defense responses in plants (Niu *et al.*, 2011). These results suggested that these TFs could also participate in the mediation of responses induced by C_{12} derivatives. In summary, the effect of these derivatives on the expression of 320 genes encoding proteins involved in diverse cellular processes including defense (e.g. PR5 and PI), signaling (e.g. ETR1, MKKK3 and BRLK3) and redox homeostasis (e.g. GST, MDAR and PDI; Tables 1,S3) provided strong evidence for the contribution of C_{12} derivatives of the HPL pathway to the control of plant responses to wounding and probably herbivory in *N. attenuata*. Future work will focus on

New
Phytologist

disentangling the potential specific roles of 9-OH-traumatin, 9-OH-traumatin-GSH, 12-OH-(9Z)-dodecenoic acid and dodecenedioic acids in the regulation of responses to wounding and herbivory and on the mechanisms underlying the formation of 9-OH-traumatin from (9Z)-traumatin by NaLOX2.

Acknowledgements

References

Allmann S, Baldwin IT. 2010. Insects betray themselves in nature to predators by rapid isomerization of green leaf volatiles. *Science* **329**: 1075–1078.

Allmann S, Halitschke R, Schuurink RC, Baldwin IT. 2010. Oxylipin channelling in *Nicotiana attenuata*: lipoxygenase 2 supplies substrates for green leaf volatile production. *Plant, Cell & Environment* **33**: 2028–2040.

Almeras E, Stolz S, Vollenweider S, Reymond P, Mene-Saffrane L, Farmer EE. 2003. Reactive electrophile species activate defense gene expression in Arabidopsis. *Plant Journal* **34**: 202–216.

Aoki S, Su Q, Li H, Nishikawa K, Ayukawa K, Hara Y, Namikawa K, Kiryu-Seo S, Kiyama H, Wada K. 2002. Identification of an axotomy-induced glycosylated protein, AIGP1, possibly involved in cell death triggered by endoplasmic reticulum–Golgi stress. *Journal of Neuroscience* **22**: 10751–10760.

Baldwin IT. 2010. Plant volatiles. *Current Biology* **20**: 392–397.

Bate NJ, Rothstein SJ. 1998. C_6-volatiles derived from the lipoxygenase pathway induce a subset of defense-related genes. *Plant Journal* **16**: 561–569.

Bonner J, English J. 1937. Purification of traumatin, a plant wound hormone. *Science* **86**: 352–353.

Bonner J, English J. 1938. A chemical and physiological study of traumatin, a plant wound hormone. *Plant Physiology* **13**: 331–348.

Browse J. 2005. Jasmonate: an oxylipin signal with many roles in plants. *Vitamins and Hormones* **72**: 431–456.

Browse J. 2009. Jasmonate passes muster: a receptor and targets for the defense hormone. *Annual Review of Plant Biology* **60**: 183–205.

Croft K, Juttner F, Slusarenko AJ. 1993. Volatile products of the lipoxygenase pathway evolved from *Phaseolus vulgaris* (L.) leaves inoculated with *Pseudomonas syringae* pv *phaseolicola*. *Plant Physiology* **101**: 13–24.

Davoine C, Falletti O, Douki T, Iacazio G, Ennar N, Montillet JL, Triantaphylides C. 2006. Adducts of oxylipin electrophiles to glutathione reflect a 13 specificity of the downstream lipoxygenase pathway in the tobacco hypersensitive response. *Plant Physiology* **140**: 1484–1493.

Dinakar C, Abhaypratap V, Yearla SR, Raghavendra AS, Padmasree K. 2010. Importance of ROS and antioxidant system during the beneficial interactions of mitochondrial metabolism with photosynthetic carbon assimilation. *Planta* **231**: 461–474.

English J, Bonner J. 1937. The wound hormones of plants I. Traumatin, the active principle of the bean test. *Journal of Biological Chemistry* **121**: 791–799.

Esterbauer H, Ertl A, Scholz N. 1976. The reaction of cysteine with α,β-unsaturated aldehydes. *Journal of Chemical Ecology* **32**: 285–289.

Farmer EE, Almeras E, Krishnamurthy V. 2003. Jasmonates and related oxylipins in plant responses to pathogenesis and herbivory. *Current Opinion in Plant Biology* **6**: 372–378.

Farmer EE, Davoine C. 2007. Reactive electrophile species. *Current Opinion in Plant Biology* **10**: 380–386.

Gardner HW. 1998. 9-Hydroxy-traumatin, a new metabolite of the lipoxygenase pathway. *Lipids* **33**: 745–749.

Gardner HW, Grove MJ. 1998. Soybean lipoxygenase-1 oxidizes 3Z-nonenal. A route to 4S-hydroperoxy-2E-nonenal and related products. *Plant Physiology* **116**: 1359–1366.

Grechkin AN. 2002. Hydroperoxide lyase and divinyl ether synthase. *Prostaglandins & Other Lipid Mediators* **68-69**: 457–470.

Grechkin AN, Kuchtina NV, Gafarova TE, Kuramshin RA. 1990. Oxidation of [1-^{14}C]linoleic acid in isolated microsomes from pea leaves. *Plant Science* **70**: 175–180.

Halitschke R, Schittko U, Pohnert G, Boland W, Baldwin IT. 2001. Molecular interactions between the specialist herbivore *Manduca sexta* (Lepidoptera, Sphingidae) and its natural host *Nicotiana attenuata*. III. Fatty acid-amino acid conjugates in herbivore oral secretions are necessary and sufficient for herbivore-specific plant responses. *Plant Physiology* **125**: 711–717.

Halitschke R, Ziegler J, Keinanen M, Baldwin IT. 2004. Silencing of hydroperoxide lyase and allene oxide synthase reveals substrate and defense signaling crosstalk in *Nicotiana attenuata*. *Plant Journal* **40**: 35–46.

Ivanova AB, Yarin AY, Antsygina LL, Gordon LK, Grechkin AN. 2001. (9Z)-12-Hydroxy-9-dodecenoic acid is an inducer of oxygen consumption and extracellular pH changes by cut wheat roots. *Doklady Biochemistry and Biophysics* **379**: 302–303.

Jung HW, Tschaplinski TJ, Wang L, Glazebrook J, Greenberg JT. 2009. Priming in systemic plant immunity. *Science* **324**: 89–91.

Kallenbach M, Alagna F, Baldwin IT, Bonaventure G. 2010. *Nicotiana attenuata* SIPK, WIPK, NPR1 and fatty acid-amino acid conjugates participate in the induction of JA biosynthesis by affecting early enzymatic steps in the pathway. *Plant Physiology* **152**: 96–106.

Kessler A, Halitschke R, Baldwin IT. 2004. Silencing the jasmonate cascade: induced plant defenses and insect populations. *Science* **305**: 665–668.

Kistner C, Matamoros M. 2005. RNA isolation using phase extraction and LiCl precipitation. In: Márquez A, ed. *Lotus japonicus handbook*. Dordrecht, the Netherlands: Springer, 123–124.

Krügel T, Lim M, Gase K, Halitschke R, Baldwin IT. 2002. *Agrobacterium*-mediated transformation of *Nicotiana attenuata*, a model ecological expression system. *Chemoecology* **12**: 177–183.

Loeffler C, Berger S, Guy A, Durand T, Bringmann G, Dreyer M, von Rad U, Durner J, Mueller MJ. 2005. B1-phytoprostanes trigger plant defense and detoxification responses. *Plant Physiology* **137**: 328–340.

Matsui K. 2006. Green leaf volatiles: hydroperoxide lyase pathway of oxylipin metabolism. *Current Opinion in Plant Biology* **9**: 274–280.

Meyer AJ, Hell R. 2005. Glutathione homeostasis and redox-regulation by sulfhydryl groups. *Photosynthesis Research* **86**: 435–457.

Mosblech A, Feussner I, Heilmann I. 2009. Oxylipins: structurally diverse metabolites from fatty acid oxidation. *Plant Physiology and Biochemistry* **47**: 511–517.

Mueller MJ. 2004. Archetype signals in plants: the phytoprostanes. *Current Opinion in Plant Biology* **7**: 441–448.

Mueller MJ, Berger S. 2009. Reactive electrophilic oxylipins: pattern recognition and signalling. *Phytochemistry* **70**: 1511–1521.

Mueller S, Hilbert B, Dueckershoff K, Roitsch T, Krischke M, Mueller MJ, Berger S. 2008. General detoxification and stress responses are

mediated by oxidized lipids through TGA transcription factors in Arabidopsis. *Plant Cell* **20**: 768–785.

Mukhtarova LS, Mukhitova FK, Gogolev YV, Grechkin AN. 2011. Hydroperoxide lyase cascade in pea seedlings: non-volatile oxylipins and their age and stress dependent alterations. *Phytochemistry* **72**: 356–364.

Mullineaux PM, Rausch T. 2005. Glutathione, photosynthesis and the redox regulation of stress-responsive gene expression. *Photosynthesis Research* **86**: 459–474.

Niu Y, Figueroa P, Browse J. 2011. Characterization of JAZ-interacting bHLH transcription factors that regulate jasmonate responses in Arabidopsis. *Journal of Experimental Botany* **62**: 2143–2154.

Noordermeer MA, Feussner I, Kolbe A, Veldink GA, Vliegenthart JFG. 2000. Oxygenation of (3Z)-alkenals to 4-hydroxy-(2E)-alkenals in plant extracts: a nonenzymatic process. *Biochemical and Biophysical Research Communications* **277**: 112–116.

Ogawa K. 2005. Glutathione-associated regulation of plant growth and stress responses. *Antioxidants & Redox Signaling* **7**: 973–981.

Prost I, Dhondt S, Rothe G, Vicente J, Rodriguez MJ, Kift N, Carbonne F, Griffiths G, Esquerre-Tugaye MT, Rosahl S *et al.* 2005. Evaluation of the antimicrobial activities of plant oxylipins supports their involvement in defense against pathogens. *Plant Physiology* **139**: 1902–1913.

Taki N, Sasaki-Sekimoto Y, Obayashi T, Kikuta A, Kobayashi K, Ainai T, Yagi K, Sakurai N, Suzuki H, Masuda T *et al.* 2005. 12-oxo-phytodienoic acid triggers expression of a distinct set of genes and plays a role in wound-induced gene expression in Arabidopsis. *Plant Physiology* **139**: 1268–1283.

Turner JG, Ellis C, Devoto A. 2002. The jasmonate signal pathway. *Plant Cell* **14**: S153–S164.

Tusher VG, Tibshirani R, Chu G. 2001. Significance analysis of microarrays applied to the ionizing radiation response. *Proceedings of the National Academy of Sciences, USA* **98**: 5116–5121.

Uchida K. 2003. 4-Hydroxy-2-nonenal: a product and mediator of oxidative stress. *Journal of Chemical Ecology* **42**: 318–343.

Vandoorn A, Kallenbach M, Borquez AA, Baldwin IT, Bonaventure G. 2010. Rapid modification of the insect elicitor N-linolenoyl-glutamate via a lipoxygenase-mediated mechanism on *Nicotiana attenuata* leaves. *BMC Plant Biology* **10**: 164.

Vick BA, Zimmerman DC. 1976. Lipoxygenase and hydroperoxide lyase in germinating watermelon seedlings. *Plant Physiology* **57**: 780–788.

Vollenweider S, Weber H, Stolz S, Chetelat A, Farmer EE. 2000. Fatty acid ketodienes and fatty acid ketotrienes: Michael addition acceptors that accumulate in wounded and diseased Arabidopsis leaves. *Plant Journal* **24**: 467–476.

Weber H, Chetelat A, Reymond P, Farmer EE. 2004. Selective and powerful stress gene expression in Arabidopsis in response to malondialdehyde. *Plant Journal* **37**: 877–888.

Wittenberg G, Danon A. 2008. Disulfide bond formation in chloroplasts. *Plant Science* **175**: 459–466.

Zimmerman DC, Coudron CA. 1979. Identification of traumatin, a wound hormone, as 12-oxo-trans-10-dodecenoic acid. *Plant Physiology* **63**: 536–541.

Supporting Information

Additional supporting information may be found in the online version of this article.

Fig. S1 Auto-oxidation of (9Z)-traumatin *in vitro*.

Fig. S2 Determination of the linearity and limit of detection of C_{12} metabolites.

Fig. S3 Accumulation of C_{12} derivatives in leaves of wild-type (WT), ir-lox2 and ir-hpl plants after wounding and fatty acid–amino acid conjugate (FAC) elicitation.

Fig. S4 Calibration curves for C_{12} standards.

Fig. S5 Quantification of *Nicotiana attenuata* hydroperoxide lyase (*NaHPL*) mRNA levels in wild-type (WT) and ir-hpl plants.

Fig. S6 Southern blot analysis of ir-hpl plants.

Table S1 Parameters used for detection of C_{12} molecules by liquid chromatography–mass spectrometry/mass spectrometry (LC-MS/MS)

Table S2 Parameters used for quantification of C_{12} molecules by liquid chromatography–mass spectrometry/mass spectrometry (LC-MS/MS)

Table S3 Complete list of genes changing expression in wounded leaves of ir-lox2/ir-lox3 plants after treatment with 9Z-traumatin : 9-OH-traumatin (1 : 1)

Table S4 Analysis of C_6 volatiles emitted by wild-type (WT) and ir-hpl plants

Methods S1 Characterization of ir-hpl plants.

Please note: Wiley-Blackwell are not responsible for the content or functionality of any supporting information supplied by the authors. Any queries (other than missing material) should be directed to the *New Phytologist* Central Office.

Table S1. Parameters used for detection of C_{12} molecules by LC-MS/MS

Reference	Compound	Capillary CID (V)	Transition [M-H]-		[M-X]-	Collison energy (V)	Retention time (min)
IS	10-OH-(2E)-decenoic acid (IS)	-35	185	>	139	15	9.9
1a	12-oxo-(9Z)-dodecenoic acid	-35	211	>	183	13.5	16.5
1b	12-oxo-(10E)-dodecenoic acid	-35	211	>	183	13.5	15.5
2a	12-OH-(9Z)-dodecenoic acid	-35	213	>	183	15.5	17.4
2b	12-OH-(10E)-dodecenoic acid	-35	213	>	183	15.5	15.5
3a	(3Z)-dodecenedioic acid	-35	227	>	183	13	18.1
3b	(2E)-dodecenedioic acid	-35	227	>	183	13	15.9
4	9-OH-12-oxo-(11E)-dodecenoic acid	-35	227	>	209	9.5	9.2

Table S2. Parameters used for quantification of C_{12} molecules by LC-MS/MS

Reference	Compound	Capillary CID (V)	Transitions [M-H]-		[M-X]-	Collison energy (V)	Retention time (min)	LoD (ng on column)
IS	10-OH-(2E)-decenoic acid (IS)	-35	185	>	139	15	11.05	0.36
1a	12-oxo-(9Z)-dodecenoic acid	-35	211	>	183	13.5	11.73	1.08
2a	12-OH-(9Z)-dodecenoic acid	-35	213	>	183	15.5	11.73	1.08
3a,b	(2E)- and (3Z)-dodecenedioic acids	-35	227	>	183	13	11.95	0.82
4	9-OH-12-oxo-(11E)-dodecenoic acid	-35	227	>	209	9.5	10.82	0.84
5	4-OH-(2E)-dodecenedioic acid	-35	243	>	225	9.5	n.d.	
6	9,12-OH-(10E)-dodecenoic acid	-35	229	>	211	9.5	n.d.	
7	9,12-OH-(10E)-dodecanoic acid	-35	231	>	213	9.5	n.d.	
8	9-OH-traumatin-GSH adduct	-35	534	>	306	16.5	10.16	0.92

n.d., not detected
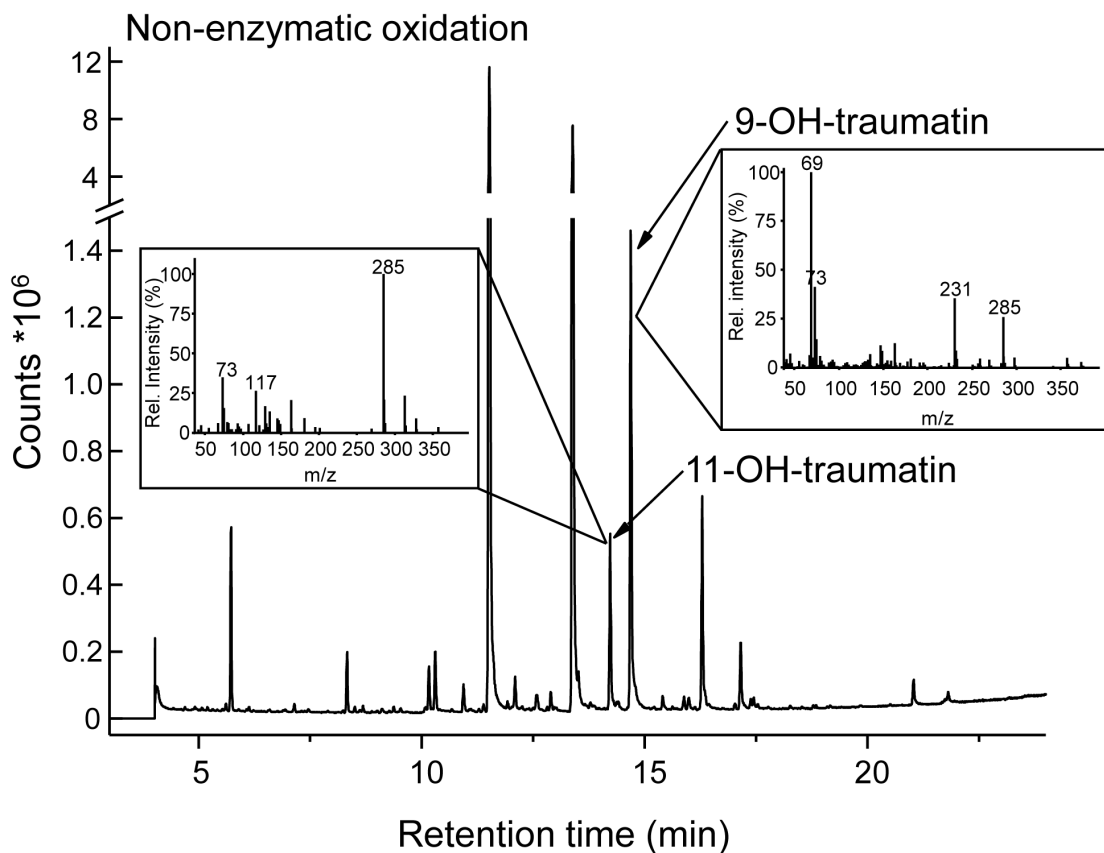
Figure S1. Auto-oxidation of (9*Z*)-traumatin *in vitro*
A solution of (9*Z*)-traumatin in methanol was air-dried at room temperature for 2 hours. After reconstituting the sample in methanol, the products were reduced with excess $NaBH_4$ and derivatized with diazomethane and MSTFA. The derivatized products were analyzed by GC-MS. Formation of 9-OH-traumatin and 11-OH-traumatin as auto-oxidation products was detected, consistently with Noordermeer *et al* (2000).

10-Hydroxy-(2*E*)-decenoic acid

$y= 5.74*10^6x + 7.55*10^5$
$r= 0.9993$
LoD: 0.36 ng

Area *10^7

(9*Z*)-traumatin

$y= 4.99*10^7x + 4.08*10^6$
$r= 0.9922$
LoD: 1.08 ng

Area *10^8

12-OH-(9*Z*)-dodecenoic acid

$y= 5.17*10^7+4.36*10^6$
$r= 0.9944$
LoD: 0.92 ng

Area *10^8

(2*E*)-traumatic acid

$y= 1.81*10^8x + 1.74*10^7$
$r= 0.9955$
LoD: 0.82 ng

Area *10^9

9-OH-Traumatin

$y= 2.30*10^7x + 4.58*10^6$
$r= 0.9953$
LoD: 0.84 ng

Area *10^8

amount (ng in column)

9-OH-Traumatin-GSH conjugate

$y= 5.56*10^6x + 1.22*10^6$
$r= 0.9943$
LoD: 0.92 ng

Area *10^7

amount (ng in column)

Figure S2. Determination of the linearity and limit of detection (LoD) for C$_{12}$ metabolites. Commercial standards and synthetic compounds were spiked at different concentrations in leaf-derived matrix obtained from ir-lox2 plants. Samples were analyzed by LC-MS/MS in the negative MRM mode and the peak areas corresponding to each analyte were integrated and plotted against the amount of analyte injected in the column (ng in column).

A

B
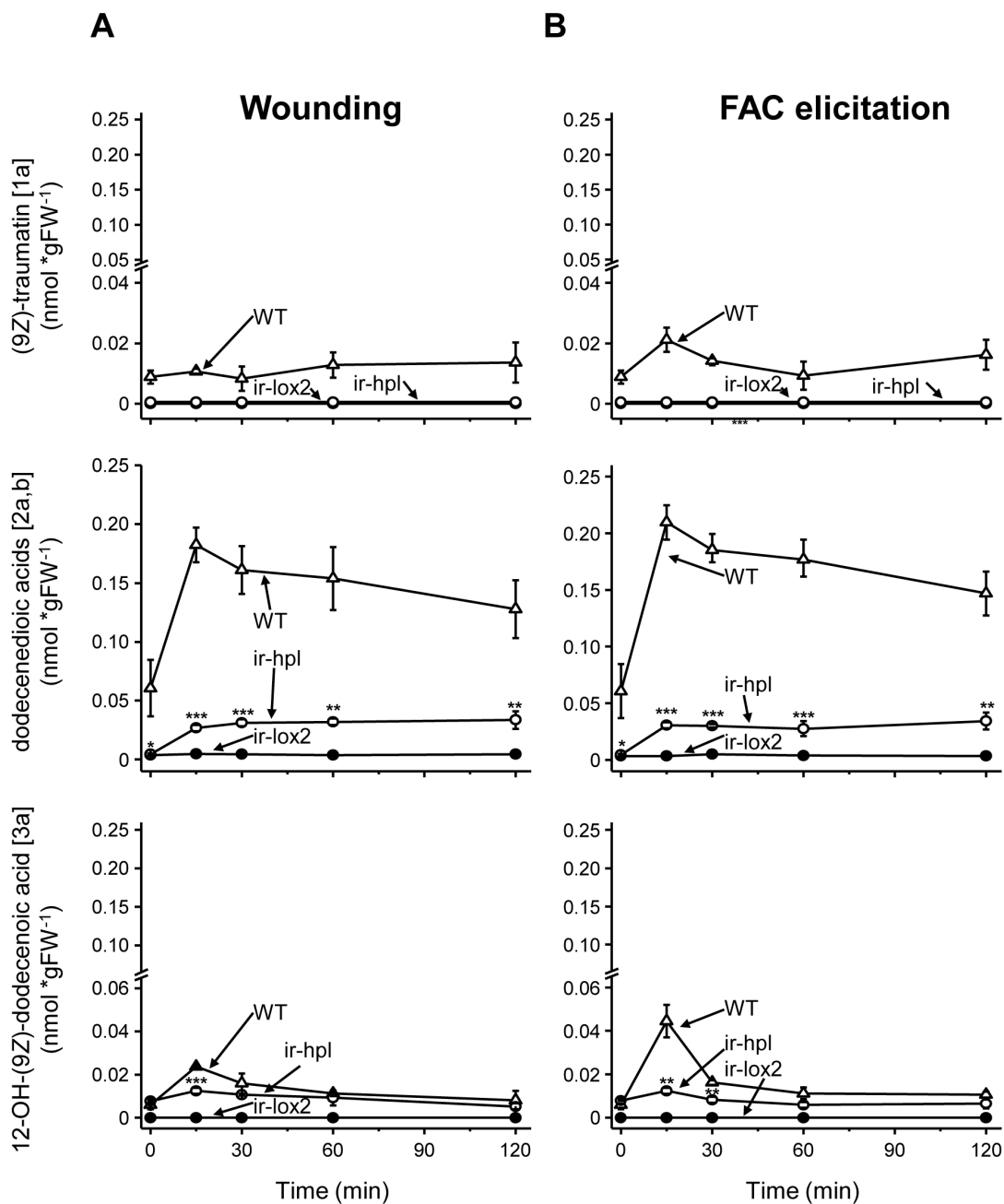
Figure S3. Accumulation of C_{12} derivatives in leaves of WT, ir-lox2 and ir-hpl plants after wounding and FAC elicitation

Leaves from WT, ir-lox2 and ir-hpl plants were either wounded with a fabric pattern wheel (**a**) or wounded plus the addition of 18:3-Glu (**b**; FAC elicitation). Leaf samples were harvested at different times, extracted and the amounts of C_{12} derivatives were quantified by LC-MS/MS (*: $P < 0.05$, **: $P < 0.01$, ***: $P < 0.001$, Student's t-test (WT vs transgenic line at same time point), $n=3$, bars indicate SE).
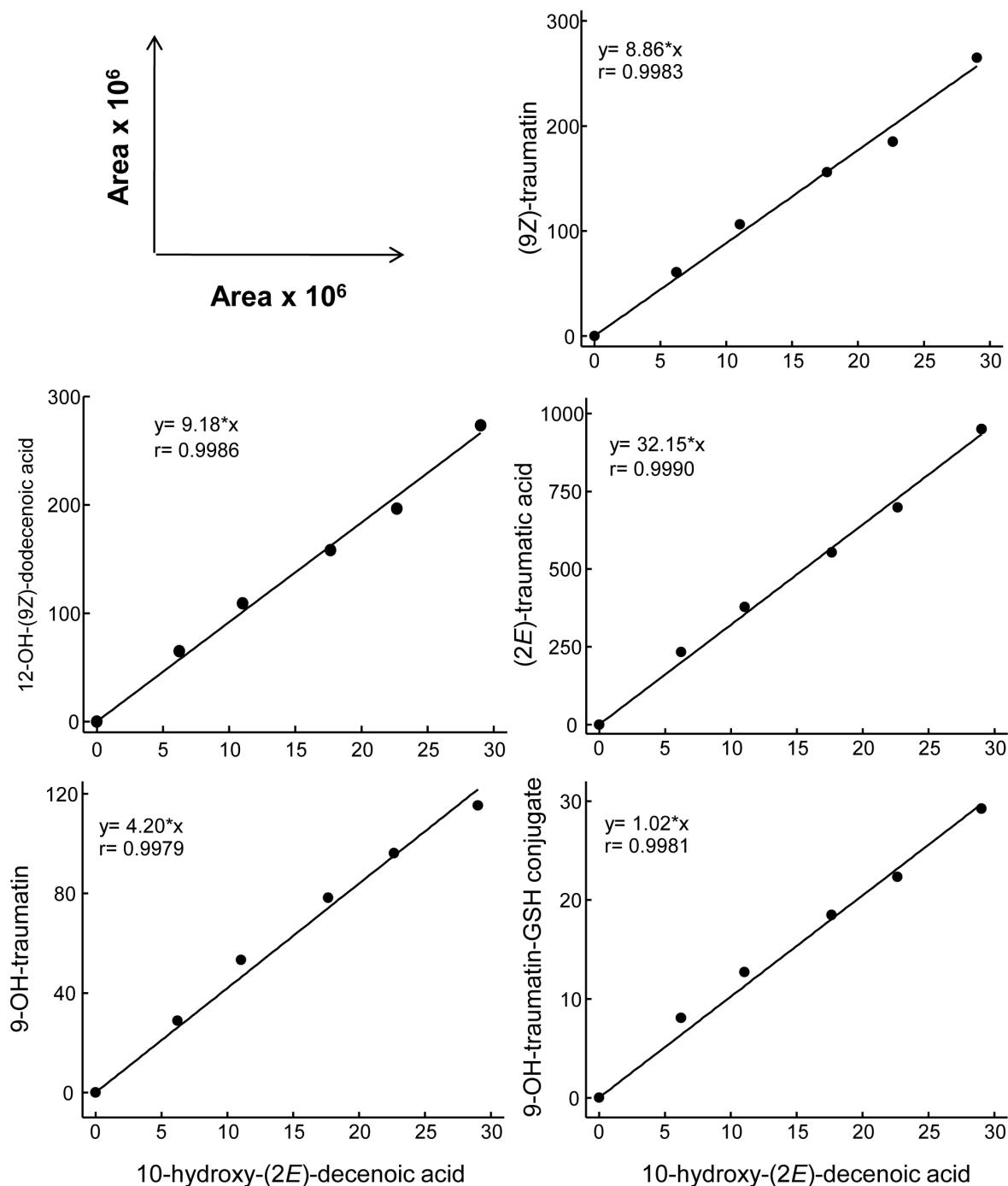
Figure S4. Calibration curves for C$_{12}$ standards.
Different amounts of C$_{12}$ standards were spiked in leaf extracts (matrix) from ir-lox2 plants and analyzed by LC-MS/MS using the parameters described in Material and Methods. Units in the Y and X axis are peak areas (x 10^6).

Appendix S1. Characterization of ir-hpl plants

Materials and Methods

Generation of transgenic ir-hpl lines

Transgenic *N. attenuata* (ir-hpl) plants reduced in the expression of NaHPL were generated via leaf disc *Agrobacterium*-mediated transformation and seedling regeneration as previously described (Krügel *et al*., 2002). The binary vector used for plant transformation was pSOL3 (Bubner et al., 2006) engineered to carry a fragment of the NaHPL cDNA (GenBank accession: AJ414400) subcloned in inverted repeat orientation (vector pSOL3HPL). T_1 transformed plants were analyzed by quantification of Na*HPL* mRNA levels by real-time quantitaive PCR in unelicited leaves and in leaves elicited with *Manduca sexta* oral secretions (OS) and for T-DNA single insertion by Southern blot hybridization (see below). Segregation analysis of hygromycin resistance in T_2 seedlings was performed on agar plates supplemented with hygromycin (0.025 mg mL^{-1}). Two lines, ir-hpl 425-4 (425) and 428-8 (428) showed the lowest levels of Na*HPL* mRNA accumulation (Figure AS1) and had a single T-DNA insertion in their genomes (Figure AS2).

For Southern blot analysis, genomic DNA of the WT and ir-hpl lines was isolated by the cetyltrimethylammonium bromide (CTAB) method. DNA samples (10 µg) were digested with EcoRV overnight at 37 C according to commercial instructions and separated on a 0.8% (w/v) agarose gel using standard conditions. DNA was blotted onto Gene Screen Plus Hybridisation Transfer membranes (Perkin Elmer Life and Analytical Sciences, Boston, MA, USA) using the capillary transfer method. A gene-specific probe for the hygromycin resistance gene *hptII* was generated by PCR using the primer pairs HYG1-18 (5′-CCGGATCGGACGATTGCG-3′) and HYG3-20 (5′-CGTCTGTCGAGAAGTTTCTG-3′). The probe was labeled with [α-^{32}P]dCTP (Perkin Elmer) using the Rediprime II kit (Amersham Pharmacia) according to commercial instruction.

Plant treatments

Leaf wounding was performed by rolling three times a fabric pattern wheel on each side of the midvein of 40-day-old rosette stage plants. For a wounding + water (w+w) treatment, 20 µL of deionized water were immediately pipetted onto the wounded leaf. For a wounding + oral secretions (w+OS) treatment, 20 µL of *Manduca sexta* oral secretion (diluted 1:3 in water, v/v) was applied to the wounds. Samples from untreated plants were used as controls.

Volatile collection and analysis

      Single leaves (+1 position) of wild type and ir-hpl plants (n=6 per genotype and treatment) were enclosed immediately after treatment between two 50 mL food-quality plastic containers (Huhtamaki, Bad Bertricher, Germany) secured with miniature claw-style hair clips. Ambient air was pulled through the collection chamber and a glass tube (ARS, Inc., Gainsville, FL, USA) packed with glass wool and 20 mg of Super Q (Alltech, Düsseldorf, Germany). Airflow was created by a vacuum pump (model DAA-V114-GB; Gast Mfg; Benton Harbour, MI, USA) at ~200 mL min^{-1}. SuperQ traps were eluted with 250 µL dichloromethane into a GC vial containing a glass insert after spiking each trap with 400 ng tetralin (Sigma-Aldrich, Germany) as an internal standard. Samples were analyzed on an Agilent 6890N gas chromatograph equipped with an Agilent 7683 autoinjector (Agilent Technologies, Böblingen, Germany) and coupled with a LECO Pegasus III time-of-flight mass spectrometer with a 4D thermal modulator upgrade (LECO, Mönchengladbach, Germany) as described by Gaquerel et al. (2009). GLVs were identified and quantified using standard solutions of (3Z)-hexenal, (2E)-hexenal, (3Z)-hexenol, (2E)-hexenol, (3Z)-hexenyl-acetate, (2E)-hexenyl-acetate, (3Z)-hexenyl-propanoate, (3Z)-hexenyl-butanoate, (2E)-hexenyl-butanoate (Sigma-Aldrich , Germany) and (2E)-hexenyl -propanoate (Bedoukian Research Inc, Danbury, USA).

Quantitative real-time PCR assay

      Total RNA was extracted from single leaves (+2 position) of WT and ir-hpl plants with TRI Reagent (Sigma-Aldrich, Germany) according to the manufacturer's instruction. Reverse transcription of 1µg of total RNA was performed using SuperScript II Reverse Transcriptase (Invitrogen, Germany) and a poly-T primer. Quantitative real-time PCR (ABI PRISM™7000, Applied Biosystems, Foster City, CA, USA) was conducted with 40 ng cDNA using the qPCR™ core reagent kit (Eurogentec, Köln, Germany) and NaHPL-specific primer pairs (FP: 5' CACTTAGACTTAGTCCACCTGTGC 3', RP: 5' AACACAAACTTTTCAGGATCATCA 3'). The PCR products were detected by gene-specific double fluorescent dye-labeled TaqMan® probes (Probe: 5' TCAGCCATTGGTAATGAGAGATCCAAAGG 3'). For calibration we used a duplicated dilution series of cDNAs which had been transcribed from induced RNA samples of the same experiment and calculated the relative transcript abundance by efficiency-correcting for each primer pair and normalizing to the *N. attenuata* actin gene (FP: 5' GGTCGTACCACCGGTATTGTG 3', RP: 5' GTCAAGACGGAGAATGGCATG 3', Probe: 5' TCAGCCACACCGTCCCAATTTATGAGG 3').

Supplemental References

Krügel T, Lim M, Gase K, Halitschke R, Baldwin IT (2002) Agrobacterium-mediated transformation of Nicotiana attenuata, a model ecological expression system. Chemoecology 12: 177-18:3

Gaquerel E, Weinhold A, Baldwin IT (2009) Molecular interactions between the specialist herbivore Manduca sexta (Lepidoptera, Sphigidae) and its natural host Nicotiana attenuata. VIII. An unbiased GCxGC-ToFMS analysis of the plant's elicited volatile emissions. Plant Physiol 149:1408-1423
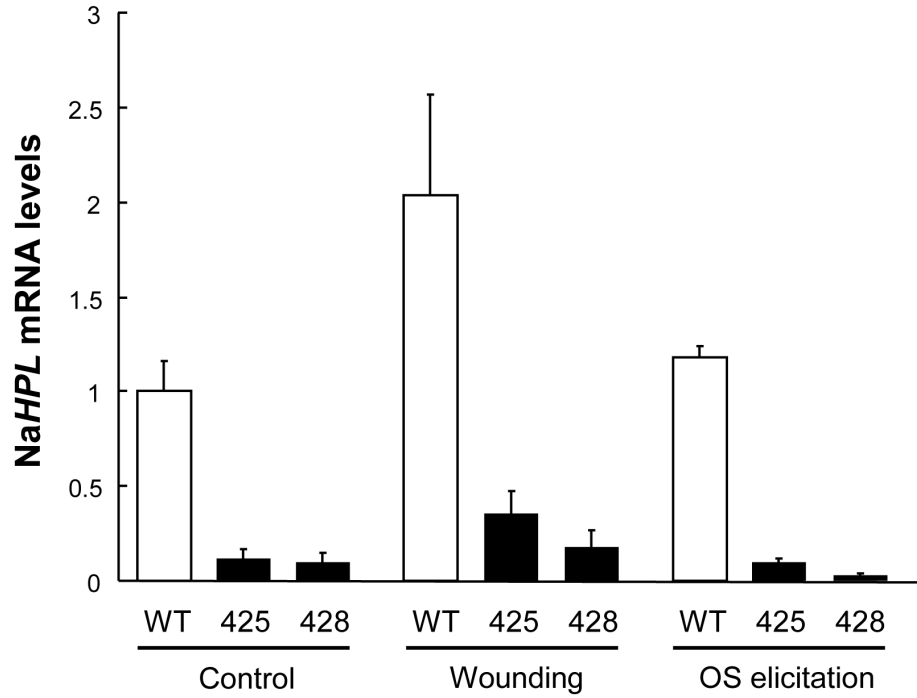
Figure AS1. Quantification of Na*HPL* mRNA levels in WT and ir-hpl plants
Total RNA was extracted from leaves of either WT or ir-hpl (lines 425 and 428) plants before (control) and 45 min after wounding and OS elicitation. The abundance of Na*HPL* transcripts was analyzed by qPCR using Na*Actin* mRNA as a reference. Na*HPL* mRNA levels represent the relative levels to the reference gene (Bars represent +/- SE, *n*=5).
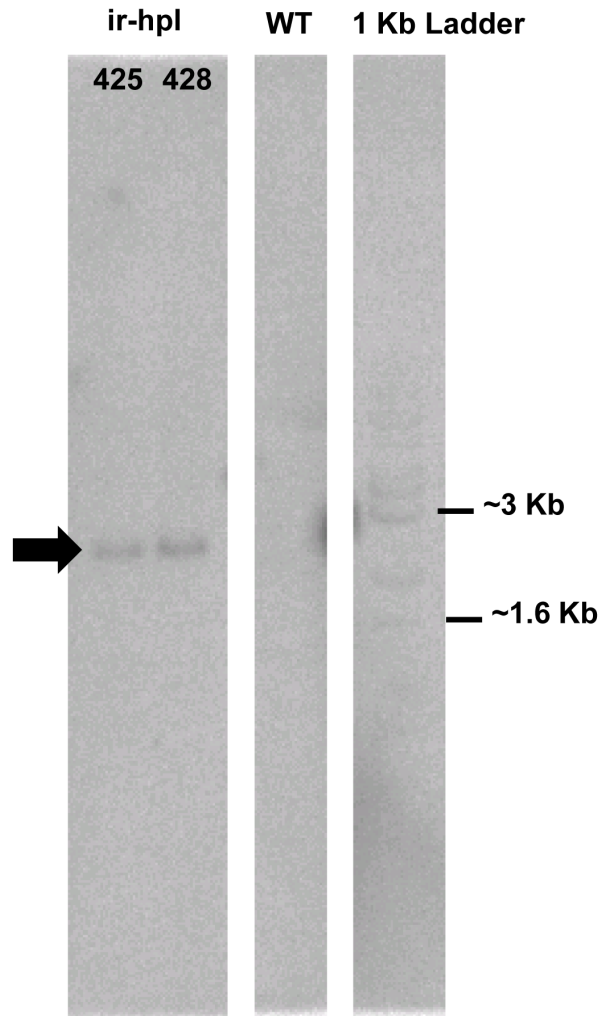
Figure AS2. Southern blot analysis of ir-hpl plants
Genomic DNA was isolated from WT and ir-hpl (lines 425 and 428) plants, digested with EcoRV and separated by agarose-gel electrophoresis using standard conditions (see Appendix S1 for methodological details). A gene-specific probe corresponding to the hygromycin resistance gene (*hptII*) was labeled with [α-^{32}P]dCTP and used for hybriditazion. The arrow points to the single T-DNA insertions in ir-hpl lines.

Table AS1. Analysis of C$_6$ volatiles emitted by WT and ir-hpl plants (*n*=6, +/- SE).

Treatment	class	Volatile	RT (s)		Relative VOC released	
			RT1	RT2	WT	irhpl (428)
Control	aldehyde	(3Z)-hexenal	174	1.93	**0.01** ± 0.005	**0.01** ± 0.002
		(2E)-hexenal	246	2.90	**0.02** ± 0.013	**n.d.**
	alcohole	(3Z)-hexenol	246	2.58	**0.24** ± 0.189	**0.02** ± 0.003
		(2E)-hexenol	270	2.73	**0.10** ± 0.091	**n.d.**
	hexenyl-ester	(3Z)-hexenyl acetate	570	2.89	**0.04** ± 0.034	**n.d.**
		(2E)-hexenyl acetate	594	2.95	**n.d.**	**n.d.**
		(3Z)-hexenyl propionate	756	2.78	**0.01** ± 0.005	**n.d.**
		(2E)-hexenyl propionate	774	2.82	**n.d.**	**n.d.**
		(3Z)-hexenyl butyrate	912	2.64	**0.03** ± 0.025	**n.d.**
		(2E)-hexenyl butyrate	930	2.70	**n.d.**	**n.d.**
	Total				**0.44** ± **0.368**	**0.03** ± **0.005**
Wounding	aldehyde	(3Z)-hexenal	174	1.93	**4.40** ± 0.592	**2.05** ± 0.371
		(2E)-hexenal	246	2.90	**1.39** ± 0.338	**0.51** ± 0.090
	alcohole	(3Z)-hexenol	246	2.58	**6.77** ± 0.495	**4.52** ± 0.729
		(2E)-hexenol	270	2.73	**3.82** ± 0.538	**1.38** ± 0.283
	hexenyl-ester	(3Z)-hexenyl acetate	570	2.89	**0.36** ± 0.034	**0.23** ± 0.042
		(2E)-hexenyl acetate	594	2.95	**0.03** ± 0.005	**0.01** ± 0.002
		(3Z)-hexenyl propionate	756	2.78	**0.03** ± 0.006	**0.03** ± 0.005
		(2E)-hexenyl propionate	774	2.82	**n.d.**	**n.d.**
		(3Z)-hexenyl butyrate	912	2.64	**0.16** ± 0.012	**0.09** ± 0.013
		(2E)-hexenyl butyrate	930	2.70	**0.02** ± 0.003	**0.01** ± 0.003
	Total				**16.99** ± **2.023**	**8.84** ± **1.539**
OS-elicitation	aldehyde	(3Z)-hexenal	174	1.93	**1.67** ± 0.417	**0.58** ± 0.089
		(2E)-hexenal	246	2.90	**2.65** ± 0.356	**1.18** ± 0.133
	alcohole	(3Z)-hexenol	246	2.58	**4.04** ± 0.629	**2.49** ± 0.207
		(2E)-hexenol	270	2.73	**5.24** ± 0.714	**2.78** ± 0.172
	hexenyl-ester	(3Z)-hexenyl acetate	570	2.89	**0.19** ± 0.031	**0.13** ± 0.022
		(2E)-hexenyl acetate	594	2.95	**0.05** ± 0.006	**0.03** ± 0.002
		(3Z)-hexenyl propionate	756	2.78	**0.03** ± 0.006	**0.03** ± 0.009
		(2E)-hexenyl propionate	774	2.82	**0.01** ± 0.001	**n.d.**
		(3Z)-hexenyl butyrate	912	2.64	**0.08** ± 0.012	**0.08** ± 0.034
		(2E)-hexenyl butyrate	930	2.70	**0.04** ± 0.005	**0.02** ± 0.006
	Total				**14.00** ± **2.179**	**7.32** ± **0.675**

Summary and Synthesis

During the 400 million-year-long history in which plants and phytophagous herbivores have co-evolved (Labandeira, 2007), both, plants and insects developed sophisticated mechanisms to recognize one another and respond accordingly. Plants have evolved mechanisms to recognize and respond to insect feeding by the perception of components present in insect oral secretions (OS), while insects have evolved mechanisms to detoxify a wide range of plant secondary metabolites. Many plant defense mechanisms are specifically induced in response to herbivory and tightly regulated by plant signaling molecules such as jasmonates, salicylic acid, abscisic acid and ethylene (Fujita et al. 2006) which are rapidly produced in response to biotic stress.

The wild tobacco *Nicotiana attenuata* responds strongly and specifically to insect attack from different feeding guilds. For example, during attack by the specialist herbivore *Manduca sexta*, the plant recognizes fatty acid amino acid conjugates (FACs), present in the insect's OS (Halitschke et al., 2001). The major FAC in *M. sexta* OS is the conjugate of α–linolenic acid and glutamic acid (18:3-Glu). In Chapter 3 we demonstrated that 18:3-Glu is rapidly oxidized by the activity of a lipoxygenase (LOX) to form additional active and inactive elicitors (Fig. 8.1). In particular, 13-oxo-13:2-Glu was an active elicitor which enhanced the biosynthesis of the phytohormone jasmonic acid (JA) and the differential emission of two monoterpenes. Metabolism of 18:3-Glu and the formation of the LOX product 13-OOH-18:3-Glu occurred within seconds; after approximately 2 min of contact with wounded leaf tissue, more than half of the applied 18:3-Glu was metabolized by LOX activity. Experiments with plants silenced in the expression of Na*LOX2* and Na*LOX3*, two LOX isoforms in *N. attenuata*, revealed that Na*LOX2* most likely catalyzes the oxidation of 18:3-Glu (Fig. 8.1). 18:3-Glu was not metabolized when applied to non-wounded leaf tissue. This suggested that cell disruption is required to bring LOX enzymes into contact with 18:3-Glu. Altogether, this study suggests a degree of specificity in the responses elicited by modified forms of 18:3-Glu, and raises the possibility that the metabolism of 18:3-Glu may play a role in the tuning of some plant defense or tolerance responses to insect herbivores.
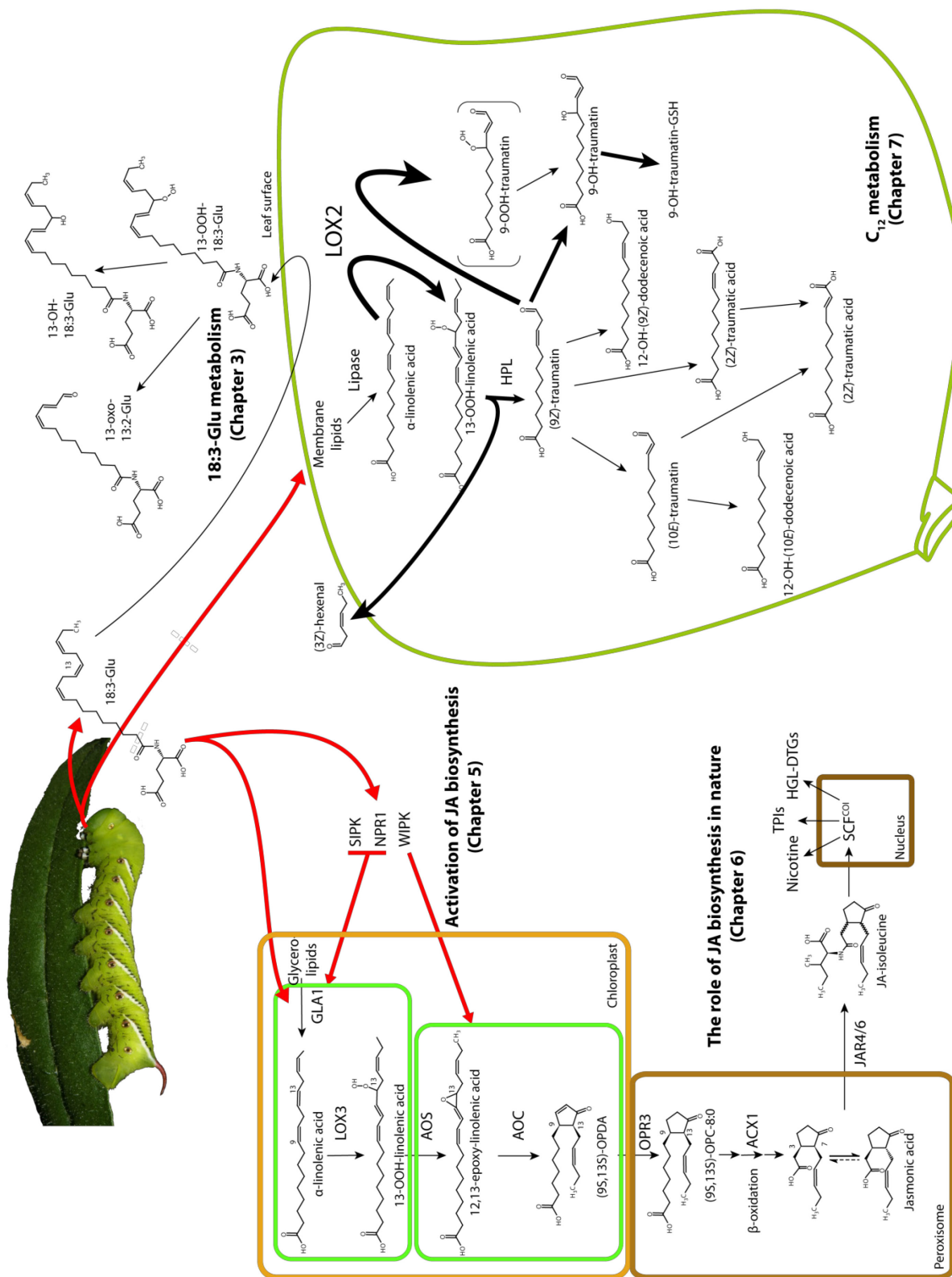
Figure 8.1: Activation and regulation of oxylipin signaling pathways in *N. attenuata* in response to herbivory. When *Manduca sexta* feeds on *Nicotiana attenuata*, the plant perceives fatty acid-amino acid conjugates like 18:3-Glu present in the insect's oral secretions. After contact with wounded leaf tissue, 18:3-Glu is rapidly modified into active and inactive metabolites catalyzed by LOX2 (Chapter 3). This metabolism of 18:3-Glu may play a role in the fine tuning of plant responses to insect herbivory. In response to herbivory, the plant induces the jasmonic acid biosynthesis. Here, 18:3-Glu together with the regulatory factors salicylate induced protein kinase (SIPK) and nonexpressor of PR-1 (NPR1) affect JA biosynthesis by enhancing the supply of α-linolenic acid through GLA1 whereas wound induced protein kinase (WIPK) affect basal allene oxide synthase (AOS) activity (Chapter 5). After stimulus, the produced JA is conjugated to isoleucine by JASMONATE RESISTANT 4 and 6 (JAR4/6) to form JA-Ile. JA-Ile binds to SCF^{COI} which participates in the activation of defense response against insect herbivores. The plants' capacity to mediate this JA signaling is essential to survive in nature (Chapter 6). Besides the activation of JA biosynthesis, leaf wounding and insect herbivory does also results in the generation of green leaf volatiles such as (3*Z*)-hexenal and C_{12} molecules such as (9*Z*)-traumatin through the cleavage of *e.g.* 13-OOH-18:3 by hydroperoxy lyase (HPL). 98% of the (9*Z*)-traumatin formed is converted into 9-OH-traumatin: two-thirds by product recycling through LOX2 and one-third by non-enzymatic oxidation. Approximately 40% of the de novo produced 9-OH-traumatin is conjugated to glutathione, consistent with this oxylipin being a reactive electrophile species (Chapter 7).

The biosynthesis of JA and its derivatives is induced within minutes after perception of wounding and herbivore elicitors (Glauser et al., 2008). These jasmonates function as signal molecules mediating plant's anti-herbivore responses. In *N. attenuata*, a strong transient burst of JA occurs within one hour after herbivore attack (Halitschke et al., 2001; Howe and Jander, 2008; Schmelz et al., 2009; Stork et al., 2009). To understand how the induction of JA biosynthesis is activated in response to wounding and herbivory, I developed a simple, rapid, specific and sensitive method for the simultaneous detection and quantification of intermediates of the JA biosynthesis pathway which are either free aliphatic molecules or small polar molecules containing free carboxyl groups (Chapter 4). I used the advantages of derivatization of free carboxyl groups in a two-step reaction with 1,1'-carbonyldiimidazole and 3-(hydroxymethyl)-pyridine. The first step formed a reactive carbimidazol amide within 1 min at room temperature. This amide was quantitatively converted into a β-picolinyl ester within 10 min at 37° C. These mild conditions allowed for the derivatization and analysis of labile signaling molecules. Furthermore, the reaction did not affect esterified carboxy groups (Christie, 2003) and could therefore be performed with crude leaf extracts. When the β-picolinyl esters were analyzed by liquid-

chromatography-electrospray ionization-mass spectrometry (LC-ESI-MS), all derivatized molecules gave a specific 3-picoline fragment ion with a mass to charge ratio (m/z) of 92 in the positive ionization mode. This fragment ion can was used to create specific transitions of the $[M+H]^+$ molecular ion to the 3-picoline moiety in multi-reaction-monitoring (MRM) mode. I tested and validated this method for 26 compounds including precursors and intermediates of JA biosynthesis such as free fatty acids and other plant signaling molecules.

The sensitive and quantitative analysis of JA biosynthesis intermediates allowed for the study of early regulatory factors that affect JA production upon insect herbivory. It has been shown that two mitogen-activated protein kinases (salicylate-induced protein kinase, SIPK, and wound-induced protein kinase, WIPK; Wu et al., 2007), and a regulatory component of the salicylic acid pathway (nonexpressor of PR-1, NPR1; Rayapuram and Baldwin, 2007) can affect the accumulation of JA in *N. attenuata*. However, it was not known how these regulators affect JA biosynthesis. I demonstrated how FAC elicitation and SIPK, WIPK, and NPR1 participate in mechanisms affecting early enzymatic steps of the JA biosynthesis pathway in *N. attenuata* (Chapter 5). I also investigated the effects of *CORONATINE INSENSITIVE1* (*COI1*) which participates in JA perception and is one of the best-characterized genes mediating downstream JA responses (Kazan and Manners, 2008; Browse, 2009). I used lines silenced in the expression of these four genes (ir-*sipk*, ir-*wipk*, ir-*npr1* and ir-*coi1*) and analyzed changes in the levels of substrates and intermediates of the JA biosynthesis pathway within 10 minutes after induction by simulated herbivory (leaf wounding and FAC elicitation). In the course of this study, a plastidial glycerolipase of the lipase A_1-I family (GLA1) essential for JA biosynthesis in *N. attenuata* (Fig 8.1) was identified. I showed that the levels of major membrane lipids did not change significantly within 10 min after simulated herbivory. Furthermore, I showed that total levels of free fatty acids (FFA) in wild-type (WT) *N. attenuata* plants did not significantly change within this period after wounding or FAC elicitation. This was consistent with data from plants silenced in GLA1 expression, in which FFA levels also did not significantly change within 10 min after stimulus. Together, the results suggested a rapid and channeled supply of 18:3 for JA biosynthesis. FFA levels were not affected by silencing *WIPK*; however, the levels of all unsaturated FFA were reduced in ir-*sipk*, ir-

npr1 and ir-*coi1* plants, suggesting a general alteration in FFA homeostasis in these plants. In contrast to FFA levels, 13-hydroperoxy-18:3 (13-OOH-18:3) levels increased linearly within 5 min after wounding, and FAC application amplified this increase. FAC elicitation did not increase 13-LOX activity or protein levels compared to unelicited plant tissue, which suggested that FAC elicitation enhances the supply of 18:3 by differential activation of GLA1. In ir-*wipk* plants, the kinetic of 13-OOH-18:3 was similar to WT upon wounding and FAC elicitation; however, in ir-*sipk* and ir-*npr1* plants levels of 13-OOH-18:3 were strongly reduced independently of reduced 13-LOX activity or protein levels. Therefore, the data indicated that the supply of 18:3 via GLA1 is one step in JA biosynthesis activated by SIPK and NPR1 (Fig 8.1). Compared to 13-LOX activity, allene oxide synthase (AOS) activity was reduced in ir-*sipk*, ir-*npr1*, ir-*coi1* as well as in ir-*wipk* plants, accompanied by a strong reduction of ($9S,13S$)-12-oxo-phytodienoic acid (OPDA) accumulation compared to WT after wounding and FAC elicitation. That these lines had similar levels of AOS mRNA compared to WT plants suggested altered posttranslational modification of AOS. WIPK-mediated mechanisms may affect basal AOS activity, which may in turn limit OPDA accumulation after elicitation (Fig 8.1). In summary, I demonstrate that signal transduction mechanisms involving SIPK, WIPK, NPR1, and the insect elicitor 18:3-Glu affect different early JA biosynthetic steps.

The activation of JA biosynthesis after herbivore attack is essential for *N. attenuata* to survive in nature. After induction, JA is conjugated to isoleucine by JASMONATE RESISTANT (JAR) to form JA-Ile (Suza and Staswick, 2008; Wang et al., 2007). JA-Ile binds to SCF^{COI} and activates the SCF^{COI} complex to mark the JAZ repressors of gene transcription for degradation. This de-represses genes involved in the biosynthesis of defense molecules, among other responses, thus activating defense (Chini et al., 2007; Thines et al., 2007). In *N. attenuata*, the best-characterized defenses molecules induced by JA are nicotine (Baldwin, 2001; Steppuhn et al., 2004), trypsine protease inhibitors (TPIs; Ussuf et al., 2001; Steppuhn and Baldwin, 2007) and 17-hydroxygeranyllinalool diterpene glycosides (HGL-DTGs; Heiling et al., 2010; Fig. 8.1). Previous reports have demonstrated that *N. attenuata* plants rendered deficient in JA biosynthesis by silencing LOX3 (as-*lox3*) suffer more damage from insect herbivores in the plant's native habitat (Kessler et al., 2004). Moreover, generalist leafhoppers of the genus *Empoasca*,

hemipterans that feed on phloem and cell contents of a broad range of host plants (Carter, 1952; Gyrisco, 1958), heavily damage as-*lox3*, whereas these insects are only rarely found on WT *N. attenuata* plants (Kessler et al., 2004). The mechanisms underlying the selection of plants for feeding by *Empoasca* leafhoppers were not known. To disentangle these mechanisms, I used *N. attenuata* plants transformed with RNAi inverted repeat (ir) constructs to silence the expression of genes involved in six specific steps of JA biosynthesis and perception; in the accumulation of the three major classes of JA-mediated defense molecules (Chapter 6; Fig. 8.1); and, in addition, plants with a JA "sink" created by ectopically expressing JMT1 (JA-O-methyl transferase1; Stitz et al., 2011). These ten different lines of transformed plants were grown in a fully randomized design in a field plot in *N. attenuata*'s native habitat, the Great Basin Desert, SW USA. A field of alfalfa (a preferred host of *Empoasca* spp) was grown adjacent to the field plot and mowing of the alfalfa field encouraged the leafhoppers to move into the *N. attenuata* plantation. I quantified the initial feeding choice of the leafhoppers by determining the canopy area damaged by *Empoasca* spp. Whereas plants silenced in JA biosynthesis, accumulation or perception were heavily damaged by *Empoasca* leafhoppers, plants deficient in the accumulation of nicotine, TPIs or HGL-DTGs were damaged similarly to control plants. To demonstrate that the initial feeding choice was a direct result of silencing JA signaling, I assayed the levels of JA and its derivatives, the presence of *Candidatus* Phytoplasma (a bacteria vectored by leafhoppers (Galetto et al., 2011; Pérez et al., 2010) and volatiles released from attacked plants, known to influence insect feeding choice (Mayer et al., 2008). The results of the field experiments demonstrated that initial *Empoasca* leafhopper feeding choice was independent of the accumulation of major defense metabolites, the presence of *Ca.* Phytoplasma spp, and emitted plant volatiles. In the glasshouse, I performed a feeding choice assay using exogenous JA treatment of plants deficient in JA biosynthesis, accumulation and perception. This treatment reduced *Empoasca* leafhopper feeding on JA biosynthesis-deficient lines, but not on plants deficient in JA perception. Together with the field experiments, these results demonstrated that the initial feeding choice by *Empoasca* leafhoppers depended on the plants' capacity to mediate JA signaling. This feeding trait was exploited in nature and *Empoasca* leafhoppers were used to discover genetic variation in JA accumulation and signaling hidden in *N. attenuata* natural

populations. *Empoasca* leafhopper introduced into a population readily selected plants for feeding that were reduced in their JA accumulation capacities compared to unattacked control plants. Furthermore, natural infestations of *Empoasca* leafhoppers in two separate native *N. attenuata* populations also identified plants with reduced JA accumulation capacities compared to their uninfested neighbors. An analysis of the progeny of these plants demonstrated that the reduction of JA accumulation is heritable and was not caused by *Empoasca* leafhopper feeding. In summary, this part of my thesis highlights the similarities that have evolved between hematophagous (blood feeding) and phytophagous insects: both feeding guilds eavesdrop on the oxylipin signals (prostaglandins and jasmonates, respectively) elicited at the attack site to select hosts with diminished defensive responses. The work also shows how an insect herbivore can be used to identify natural variation in a major defense signaling pathway in plants.

Together with many other important studies reviewed, for example in (Howe and Jander, 2008), my thesis demonstrated the fundamental role of the rapid activation of the JA biosynthesis pathway in response to insect herbivory. But the accumulation of JA is only one response in plants induced after insect herbivore attack. The hydroperoxide lyase (HPL) pathway, for example, generates the green leaf volatiles (GLVs) hexanal and (3Z)-hexenal as a result of the cleavage of 13*S*-OOH-linoleic acid (13*S*-OOH-18:2) and 13*S*-OOH-18:3 by HPL. GLVs play essential roles as signaling molecules in indirect plant defenses (Croft et al., 1993; Matsui, 2006; Allmann and Baldwin, 2010; Baldwin, 2010). In *N. attenuata* leaves, the biosynthesis of hexanal and (3Z)-hexenal requires the activity of Na*LOX2* (Allmann et al., 2010). In recent years, research has been focused primarily on the biochemical and functional characterization of GLVs during herbivore attack. However, the other half of the cleaved 13*S*-OOH-18:2 and 13*S*-OOH-18:3 forms 12-oxo-(9Z)-dodecenoic acid ((9Z)-traumatin, Fig. 8.1; Vick and Zimmerman, 1976). Less attention has been paid to the metabolism and signal capacities of (9Z)-traumatin and other C_{12} derivatives of the HPL pathway. As a result, the metabolic fluxes and fates of these molecules under stress conditions are largely unknown in plants. (9Z)-traumatin undergoes rapid modifications by diverse enzymatic and non-enzymatic reactions, generating multiple potential chemical signals (Zimmerman and Coudron, 1979; Ivanova et al., 2001). In my thesis, I performed a detailed analysis of the fluxes and metabolism of C_{12} derivatives in *N.*

attenuata plants induced by wounding and FAC elicitation (Chapter 7). I developed a LC-MS/MS based method for the quantification of C_{12} derivatives and demonstrated that in *N. attenuata*, approximately 98% of the initially produced (9*Z*)-traumatin was converted into 9-hydroxy-10(*E*)-traumatin (9-OH-traumatin). In contrast, the remaining 2% of the (9*Z*)-traumatin was rapidly metabolized by either rearrangement of the *Z*-C_9-C_{10} double bond to *E*-C_{10}-C_{11} to form 12-oxo-(10E)-dodecenoic acid ((10*E*)-traumatin, Fig 8.1), by auto-oxidation of the aldehyde group to form (3Z)- and (2E)-dodecenedioic acid ((3*Z*)- and (2E)-traumatic acid Fig 8.1), or by reduction of the aldehyde group to form (9Z)- and (10E)-12-hydroxydodecenoic acid ((9*Z*)- and (10*E*)-12-OH-dodecenoic acid, Fig 8.1). For the formation of 9-OH-traumatin, both, enzymatic and non-enzymatic mechanisms have been proposed in other plant species (Gardner, 1998; Noordermeer et al., 2000) and I demonstrated that both mechanisms occur in *N. attenuata*. I used protein extracts from WT and ir-*lox2* plants and performed *in vitro* assays with synthetic (9*Z*)- and (10*E*)-traumatin. By using heat inactivation and LOX inhibitors, I could demonstrate that one third of *de novo* produced 9-OH-traumatin is synthesized non-enzymatically, but two thirds are produced enzymatically by product recycling through LOX2 activity. 9-OH-traumatin is a reactive electrophile species (Gardner et al. 1998) and approximately 40% of the produced 9-OH-traumatin was conjugated to glutathione within 1 h after elicitation. In summary, in this part of my thesis I disentangled the metabolism of C_{12} derivatives in *N. attenuata* leaves upon wounding and FAC elicitation by developing a method for the quantification of C_{12} metabolites. Additionally, I could show by microarray analysis that C_{12} derivatives are potential signaling molecules for the induction of gene expression during the response to wounding and herbivory.

Oxylipins are fundamental in orchestrating responses to biotic and abiotic stresses. They comprise a large family of many different structures and can be found in almost all living organisms. Their function as signaling molecules most likely co-evolved in these organisms. In this thesis, I focused on two major oxylipin signaling pathways found in plants, the AOS pathway responsible for JA production and the HPL pathway responsible for the production of GLVs and C_{12} metabolites. I showed that metabolism of insect elicitors at the wound site can tune the induction of oxylipin signaling pathways, how these pathways are activated upon insect herbivore attack and which function these signaling

___

pathways fulfill in nature. To understand how oxylipin signaling has shaped intra- and inter-specific interactions in nature, we have to know how oxylipin biosynthesis is regulated and how oxylipin signaling affects the interaction of plants with insects in nature.

References

Allmann, S., and Baldwin, I.T. (2010). Insects betray themselves in nature to predators by rapid isomerization of green leaf volatiles. Science **329,** 1075-1078.

Allmann, S., Halitschke, R., Schuurink, R., and Baldwin, I. (2010). Oxylipin channelling in Nicotiana attenuata: lipoxygenase 2 supplies substrates for green leaf volatile production. Plant Cell Environ **33,** 2028-2040.

Baldwin, I.T. (2001). An ecologically motivated analysis of plant-herbivore interactions in native tobacco. Plant Physiology **127,** 1449-1458.

Baldwin, I.T. (2010). Plant volatiles. Curr Biol **20,** R392-397.

Browse, J. (2009). Jasmonate Passes Muster: A Receptor and Targets for the Defense Hormone. Annu. Rev. Plant Biol **60,** 183-205.

Carter, W. (1952). Injuries to plants caused by insect toxins.2. Botanical Review **18,** 680-721.

Chini, A., Fonseca, S., Fernández, G., Adie, B., Chico, J., Lorenzo, O., García-Casado, G., López-Vidriero, I., Lozano, F., Ponce, M., Micol, J., and Solano, R. (2007). The JAZ family of repressors is the missing link in jasmonate signalling. Nature **448,** 666-671.

Christie, W.W. (2003). Lipid Analysis; Isolation, Separation, Identification and Structural Analysis of Lipids. **15**. 3rd edition. Bridgewater, England: The Oily Press.

Croft, K., Juttner, F., and Slusarenko, A.J. (1993). Volatile Products of the Lipoxygenase Pathway Evolved from Phaseolus vulgaris (L.) Leaves Inoculated with Pseudomonas syringae pv phaseolicola. Plant Physiol **101,** 13-24.

Fujita, M., Fujita, Y., Noutoshi, Y., Takahashi, F., Narusaka, Y., Yamaguchi-Shinozaki, K., and Shinozaki, K. (2006). Crosstalk between abiotic and biotic stress responses: a current view from the points of convergence in the stress signaling networks. Curr. Opin. Plant Biol. **9**, 436-442.

Galetto L, Marzachì C, Demichelis S, Bosco D. (2011), Host Plant Determines the Phytoplasma Transmission Competence of Empoasca decipiens (Hemiptera: Cicadellidae). J Econ Entomol 104: 360-366

Gardner, H.W. (1998). 9-Hydroxy-traumatin, a new metabolite of the lipoxygenase pathway. Lipids **33,** 745-749.

Glauser, G., Grata, E., Dubugnon, L., Rudaz, S., Farmer, E.E., and Wolfender, J.L. (2008). Spatial and temporal dynamics of jasmonate synthesis and accumulation in Arabidopsis in response to wounding. J Biol Chem **283,** 16400-16407.

Gyrisco, G.G. (1958). Forage insects and their control. Annual Review of Entomology **3,** 421-448.

Halitschke, R., Schittko, U., Pohnert, G., Boland, W., and Baldwin, I.T. (2001). Molecular interactions between the specialist herbivore Manduca sexta (Lepidoptera, Sphingidae) and its natural host Nicotiana attenuata. III. Fatty acid-amino acid conjugates in herbivore oral secretions are necessary and sufficient for herbivore-specific plant responses. Plant Physiology **125,** 711-717.

Heiling, S., Schuman, M.C., Schoettner, M., Mukerjee, P., Berger, B., Schneider, B., Jassbi, A.R., and Baldwin, I.T. (2010). Jasmonate and ppHsystemin Regulate Key Malonylation Steps in the Biosynthesis of 17-Hydroxygeranyllinalool Diterpene Glycosides, an Abundant and Effective Direct Defense against Herbivores in Nicotiana attenuata. Plant Cell **22,** 273-292.

Howe, G.A., and Jander, G. (2008). Plant Immunity to Insect Herbivores. Annual review of plant biology **59,** 41-66.

___

Ivanova, A.B., Yarin, A.Y., Antsygina, L.L., Gordon, L.K., and Grechkin, A.N. (2001). (9Z)-12-Hydroxy-9-dodecenoic Acid Is an Inducer of Oxygen Consumption and Extracellular pH Changes by Cut Wheat Roots. Doklady Biochemistry and Biophysics **379,** 302-303.

Kazan, K., and Manners, J. (2008). Jasmonate Signaling: Toward an Integrated View. Plant Physiology **146,** 1459-1468.

Kessler, A., Halitschke, R., and Baldwin, I.T. (2004). Silencing the jasmonate cascade: induced plant defenses and insect populations. Science **305,** 665-668.

Labandeira, C. (2007). The origin of herbivory on land: Initial patterns of plant tissue consumption by arthropods. Insect Science **14,** 259-275.

Matsui, K. (2006). Green leaf volatiles: hydroperoxide lyase pathway of oxylipin metabolism. Curr Opin Plant Biol **9,** 274-280.

Mayer, C.J., Vilcinskas, A., Gross, J. (2008). Phytopathogen lures its insect vector by altering host plant odor. J Chem Ecol **34,** 1045-1049.

Noordermeer, M.A., Feussner, I., Kolbe, A., Veldink, G.A., and Vliegenthart, J.F.G. (2000). Oxygenation of (3Z)-alkenals to 4-hydroxy-(2E)-alkenals in plant extracts: A nonenzymatic process. Biochemical and Biophysical Research Communications **277,** 112-116.

Pérez, K.A., Piñol, B., Rosete, Y.A., Wilson, M., Boa, E., Lucas, J. (2010). Transmission of the Phytoplasma Associated with Bunchy Top Symptom of Papaya by Empoasca papayae Oman. J Phytopathol **158,** 194-196

Rayapuram, C., and Baldwin, I.T. (2007). Increased SA in NPR1-silenced plants antagonizes JA and JA-dependent direct and indirect defenses in herbivore-attacked Nicotiana attenuata in nature. Plant Journal **52,** 700-715.

Schmelz, E.A., Engelberth, J., Alborn, H.T., Tumlinson, J.H., and Teal, P.E.A. (2009). Phytohormone-based activity mapping of insect herbivore-produced elicitors. Proceedings of the National Academy of Sciences **106,** 653-657.

Steppuhn, A., and Baldwin, I.T. (2007). Resistance management in a native plant: nicotine prevents herbivores from compensating for plant protease inhibitors. Ecology Letters **10,** 499-511.

Steppuhn, A., Gase, K., Krock, B., Halitschke, R., and Baldwin, I.T. (2004). Nicotine's defensive function in nature. Plos Biology **2,** 1074-1080.

Stork, W., Diezel, C., Halitschke, R., Galis, I., and Baldwin, I.T. (2009). An ecological analysis of the herbivory-elicited JA burst and its metabolism: plant memory processes and predictions of the moving target model. J Chem Ecol **4,** e4697.

Stitz, M., Gase, K., Baldwin, I.T., Gaquerel, E. (2011) Ectopic expression of AtJMT in Nicotiana attenuata: creating a metabolic sink has tissue-specific consequences for the jasmonate metabolic network and silences downstream gene expression. Plant Physiol **157,** 341-354.

Suza, W.P., and Staswick, P.E. (2008). The role of JAR1 in Jasmonoyl-L: -isoleucine production during Arabidopsis wound response. Planta **227,** 1221-1232.

Thines, B., Katsir, L., Melotto, M., Niu, Y., Mandaokar, A., Liu, G.H., Nomura, K., He, S.Y., Howe, G.A., and Browse, J. (2007). JAZ repressor proteins are targets of the SCFCO11 complex during jasmonate signalling. Nature **448,** 661-U662.

Ussuf, K.K., Laxmi, N.H., and Mitra, R. (2001). Proteinase inhibitors: Plant-derived genes of insecticidal protein for developing insect-resistant transgenic plants. Current Science **80,** 847-853.

Vick, B.A., and Zimmerman, D.C. (1976). Lipoxygenase and hydroperoxide lyase in germinating watermelon seedlings. Plant Physiol **57,** 780-788.

Wang, L., Halitschke, R., Kang, J.H., Berg, A., Harnisch, F., and Baldwin, I.T. (2007). Independently silencing two JAR family members impairs levels of trypsin proteinase inhibitors but not nicotine. Planta **226,** 159-167.

Wu, J.Q., Hettenhausen, C., Meldau, S., and Baldwin, I.T. (2007). Herbivory rapidly activates MAPK signaling in attacked and unattacked leaf regions but not between leaves of Nicotiana attenuata. Plant Cell **19,** 1096-1122.

Zimmerman, D.C., and Coudron, C.A. (1979). Identification of Traumatin, a Wound Hormone, as 12-Oxo-trans-10-dodecenoic Acid. Plant Physiol **63,** 536-541.

Zusammenfassung

Während der seit 400 Millionen Jahren andauernden Evolutionsgeschichte von Pflanzen und pflanzenfressenden Insekten, haben sowohl Pflanzen als auch Insekten raffinierte Mechanismen entwickelt, um die Anwesenheit des jeweils anderen zu bemerken und dementsprechend zu reagieren. Während Pflanzen gelernt haben, ein fressendes Insekt anhand von Substanzen im Oralsekret (OS) des Insekts zu identifizieren, haben Insekten gelernt, eine Vielzahl giftiger Pflanzenmetabolite zu entgiften. Die pflanzlichen Verteidigungsmechanismen sind dabei größtenteils nicht ständig aktiv, sondern werden erst induziert, sobald ein Pflanzenfresser beginnt an der Pflanze zu fressen. Die Aktivierung dieser Verteidigungsmechanismen geschieht nicht unkontrolliert, sondern wird durch eine Vielzahl von Signalmolekülen sehr genau reguliert. Diese Substanzen, zu denen u.a. Jasmonate, Salizylsäure, Abzisinsäure und Ethylen gehören, werden unverzüglich nach Insektenfraß in der Pflanze gebildet und koordinieren die Verteidigung der Pflanze.

Der wilde Tabak *Nicotiana attenuata* reagiert intensiv und spezifisch auf den Fraß unterschiedlichster Insektenarten. Beispielsweise wird eine fressende Raupe des Tabakschwärmers *Manduca sexta* anhand der im OS der Raupe vorhandenen Fettsäure-Aminosäure-Konjugate (FAC) erkannt. Das quantitativ häufigste FAC im *M. sexta* OS ist das Konjugat von α–Linolensäure und Glutaminsäure (18:3-Glu). In Kapitel 3 konnten wir zeigen, dass dieses FAC bei Kontakt mit der verwundeten Blattoberfläche sofort metabolisiert wird. Diese enzymatische Reaktion wurde durch Lipoxygenase (LOX) katalysiert und generierte aktive und inaktive Metaboliten. Vor allem das gebildete 13-oxo-13:2-Glu war ein aktives Signalmolekül und verstärkte im Vergleich zu mechanischer Verwundung die Biosynthese von Jasmonsäure (JA) sowie die Emission zweier Monoterpene. Die Metabolisierung von 18:3-Glu nach Kontakt mit dem verwundeten Blattmaterial geschah sehr schnell, innerhalb von Sekunden war das LOX-Produkt 13-OOH-18:3-Glu nachweisbar und bereits nach 2 Minuten war ungefähr die Hälfte des aufgetragenen 18:3-Glu verstoffwechselt. Durch die Verwendung von Pflanzen, mit

reduzierter Expression zweier *N. attenuata* LOX Isomere, *LOX2* und *LOX3*, konnten wir zeigen, dass höchstwahrscheinlich LOX2 die 18:3-Glu Metabolisierung katalysiert. Dies geschah jedoch ausschließlich bei Verwundung von Blattmaterial woraus man schießen kann, dass die Zerstörung von Pflanzenzellen notwendig ist, um LOX Enzyme in Kontakt mit 18:3-Glu zu bringen. Zusammengenommen ließ sich aus den erhaltenen Daten schließen, dass die Metabolisierung von 18:3-Glu eine Feinabstimmung der pflanzlichen Verteidigungsmechanismen darstellt und es sich hierbei um eine weitere Stufe der insektenspezifisch gesteuerten Abwehr handelt.

Eine grundlegende Reaktion der Pflanze ist die unmittelbare Aktivierung der JA Biosynthese und ihrer Derivate innerhalb weniger Minuten nach Insektenfraß. Diese so genannten Jasmonate steuern die pflanzlichen Verteidigungsmechanismen gegen Herbivoren. In *N. attenuata* akkumuliert JA transient innerhalb einer Stunde nach Insektenfraß. Um zu untersuchen, wie genau die JA Biosynthese nach Verwundung und Insektenfraß aktiviert wird, entwickelte ich eine einfache, schnelle, sowie spezifische und sensitive analytische Methode um Zwischenprodukte der JA Biosynthese simultan zu detektieren und zu quantifizieren. Die Methode konnte für Moleküle mit freien Carboxylgruppen genutzt werden, die durch eine zweistufige Reaktion derivatisiert wurden. Die erste Reaktion bildete bei Raumtemperatur innerhalb 1 Minute aus der Carbonsäure mit 1,1'-carbonyldiimidazol eine reaktives Carbimidazol das in der zweiten Reaktion innerhalb von 10 Minuten bei 37°C mit 3-hydroxymethyl)-pyridine quantitativ zu einen β–Picolinylester reagierte. Diese milden Bedingungen ermöglichten auch die Derivatisierung und Analyse sensibler Moleküle. Außerdem wurden durch die Reaktion veresterte Carboxylgruppen nicht umgeestert. Daher konnten auch nicht aufgearbeitete Proben verwendet werden. Wurden β–Picolinylester flüssigkeitschromato-graphisch (LC) aufgetrennt und nach positiver Elektrosprayionization (ESI) massen-spektrometrisch (MS) analysiert, ergaben alle β–Picolinylester ein spezifisches Fragmention mit einem Masse-Ladungs-Verhältnis (m/z) von 92. Dieses Fragmention wurde benutzt, um die β–Picolinylester im MS-multi-reaction monitoring (MRM) Modus anhand des Übergangs vom Molekülion $[M+H]^{+}$ zum Ion m/z= 92 zu quantifizieren. Die entwickelte Methode wurde für 26 verschieden Substanzen getestet und validiert.

Zusammenfassung

Die quantitative Bestimmung von Zwischenprodukten der JA Biosynthese ermöglichte die Untersuchung von Faktoren, die die JA Produktion nach Insektenbefall beeinflussen. Zuvor konnte bereits gezeigt werden, dass zwei mitogen-aktivierte Proteinkinasen (salizylat-induzierte und durch Verwundung induzierte Proteinkinase, SIPK und WIPK) und eine regulatorische Komponente des Salizylsäuresignalweges (nonexpressor of PR1, NPR1) die JA Produktion in *N. attenuata* beeinflussen. Allerdings war bisher nicht bekannt, wie die JA Biosynthese durch diese Komponenten reguliert wird. Ich konnte zeigen wie SIPK, WIPK und NPR1 die frühen enzymatischen Schritte der JA Biosynthese in *N. attenuata* nach Verwundung und FAC Applikation (W+FAC) beeinflussen. Des Weiteren untersuchte ich Effekte von *CORONATINE INSENSITIVE 1* (COI1), einem Gen das an der Wahrnehmung von JA und der Steuerung von JA regulierten Abläufen in der Pflanze beteiligt ist, und hierbei eines der am besten erforschten Gene darstellt. Mit Hilfe von transgenen Linien, die jeweils in der Transkription eines dieser Gene reduziert waren (ir-*sipk*, ir-*wipk*, ir-*npr1* und ir-*coi1*), analysierte ich quantitative Änderungen von Substraten und Intermediaten der JA Biosynthese innerhalb von 10 Minuten nach W+FAC. Im Verlauf dieser Arbeit wurde eine Lipase (GLA1) identifiziert, die wesentlich an der JA Biosynthese in *N. attenuata* beteiligt ist. Ich konnte zeigen, das sich in Wild-Typ (WT) Pflanzen innerhalb von 10 min nach W+FAC weder die Menge an Membranlipiden noch an freien Fettsäuren (FFA) signifikant änderte. Innerhalb dieser Zeit blieb der Gehalt an FFA auch konstant wenn die Expression von GLA1 reduziert wurde. Diese Daten ließen darauf schließen, dass 18:3 durch einen schnellen und gerichteten Mechanismus für die JA Biosynthese bereitgestellt wird. In ir-*sipk*, ir-*npr1* und ir-*coi1* Pflanzen war die Menge aller ungesättigten FFA im Vergleich zu WT Pflanzen reduziert, wodurch man in diesen Pflanzen von einer generellen Änderung der homöostatischen FFA Menge ausgehen konnte. In Gegensatz zu FFA stieg der Gehalt an 13-hydroperoxi-18:3 (13-OOH-18:3) innerhalb von 5 min nach Verwundung linear an. FAC Applikation verstärkte diesen Effekt noch, änderte jedoch nicht die Aktivität von 13-LOX oder den Proteingehalt. Dies indizierte, das FAC Applikation den 13-OOH-18:3 Gehalt dadurch erhöhte, das GLA1, und somit die Bereitstellung von 18:3, aktiviert wurde. In ir-*wipk* Pflanzen glich der Gehalt an 13-OOH-18:3 dem von WT Pflanzen, war jedoch in ir-*sipk* und ir-*npr1* Pflanzen stark reduziert. Da auch hier die Aktivität und der

Proteingehalt an 13-LOX unverändert in Vergleich zu WT war, ließ sich daraus schlussfolgern, dass SIPK und NPR1 die Bereitstellung von 18:3 durch GLA1 aktivieren und dadurch die JA Biosynthese regulieren. Im Gegensatz zur 13-LOX Aktivität, war die Aktivität von Allene oxide synthase (AOS) sowohl in ir-*sipk*, ir-*npr1*, ir-*coi1* als auch in ir-*wipk* Pflanzen reduziert, was sich auch in einem verminderten Gehalt an (9*S*,13*S*)-12-oxo-phytodienonsäure (OPDA) widerspiegelte. WIPK-vermittelte Prozesse könnten die Grundaktivität von AOS beeinflussen, wodurch die Akkumulierung von OPDA nach W+FAC beeinflusst wird. Zusammenfassend konnte ich zeigen, dass FACs und die Mechanismen der Signalübertragung an denen SIPK, WIPK und NPR1 beteiligt sind, unterschiedliche Stufen der JA Biosynthese beeinflussen.

Um in der Natur zu überleben, ist die Aktivierung der JA Biosynthese nach Insektenfraß von essentieller Bedeutung. JA wird durch JASMONATE RESISTANT (JAR) mit Isoleucine zu JA-Ile konjugiert, welches an den SCF^{COI}-Komplex bindet. Diese Bindung führt zur Markierung und zum Abbau von JAZ Proteinen, welche die Transkription von Genen spezifisch unterdrücken. Dadurch werden Gene reaktiviert die an der Biosynthese von Verteidigungssubstanzen beteiligt sind. In *N. attenuata* zählen Nikotin, Trypsin-Protease Inhibitoren und glykosidische 17-hydroxi-geranyllinalool-diterpene (HGL-DTGs) zu den am besten untersuchten JA induzierten Verteidigungs-substanzen. Wird die JA Biosynthese in *N. attenuata* Pflanzen ausgeschaltet, im Speziellen durch gentechnische Verminderung der LOX3 Transkription (as-*lox3*), werden die Pflanzen in ihrem natürlichen Lebensraum, der Great Basin Wüste im Südwesten der USA, vermehrt von Herbivoren befallen. Mehr noch, Zwergzikaden der Spezies *Empoasca*, die normalerweise nur selten auf wilden *N. attenuata* Pflanzen zu finden sind, verursachten starken Schaden an as-*lox3* Pflanzen. Die zugrunde liegenden Mechanismen sind jedoch weitgehend unerforscht. Daher benutzte ich zehn verschieden transformierte Linien von *N. attenuata*, um diese Mechanismen genauer zu untersuchen. Die zehn Linien setzten sich aus sechs Linien mit verminderter Genexpression von JA Biosynthese- und JA Wahrnehmungsgenen, aus drei Linien mit verminderter Akkumulierung von JA regulierten Verteidigungssubstanzen, und aus einer Linie mit einer durch Überexpression von JMT1 (JA-O-methyl transferase1) generierten JA Senke zusammen. Alle transformierten Linien wurden im Feldversuch auf *Empoasca* Schaden untersucht. Während Pflanzen, die an der

JA-Biosynthese, -Wahrnehmung oder durch eine JA Senke manipuliert wurden, stark durch *Empoasca* Zwergzikaden befallen waren, zeigten Pflanzen, die weniger Nikotin, TPI oder HGL-DTG akkumulieren, kaum das für *Empoasca* typische Schadbild. Um zu zeigen, dass die Wahl der Wirtspflanze durch *Empoasca* direkt mit der Manipulation der JA Signalkaskade in Verbindung steht, untersuchte ich außer dem Fraßschaden auch die Gehalte an JA und JA-Derivaten, das Vorhandensein von *Candidatus* Phytoplasma (Bakterien, die durch Zwergzikaden übertragen werden) und die Emission flüchtiger Stoffe von attackierten Pflanzen. Zusätzlich untersuchte ich das Fressverhalten von *Empoasca* in Gewächshausexperimenten in denen ich Linien mit reduzierter JA-Biosynthese, -Akkumulierung oder -Wahrnehmung benutzte um durch exogenes JA die Resistenz gegen *Empoasca* wiederherzustellen. Dies gelang, wenn die Biosynthese von JA, jedoch nicht wenn die Wahrnehmung von JA in den Pflanzen manipuliert war. Zusammengenommen konnten die Feld- und die Gewächshausversuche zeigen, dass die Größe des Schadens von *Empoasca* an *N. attenuata* Pflanzen davon abhängt, wie gut die JA Signalkaskade in der Pflanze vermittelt wird. Das Fressverhalten von *Empoasca* bot die Möglichkeit, um Variationen der JA-Signalkaskade in natürlichen *N. attenuata* Populationen zu untersuchen. Brachte man *Empoasca* in eine natürliche *N. attenuata* Population ein, oder untersuchte man den natürlichen Befall von *Empoasca* innerhalb von Populationen, fand man die Insekten, und den durch sie verursachten Schaden, ausschließlich an Pflanzen, die eine verminderte JA Biosynthesekapazität aufwiesen. Zusammenfassend zeigte dieser Teil meiner Ergebnisse, wie anhand von Insektenschäden ein tieferer Einblick in die natürliche Variation eines grundlegenden Verteidigungsmechanismus' von Pflanzen erhalten werden kann.

In meiner Arbeit konnte ich die elementare Rolle der Aktivierung der JA Signalkaskade in der Pflanze nach Insektenbefall unterstreichen. Jedoch ist die Produktion von JA nur ein Aspekt der Pflanzenverteidigung nach Herbivorie. Beispielsweise führt die Verwundung von Pflanzenmaterial zur unverzüglichen Emission so genannter grüner Blattduftstoffe (GLVs) durch die Spaltung von 13*S*-OOH-linolsäure (13*S*-OOH-18:2) und 13*S*-OOH-18:3 durch Hydroperoxi-Lyase (HPL). In *N. attenuata* Pflanzen wird die Bildung von GLVs, bzw. die Synthese der benötigten Peroxide, durch die LOX isoform LOX2 geregelt. Pflanzen mit reduzierter Expression an LOX2 (ir-*lox2*) zeigen eine

substantiell verminderte Emission an GLVs. GLVs spielen eine bedeutende Rolle als Signalmoleküle in der indirekten Pflanzenverteidigung und die biochemische und funktionelle Charakterisierung von GLVs während Insektenfraßes war innerhalb der letzten Jahre Bestandteil vieler Studien. Dabei wurde jedoch die potentielle Funktion der anderen Spaltprodukte der Reaktion von 13S-OOH-18:2 und 13S-OOH-18:3 mit HPL vernachlässigt. Die Spaltung führt ebenfalls zur Bildung von 12-oxo-(9Z)-dodecenoic acid ((9Z)-traumatin). Nach der Synthese wird (9Z)-traumatin durch eine Vielzahl von enzymatischen und nicht-enzymatischen Reaktionen modifiziert wodurch eine Reihe potentieller Signalmoleküle entstehen. Als Teil meiner Arbeit entwickelte ich eine LC-MS/MS basierte Methode zur quantitativen Bestimmung dieser C_{12} Stoffwechselprodukte und analysierte das Verhalten dieser Stoffe nach W+FAC. Ich konnte zeigen, dass circa 98% des entstandenen (9Z)-traumatins in 9-hydroxi-10(E)-traumatin (9-OH-traumatin) umgewandelt wurden und die restlichen 2% in andere Substanzen, entweder durch Umlagerung der Doppelbindung oder Oxidation bzw. Reduktion der Aldehydgruppe. Die Bildung von 9-OH-traumatin kann sowohl enzymatisch als auch nicht enzymatisch ablaufen und ich konnte zeigen, dass in *N. attenuata* beide Mechanismen vorkommen. Ich verwendete Proteinextrakte aus WT und ir-*lox2* und führte *in vitro* Reaktionen mit synthetischem (9Z)-traumatin und (10E)-traumatin durch. Durch Inaktivierung von LOX Enzymen mittels Erhitzen oder spezifischen Inhibitoren konnte ich nachweisen, dass ein Drittel des gebildeten 9-OH-traumatins nicht-enzymatisch entsteht, jedoch zwei Drittel enzymatisch durch Produktrecycling via LOX2. 9-OH-traumatin ist ein reaktives, elektrophiles Molekül und wurde in *N. attenuata* innerhalb 1 Stunde nach W+FAC zu circa 40% mit Glutathion konjugiert. Zusammen genommen, konnte ich durch die Entwicklung einer Methode zur quantitativen Bestimmung von C_{12} Molekülen, in diesem Teil meiner Arbeit den Stoffwechsel von C_{12} Molekülen in *N. attenuata* aufzeigen. Mithilfe eines Microarrays konnte ich außerdem zeigen, dass diese Moleküle eine potentielle Signalfunktion für die Aktivierung von Genexpression nach W+FAC besitzen.

Zusammenfassung

Oxidationsprodukte ungesättigter Fettsäuren, sogenannte Oxylipine, spielen eine entscheidende Rolle bei der Regulation von Antworten auf biotischen und abiotischen Stress. Diese Substanzgruppe besteht aus einer Vielzahl von Molekülen und kann in fast allen Lebewesen nachgewiesen werden. In der vorliegenden Arbeit habe ich die zwei größten Oxylipinsignalkaskaden der Pflanzen untersucht: Die AOS-Signalkaskade, die zur Bildung von JA führt, und die HPL-Signalkaskade die zur Bildung von GLVs und C_{12} Molekülen führt. Ich habe gezeigt, wie diese Signalkaskaden nach Insektenbefall aktiviert werden, wie die Verstoffwechselung von Molekülen im Insekten OS diese Aktivierung optimieren kann und welche Rolle diesen Signalkaskaden in der Natur zukommt. Um zu verstehen, wie Oxylipinsignale intra- und interspezifische Wechselbeziehungen geformt haben, muss man wissen wie die Oxylipinbiosynthese reguliert ist und wie Oxylipinsignale die Wechselbeziehung von Pflanzen und Insekten in der Natur beeinflussen.

Acknowledgements

Finally it is time to thank the many people who supported me during my time as a Ph.D. student in many different ways. A big thank you to all of you, you really paved the way to this thesis.

Ian, I want to thank you for the opportunity you gave me to work in this really fascinating research area. I enjoyed discussions with you in Jena but especially during the three field seasons in Utah. Thank you for the great ideas you always had to support achieving my research goals but also for critical comments that shaped me as a scientist. Your passion for science is impressive. **Gustavo**, you hired me as a Ph.D. student and I know it was not always easy to supervise me. However, you never lost your humor and your straight way of doing science and your talent always to think in the big picture formed my way of doing science. You always had a sympathetic ear and solutions to all the problems and questions that arose and always offered a helping hand if necessary. Thank you for this. **Georg Pohnert**, I want to thank you for your courage to be my university supervisor regardless that you haven't seen me quite often during my work on this thesis. **Arjen**, **Alejandro**, **Fiametta**, **Paola**, **Silke**, **Antje**, **Ian** and **Gustavo**, as my coauthors in the manuscripts presented here, I want to thank you for the great efforts you made to convert experiments and crude data into a publishable format. I want to thank **Merry**, **Gustavo**, **Alex**, **Arne**, **Mari** and **Micha** for proofreading the introduction, summary and Zusammenfassung part of my thesis.

I thank the **GuBo group** (past and present members) for the great working atmosphere we had. I want to thank **Tamara**, **both Andreas**' and all other **gardeners** for growing and taking care of thousands of plants that I used during this work. At our field station in Utah, experiments would not have been possible without the work of **Danny**, **Celia** and **Ian**. Our service group team (**Klaus**, **Thomas**, **Matthias**, **Antje**, **Eva**, **Susi** and **Wibke**) is thanked for taking care of equipment, plant transformations and all the other little things that are required to keep the department running. All my experiments in Utah would not have been possible without the help of **Danny**, **Celia**, **Merry**, **Micha**, **Silke**, **Arne**, **Paola**, **Mari** and **Will**. Thank you for this and I'm really sorry for starting

---

Acknowledgements

Curriculum vitae

Personal details:

Name: Mario Kallenbach

Date of birth: 29.11.1980

Place of birth: Gotha, Germany

Nationality: German

Current address: Theo-Neubauer-Straße 8, 07743 Jena

Email: mkallenbach@ice.mpg.de

Education:

August 2007-present:

> Ph.D. student at the Max-Planck Institute for Chemical Ecology Jena

October 2001-March 2007:

> Diploma student of Environmental Chemistry at the Friedrich Schiller University Jena, completed with a Diploma thesis entitled: "Biofilme natürlicher Substrate - Homogenitätsuntersuchen und Eignungsprüfung zur Aufdeckung anthropogener Belastungen" supervised by Prof. Jürgen Einax at the FSU Jena, Institute of Inorganic and Analytical Chemistry

September 1991-July 1999:

> Grammar school at Arnoldischule Gotha

September 1987-August 1991:

> Primary school at Bertha-von-Suttner school, Mechterstädt

Publications

2011

Kallenbach, M., Gilardoni, P. A., Allmann, S., Baldwin, I. T., Bonaventure, G. (2011). C12 derivatives of the HPL pathway are produced by product-recycling through LOX2 1 in Nicotiana attenuata leaves. New Phytologist, 191(4), 1054-1068.

2010

Kallenbach, M., Alagna, F., Baldwin, I. T., Bonaventure, G. (2010). Nicotiana attenuata SIPK, WIPK, NPR1 and fatty acid-amino acid conjugates participate in the induction of JA biosynthesis by affecting early enzymatic steps in the pathway. Plant Physiology, 152, 96-106.

van Doorn, A., **Kallenbach, M.**, Borquez, A., Baldwin, I. T., Bonaventure, G. (2010). Rapid modification of the insect elicitor N-linolenoyl-glutamate via a lipoxygenase-mediated mechanism on Nicotiana attenuata leaves. BMC Plant Biology, 10, 164.

2009

Kallenbach, M., Baldwin, I. T., Bonaventure, G. (2009). A rapid and sensitive method for the simultaneous analysis of aliphatic and polar molecules containing free carboxyl groups in plant extracts by LC-MS/MS. Plant Methods, 5, 17.

Oral Presentations

Kallenbach M,*, Kinetic studies on jasmonic acid biosynthesis intermediates activated by FAC signaling. 8th IMPRS Symposium, MPI for Chemical Ecology, Dornburg, DE, Mar 2009

Poster Presentations

Kallenbach M. Jasmonic acid as a direct defense against herbivores: Empoasca spp. choose their host plants by eavesdropping on aposomatic JA. 10th IMPRS Symposium, MPI for Chemical Ecology, Dornburg, DE, Feb 2011

Kallenbach M. Profiling the derivatives of the HPL pathway in N. attenuata: Hydroxylated C12 alkenal as major product of NaLOX2. 9th IMPRS Symposium, MPI for Chemical Ecology, Dornburg, DE, Feb 2010

Kallenbach M., Baldwin I.T., Bonaventure G. Early metabolic responses activated by FAC perception in N. attenuata. Oxylipin Symposium, University of Lausanne, Lausanne, CH, Aug 2008

Kallenbach M. The early metabolic responses activated by FAC perception in Nicotiana attenuata. 7th IMPRS Symposium, MPI for Chemical Ecology, Dornburg, DE, Feb 2008

Kallenbach M. The early metabolic responses activated by FAC perception in Nicotiana attenuata. IMPRS Evaluation Symposium, MPI for Chemical Ecology, Jena, DE, Sep 2007

Selbständigkeitserklärung

Ich erkläre, dass ich die vorliegende Arbeit selbständig und unter Verwendung der angegebenen Hilfsmittel und Quellen angefertigt habe.

Ort, Datum   Unterschrift des Verfassers